University of Kent at Canterbury

New strategies for the introduction of ^{18}F into peptides for imaging with Positron Emission Tomography

Helen L. Sladen

A thesis submitted to the University of Kent at Canterbury for the degree of Doctor of Philosophy in the Faculty of Science, Technology and Medical Studies.

Research School of Biosciences

June 2009.

Declaration

No part of this thesis has been submitted in support of an application for any other degree or qualification to the University of Kent at Canterbury or any other University or Institute of Learning.

Helen L. Sladen

Research School of Biosciences

June 2009

Acknowledgements

I would like to thank my supervisors, Professor Blower and Dr Biagini for all their support and assistance throughout this project. I would also like to thank Kevin Howland for the peptide synthesis, Dave Smith for the elemental analysis, EPSRC Swansea Mass Spectrometry Centre for the mass spectra and Michelle Rowe for her help with the 2D NMR and DEPT analysis.

Thanks to the friends I have made in lab 310 (Beulah, Ali, Anica, Hazel, Glen and David) for their friendship and others, namely Louise, Danielle, Gloria, Uzma, Lee, Carol, Steve and David for friendship and support throughout the years of this project. It has been much appreciated. Lastly, thanks to Buddy for constantly trying to distract me but also making life entertaining for me while writing up.

Abstract

PET is a potent imaging technique that uses positron emitting radionuclides such as ^{18}F, which is used either in the form of [^{18}F]FDG or attached to another biomolecule for diagnosis of disease and monitoring of treatment. The major disadvantage of labelling molecules with ^{18}F is their time-consuming, multiple step preparation.

This thesis presents two different novel strategies that both aim to decrease the number of steps required to prepare ^{18}F labelled peptides. The first strategy involved using the metal ruthenium as a binding site for ^{18}F in a one-step labelling technology involving halide anion exchange. The second approach involved a chemoselective reaction between the hydrazine functionalised compounds HYBA or HYNIC and a labelled aromatic aldehyde to form a hydrazone. In the second strategy, a peptide is synthesised with a HYBA or HYNIC molecule attached to it. Following this, ^{18}F labelled benzaldehyde is reacted with the peptide to give a 1 + 1 labelling strategy. Before using this methodology for labelling with ^{18}F, the chemoselectivity of the hydrazone formation was thoroughly tested by conducting competition reactions. The competition reactions involved a reaction between an aromatic aldehyde and HYBA in the presence of a competing amine. The reaction was found to be selective between the aldehyde and HYBA, even with increased equivalents of the competing amine present in the reaction mixture. Rate monitoring reactions were carried out in the presence of the competing amine, benzylamine, to see how quickly the hydrazone product formed at room temperature and at 50°C. The formation of the hydrazone was found to be quick and clean, even at room temperature. Amino acid synthons, two containing HYBA and two containing HYNIC, were synthesised to be incorporated into the peptide 'nanogastrin' for chemoselective labelling. These hydrazine containing peptides were then to be radiolabelled with [^{18}F]fluorobenzaldehyde. Early indications are that this approach to radiolabelling works as theorised.

Contents

Abbreviations

ABAME	4-aminobutyric acid methyl ester
Ala	alanine
Amu	atomic mass unit
Asp	aspartic aicd
BA	benzylamine
Boc	butoxycarbonyl
br	broad
c.a	carrier added
CCK-1	cholecystokinin type 1 (A)
CCK-2	cholecystokinin type 2 (B)
c.f	carrier free
Ci	curie
CNS	central nervous system
COSY	correlation spectroscopy
CT	Computer Tomography
d	doublet
dd	doublet of doublets
DCC	1,3-dicyclohexylcarbodiimide
DCM	dichloromethane
DEPT	Distortionless Enhancement by Polarization Transfer
DIEA	diisopropyl ethylamine
DMF	*N, N*-dimethylformamide
DMSO	dimethylsulphoxide
DTPA	diethylenetriamine pentaacetic acid

EDC	1-ethyl-3(3-dimethylaminopropyl)carbodiimide hydrochloride
EDTA	ethylenediamine tetraacetic acid
EOB	end of bombardment
EtOAc	ethyl acetate
EtOH	ethanol
ESI	electrospray
[^{18}F]FB-CHO	[^{18}F]Fluorobenzaldehyde
Fmoc	9-fluorenylmethoxycarbonyl
FPB	4-formylphenyl boronic acid
FDG	2-fluorodeoxy-D-glucose
GI	gastrointestinal
Glu	glutamine
Gly	glycine
HBTU	*O*-(benzotriazol-1-yl)-1,1,3,3-tetramethyluronium hexafluorophosphate
HF	hydrofluoric acid
HOBt	1-hydroxybenzotriazole
HPLC	high performance liquid chrmoatography
HYBA	4-hydrazinobenzoic acid
HYNIC	6-hydrazinonicotinic acid
IBAE	4-iodobenzoic acid active ester
IgG	immunoglobulin G
IR	infra red
LC-MS	liquid chromatography - mass spectrometry
LET	linear energy transfer
Lys	lysine
m	medium

m	multiplet
M	molecular ion
MBq	megabequerels
Met	methionine
n.c.a	no carrier added
NHS	*N*-hydroxysuccinimide
MHz	megahertz
MRI	Magnetic Resonance Imaging
MS	mass spectrometry
MTC	medullary thyroid cancer
m/z	mass to charge ratio (MS)
NMR	nuclear magnetic resonance
ov	overlapping
PET	Positron Emission Tomography
Phe	phenylalanine
PNS	peripheral nervous system
ppm	parts per million
q	quartet
RCP	radiochemical purity
RCY	radiochemical yield
RGD	Arg-Gly-Asp peptide
RP	reverse phase
RT	room temperature
Ru(III) EDTA	Ruthenium(III) {[2-(Bis-carboxymethyl-amino)-ethyl]-carboxymethyl-amino}-acetic acid
s	singlet (NMR)
s	strong (IR)

SPPS	solid phase peptide synthesis
SPECT	Single Photon Emission Computer Tomography
str	stretch
t	triplet
TEA	triethylamine
TFA	trifluoroacetic acid
TIS	triisopropylsilane
TLC	thin layer chromatography
TPPTS	trisodium triphenylphosphine-3,3',3"-trisulfonate
Trp	tryptophan
Tyr	tyrosine
UV	ultra violet
w	weak

Chapter 1

1.0 Introduction

1.1 Introduction to PET and SPECT

1.1.1 PET

Positron Emission Tomography or PET, which is currently likely to be the most advanced technology for studying *in vivo* molecular interactions (Valk et al. 2003), is used to monitor the concentration and movement of a positron emitting isotope in living tissue. PET is a potent non-invasive imaging technique for investigating biochemical, physiological and pharmacological processes in the human body including blood flow, glucose metabolism, receptor properties, enzyme activity and drug distribution and mechanisms. Diseases are biological processes and molecular imaging with PET is insightful and educational about these processes (Phelps 2000).

PET is being increasingly used for the evaluation of patients with known or suspected cancer at all stages of the management process, from staging to follow up treatment. The role of PET in therapeutic monitoring is rapidly growing due to its ability to provide earlier firm identification of non-responders than can be provided by conventional non-invasive imaging techniques. The potential therefore is an earlier change to alternative treatment that may be more effective or to avoid unnecessary toxicity related to unsuccessful treatment. It may also prevent early withdrawal of effective therapy (Hicks 2005). In many cases, diagnostic sensitivity and accuracy are 85-90% or better whether addressing primary lesions, metastases or recurrences (Conti et al. 1996).

According to Schubiger (2007), PET has the sensitivity necessary to visualise the interactions between physiological targets and ligands, for example, brain receptors as targets and neurotransmitters as ligands. PET is therefore excellent for monitoring drug distribution, pharmacokinetics and pharmacodyamics for most of the body's organs. The sensitivity of

PET is 10^{-9} to 10^{-12} mol as opposed to the imaging techniques, MRI (Magnetic Resonance Imaging) and CT (Computer Tomography) which are 10^{-5} and 10^{-3} mol respectively (Schubiger 2007, Rudin 2003). PET can detect changes at the cellular level and so detect the early onset of disease before it would be evident using other imaging techniques, such as CT and MRI. PET is less expensive and may yield more information than exploratory surgery. Compared to MRI and CT, PET can differentiate between malignant and benign tumours.

1.1.2 SPECT

Single Photon Emission Computer Tomography or SPECT is, like PET, also a technology used for imaging. SPECT is a commonly used and highly sophisticated method of imaging with instruments available in most hospitals worldwide (Adam and Wilbur 2004). SPECT relies on emission of a single gamma photon with enough energy (> 100 keV) to escape from the body and be detected. After injection of the radionuclide into the patient, these gamma photons are released from target areas. The photons are captured on a gamma camera that rotates around the patient. This gives an image of the radiopharmaceutical distribution (Marsden 2003). ^{99m}Tc from the ^{99}Mo/^{99m}Tc generator is ideal for use with SPECT as it decays to ^{99}Tc with emission of gamma photons with an ideal energy of 140 keV. These photons are emitted in high abundance. The half-life of six hours is long enough for extended procedures to be carried out, but short enough to minimise the radiation dose to the patient. Radiation from the low concentrations used for imaging is relatively harmless (Sattelberger and Atcher 1999). Technetium has no stable isotope and is a synthetic element. The m in the name ^{99m}Tc stands for metastable nuclear isotope. It does not change into another element upon decay. In routine medical practice, due to its ideal properties for SPECT and the widespread use of this imaging technique, ^{99m}Tc is still the radionuclide of choice (Okarvi 2001).

PET is not as widely available as SPECT due partly to the synthesis of SPECT radiopharmaceuticals based on ^{99m}Tc being produced in a 'kit' form. The result of this is that the labelling procedure is simple and quick and can be carried out by a technician rather than a radiochemist. The ^{99m}Tc (as pertechnetate ion) is added to a pre-prepared, sterile mixture of labelling precursors and additives. No final purification is necessary before injection into the patient (Schirrmacher et al. 2007). This kit technology is not available for the ^{18}F radiopahrmaceuticals that are used in PET. Another reason that SPECT is more widely used

than PET is that ^{99m}Tc is produced by generators that are present in all hospitals where SPECT is carried out, whereas ^{18}F must be made by a cyclotron. Cyclotrons are too big and expensive for most hospitals to own, meaning ^{18}F must often be produced in a different location to where it is used, causing problems with loss due to decay of the ^{18}F nucleus during transit.

1.1.3 Production of radionuclides and positron emission

In PET, a biologically active molecule is labelled with a positron (β^+) emitting radionuclide (Phelps 2000). A radionuclide is an unstable nuclide that decays to achieve stability. Radionuclides are unstable because they have too many neutrons, too few neutrons or have too many protons and neutrons. The positron emitting radionuclides used in PET are all proton rich and neutron poor.

Examples of positron emitting radionuclides used in PET are ^{18}F, ^{11}C, ^{15}O, ^{13}N, ^{62}Cu and ^{64}Cu. Fluorine-18 (^{18}F) is the radionuclide of choice as it decays nearly 100% by positron emission with low positron energy (635 KeV). This results in a low radiation dose to the patient. It also has a short range of emission in tissue which, in turn, allows for high resolution imaging. A more detailed discussion about ^{18}F can be found in section 1.3. As PET radionuclides have short half-lives, PET investigations need to take place near or at the site of production of the radionuclides.

Radioisotope	Half-life	Nuclear reaction
Carbon-11	20.4 minutes	^{14}N (p, α) ^{11}C
Nitrogen-13	9.96 minutes	^{16}O (p, α) ^{13}N
Oxygen-15	2.07 minutes	^{15}N (p, n) ^{15}O
Fluorine-18	109.7 minutes	^{18}O (p, n) ^{18}F

Table 1.0 Short-lived PET radionuclides with half-lives and nuclear reaction for production. The longer half-life of ^{18}F has advantages for production and makes longer imaging times possible

A cyclotron is a particle accelerator and is used for production of radionuclides. This produces radionuclides which are deficient in neutrons and that are carrier free. There are small cyclotrons available which are used for the production of the positron emitting nuclides ^{18}F, ^{11}C, ^{15}O, ^{13}N (Hendry et al. 1986) and for production of ^{61}Cu, ^{60}Cu, ^{64}Cu, ^{124}I, ^{89}Zr. The advantage of these small cyclotrons is that they can be installed at a PET centre. A cyclotron accelerates a particle and produces a beam (proton, deuteron or alpha particle) to bombard a stable element, such as ^{18}O. This brings about nuclear reactions leading to the production of the desired radionuclides.

PET requires the preparation of a positron emitting radiotracer. A positron is an antielectron, in other words it is the antimatter equivalent of the electron. It has the same mass as an electron, with a charge of +1 and a spin of a ½.

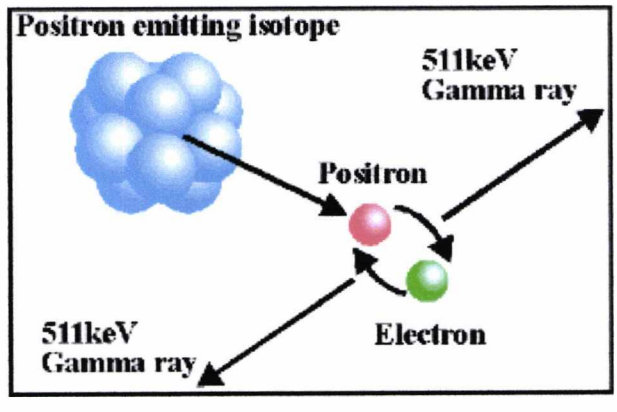

Figure 1.0 In PET, a low energy positron will meet an electron in the body and they will annihilate each other. This results in the release of two 511 KeV γ-rays at 180° to each other (McCarthy et al. 1994)

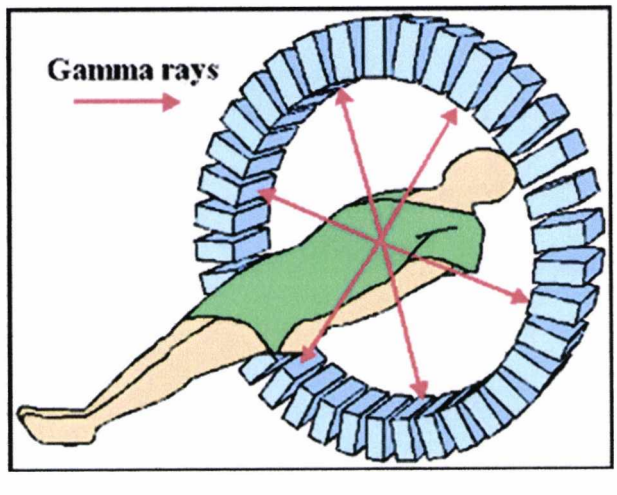

Figure 1.1 Detection of the γ-rays emitted from a patient occurs by a ring of bismuth germinate detectors

An explanation of some of the terminology used in radiochemistry is appropriate here, as these terms will be used throughout this chapter. Specific activity is defined as the ratio of the amount of radioactivity per unit mass or molar quantity. Specific activity can have a large effect on radiolabelling chemistry and the ability to conduct imaging or therapy. For example, high specific activity ^{18}F may be several thousand Curies (Ci/mmol where 1 mCi = 37 MBq) or megabequerels for [^{18}F]fluoride from a water target compared to only 1 Ci/mmol for carrier added [^{18}F]F_2 from a gas target (Adam and Wilbur 2004). The theoretical maximum specific activity is a function of the half-life where there is no dilution of the radionuclide by other isotopes of the compound and is therefore said to be 'carrier free' (c.f.). A c.f. compound is a radiolabelled compound not diluted with compound labelled with stable isotope (carrier). N.c.a. or no carrier added means a compound is not diluted with stable isotope labelled compound and c.a. is carrier added i.e. a known amount of carrier is added to the labelled compound. Having carrier free radionuclides is an advantage as large amounts of compound labelled with stable isotope could saturate receptors and prevent the radiolabelled compound being taken up. All quantities of radioactivity, specific activity and radiochemical yield (RCY, which is defined as the yield of a radiochemical separation expressed as a fraction of the activity originally present) must be related to the same reference time point. End of bombardment (EOB) normalises all radioactivity measurements to the end of cyclotron irradiation time. End of synthesis (EOS) normalizes all radioactivity measurements to the end of chemical synthesis. (Sutcliffe-Goulden 2001)

1.2 Radiotherapy

Radionuclides with different decay properties from those used for imaging in SPECT and PET can be used for radiotherapy.

Radiation interacts with biological tissues through absorption of energy to either excite electrons or ionise atoms in its path. When the absorbed energy of radiation is sufficient to eject one or more electrons, ionisation occurs. This energy of radiation is dispersed and is more than enough to break chemical bonds. The largest component of cells (80%) is water and so water is the molecule most likely to be ionised. Ionised water molecules rapidly cause hydroxyl free radicals to form, which cause damage to the cell. This is an indirect action of radiation damage as the damage is not caused by the radiation itself. Cellular repair mechanisms can offset the damage to some extent, but when the damage is too extensive, cell

death occurs. Direct action of the radiation can also occur via electrons, protons, neutrons and α-particles, which can collide with DNA. These interactions transfer a large amount of energy in the distance travelled and are considered to have high linear energy transfer (LET). LET is an important concept in radiotherapy as the effectiveness of the radiation at cell killing increases as the LET of the radiation increases (Adam and Wilbur 1994). Radionuclides for therapy have particle emissions that produce more ionisation in biological tissue than the radionuclides used in imaging, in other words, the radionuclide should have the right energy to penetrate the tumour and accumulate there, killing the surrounding cells. The half-life should be several hours or days. Therapeutic radionuclides are usually β^- emitters. The energy from these β^- emitters is absorbed within a few millimetres of tissue meaning the β^--particle travels well beyond the cell to which it is attached and therefore not every cell need have the radionuclide associated with it (Adam and Wilbur 2004). α-particles have a range in tissue of 50-70 μm (for ^{211}At). α-particles have more interaction with tissue than β^--particles which means they are able to transfer more energy and are therefore considered to have very high LET. α-particles are therefore very attractive for use in therapy. It is estimated to take several hundred β^- emitting radionuclides to kill a cell due to the fact that most of the energy is deposited outside the cell, or 1 to 14 α emitting radionuclides. Astatine-211, Bi-213 and Ra-223 are all α emitting radionuclides suitable for use in humans. Development of α emitting radionuclides is currently an area of intensive research. Auger electrons can be used for radiotherapy if they can enter the cell nucleus (Liu and Edwards 2001). Auger electrons are produced by electron capture decay. As electrons drop from the L shell to the K shell to fill spaces created by captured electrons, photons of energy specific to the particular element are emitted. This energy is transferred to an electron in an outer shell, which is then emitted from the atom as an Auger electron. Auger electrons have been shown to be very toxic when incorporated into mammalian DNA (Kassis et al 1982). Auger electrons do not transfer their energy very far and this fact means the Auger electron has very high LET. They cause little damage to non-target tissue.

1.3 Fluorine-18

^{18}F has become the choice radionuclide in PET (Dolle 2005) in a similar way to ^{99m}Tc in SPECT. ^{18}F has optimal chemical and nuclear properties for PET. It is easy to manufacture and can be used in comparatively high radioactive quantities (Okarvi 2001). ^{18}F can be produced in good yields, even with low energy cyclotrons. It has ideal emissions in that it has

low positron energy, typically 635 keV, which not only limits the dose to patients, but also results in an essentially short range of emission in tissue (Wilbur 1992, Kilbourn 1987), providing high resolution images. ^{18}F has a half-life of 109.7 minutes which allows time consuming multiple step radiosyntheses along with extended PET studies of slower biochemical processes. The half-life is important as too short and it will decay before it is metabolised; too long and the nuclide will still be present long after the applicable metabolism has occurred resulting in wasteful use of the radioactive dose. The relatively long half-life of ^{18}F permits transport of ^{18}F pharmaceuticals to hospitals without on-site cyclotron facility (Stocklin 1998, Varagnolo 2000).

1.3.1 Basic ^{18}F radiolabelling methods

In general, radiolabelling of target molecules must be quick and involve as few reaction steps as possible to get high radiochemical yields and high specific activity. Indeed, for reasons of economy (decay of radioactivity), reliability (routine production in remote controlled devices) and radiation protection (of the radiochemist), the nuclide should ideally be added as the last step.

The fluorine atom is small and can accept a hydrogen bond. Though the carbon-fluorine bond is very strong, labelling molecules with ^{18}F has its challenges. 'True' or isotopic labelling is limited to molecules with a fluorine atom, however there are no naturally occurring fluorine-containing compounds in the body and fluorine-containing biomolecules are often not suitable substrates in normal metabolic pathways as they can act as enzyme inhibitors. Unlike ^{18}F, radionuclides such as ^{15}O, ^{13}N, ^{11}C are able to give isotopic or 'true' labelling, as the elements carbon, nitrogen and oxygen are obviously very common in nature. The radiolabelled tracers are indistinguishable from the stable isotope equivalent molecules.

^{18}F is most commonly used by replacing hydrogen in organic molecules. This significantly affects the chemical and biochemical properties of the molecule. This can be an advantage, for example using [^{18}F]FDG, which is discussed in more detail in section 1.3.2.

Fluorination in non-radiochemistry is theoretically transferable to radiochemistry. However when used n.c.a, these methods produce low RCY (Atkins et al. 1972, Tewson and Welch 1979). Methods used to introduce non radioactive fluorine into aromatic organic compounds include the Wallach reaction (Wallach 1886) or solid diazonium tetrafluoroborates in the

Balz-Schiemann reaction with better yields (Balz and Scheimann 1927). These are dediazoniation reactions in which the fluorine replaces a decomposing diazonium moiety. Both of these reactions use S_N1 type nucleophilic substitution and so the reactive carbocation can react with any nucleophile present giving rise to side reactions. (Coenen 2007).

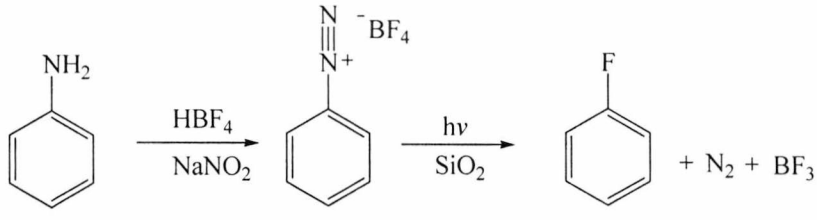

Scheme 1.0 Balz-Schiemann reaction

Labelling with ^{18}F is either by electrophilic substitution or nucleophilic substitution. Electrophilic substitution is c.a. using $[^{18}F]F_2$ gas, where only one (at most) of the fluorine atoms present is ^{18}F. The electrophilic route therefore leads to low specific radioactivity. The nucleophilic route is the most important, gives high specific radioactivity and can be direct or indirect. Both nucleophilic and electrophilic routes yield unwanted radioactive and non-radioactive by-products that must be removed from the desired product by high performance liquid chromatography (HPLC). The use of a prosthetic group for labelling a peptide or other biomolecule, is an indirect method which allows for mild and site specific labelling. The nucleophilic substitution (via S_N2 mechanism) is based on n.c.a $[^{18}F]$fluoride. The n.c.a. $[^{18}F]$fluoride is obtained as an aqueous solution and so is hydrated. ^{18}F forms hydrogen bonds which decrease its nucleophilicity and so labelling takes place under polar, aprotic conditions (Coenen 2007). This produces highly reactive ^{18}F. Anhydrous acetonitrile is a commonly used solvent for labelling. Anion exchange resins are then used to separate $[^{18}F]$fluoride and recover ^{18}O enriched target water. The last of the water is removed by azeotropic distillation under a stream of nitrogen and thermal drying at temperatures of between 80°C - 110°C. For anion activation the bicyclic aminopolyether kryptofix 222, in combination with K_2CO_3, is very commonly used.

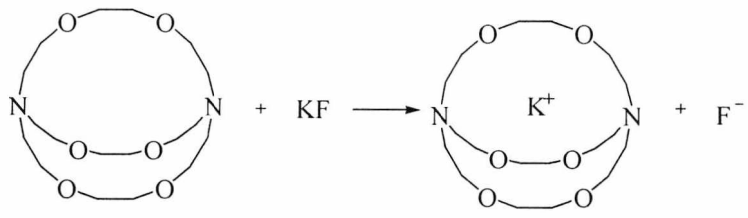

Scheme 1.1 To show synthesis of $[K/K222]^+/F^-$. K222 sequesters the potassium ion to provide a 'naked', reactive form of fluoride

For direct fluorination, halogens or sulfonic acid esters such as mesylate, tosylate or triflate act as a leaving group. Of these, triflate is the best (Coenen et al. 1986). Triflate or trifluoromethanesulfonate ($^-$OTf) anion is the conjugate base of CF_3SO_3H which is a stronger acid than even sulphuric acid. It is therefore an excellent leaving group. Fluorine in polar aprotic solvents has a strong basic character which can lead to elimination reactions occurring alongside substitution reactions. To label an aromatic molecule with [^{18}F]fluoride, an activated benzene ring must be present with electron withdrawing groups, e.g. NO_2, CN or COR, in the *ortho-* or *para-* position to the leaving group. Benzaldehydes are very useful for labelling as the aldehyde group is highly electrophilic in character.

As stated, nucleophilic *homo*aromatic substitutions with [^{18}F] require activated rings with a good leaving group, such as a nitro- group, a halogen or a trimethylammonium group together with a strong electron withdrawing substituent e.g. NO_2, CN or COR, preferably placed *para-* to the leaving group. More recently there has been interest in *hetero*aromatic rings, especially the pyridine series. This is because of the discovery of some important nicotinic acid receptor drug families with a fluoropyridine moiety (Dolle 2007). Indeed, it has been found that nucleophilic *hetero*aromatic substitution at the *ortho-* position with a 2-fluoropyridinyl moiety with n.c.a. [^{18}F] is the most efficient way of producing radiopharmaceuticals of high specific activity when compared to *homo*aromatic and aliphatic nucleophilic radiofluorination (Dolle 2005).

1.3.2 [^{18}F]-2-fluorodeoxy-D-glucose

[^{18}F]-2-fluorodeoxy-D-glucose ([^{18}F] FDG) is a glucose analogue labelled in the 2 position with [^{18}F]fluoride.

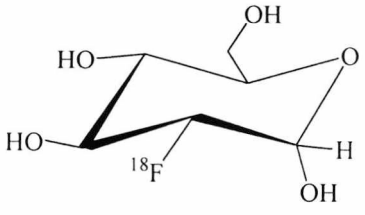

Figure 1.2 [^{18}F]-2-fluorodeoxy-D-glucose

[^{18}F]FDG is the most widely used PET radiopharmaceutical in oncology (Gallagher 1978, Reivich et al. 1979) and has been for many years. Chemically it is an analogue of glucose, although as a metabolite it is not treated exactly as glucose *in vivo*. However, [^{18}F]FDG is still ideal for imaging glucose uptake (Hicks 2005). This is discussed in more detail later. [^{18}F]FDG is readily produced in large quantities. It is very useful as tumour cells have a hypermetabolic state, which means they have an increased rate of glycolysis and therefore [^{18}F]FDG accumulates in tumour cells (Yasuda and Shohtsu 1997). Tumour cells also have increased amino acid transport, protein synthesis and increased DNA synthesis. They can have increased or decreased receptor expression and increased or decreased blood flow. [^{18}F]FDG is used for diagnosis and monitoring of treatment in malignant disease. Whole body PET images, feasible because of the relatively long half-life of [^{18}F]FDG, can also detect any metastases from the primary tumour.

[^{18}F]FDG is transported across the cell membrane and phosphorylated to [^{18}F]FDG-6-phosphate ([^{18}F]FDG-6P). Unlike glucose-6-phosphate, [^{18}F]FDG-6P is not further metabolised, remaining trapped in the cell. It therefore accumulates in tissue with a high glucose uptake. This allows imaging of the tumour from the [^{18}F] trapped in the cell in the form of [^{18}F]FDG-6P. The drawback to this is that it is also taken up by normal healthy tissues that use glucose as fuel such as the brain, digestive tract, thyroid gland, skeletal muscle, myocardium, bone marrow and the genitourinary tract. Benign pathological uptake occurs in healing bone, lymph nodes, joints and sites of infection. It is also utilised in the aseptic inflammatory response (Shreve et al. 1999). This is why more selective radiopharmaceuticals are also needed.

A real strength of PET scanning with [^{18}F]FDG is that the metabolic information provided is complementary to results from standard clinical and morphological examinations (Conti et al. 1996). Simultaneous acquisition of PET and CT images enables physicians to more precisely discriminate between physiologic and malignant [^{18}F]FDG uptake and more accurately localise lesions (Kluetz et al. 2000). Still, the limitation of [^{18}F]FDG PET has lead to researchers looking for other more selective molecules to label with positron emitting nuclides.

Figure 1.3 An [^{18}F]FDG image

1.4 Clinical considerations in the production of labelled compounds for PET

Since radiopharmaceuticals are administered usually by intravenous injection, they must meet the same strict criteria that exist for the production of pharmaceuticals (Parker et al. 1984). All conventional injectable pharmaceutical products are required to pass sterility and pyrogen tests before they are released for administration. This requirement cannot be met for many radiopharmaceuticals due to the fact that the time required for testing is very long compared

with the half-life of the radionuclide. The need to be able to produce, on a routine basis, high quality radiopharmaceuticals which can be safely administered to patients has led to the development of the radiopharmaceutical 'kit'. These kits contain all the non-radioactive ingredients required for the preparation of an injectable radiopharmaceutical in a pre-packaged, sterile form which has been subjected to full quality control testing prior to use. These kits are designed so that the preparative procedure is reduced to a few simple operations which can be carried out under aseptic conditions. A single-stage procedure is desirable as each additional step increases the risk of introducing microbial contamination into the preparation (Parker et al. 1984). These kits are available only for ^{99m}Tc on the whole, not for ^{18}F.

1.5 Novel labelling strategies

There are potentially hundreds of ^{18}F labelled radiotracers, mostly small monomeric molecules. Increasingly, there are also more complex structures where labelling depends on multiple step synthesis. (Wuest 2007). Surface receptors on cells are good targets for imaging probes. Many alternative compounds for better tumour characterisation are being evaluated. These compounds can be divided into general tracers for evaluating non-specific aspects of tumour metabolism, such as protein synthesis, amino acid transport, nucleic acid synthesis, or membrane component synthesis and specific tracers for receptors or gene expression (Couturier 2004). Some examples of these compounds are as follows:

Fluorinated analogues of amino acids are useful because increased transport and/or protein synthesis in tumour cells has been demonstrated (Couturier 2004). For example L-3-[^{18}F]-α-methyl tyrosine which has been shown to be clinically useful in the diagnosis of malignant tumours (Inoue 2001). Tyrosine tracers are used for brain and protein metabolism studies (Adam and Wilbur 2004).

Peptides such as [^{18}F]fluoro-octreotide are used for somatostatin receptor imaging. Somatostatin is a cyclic peptide that is secreted in the brain, the digestive tract and the thyroid. Octreotide is a somatostatin analogue with a longer biological half-life. Octreotide is indicated for treatment of neuroendocrine tumours such as carcinoids (Couturier 2004) and labelled forms can help visualise whether somatostatin receptor-positive tumours have occurred (Kwekkeboom 2000). More is discussed about peptides including octreotide later in this chapter.

Thymidine Kinase TK1 expression is strictly controlled in normal cells, but is frequently over expressed in proliferating tumour cells (Couturier 2004) This enables the use of fluorinated nucleosides such as [^{18}F]3'-fluoro-3'-deoxythymidine for imaging tumour cells that over express TK1.

Fluorinated analogues of membrane phospholipids such as choline analogues can be used for imaging due to the fact that the malignant transformation in cells is associated with increased levels of choline and may possibly be used as a supportive indicator of progression of some tumours (Tedeschi 1997).

Fluorinated analogues of oestrogen, e.g. [^{18}F]fluoroestradiol, an oestrogen receptor ligand, can be used to study oestrogen receptors which are often over expressed in breast cancer, as oestrogen plays a major role in the development of breast cancer. This can also be used to monitor the response to treatment for breast cancer with drugs such as tamoxifen. Fluorinated analogues of progesterone can be used for imaging tumours expressing progesterone receptors (Couturier 2004).

It is established that hypoxia to some extent protects tumour cells against irradiation and some chemotherapeutic agents. Therefore hypoxia could be an important factor in resistance to treatment. Hypoxic cells can be found in numerous solid tumours (Couturier 2004). There are fluorinated tracers that make it possible to assess hypoxia e.g nitroimidazoles, such as [^{18}F]EF5 (Adam and Wilbur 2004).

In many malignant endothelial cancer cells, the folate receptor is over expressed, while in normal tissue restricted expression is found (Garin-Chesa et al. 1993, Weitmann et al. 1992). The over expression ranges from 30 times the normal expression in ovarian carcinoma to 1400 times in endometrial cancer (Garin-Chesa et al. 1993). ^{18}F labelled folate has been developed using click chemistry. The tracer showed good *in vitro* properties (Ross et al. 2008). Click chemistry is a concept in chemistry (generally, not just in the field of radiolabelling) where the object is to generate compounds quickly and reliably by joining small modular units. Ideally reactions should have high yields, inoffensive by-products, stereospecificity, simple reaction conditions with the use of water (preferably) as the solvent. In general terms, products should be easy to purify by crystallisation and should be stable under physiological conditions (see page 20 for an example of radiolabelling using click chemistry).

The use of a prosthetic group is necessary for the labelling of peptides with ^{18}F because of the limitations of the nucleophilic introduction of ^{18}F, such as the harsh basic conditions, which precludes the direct labelling of bioactive molecules (such as peptides) with H-acidic functions (Guhlke 1994). The prosthetic group, for example, trimethylammonium triflate, is radiolabelled with ^{18}F.

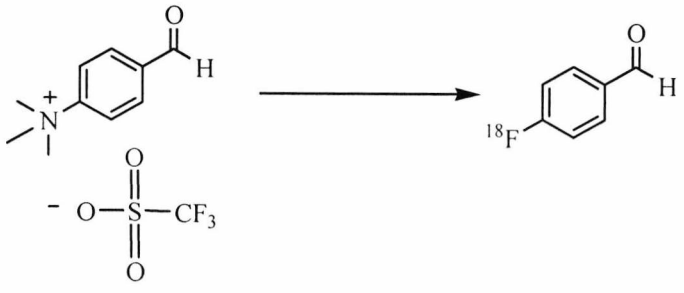

Scheme 1.2 Radiolabelling of trimethylammonium triflate with [^{18}F] to produce [^{18}F]fluorobenzaldehyde

[^{18}F]fluorobenzaldehyde is then attached to the peptide via a specific functional group. This is covered in more detail in the section on labelling peptides. When synthesising ^{18}F, the addition of K_2CO_3 is necessary to prevent the release of H[^{18}F]F during the drying process but leads to complications when the compound to be labelled, such as peptides, are base sensitive. The syntheses of ^{18}F labelled prosthetic groups are multiple step ones.

1.6 Peptides

The idea of using peptides in PET is that they are specific, unlike [^{18}F]FDG, so will be taken up selectively in tissues due to the presence of a specific receptor for a particular peptide. Peptides are useful for imaging disease states such as cancer and inflammation because they take advantage of a distinct cellular target, such as a receptor, being present on the cell. Receptors are often over expressed on tumour cells. Peptides will bind to their receptors with high specificity and affinity (Ting et al. 2008).

The first step towards peptide use in PET was the use of monoclonal antibodies used to target specific receptors expressed in disease. Monoclonal antibodies were labelled with ^{99m}Tc or ^{111}In. However, monoclonal antibodies are too large to have ideal pharmacokinetics and over the last few years, biospecific imaging agents have taken over from large proteins. These biospecific imaging agents evolved from antibody fragments to antigen binding domain fragments to biologically active peptides (Fischman et al. 1993). Peptides are smaller than

antibodies, synthesised more easily and less likely to cause an immunogenic response. Their smaller size means that unbound peptides are cleared from the blood more quickly than unbound antibodies are, resulting in high target to background ratio and so improving image quality. Peptides penetrate tumours more easily and possess binding affinities for their receptors that are comparable or even greater than antibody binding affinities. Peptides are rapidly taken up by target tissue as opposed to monoclonal antibodies that are taken up far more slowly (Okarvi 2001).

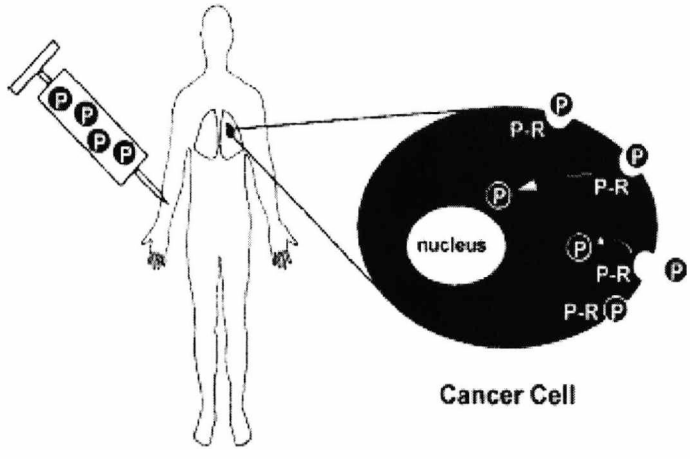

Figure 1.4 Peptide receptor targeting of cancer cells. The radiolabelled peptide (P) is injected intravenously into the patient and distributed in the whole body. If the patient has a tumour with cancer cells expressing the corresponding peptide receptor (P-R), the radiopeptide will bind to it and internalise the receptor into the cell where the radioactivity will accumulate. Whole body PET will detect the radioactivity accumulated in the tumour, and the remaining radioactivity in the body will be cleared through the kidneys (Reubi 2003)

Biologically active molecules that selectively interact with specific cell types are attractive vehicles for the delivery of radioactivity to target tissues. The affinity of the peptide for the receptor facilitates retention of the radiolabelled peptide in receptor expressing tissue. Various receptors are over expressed in particular tumour types and peptides binding to these sites can be used to visualise tumour lesions scintigraphically. In most cases the desired pharmacokinetic characteristics may be engineered into the peptide molecule. Peptides are relatively small so a non-target bound radiotracer is eliminated rapidly from the body, reducing background radiation and allowing good target definition. Small peptides are rapidly taken up by the target tissue. They can be manipulated chemically to optimise their affinity for a particular binding site and display a more specific distribution (Okarvi 2001).

It has been predicted that in the next few years, 50% of all drugs entering clinical trials will be peptides. (Wester and Schottelius 2007). Reasearch in genomics and proteomics will uncover new as well as known targets upregulated in certain disease states. It will be possible to develop specific peptide ligands that can bind to these targets. Bioactive peptides are expected to become a very important class of tracers in PET.

1.6.1 Labelling peptides

It is not possible to label peptides directly with ^{18}F as strong basic conditions are required, which results in denaturing of sensitive organic compounds and deprotonation of acidic moieties found on the peptide (Guhlke 1994). This is why other labelling strategies are being developed. Labelling with a prosthetic group is one way of labelling without exposing the peptide to harsh conditions. The prosthetic group can be a small organic molecule which can be labelled separately and then attached to the peptide via a specific functional group, for example an amino or sulfhydryl group or a bigger molecule, such as HYNIC (King et al. 2007). This group is called a bifunctional chelating agent and is therefore used as a means of binding a small radiolabelled prosthetic group to a peptide. The radiolabelled bifunctional chelator-peptide must be thermodynamically stable and kinetically inert to survive under physiological conditions (Heppeler et al. 2000). Labelling in this manner is an area of intense research as bioconjugation of a small organofluoride precursor to a large molecule is often not high yielding even though often a large excess of the biomolecule is added to drive the reaction forward (Ting et al. 2008). Another problem is that labelling peptides using ^{18}F prosthetic groups often increases the lipophilicity of the peptide which can have consequences on *in vivo* behaviour of the peptide (Schirrmacher et al. 2007).

1.6.1.1 Non-selective labelling

^{18}F acylation is the most common method of ^{18}F labelling, it is a non-selective means of radiolabelling. Labelling a biomolecule can be a selective or non-selective process. Chemoselectivity and regioselectivity mean that the exact location of the ^{18}F on the biomolecule can be chosen and applied with only the desired product being synthesised. Non-selective labelling does not give this ability, it relies on labelling synthons such as carboxylic acids or active esters which target primary amino functions either at the *N*-terminus of peptides (α-NH_2) or lysine residues (ε-NH_2) (Schirrmacher et al. 2007). Active esters can be

used to form an amide bond between the carboxyl group of bifunctional chelating agent and an amino group in a peptide ligand (Fichna and Janecka 2003).

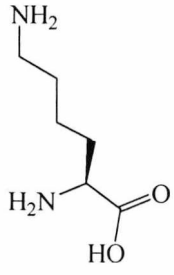

Figure 1.5 L-lysine

Due to the abundance of lysine residues in proteins, proteins and peptides are then labelled in a non-selective manner meaning it is not possible to know exactly where on a molecule the label is and that many impurities will also be synthesised alongside the product of interest. A good example of this can be given using annexin V, as there are at least 23 potential sites for a reaction to occur between the annexin V and *N*-succinimidyl 4-[^{18}F]fluorobenzoate ([^{18}F]SFB), some near the active binding site of the protein (Li et al. 2008). Separation of the unconjugated molecule, present as an impurity, from the desired product can lead to a large reduction in specific activity (Ting et al 2008). Labelling with *N*-succinimidyl 4-[^{18}F] fluorobenzoate continues to be the most common way of radiolabelling because of high metabolic stability (Vaidyanathan and Zalutsky 1992, 1994, Wester et al. 1996) and good conjugation yields (Wester et al. 1996). [^{18}F]SFB can be used in the ^{18}F-fluoroacylation of lysine and is the most suitable prosthetic group used in the labelling of proteins and peptides with a wide range of applications. This was found by Wester et al. (1996) when several different prosthetic groups for a number of different peptides were compared. [^{18}F]SFB and another commonly used prosthetic group 4-nitrophenyl-2-[^{18}F]fluoropropionate ([^{18}F]NPFP), were investigated using four different proteins; human serum albumin, transferrin, avidin, and immunoglobulin G. Wester et al (1996) found that although [^{18}F]SFB may be the best method for labelling with respect to maximising conjugate yields and *in vivo* stability, it is a time consuming and non-selective method of radiolabelling. Synthesis of labelled peptides with prosthetic groups can take several additional steps after adding the ^{18}F label (Wust et al. 2003). A one-step labelling preparation via [^{18}F]fluoroacylation has been carried out (Lang

and Eckelmann 1994) but this method suffered from low yields of *N*-succinimidyl-4-([^{18}F]fluoromethyl)benzoate (18-25% within 30 minutes) as well as defluorination (Magata et al. 2000). This has prevented the use of this method for routine applications. Another disadvantage of [^{18}F] acylation is the necessary use of protective peptide precursors for conjugation with the prosthetic group as this required deprotection after peptide synthesis, adding another post-labelling step to this route of [^{18}F] radiopharmaceutical synthesis (Poethko et al 2004a).

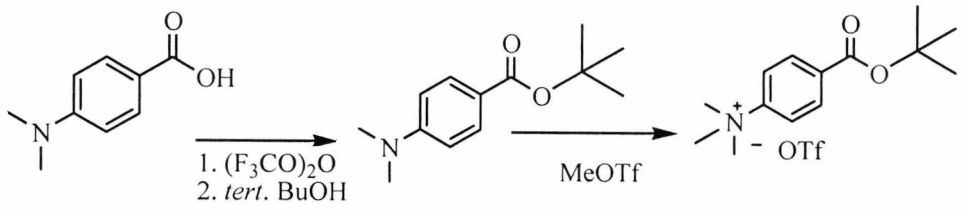

Scheme 1.3 Synthesis of triflate salt

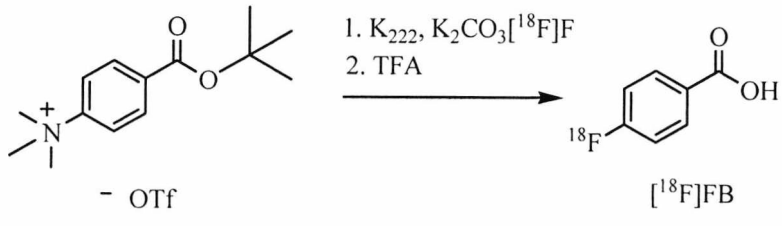

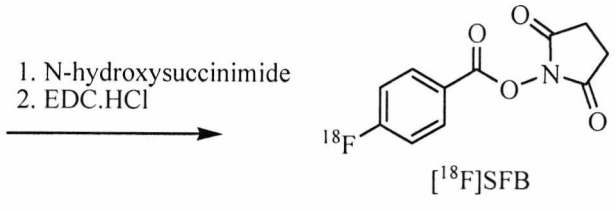

Scheme 1.4 Radiosynthesis of [^{18}F]SFB

Product 1

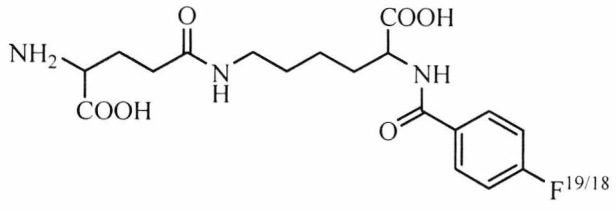

Product 2

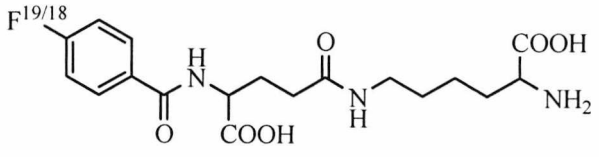

Product 3

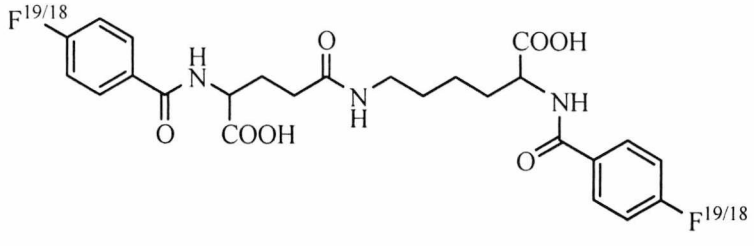

Scheme 1.5 Formation of three fluorobenzoylated peptides; products 1, 2 and 3

The steps involved (shown above) are numerous and time consuming meaning this labelling technology takes hours, requiring high levels of radioactivity to compensate for loss through decay. Extensive purification must also be carried out after synthesis. Care must be taken to ensure the end product is sterile to allow for injection into patients. The more steps taken for the production process, the harder this becomes. This, then, is not an ideal way to label biomolecules with ^{18}F. Despite all this, labelling biomolecules with [^{18}F]SFB continues to be the most common method of radiolabelling and a number of improvements have been made in the synthesis of [^{18}F]SFB, including automation (Vaidyanathan and Zalutsky 2006).

1.6.1.2 Chemoselective labelling

In recent years, chemoselective labelling has become a hot topic in ^{18}F radiochemistry with many new methods being published. Chemoselectivity depends on the implementation of a particular methodology meaning a specific reaction is favoured above other potential reactions. Below some of this new methodology for radiolabelling biomolecules with ^{18}F is discussed.

Site specific labelling is desirable as it produces a homogenous product leading to reproducibility in labelling and imaging (Flavell et al. 2008). Other than the ideal one step only procedure, the next best labelling strategy using peptides would be a 1 + 1 step strategy. Step 1 would be a high yield synthesis of an ^{18}F labelled prosthetic group. This should be stable so it would not be defluorinated *in vivo*. Step 2 would be a one step chemoselective conjugation to a specifically functionalised, unprotected peptide precursor. The second step should be done in aqueous media and under mild conditions to protect the peptide from denaturation.

Click chemistry has been used to develop a chemoselective ^{18}F labelling strategy. This uses the 1,3-dipolar Huisgen cycloaddition reaction of terminal alkynes with azides, yielding 1,4-disubstituted 1,2,3-triazoles under mild conditions. The alkynes and azides are relatively easy to introduce into molecules; they are stable to the majority of organic synthetic reaction conditions and can therefore be introduced into the target molecules at the most convenient time (Bock et al. 2006). Uncatalysed, the Huisgen cycloaddition reaction usually yields mixtures of 1,4- and 1,5- disubstituted triazoles and proceeds at a slow pace. Huisgen and Meldal discovered recently that Cu(I) catalysis leads to 1,4 regioisomers only and increases reaction rates many times, meaning that now this methodology could be useful for PET (Appukkuttan et al. 2004). Marik and Sutcliffe (2006) described a procedure for obtaining ^{18}F fluorinated peptides by reacting ω-[^{18}F]fluoroalkynes with peptides bearing *N*-(3-azidopropionyl)-groups that did not need HPLC purification. The labelled peptides were obtained were obtained 54-99% RCY.

Recently it has been discovered that a fluorination enzyme, wild type fluorinase (isolated from the bacterium *Streptomyces cattleya*) is capable of forming C-F bonds (Schaffrath et al. 2003). The enzyme fluorinase was used to incorporate ^{18}F into 5'-[^{18}F]fluoro-5'-

deoxyadenosine as a potential tumour imaging agent (Martarello et al. 2003). However, the problem with this method of radiolabelling was that the reaction the fluorinase catalyses is reversible and because of this, suffered from a RCY of only 1% (decay corrected). It was found that by coupling other enzymes to the fluorinase, more of the labelled compound was isolated. This helped achieve much higher RCYs of 45-75% (Deng et al. 2006) but the synthesis time of 1-4 hours was too long for routine use in a clinical setting.

A recent finding using protic solvents for nucleophilic reactions has shown surprising results. Solvents such as tertiary alcohols have been shown to facilitate nucleophilic reactions with alkali metal fluorides. This was an unexpected result as anion nucleophilicity is normally reduced as a result of the interaction with the partial positive charge present in protic solvents. Kim et al. (2006) showed that cold fluorinations of compounds using CsF in tert-amyl alcohol gave the corresponding fluorinated products in good to excellent yields at temperatures between 25-90°C. Selectivity is shown towards nucleophilic reactions by reducing the amount of impurities produced in side reactions such as alkenes, alcohols and ethers. Lee et al. (2007) demonstrated an automated high RCY synthesis of a radioligand for dopamine transporter imaging using t-BuOH as a solvent. This chemistry is not fully understood yet. One characteristic is that the reactivity of the halide ions in these solvents seems to be reversed i.e. F^- is more reactive than Br^- (Schirrmacher et al. 2007).

Lysine residues in proteins may be common but cysteine residues are much less so and are the only amino acid to contain a free thiol moiety. Thiol reactive prosthetic groups (free sulfhydryl –SH groups) are not commonly found in many peptides or proteins.

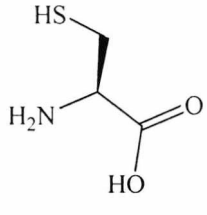

Figure 1.6 L-cysteine

This is the basis for another chemoselective labelling strategy. These strategies are mostly based on a maleimide group for thiol specific Michael addition reactions. This means that labelling specifically with thiol reactive prosthetic groups gives control and therefore

selectivity over labelling. The problem with this method is that the labelling requires a multiple step approach (2 to 4 steps), which limits the technique in a clinical setting (Wester and Schottelius 2007) and relies on there being one accessible cysteine residue available for site specific labelling. Toyokuni et al. (2003) synthesised *N*-{4-[(4-[^{18}F]fluorobenzylidene)aminooxy]butyl}maleimide ([^{18}F]FBABM). The radiosynthesis was labour intensive, taking one hour and needed HPLC purification. The secondary thiol reactive labelling precursor gave a decay corrected RCY of 35%. The conjugation reaction with a model peptide glutathione, occurred in 30 minutes at room temperature in yields of 70%. Overall, from a clinical point of view, this is a rather long preparation time for an ^{18}F labelled peptide. As this method depends on there being one accessible cysteine residue only on a peptide, it has limited application. The two-step two pot synthesis of [^{18}F]FBABM is shown below.

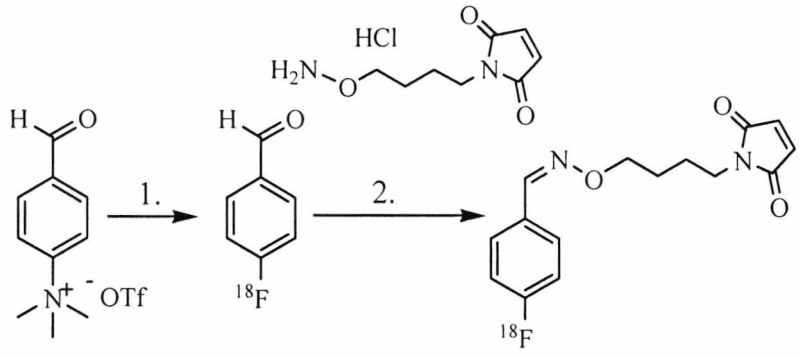

Scheme 1.6 Synthesis of [^{18}F]FBABM. (1) K^{18}F, kriptofix 222, ACN, 100°C for 15 min. (2) Addition of maleimide, MeOH at RT for 15 min

Another study taking a similar approach to that above investigated labelling a modified version of the protein annexin V, called annexin V-128 which is a mutated form of the protein with one cysteine residue (Li et al. 2008). Their method of synthesising the [^{18}F]FBABM shown above was an improvement on the method by Toyokuni et al. (2003) by not having to use C18 SepPak purification and carrying out the two-step reaction in one pot in a process that could be automated and that gave similar RCYs to the two-step, two pot synthesis above (23% RCY) in 92 minutes.

Glaser et al. (2004) prepared ^{18}F prelabelled thiols for chemoselective alkylation with a chloroacetyl-modified peptide. The chloroacetyl function was used to chemoselectively enable the binding of the ^{18}F prosthetic group to the model peptide $ClCH_2C(O)$-

LysGlyPheGlyLys. (3-[^{18}F]fluoropropylsulfanyl)triphenylmethane, (2-{2-[2-(2-[^{18}F]fluoroethoxy)ethoxy]ethoxy}ethylsulfanyl)triphenylmethane and 4-[^{18}F]fluoromethyl-*N*-[2-triphenylmethanesulfanyl)ethyl]benzamide were prepared from the corresponding methanesulfonyl precursors. After removal of the triphenylmethane protecting group, the ^{18}F-fluorothiols were reacted with the model peptide. The decay corrected RCYs of the ^{18}F-labelled isolated peptides were 10%, 32% and 1% respectively. The method involves only two steps that involve handling ^{18}F and the peptides needed no purification. The conclusion was that using ^{18}F-fluorothiols for chemoselective labelling of peptides showed considerable potential.

Formation of an oxime bond between 4-[^{18}F]fluorobenzaldehyde and a peptide functionalised with an aminooxy-group is the basis of another chemoselective means of radiolabelling biomolecules. Coupling with the carbonyl component can be performed in aqueous media (Poethko et al, 2004a, 2004b).

Figure 1.7 An aldoxime A ketoxime

The oxime strategy meets the 1 + 1 step strategy requirement and has been successfully applied with a variety of peptides (Poethko at al 2004a and 2004b). The efficiency of the oxime bond formation with a variety of aminooxy functionalised peptides (minigastrin, RGD and octreotide) was found to be strongly dependent on pH, peptide concentration, reaction time and reaction temperature (Poethko et al 2004a). Optimal results at low peptide concentrations (0.5 mM) were obtained within 15 minutes at 60°C, pH 2-3, independent of the peptide used with a 60-80% RCY.

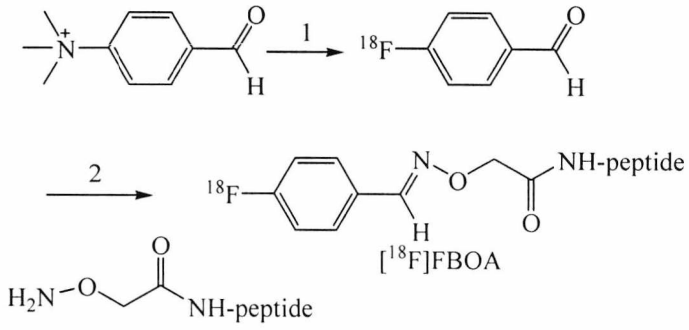

Scheme 1.7 Radiosynthesis of [^{18}F]FB-CHO and conjugation to aminooxy-functionalised peptides via oxime formation. Reaction conditions: (1) [K222]+ ^{18}F- for 15 min at 60°C in dimethylsulfoxide, followed by cartridge purification and elution with MeOH. (2) Aminooxy peptide (0.5 mmol/l) in H_2O, MeOH and trifluoroacetic acid (pH 2.5), 15 min at 60°C. [^{18}F]FBOA is *N*-(4-[^{18}F]fluorobenzylidene)oxime (Poethko et al. 2004a)

The specificity of [^{18}F]FBOA formation with the aminooxy group was investigated in an amino acid competition experiment. Cysteine, arginine, histidine, serine and lysine were incubated with [^{18}F]fluorobenzaldehyde ([^{18}F]FB-CHO) both in the presence and absence of an equimolar amount of 2-aminooxyacetic acid under conditions of 60°C for 25 minutes. In the absence of 2-aminooxyacetic acid, 15% of the [^{18}F]FB-CHO reacted to form a radiolabelled conjugate that was identified as the reaction product with cysteine. In the presence of the 2-aminooxyacetic acid, the RCY of the [^{18}F]FBOA-OH was 93% within 25 minutes in all cases demonstrating the high specificity of [^{18}F]FB-CHO for the aminooxy group. This method of labelling represents a rapid two-step, high yield method for the [^{18}F] labelling of peptides and proteins. The whole labelling process from EOB took place within thirty minutes with reasonable RCY and produced no side products. Maximum RCY occurred at between pH 2 and 4 with almost no [^{18}F]FBOA formation above pH 5. HPLC separation of the [^{18}F]FBOA labelled peptides was still necessary (Poethko et al. 2004b).

Flavell et al. (2008) have developed a two-step site specific approach for the purpose of labelling leptin, a peptide hormone, resistance to which is implicated in obesity. An aminooxy-reactive group was incorporated into the C-terminus of leptin. This was derivatised with [^{18}F]FB-CHO using an aniline-accelerated radiochemical oximation reaction. Interestingly, the use of aniline as a catalyst in this reaction has been shown to dramatically accelerate the reaction in oxime conjugations, it allows the reaction to proceed in good yield at a lower concentration of the aminooxy precursor and at lower temperature than had been described previously (Poethko et al. 2004a). The approach in this study centred on the use of

[^{18}F]FB-CHO forming an oxime bond with a cysteine residue derivatised with an aminooxy group. The total synthesis time was 120 minutes and the radiochemical purity of the protein was greater than 95%. This modified leptin molecule was shown to be biologically active.

Formation of a hydrazone bond between an aldehyde and a hydrazine group is another example of a chemoselective reaction. (Bruus-Jensen et al 2006).

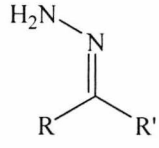

Figure 1.8 A hydrazone bond

Products with the 4-[^{18}F]fluorobenzoyl moiety have increased lipophilicity but have been used widely for labelling peptides.

Hydrazones share the optimal labelling requirements as detailed above with the oxime strategy. Hydrazone bond formation is chemoselective and highly efficient between, for example, [^{18}F]FB-CHO and a hydrazine group on a molecule such as HYNIC (6-hydrazinonicotinic acid) (Bruus-Jensen et al 2006). The chemoselectivity between the hydrazine functionalised molecule and a carbonyl compound has led to this chemistry being developed into a commonly used and highly sensitive analytical test for detection and quantification of carbonyls (Houdier et al. 1999). HYNIC derivatised peptides are already widely in use in nuclear medicine as precursors for ^{99m}Tc labelling.

Hydrazones are reasonably stable under neutral conditions and therefore should also be so *in vivo*. Hydrazones are formed and cleaved under acidic conditions. It has been suggested that after receptor mediated internalisation, hydrazone-modified peptides may possibly release their prosthetic groups, as the conditions in endosomes and lysosomes are acidic (Padilla De Jesús et al. 2002). This may increase cellular retention of radioactivity by the target cells.

Bruus-Jensen et al. (2006) investigated the chemoselectivity of the HYNIC reaction with [^{18}F]FB-CHO by designing a set of conjugation experiments in the presence and absence of the potentially competing amino acids arginine, histidine cysteine and glycine. When [^{18}F]FB-CHO was reacted with the HYNIC with no amino acids present, the reaction produced the

hydrazone in 70% radiochemical yield in 10 minutes at 90°C in aqueous buffered media containing varying amounts of organic solvent. When the same reaction was repeated with each of the amino acids above added in 5-fold excess over HYNIC (in separate reactions), there was no significant reduction in hydrazone production. Hydrazone production was shown to be temperature-dependent. Maximum yields of the HYNIC conjugated peptide [^{18}F]FB-CH=N-HYNIC-Tyr^3-Thr^8-octreotide were obtained at 65-70°C. No reactions with unprotected peptide side chains containing arginine, cysteine, histidine, lysine or serine occurred during the [^{18}F]FB-CHO labelling of the HYNIC-peptides (Bruus-Jensen et al. 2006).

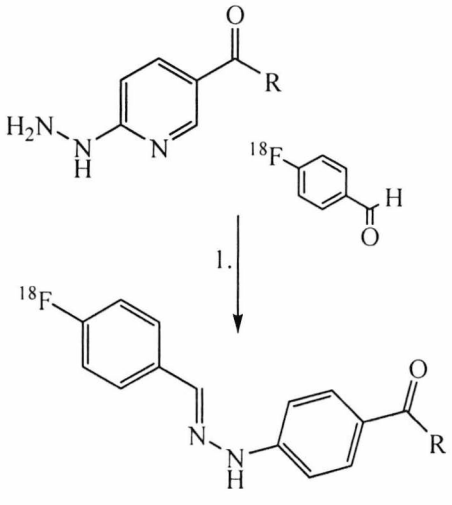

Scheme 1.8 Scheme to show the chemoselective radiofluorination reaction via hydrazone bond formation between HYNIC or a HYNIC-functionalised peptide and [^{18}F]FB-CHO.(1) MeCN/KH_2PO_4 buffer, ΔT, 10 min. R = OH, -Tyr^3-Thr^8-octreotide, -Tyr^3-Thr^8(NH_2)-octreotide, -substance-P (Bruus-Jensen et al. 2006)

Hydrazone formation was affected by pH, with the highest yields found at lower pH levels e.g. lower yields were found at pH>5.5 and this reflects the dependence of hydrazone formation on proton catalysis. The reverse is also true, that at lower pH, more hydrazone degradation is also occurring as the reaction is in equilibrium. The hydrazone bond is therefore kinetically more stable at a higher pH. The hydrazone methodology therefore represents a rapid two-step, high yielding technology that can be applied to labelling of peptides which are stable at neutral pH, including in blood (Bruus-Jensen et al. 2006). RCY was 85% in 15 minutes.

Chang et al. (2005) found that purified [^{18}F]fluorobenzaldehyde coupled to HYNIC-HSA (human serum albumin, an example of a protein that may be used *in vivo* as a blood pool imaging agent), via hydrazone formation was very stable in buffered aqueous media for 6 hours at pH 7.4 at room temperature and in human serum at 37°C. The yields obtained were 25-90%. The higher yields only being reached with high concentrations of protein (2mg/ml) and high reaction temperatures (50-60°C) and long reaction times (20-30 minutes) (Chang et al 2005). Biodistribution studies in mice showed no significant effects on the biological properties of the HSA after introduction of HYNIC as a bifunctional chelating agent. Chang et al. (2005) found that the hydrazone formation methodology used here was more favourable than the oxime methodology as HYNIC has already been verified as a bifunctional chelating agent for use with ^{99m}Tc, giving the advantages already mentioned of uniting labelling technology for SPECT and PET. It is mentioned also that while the use of thiol containing (Glaser et al. 2004) and thiol reactive ^{18}F labelling synthons (Toyokuni et al. 2003) may show high labelling efficiencies, highly reactive and unstable thiols have the ability to cause storage and preparation problems.

Lee et al. (2006) labelled the $\alpha_v\beta_3$ integrin binding peptide (RGD or Arg-Gly-Asp peptide) via hydrazone bond formation between c(RGDyK)-HYNIC and [^{18}F]FB-CHO. The peptide RGDyK is a cyclic peptide containing the residues y (D-tyrosine), an unnatural amino acid and K (lysine) as well as RGD. Conjugation efficiency was again found to be affected by pH. The highest conjugation efficiency was found at pH 4.5 (95% efficiency) with efficiencies being 10% less at other pH values. Conjugation efficiency was also dependent on the stoichiometric amount of the peptide, which was greatest when the peptide was present in the biggest excess. It was also dependent on temperature, with higher conjugation efficiencies being found at high temperatures (room temperature 85.4%, 50°C 95.6% and 90°C 93.1%). The optimal conditions for conjugation were therefore pH 4.5 at 50°C for 20 minutes using excess peptide. The decay corrected RCY was 15.4% and the total synthesis time from EOB was 90 minutes. The specific activity was found to be 20.5 GBq/μmol at the end of synthesis. The study also indicated that binding of [^{18}F]RGDyK to the mouse model of ischaemic muscle occurred and was specific.

Rennen et al. (2007) report the use of HYNIC as a bifunctional chelating agent in the [^{18}F] fluorination of a non-peptide compound; LTB4. The LTB4 receptor is expressed on polymorphonuclear granulocytes and is involved in leukocyte function during the

inflammatory response. [^{18}F]-MB67 (MB67 is an antagonist of LTB4) was stable in PBS at 37°C for at least 4 hours. It was synthesised with a specific activity of 1200 GBq/mmol, 65-85% RCY. The [^{18}F]-MB67 was compared to [^{99m}Tc]-MB67 (both synthesised using HYNIC) *in vivo*. There were some similarities between the metabolism of both compounds, but also some differences. There was lower uptake in the abscess and spleen of [^{18}F]-MB67, thought to be due to some physicochemical differences between the two compounds, which may reduce the ability of [^{18}F]-MB67 to bind to its receptors on neutrophils. In [^{18}F]-MB67, the prosthetic group is uncharged, whereas with [^{99m}Tc]-MB67, the ^{99m}Tc core with surrounding coligands is charged. The lipophilicity of a biomolecule is increased by the addition of another benzyl group which can affect the biological properties of the molecule as was seen for [^{18}F]FB-octreotide (Bruus-Jensen et al. 2006). It was found that although specific abscess uptake was shown the relatively low specific activity of the [^{18}F]-MB67 may limit this approach to labelling.

Shao and Tam (1995) found that the hydrazone bond containing peptide [^{18}F] FB-CH=N-HYNIC-TOCam showed rapid release of [^{18}F]fluorobenzaldehyde. At pH 4, 65% and at pH 7, 87% of the intact labelled peptide was detected after 5 hours. The lower stability of the intact peptide in acidic media does not have a significant effect on the pharmacokinetics. Shao and Tam (1995) also found that the oxime bond was more stable in aqueous media than the hydrazone bond. The oxime bond was stable in the pH range 3-7 over 24 hours and was only slightly degraded at pH 9 (21% of compound degraded) (Shao and Tam 1995).

In summary, hydrazone bond formation is as efficient as oxime formation. Both the oxime and the hydrazone conjugation methods are rapid, show good RCYs (85% in 15 minutes), work at room temperature, produce peptides relatively stable at neutral pH and can be carried out in aqueous media in a 1 + 1 manner. An advantage of the hydrazone methodology over the oxime methodology is that as HYNIC is already used as a bifunctional chelating agent for labelling peptides with ^{99m}Tc, it would be advantageous to use the same methodology for labelling with ^{18}F as the same precursors could be used for both SPECT and PET (Bruus-Jensen et al. 2006).

1.6.2 Examples of peptides used in PET

The application of radiolabelled small bioactive peptides for diagnostic imaging is rapidly gaining importance in nuclear medicine (Okarvi 1999). Traditionally, imaging agents were large proteins (polyclonal antibodies with low specificity), then became smaller monoclonal antibodies and fragments with relatively high specificity, and eventually became even smaller molecular recognition units such as single-chain antigen binding domain fragments, and finally to receptor specific regulatory peptides (Okarvi 2001).

At the moment, there are not many peptides used in clinical PET. The peptides investigated are limited to analogues of peptides such as somatostatin, gastrin, neurotensin or RGD-peptides (see table 1.1). RGD-peptides are cyclic pentapeptides containing an Arg-Gly-Asp sequence. The somatostatin receptor ligand, octreotide, was the first clinically relevant peptide to be labelled with 4-nitrophenyl 2-[^{18}F]fluoropropionate (Guhlke et al 1994). Cyclic peptapeptides (such as the RGD peptide) bind with high affinity to $\alpha_v\beta_3$ integrins and have been proposed as tracers for determination of integrin status to help quantify angiogenic processes. (Wester and Schottelius 2007). Below is a table with some of the peptides presently used in PET and their characteristics.

Regulatory Peptide	No. of amino acid residues	Receptor Type (subtypes)	*In vivo* activity
SST (somatostatin)	14	SST receptors (sst1-5)	Inhibition of hormone and exocrine secretion
BN/GRP (bombesin/gastrin releasing peptide	14	BN/GRP receptors (GRP, NMB, BRS-3)	Gut hormone release, regulation of exocrine secretion
VIP (vasoactive intestinal peptide)	28	VIP receptors (-)	Vasodilation, water and electrolyte secretion in the gut
RGD-containing peptides	-	GPIIb/IIIa/platelet and vitronectin/integrin receptors	Inhibition of adhesive and aggregatory functions of platelets
α-MSH (α-melanocyte stimulating hormone)	13	α-MSH receptors (-)	Melanogenesis
NT (neurotensin)	13	NT receptors (NT1-3)	Vasoconstriction, regulation of cardiac activity, raise in vascular permeability
SP (substance P)	11	SP receptors (NK1)	Hypotension, salivary gland secretion, transmission of pain

Table 1.1 General characteristics of selected peptides for comparison (Fichna and Janecka 2003)

The $\alpha_v\beta_3$ integrin is one that is expressed in several cancers and is upregulated in tumour vasculature. (Haubner et al. 1999). Integrins are glycoproteins expressed on most cells with a nucleus. They are essential adhesion molecules in many biological processes including cell growth, tissue development, platelet aggregation, inflammation, wound healing and tumour metastases. Peptides and proteins with the RGD sequence are ligands for the $\alpha_v\beta_3$ integrin,

such as Von Willebrand factor, thrombospondin, fibrinogen, osteopontin and collagen. It is expressed on melanoma cells, glioblastoma cells, smooth muscle cells, endothelial cells, fibroblasts and osteoclasts. The $\alpha_v\beta_3$ integrin is involved in cell growth promotion, inhibition of apoptosis, increased protease production, promotion of tumour cell invasion, especially melanoma and glioblastoma. It is potentially involved in angiogenesis and therefore of importance in tumour growth. RGD cyclic pentapeptides have been used as antagonists for RGD-directed integrins. Humphries et al. (1986) demonstrated that it was possible to prevent melanoma metastasis by co-injection of RGD peptide with the tumour cells, possibly because of competition with the integrins for binding sites. The RGD peptide has been shown to induce apoptosis of angiogenic blood vessels *in vivo* (Brooks et al. 1994).

Somatostatin is a fourteen amino acid peptide. It has a biological half-life of a few minutes. Indeed, the drawback of labelled peptides for imaging is that they often have a short plasma half-life because they are sensitive to proteolysis. To improve *in vivo* stability somatostatin has been shortened to an eight amino acid sequence, two D amino acids have been incorporated, one at the *N*-terminal, and the *C*-terminal has been made into an alcohol to give the peptide octreotide. Octreotide, an octapeptide, has a biological half-life of about 2 hours and has been used in SPECT with ^{99m}Tc, ^{111}In, and ^{123}I (Heppeler et al. 2000 abstract). Cancer cells quite often express cell-signalling receptors for proteins such as somatostatin. Somatostatin is a neuropeptide which acts on the pituitary gland to inhibit the secretion of growth hormone. In fact, most human neuroendocrine tumours originating from tissue upon which somatostatin acts, have preserved their somatostatin receptors. Examples include carcinoid tumours, small cell carcinomas and paragangliomas. Small peptide analogues of proteins, such as octreotide, can be synthesized by solid phase synthesis and then radiolabelled with ^{18}F. When this is injected into a patient for imaging purposes, the peptide will bind to receptors specific for somatostatin and they therefore act as markers for imaging tumours.

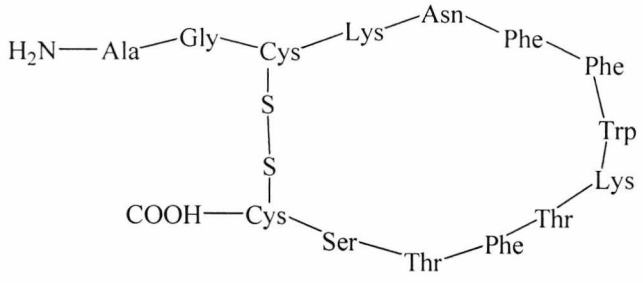

Figure 1.9 Somatostatin; a fourteen amino acid neuropeptide

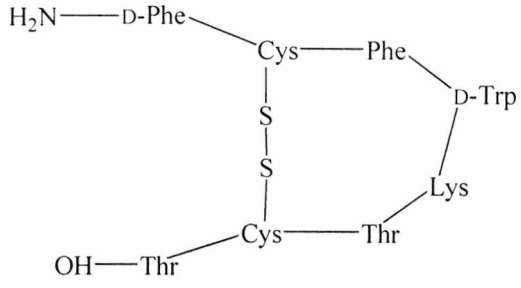

Figure 1.10 The analogue of somatostatin; octreotide

Somatostatin analogue peptides have been used successfully in therapy as well as in imaging. Peptide-receptor radionuclide therapy in neuroendocrine tumour patients with radiolabelled somatostatin analogues has resulted in symptomatic improvement, prolonged survival and enhanced quality of life. The side effects of this type of therapy are few and mostly mild, especially when using kidney protective agents. If peptide-receptor therapy was to become more widespread, it could be the first treatment choice for patients with metastasised or inoperable tumours (de Visser et al. 2008).

Gastrin is a linear peptide hormone produced by the G cells of the duodenum and the pyloric antrum of the stomach. In Zollinger-Ellison syndrome, gastrin is produced at excessive levels, often by a gastrinoma (gastrin producing tumour; mostly benign) of the pyloric antrum or the pancreas. CCK-2 is a human protein receptor for CCK and gastrin which are regulatory peptides of the brain and gastrointestinal (GI) tract (Mather et al. 2007). Gastrin is discussed in greater detail in the introduction to chapter 4 as a shortened analogue of gastrin is the peptide used for radiolabelling in this project.

Annexin V is a cytoplasmic protein that is useful in detecting cell apoptosis by binding to phosphatidylserine which is exposed on the outer surface of cells during the apoptotic process. Apoptosis is programmed cell death and is such an essential process that when it is dysregulated, it can lead to cancer and neurodegenerative disorders (Johnstone et al. 2002). Many anti-cancer therapies work by induction of apoptosis in tumour cells. This protein has been used successfully for synthesis of [^{18}F] labelled annexin V (Li et al. 2008).

Bombesin is a 14 amino acid peptide originally isolated from frog skin. Its mammalian equivalent is the 27 amino acid peptide GRP (gastrin releasing peptide) (Moody et al. 1985). Receptors are expressed in the central nervous system (CNS) and peripheral tissue such as the pancreas or GI tract. The receptors are found on lung, prostate, breast, gastric, colon and pancreatic tumours. Since bombesin/GRP peptides are mostly autocrine growth factors, inhibiting the peptide from reaching its receptor would result in prevention of tumour growth (Breeman et al 1999).

Vasoactive intestinal peptide (VIP) is a 28 amino acid neuroendocrine mediator. It is one of the inhibitory neurotransmitters in the gut (Brechbiel and Gansow 1991). VIP receptors are expressed on CNS and pancreatic tissues along with adenocarcinomas (Fichna and Janecka 2003).

Labelled analogues of the tridecapeptide α-Melanocyte stimulating hormone are used for melanoma tumour imaging. Receptors for α-MSH are over expressed on melanoma cells (Tatro et al. 1990).

Neurotensin is a 13 amino acid neurotransmitter in the CNS. It is also a local hormone that stimulates growth. Analogues of neurotensin are used for detecting pancreatic, prostate, lung or colon carcinomas and meningiomas (Fichna and Janecka 2003).

Substance P is an 11 amino acid neuromodulator and neurotransmitter which is over expressed in breast, thyroid and glial tumours (Hennig et al. 1995).

Multimers of peptides, as opposed to the monomer or dimer have shown improved imaging (Poethko etal 2004b). Tumour uptake and tumour to organ ratios increased in the series monomer < dimer < tetramer.

From the above discussion on peptides in PET, it can be seen that their increased use in nuclear medicine would give excellent scope for maximising the potential of PET. The current practice for labelling peptides with ^{18}F consists of first labelling the prosthetic group, a multiple step procedure, which is subsequently incorporated into the peptide or protein, followed by a purification step. A kit based approach to the preparation of ^{18}F peptides for PET, possibly based on one of the chemoselective methods of labelling discussed above, would be commercially attractive and therefore beneficial to the patient because it would make production simpler and novel imaging methods accessible to a wider market, in the same way that the widespread use of gamma camera imaging has been made possible by the use of the ^{99m}Tc kit.

1.7 Radiohalogens in imaging and therapy

Mainly it is the radionuclides ^{18}F, ^{15}O, ^{13}N, ^{11}C with short half-lives that are used in PET centres. However, there are many other radionuclides that have applications or potential applications in imaging or radiotherapy.

A brief overview of the halogens bromine, iodine and astatine with regard to their applications in nuclear medicine will be given here.

There are 23 radionuclides of bromine in addition to the two stable isotopes (^{79}Br and ^{81}Br), 34 radionuclides of iodine in addition to the stable ^{127}I and 31 radionuclides of astatine with no stable nuclides. (Adam and Wilbur 2004).

Radiohalogen	Half-life	Type of emission	Application
^{18}F	109.7 m	β^+	PET Imaging
^{122}I	3.6 m	β^+	PET Imaging
^{123}I	13.2 h	γ	SPECT Imaging
^{124}I	4.2 d	β^+	PET Imaging
^{125}I	59.4 d	Auger e^-	Therapy
^{131}I	8.0 d	β^-	Therapy
^{75}Br	97 m	β^+	PET Imaging
^{76}Br	16.2 h	β^+	PET Imaging
^{77}Br	57.0 h	Auger e^-	Therapy
^{211}At	7.2 h	α	Therapy

Table 1.2 Radiohalogens used in imaging and therapy, including ^{18}F for comparison (Adam and Wilbur 2004)

The radionuclides above have relatively short half-lives and have high theoretical specific activity.

^{75}Br has a half-life of 97 minutes. It has higher positron energy than ^{18}F and decays only 71% by positron emission which contributes to the resolution being less satisfactory than for ^{18}F (Adam and Wilbur 2004).

^{76}Br has a half-life of 16.2 hours and is used as an imaging agent. It again suffers in comparison to ^{18}F in terms of resolution as it decays only 54% by positron energy (Adam and Wilbur 2004).

^{77}Br has a half-life of 57 hours and decays partially by Auger electron emission. Due to its limited availability as well as its two higher energy gamma rays and low percent positron energy (1%), it is less desirable as a PET or SPECT nuclide (Adam and Wilbur 2004). Bromine nuclides can be incorporated into steroids (Downer et al 2001). Antisense ligand

nucleotides have been labelled with ^{76}Br (Wu et al 2000, 2004). Brominated antibodies have been made and their biodistribution has been compared to other halogenated antibodies (Orlova et al 2002, Winberg et al 2004).

Radiobromine labelled molecules are appealing as the chemistry is more easily carried out than fluorine chemistry. The carbon-bromine bond is stronger than the carbon-iodine bond and the bromine atom is smaller than the iodine atom. Bromine radionuclides are not as available as iodine radionuclides, they can be produced on a cyclotron but their targets and isotope extraction procedures are complicated. They are not widely used because of this. (Adam and Wilbur 2004).

^{122}I is a positron emitting halogen. It has favourable imaging properties, but a very short half-life of 3.6 minutes. The very short half-life makes it difficult to carry out complex organic chemistry. It can be used for imaging blood flow, but not for any long physiological process. It therefore has limited use. (Adam and Wilbur 2004).

^{123}I is a SPECT radionuclide that is available commercially and widely used. It has very good imaging properties and a reasonable half-life of 13.2 hours (Adam and Wilbur 2004).

^{124}I is a positron emitting nuclide with a relatively long half-life of 4.18 days. It has both imaging and therapeutic potential. An androgen radiolabelled with ^{124}I has been described (Downer et al 2001). Both iodine and bromine radionuclides make possible long-lasting steroid hormones for both therapy and imaging.

^{125}I is an Auger electron emitting radionuclide. 5-[^{125}I]iodo-2'-deoxyuridine has been administered and incorporated into growing cancer cells. [^{125}I]iodo-2'-deoxyuridine is incorporated into the DNA and kills the cell (Kassis et al.1998).

The decay of ^{131}I is β^- decay accompanied by x-rays and γ-rays ranging in energy from 80 to 723 keV (Gansow 1991). Radioisotope therapy is targeted therapy, for example, radioiodine in the form of ^{131}I is absorbed specifically by the thyroid gland. This is used as treatment for thyroid cancer or thyrotoxicosis and is the most commonly used radiohalogen in therapy (Adam and Wilbur 2004). ^{131}I is undesirable for imaging because of its long half life (8.05 d), cytotoxic β^- radiation and also because of the image background associated with the higher energy γ-rays. ^{131}I has been used with antibodies in animals and humans for therapy with only modest success, possibly because of the low energy of the β^- emission. Deiodination of the

antibodies may occur and lead to uptake in the gut and thyroid, delivering non-specific radiation doses (Gansow 1991).

An advantage of iodine over fluorine is that iodide is easily oxidised to an electrophilic form of iodine. It can be used in electrophilic chemistry without having to add carrier iodine. A disadvantage of radiolabelling with iodine is that the carbon-iodine bond is less stable to cleavage *in vivo*. Aromatic C-I bonds are more stable than aliphatic C-I bonds.

Labelling organic molecules with astatine usually follows the same procedures for labelling with iodine. The carbon-astatine bond stability is lower than the carbon-iodine bond. This causes problems when labelling proteins directly with ^{211}At, a procedure which is possible with iodine. Methods for introducing ^{211}At labelled aromatic compounds that could be conjugated to a protein have been developed (Wilbur 1992). The most commonly used reagents for ^{211}At labelling of proteins are the *para*astatobenzoate *N*-hydroxysuccinimide ester [^{211}At]PAB (Wilbur et al. 1989) and the *meta*astatobenzoate *N*-hydroxysuccinimide ester [^{211}At]ATE (Zalutsky and Narula 1988) shown below.

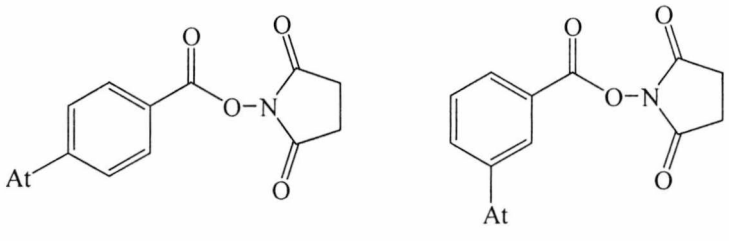

Figure 1.11 [^{211}At]PAB and [^{211}At]ATE

These reagents have been shown to be stable to deastatination on slowly metabolised proteins, such as monoclonal antibodies (MW ~ 150 kDa), but not on smaller Fab' fragments (MW ~ 50 kDa). Due to the *in vivo* instability limiting the use of ^{211}At and also because it is a highly desirable potential therapy radionuclide, it is an area of active research (Adam and Wilbur 2004).

1.8 Boron and silicon as binding sites for fluorine.

The use of boron and silicon as binding sites for fluorine instead of the more conventional carbon is an area relatively few groups have researched (Schirrmacher et al. 2007). The first use of silicon for radiolabelling with ^{18}F dates back to 1985 when Rosenthal et al. (1985)

radiolabelled chlorotrimethylsilane with ^{18}F in aqueous acetonitrile to yield the corresponding Si-^{18}F compound in 65% RCY. However, *in vivo*, the Si-^{18}F compound hydrolysed quickly to give the silanol. When [^{18}F]fluorotrimethylsilane was inhaled by rats, most of the radioactivity was found in the bones of the rats due to the fast hydrolysis of the Si-^{18}F bond. Unbound ^{18}F is always metabolised to the bone structure *in vivo*. In this paper Rosenthal suggested the use of more sterically hindered Si-^{18}F compounds to try and avoid the problem of hydrolysis *in vivo*. More recently than this Ting et al. (2005), labelled the compounds *p*-aminophenylboronylpinacolate and (aminopropyl)triethoxysilane for targeting the protein avidin to determine ^{18}F incorporation into these compounds. The expected trifluoroborate and tetrafluorosilicate compounds were formed after treatment with cold fluoride. This translated well to labelling with ^{18}F and the labelling efficiency was found to be very high at 80-100%. In aqueous buffer, the [^{18}F]-trifluoroborate was found not to decompose at all and the [^{18}F]-tetrafluorosilicate was reasonably stable with a rate constant of hydrolysis of 0.01 min^{-1}. In serum or whole blood, no drop in ^{18}F radioactivity was observed. A very positive point about this methodology is that the ^{18}F chemistry works well under aqueous conditions (Schirrmacher et al. 2007).

Another approach to labelling utilising the Si-^{18}F bond has been named SiFA which is an abbreviation for **Si**licon-**F**luoride-**A**cceptor. This approach operates via isotopic exchange of ^{19}F for ^{18}F. When $^{18}F^-$ in acetonitrile was added to nanomolar quantities of di-*tert*-butyl-phenyl-fluorosilane, the isotopic exchange was very efficient, taking place within 15 minutes at room temperature with high RCY. A SiFA compound has a silicon core, two tert-butyl groups and a phenyl system that is amenable to modifications for chemoligation (Schirrmacher et al. 2007). RCYs of 80-95% have been possible using this approach (Haka et al. 1989). This chemistry has been applied to chemoselectively labelling a peptide via the use of an aminooxy functionality with a SiFA derivatised with an aromatic aldehyde (Poethko et al. 2004a). This produced a stable product and this methodology was then applied to an aminoxy peptide Tyr^3-octreotate which was coupled to *p*-(di-*tert*-butylfluorosilyl)benzaldehyde. The peptide was labelled with ^{18}F in RCYs of 95-97% after 10-15 minutes at room temperature. No HPLC purification of the labelled peptide was necessary as purification could be achieved using solid phase extraction. The drawbacks are that the specific activity of the labelled peptide was too low for imaging and that the

introduction of SiFA compounds increases the lipophilicity of the labelled peptide, which may alter its metabolism *in vivo*.

Ting et al (2008) researched the use of an arylboronic acid ester functionality as a chemoselective captor of aqueous [^{18}F]fluoride to give an aryltrifluoroborate anion labelled with [^{18}F] ($ArBF_3^-$). An electron-withdrawing substituent or a protonated species which can be involved in hydrogen bonding enhances the reactivity of arylboronic acid with fluoride. The approach of Ting et al. (2008) used carrier [^{19}F]fluoride to favour the synthesis of $ArBF_3$. Biotin was used as the biomolecule for imaging in this study. Biotin has a very high affinity for the protein avidin. The study demonstrated that [^{18}F]trifluoroborate was stable *in vivo*, stating that biotinyl-ArB[^{18}F][^{19}F]$_2^-$ appeared to be metabolised as a stable non-coordinating anion with no accumulation of free [^{18}F]fluoride in the bone. This demonstrates the stability of the C-B and the B-F bonds *in vivo*. The $ArBF_3^-$ cleared very quickly from the body which could be problematic, as the radiopharmaceutical needs to have enough time to reach its target, on the other hand, the remaining unbound radiopharmaceutical needs to clear quickly enough to give a high signal-to-noise ratio. The work done in this study validates the claims that boronic esters are potentially useful as readily labelled precursors for PET imaging (Ting et al. 2008). The use of boronic esters to capture [^{18}F]fluoride would be a one step method of labelling a biomolecule rather than the more conventional C-F bond chemistry that uses a 1 + 1 labelling approach at best.

1.9 Aims and objectives

Two strategies were evaluated:

1.9.1 Use of a metal as a fluoride binding site. The aim of the work undertaken for this strategy was to develop a novel one step labelling strategy to introduce ^{18}F into peptides using a metal as a binding site for ^{18}F. The inspiration for this idea came from the affinity that boron has for fluorine which has been exploited using boron as a binding site for fluorine in radiolabelling with ^{18}F. By extrapolation of this idea, a metal with a high affinity for fluorine could be used in a similar way. A chelated metal could be incorporated into a peptide and used as a site specific binding site for ^{18}F. This approach using a metal (ruthenium) chelated to EDTA was investigated. In order that this thesis is presented in a clear and logical

manner, the ruthenium work has been separated and is contained, along with the introduction to this work, in chapter 5 (the last chapter).

1.9.2 Use of hydrazone bond formation. The hydrazone route was applied with the aim still being to decrease the number of steps necessary to incorporate ^{18}F into a peptide. A thorough investigation into the chemoselectivity of the hydrazine functionalised compound HYBA for an aldehyde followed. HYNIC has been used extensively for radiolabelling with ^{99m}Tc for SPECT. For ^{99m}Tc, HYNIC is preferable as a bifunctional chelating agent to HYBA for reasons of stability (King et al. 2007). However for labelling with ^{18}F, there are no stability issues when using HYBA and using HYBA is a more cost effective way of radiolabelling peptides. Use of HYBA may also be preferential to HYNIC because of having no nearby acid/base catalyst (the pyridine nitrogen). A new amino acid derivative Fmoc-Lys-HYBA-Boc was synthesised to be attached to a peptide and then radiolabelled in a 1 + 1 strategy. Gastrin analogue peptides were the peptides used for radiolabelling and the radiolabelling of these peptides was to be carried out via a chemoselective strategy utilising hydrazone bond formation using HYBA and also HYNIC for comparison.

References

Adam MJ, Wilbur DS (2004). Radiohalogens for imaging and therapy. *Chemical Society Review* **34**, 153-163.

Appukkuttan P, Dehaen W, Fokin VV, et al. (2004). A microwave-assisted click chemistry synthesis of 1,4-disubstituted 1,2,3-triazoles via a copper(I)-catalyzed three-component reaction. *Organic Letters* **6,** 4223-4225.

Atkins HL, Christmann DR, Fowler JS, Hauser W, Hoyte RM, Kloper JF, Lin SS, Wolfe AP (1972). Organic radiopharmaceuticals labelled with of short half-life. V. ^{18}F labelled 5- and 6-fluorotryptophan. *Journal of Nuclear Medicine* **13**, 713-719.

Bakker WH, Albert R, Bruns C, et al. (1991). [In-111]-DTPA-D-Phe-octreotide, a potential radiopharmaceutical for imaging of somatostatin receptor positive tumours. *Life Science* **49**, 1583-1591.

Balz G, Schiemann G (1927). Uber aromatische Fluorverbindungen, I.: Ein neues Verfahren zu ihrer Darstellung. *Chemische Berichte* **60**, 1186-1190.

Block D, Coenen HH, Stocklin G (1988). NCA F-18-Fluoroacylation via fluorocarboxylic acid esters. *Journal of Labelled Compounds and Radiopharmaceuticals* **25**, 185-200.

Block D, Klatte B, Knochel A, Beckmann R, Holm U (1986). NCA [F-18] labelling of aliphatic-compounds in high yields via aminopolyether-supported nucleophilic substitution. *Journal of Labelled Compounds and Radiopharmaceuticals* **23**, 467-477.

Blok D, Feitsma RIJ, Vermeij P, Pauwels EKJ (1999). Peptide radiopharmaceuticals in nuclear medicine. *European Journal of Nuclear Medicine* **26**, 1511-1519.

Bock VD, Hiemstra H, van Maarseveen JH (2006). Cu-I-catalyzed alkyne-azide "click" cycloadditions from a mechanistic and synthetic perspective. *European Journal of Organic Chemistry* **1**, 51-68.

Brechbiel MW, Gansow OA (1991). Backbone substituted DTPA ligands for 90Y radioimmunotherapy. *Bioconjugate Chemistry* **2**, 187-194.

Breeman WA, Hofland LJ, de Jong M, Bernard B, Srinivasan A, Kwekkeboom DJ, Visser T, Krenning EP (1999). Evaluation of radiolabelled bombesin analogues for receptor-targeted scintigraphy and radiotherapy. *International Journal of Cancer* **81**, 658-665.

Brooks PC, Montgomery AMP, Rosenfeld M, Reisfeld, RA, Hu T, Klier G, Cheresh DA (1994). Integrin alpha(V)Beta(3) antagonists promote tumour regression by inducing apoptosis of angiogenic blood-vessels. *Cell* **79**, 1157-1164.

Bruus-Jensen K, Poethko T, Schottelius M, Hauser A, Schwaiger M, Wester HJ (2006). Chemoselective hydrazone formation between HYNIC-functionalized peptides and ^{18}F-fluorinated aldehydes. *Nuclear Medicine and Biology* **33**, 173-183.

Chang YS, Jeong JM, Lee YS, Kim HW, Rai GB, Lee SJ, Lee DS, Chung JK, Lee MC (2005). Preparation of ^{18}F-human serum albumin: a simple and efficient protein labelling method with ^{18}F using a hydrazone-formation method. *Bioconjugate Chemistry* **16**, 1329-1333.

Coenen HH (2007). Fluorine-18 labelling methods: Features and possibilities of basic reations. *PET Chemistry the Driving Force in Molecular Imaging*. Chapter 2. Schubiger PA, Lehmann L, Friebe M (editors). Springer-Verlag Berlin Heidelberg 2007.

Coenen HH, Klatte B, Knochel A, Schuller M, Stocklin G (1986). Preparation of n.c.a. [17-^{18}F]-fluoroheptadecanoic acid in high yields via aminopolyether supported, nucleophilic fluorination. *Journal of labelled compounds and radiopharmaceuticals* **23**, 455-467.

Conti PS, Lilien DL, Hawley K, Keppler J, Grafton ST, Bading JR (1996). PET and [^{18}F]-FDG in Oncology: A clinical update. *Nuclear Medicine and Biology* **23**, 717-735.

Couturier O, Luxen A, Chatel J-F, Vuillez J-P, Rigo P, Hustins R (2004). Fluorinated tracers for imaging cancer with positron emission tomography. *European Journal of Nuclear Medicine* **31**, 1182-1206.

Deng H, Cobb SL, Gee AD, et al. (2006) Fluorinase mediated C-F-18 bond formation, an enzymatic tool for PET labelling. *Chemical Communications* **6,** 652-654.

Dolle F (2005). Fluorine-18-labelled fluoropyridines: advances in radiopharmaceutical design. *Current Pharmaceutical Design* **11**, 3221-3235.

Dolle F (2007). [^{18}F]fluoropyridines: From conventional radiotracers to the labelling of macromolecules such as proteins and oligonucliotides. *PET Chemistry the Driving Force in Molecular Imaging*. Chapter 5. Schubiger PA, Lehmann L, Friebe M (editors). Springer-Verlag Berlin Heidelberg 2007.

Downer JB, Jones LA, Engelbach JA, Lich LL, Mao W, Carlson KE, Katzenellenbogen JA, Welch MJ (2001). Comparsison of animal models for the evaluation of radiolabelled androgens. *Nuclear Medicine and Biology* **28**, 613-626.

Fichna J and Janecka A (2003). Synthesis of target-specific radiolabelled peptides for diagnostic imaging. *Bioconjugate Chemistry* **14**, 3-17.

Fischman AJ, Babich JW, Strauss HW (1993). A ticket to ride: peptide radiopharmaceuticals. *Journal of Nuclear Medicine* **34**, 2253-2263.

Flavell RR, Kothari P, Bar-Dagan M, Synan M, Vallabhajosula, Friedman JM, Muir TW, Ceccarini G (2008). Site-specific ^{18}F-labelling of the protein hormones leptin using a general two-step ligation procedure. *Journal of the American Chemical Society* **130**, 9106-9112.

Gansow OA (1991). Newer approaches to the radiolabelling of monoclonal antibodies by the use of metal chelates. *Nuclear Medicine and Biology* **18**, 369-381.

Garin-Chesa P, Campbell I, Saigo PE, Lewis JL Jr, Old LJ, Rettig WJ (1993). Trophblast and ovarian cancer antigen LK26. Selectivity and specificity in immunopathology and molecular identification as a folate-binding protein. *American Journal of Pathology* **142**, 557-567.

Glaser M, Karlsen H, Solbakken M, Arukwe J, Brady F, Luthra SK, Cuthbertson A (2004). ^{18}F-fluorothiols: a new approach to label peptides chemoselectively as potential tracers for positron emission tomography. *Bioconjugate Chemistry* **15**, 1447-1453.

Guhlke S, Wester H-J, Bruns C, Stocklin G (1994). (2-[^{18}F]fluoropropionyl-($_{D}$)phe^{1})-octreotide; a potential radiopharmaceutical for quantitative somatostatin receptor imaging with PET: Synthesis, radiolabeling, *in vitro* validation and biodistribution in mice. *Nuclear Medicine and Biology* **21**, 819-825.

Guo M, Sun H, McArdle HJ, Gambling L, Sadler PJ (2000). Ti(IV) uptake and release by human serum transferrin and recognition of Ti(IV)-transferrin by cancer cells: understanding the mechanism of action of the anticancer drug titanocene dichloride. *Biochemistry* **39**, 10023-10033.

Haka MS, Kilbourne MR, Watkins GL et al. (1989). Aryltrifluoromethanesulfonates as precursors to aryl [F-18] fluorides-improved synthesis of [F-18] GBR-13119. *Journal of Labelled Compounds & Radiopharmaceuticals* **27**, 823-833.

Haubner R, Gratias R, Diefenbach B, Goodman SL, Jonczyk A, Kessler H (1996). Structural and functional aspects of RGD-containing cyclic pentapeptides as highly potent and selective integrin alpha(v)beta(3) antagonists. *Journal of the American Chemical Society* **118**, 7461-7472.

Haubner R, Wester HJ, Mang C, Senekowitsch-Schmidtke R, Kessler H, Schwaiger H (2000). Synthesis and first evaluation of a [F-18]SAA-labelled RGD-peptide for monitoring the alpha(v)beta(3) integrin expression. *Journal of Nuclear Medicine* **41**, 162.

Haubner R, Wester HJ, Reuning U, Senekowitsch-Schmidtke R, Diefenbach B, Kessler H, Stocklin G, Schwaiger M (1999). Radiolabelled alpha(v)beta(3) integrin antagonists: A new class of tracers for tumour targeting. *Journal of Nuclear Medicine* **40**, 1061-1071.

Hendry GO, Straatmann MG, Carroll, LR, Ramsey FA, Wieland B (1986). Design and Performance of a small clinical cyclotron. *Journal of Nuclear Medicine* **27**, 1018.

Hennig IM, Laissue JA, Horisberger U, Reubi JC (1995). Substance-P receptors in human primary neoplasms: tumoural and vascular localisation. *International Journal of Cancer* **61**, 786-792.

Heppeler A, Froidevaux S, Eberle AN, Maecke HR (2000). Receptor targeting for tumour localisation and therapy with radiopeptides. *Current Medicinal Chemistry* **7**, 971-994.

Hicks RJ (2005). The role of PET in monitoring therapy. *Cancer Imaging* **5**, 51-57.

Houdier S, Legrand M, Boturyn D, Croze S, Defranq E, Lhomme J (1999). A new fluorescent probe for sensitive detection of carbonyl compounds. *Analytica Chimica Acta* **382**, 253-256.

Humphries MJ, Olden K, Yamada KM (1986). A synthetic peptide from fibronectin inhibits experimental metastasis of murine melanoma cells. *Science* **233**, 467-470.

Inoue T. Koyama K, Oriuchi N, Alyafei S, Yuan Z, Suzuki H (2001). Detection of malignant tumours: Whole-body PET with fluorine 18 α-methyl-tyrosine versus FDG-preliminary study. *Radiology* **220**, 54-62.

IUPAC Compendium of Chemical Terminology (1997). 2nd Edition

Johnstone RW, Ruefli AA, Lowe SW (2002). Apoptosis: a link between cancer genetics and chemotherapy. *Cell* **108**, 153-164.

Kassis AI, Adelstein SJ, Haydock S, Sastry KSR, McElvany KD, Welch MJ (1982). Lethality of Auger electrons from the decay of bromine-77 in the DNA of mammalian cells. *Radiation Research* **90**, 362-373.

Kassis AI, Wen PY, Van den Abbeele AD, Baraowska-Kortylewicz J, Makrigiorgos GM, Metz KR, Matalka KZ, Cook CU, Sahu SK, Black PM, Adelstein SJ (1998). 5-[I-125]iodo-2'-deoxyuridine in the radiotherapy of brain tumours in rats. *Journal of Nuclear Medicine*. **39**, 1148-1154.

Kilbourn MS, Dence CS, Welch MJ, Mathias CJ (1987). Fluorine-18 labeling of proteins. *Journal of Nuclear Medicine* **28**, 462-470.

Kim DW, Ahn DS, Oh YH, et al. (2006). A new class of S(N)2 reactions catalyzed by protic solvents: Facile fluorination for isotopic labeling of diagnostic molecules. *Journal of the American Chemical Society* **128**, 16394-16397.

King RC, Surfraz MB-U, Biagini SCG, Blower PJ, Mather SJ (2007). How do HYNIC-conjugated peptides bind technetium? Insights from LC-MS and stability studies. *Dalton Transactions* 4998-5007.

Kluetz PG, Meltzer CC, Villemange VL, Kinahan PE, Chandler S, Martinelli MA, Townsend DW (2000). Combined PET/CT imaging in oncology: Impact on patient management. *Clinical Positron Imaging*, **3**, 223-230.

Koepf-Maier P, Preiss F, Marx T, Klapoetke T, Koepf H (1986). Tumour inhibition by titanocene complexes: activity against sarcoma 180. *Anticancer Research* **6**, 33-37.

Kwekkeboom D, Krenning EP, de Jong M (2000). Peptide receptor imaging and therapy. *Journal of Nuclear Medicine* **41**, 1704-1713.

Lang L, Eckelmann WC (1994). One-step synthesis of 18F labelled [^{18}F]-N-succinimidyl-4-(fluoromethyl)benzoate for protein labelling. *Applied Radiation and Isotopes* **45**, 1155-1163.

Lee SJ, Oh SJ,Chi DY, et al. (2007). One-step high-radiochemical-yield synthesis of [F-18]FP-CIT using a protic solvent system. *Nuclear Medicine and Biology* **34,** 345-351.

Lee Y-S, Jeong JM, Kim HW, Chang YS, Kim YJ, Hong MK, Rai GB, Chi DY, Kang WJ, Kang HK, Lee DS, Chung J-K, Lee MC, Suh Y-G (2006). An improved method of 18F peptide labelling: hydrazone formation with HYNIC-conjugated c(RGDyK). *Nuclear Medicine and Biology* **33**, 677-683.

Li X, Link JM, Stekhova S, Yagle KJ, Smith C, Krohn KA, Tait JF (2008). Site-specific labelling of annexin V with F-18 for apoptosis imaging. *Bioconjugate Chemistry* **19**, 1684-1688.

Liu S, Edwards D (2001). Bifunctional chelators for therapeutic lanthanide radiopharmaceuticals. *Bioconjugate Chemistry* **12** 7-34.

Magata Y, Lang L, Kiesewetter DO, Jagoda EM, Channing MA, Ecklemann WC (2000). Biologically stable [^{18}F]-labelled benzylfluoride derivatives. *Nuclear Medicine and Biology* **27**, 163-168.

Marik J, Sutcliffe JL (2006). Click for PET: rapid preparation of [F-18]fluoropeptides using Cu-I catalyzed 1,3-dipolar cycloaddition. *Tetrahedron Letters* **47**, 6681-6684.

Marsden PK (2003). Detector technology challenges for nuclear medicine and PET. *Nuclear Instruments and Methods in Physics research section A* **513**, 1-7.

Martarello L, Schaffrath C,Deng H, et al. (2003). The first enzymatic method for C-F-18 bond formation: the synthesis of 5 '-[F-18]-fluoro-5 ' deoxyadenosine for imaging with PET. *Journal of Labelled Compounds & Radiopharmaceuticals* **46**, 1181-1189.

Mather SJ, McKenzie AJ, Sosabowski JK, Morris TM, Ellison D, Watson SA (2007). Selection of radiolabelled gastrin analogues for peptide receptor-targeted radionuclide therapy. *The Journal of Nuclear Medicine* **48**,615-622.

McCarthy TJ, Schwartz SW, Welch MJ (1994). Nuclear Medicine and positron emission tomography: An overview. *Journal of Chemical Education* **71**, 830-836.

Moody TW, Carney DN, Cuttita F, Quattrocchi K, Minna JD (1985). High affinity receptors for bombesin/GRP-like peptides on human small cell lung cancer. *Life Science* **37**, 105-113.

Okarvi SM (1999). Recent developments in ^{99m}Tc-labelled peptide-based radiopharmaceuticals: an overview. *Nuclear Medicine Communications* **20**, 1093-1112.

Okarvi S (2001). Recent progress in fluorine-18 labelled peptide radiopharmaceuticals. *European Journal of Nuclear Medicine* **28**, 929-938.

Okarvi S (2002). Development of peptide-based radiopharmaceuticals as tumour imaging agents. *Journal of Nuclear Medicine* **43**, 1483.

Orlova A, Hoglund J, Lubberink M, Lebeda O, Gedda L, Lundqvist H, Tolmachev V, Sundin A (2002). Comparative biodistribution of the radiohalogenated (Br, I and At) antibody A33. Implications for *in vivo* dosimetry. *Cancer Biotherapy and Radiopharmaceuticals* **17**, 385-396.

Padilla De Jesús OL, Ihre HR, Gagne L, Fréchet JMJ, Szoka FC (2002). Polyester dendritic systems for drug delivery applications: in vitro and *in vivo* evaluation. *Bioconjugate Chemistry* **13**, 453-700.

Parker RP, Smith PHS, Taylor DM (1984). Basic Science of Nuclear Medicine. *2nd Ed.*

Phelps ME (2000). Positron emission tomography provides molecular imaging of biological processes. *Proceedings of the National Academy of Sciences* **97**, 9226-9233.

Phelps ME (2000). PET: the merging of biology and imaging into molecular imaging *Journal of Nuclear Medicine* **41**, 661-681.

Poethko T, Schottelius M, Thumshirn G, Hersel U, Herz M, Henriksen G, Kessler H, Schwaiger M, Wester HJ (2004a). Two-step methodology for high-yield routine radiohalogenation of peptides: ^{18}F-labeled RGD and octreotide analogs. *Journal of Nuclear Medicine* **45**, 892-902.

Poethko T, Schottelius M, Thumshirn G, Herz M, Haubner R, Henriksen G, Kessler H, Schwaiger M, Wester HJ (2004b). Chemoselective pre-conjugate radiohalogenation of unprotected mono- and multimeric peptides via oxime formation. *Radiochimica Acta* **92**, 317-328.

Rennen HJJ, Laverman P, van Eerd EM, Oyen WJG, Corstens FHM, Boerman OC (2007). PET imaging of infection with a HYNIC-conjugated LTB4 anatagonist labelled with F-18 via hydrazone formation. *Nuclear Medicine and Biology* **34**, 691-695.

Reubi JC (2003). Peptide receptors as molecular targets for cancer diagnosis and therapy. *Endocrine Reviews* **24**, 389-427.

Rosenthal MS, Bosch AL, Nickles RJ, et al. (1985). Synthesis and some characteristics of no-carrier added [F-18] fluoromethylsilane. *International Journal of Applied Radiation and Isotopes* **36**, 318-319.

Ross TL, Honer M, Lam PYH, Mindt TL, Groehn V, Schibli R, Schubiger PA, Ametamey SM (2008). Fluorine-18 click radiosynthesis and preclinical evaluation of a new F-labelled folic acid derivative. *Bioconjugate Chemistry* **19**, 2462-2470.

Rudin M, Weissleder R (2003). Molecular imaging in drug discovery and development. *Nature Reviews* **2**, 123-131.

Sakamoto H, Nakai Y, Ohashi Y, Matsuda M, Sakashita T, Nasako Y (1998). Monitoring of response to radiotherapy with fluorine-18 deoxyglucose PET of head and neck squamous cell carcinomas. *Acta Oto-Laryngologica*, **118**, **S38**, 254-260(7).

Sattelberger AP and Atcher RW (1999). Nuclear medicine finds the right chemistry. *Nature Biotechnology* **17**, 849-850.

Schaffrath, C; Deng, H; O'Hagan, D (2003). Isolation and characterisation of 5 '-fluorodeoxyadenosine synthase, a fluorination enzyme from Streptomyces cattleya. *FEBS LETTERS* **547**, 111-114.

Schirrmacher R, Wängler C, Schirrmacher E (2007). Recent developments and trends in ^{18}F-radiochemistry: Syntheses and applications. *Mini-Reviews in Organic Chemistry* **4**, 317-329.

Shao J, Tam JP (1995). Unprotected peptides as building blocks for the synthesis of peptide dendrimers with oxime, hydrazone and thiazolidine linkages. *Journal of the American Chemical Society* **117**, 3893-3898.

Schubiger PA (2007). Molecular Imaging with PET – Open questions? *PET Chemistry the Driving Force in Molecular Imaging*. Chapter 1. Schubiger PA, Lehmann L, Friebe M (editors). Springer-Verlag Berlin Heidelberg 2007.

Shreve PD, Anzai Y, Wahl RL (1999). Pitfalls in oncologic diagnosis with FDG PET imaging: Physiologic and benign variants. *Radiographics,* **19**, 61-77.

Stocklin GL (1998). Is there a future for clinical fluorine-18 radiopharmaceuticals (excluding FDG) *European Journal of Nuclear Medicine* **25**, 16-12-1616.

Sutcliffe-Goulden J (2001). *PhD Thesis.*

Tatro JB, Atkins M, Mier JW, Hardarson S, Wolfe H, Smith T, Entwistle ML, Reichlin S (1990). Melanotropin receptors demonstrated in situ in human melanoma. *Journal of Clinical Investigation* **85**, 1825-1832.

Tedeschi G, Lundbom N, Raman R, Bonavita S, Duyn JH, Alger JR (1997). Increased choline signal coinciding with a malignant degeneration of cerebral gliomas: A serial proton magnetic resonance spectroscopy imaging study. *Journal of Neurosurgery* **84**, 526-524.

Tewson TJ, Welch MJ (1979). Preparation of fluorine-18 aryl fluorides: piperidyl triazenes as a source of diazonium salts. *Journal of the Chemical Society Chemical Communications*, 1149-1150.

Ting R, Adam MJ, Ruth TJ, et al. (2005). Arylfluoroborates and alkylfluorosilicates as potential PET imaging agents: High-yielding aqueous biomolecular F-18-labeling. *Journal of the American Chemical Society* **127,** 13094-13095.

Ting R, Harwig C, auf dem Keller U, McCormick S, Austin P, Overall CM, Adam MJ, Ruth TJ, Perrin DM (2008). Toward [^{18}F]-labelled aryltrifluoroborate radiotracers: *In vivo* positron emission tomography imaging of stable aryltrifluoroborate clearance in mice. *Journal of the American Chemical Society* **130**, 12045-12055.

Toyokuni T, Walsh JC, Dominguez A, Phelps ME, Barrio JB, Gambhir SS, Satyamurhy N (2003). Synthesis of a new heterobifunctional linker, *N*-[4-(aminooxy)butyl]maleimide for facile access to a thiol-reactive ^{18}F-labelling agent. *Bioconjugate Chemistry* **14**, 1253-1259.

Vaidyanathan G, Zalutsky MR (1992). Labelling proteins with fluorine-18 using *N*-succinimidyl 4-[^{18}F]fluorobenzoate. *Nuclear Medicine and Biology* **19**, 275-281.

Vaidyanathan G, Zalutsky MR (1994). Improved synthesis of *N*-succinimidyl 4-[^{18}F]fluorobenzoate and its application to the labelling of a monoclonal antibody fragment. *Bioconjugate Chemistry* **54**, 352-356.

Vaidyanathan G, Zalutsky MR (2006). Synthesis of *N*-succinimidyl 4-[^{18}F]fluorobenzoate, an agent for labelling proteins and peptides with ^{18}F. *Nature Protocols* **1**, 1655-1661.

Valk PE, Bailey DL, Townsend DW, Maisey MN (2003). Positron emission tomography – basic science and clinical practice. Valk PE, Bailey DL, Townsend DW, Maisey MN (eds). *Springer*, London-Berlin-Heidelberg-New York-Hong Kong-Milan-Paris-Tokyo, pp 1-884.

Van de Wiele C, Oltenfreiter R, De Winter O, Signore A, Slegers G, Dierckx RA (2002). Tumour angiogenesis pathways: related clinical issues and implications for nuclear medicine imaging. *European Journal of Nuclear Medicine and Molecular Imaging* **29**, 699-709.

Varagnolo L, Stokkel MPM, Mazzi U, Pauwels EKJ (2000). ^{18}F-labeled radiopharmaceuticals for PET in oncology, excluding FDG. *Nuclear Medicine and Biology* **27**, 103-112.

De Visser M, Verwijnen SM, de Jong M (2008). Improvement strategies for peptide receptor scintigraphy and radionuclide therapy. *Cancer Biotherapy and Radiopharmaceuticals* **23**, 137-157.

Wallach O (1886). Uber das Verhalten einiger Diazo- und Diazoamidoverbindungen. *Justus Leibigs Annalen der Chemie* **235**, 242-255.

Walsh JC, Fleming LM, Satyamurthy N, Barrio JR, Phelps ME, Gambhir SS, Toyokuni T (2000). Application of silicon-fluoride chemistry for development of amine-reactive F-18 labeling agents for biomolecules. *Journal of Nuclear Medicine* **41**, 249P-249P1098.

Weitmann SD, Lark RH, Coney LR, Fort DW, Frasca V, Zurawski VRJr, Kamen BA (1992). Distribution of the folate receptor GP38 in normal and malignant cell lines and tissues. *Cancer Research* **52**, 3396-3401.

Welch MJ, Laforest R, Lewis JS (2007). Production of non-standard PET radionuclides and the application of radiopharmaceuticals labelled with these nuclides. *PET Chemistry the Driving Force in Molecular Imaging*. Chapter 6. Schubiger PA, Lehmann L, Friebe M (editors). Springer-Verlag Berlin Heidelberg 2007.

Wester HJ, Hamacher K, Stocklin G (1996). A comparative study of NCA fluorine-18 labelling of proteins via acylation and photochemical conjugation. *Nuclear Medicine and Biology* **23**, 365-372.

Wester HJ, Schottelius M (2007). Fluorine-18 labelling of peptides and proteins. *PET Chemistry the Driving Force in Molecular Imaging*. Chapter 4. Schubiger PA, Lehmann L, Friebe M (editors). Springer-Verlag Berlin Heidelberg 2007.

Wilbur DS (1992). Radiohalogenation of proteins: An overview of radionuclides, labeling methods and reagents for conjugate labeling. *Bioconjugate Chemistry* **3**, 433-470.

Wilbur DS, Hadley SW, Hylarides MD, Abrams PG, Beaumier PA, Morgan AC (1989). Development of a stable radioiodinating reagent to label monoclonal-antibodies for radiotherapy of cancer. *Journal of Nuclear Medicine* **30**, 216-226.

Winberg KJ, Persson M, Malmstrom PU, Sjoberg S, Tolmachev V (2004). Radiobromination of anti-HER2/neu/ErB-2 monoclonal antibody using the *p*-isothiocyanatobenzene derivative of the [^{76}Br]undecahydro-bromo-7,8-dicarba-nido-undecaborate(1-) ion. *Nuclear Medicine and Biology* **31**, 425-433.

Wu F, Lendvai G, Yngvu U, Eriksson B, Langstrom B, Bergstrom M (2004). Hybridisation of [^{76}Br]-labelled antisense oligonucleotides to chromogranin A mRNA verified by RT-PCR. *Nuclear Medicine and Biology* **31**, 1073-1078.

Wu F, Yngvu U, Hedberg E, Honda M, Lu L, Eriksson B, Watanabe Y, Bergstrom M, Langstrom B (2000). Distribution of ^{76}Br-labelled antisense oligonucleotides of different length determined ex vivo in rats. *European Journal of Pharmaceutical Science* **10**, 179-186.

Wuest F (2007). Fluorine-18 labelling of small molecules: The use of ^{18}F-labelled aryl fluorides derived from no-carrier-added [^{18}F]fluoride as labelling precursors. *PET Chemistry the Driving Force in Molecular Imaging*. Chapter 3. Schubiger PA, Lehmann L, Friebe M (editors). Springer-Verlag Berlin Heidelberg Germany 2007.

Wust F, Hultsch C, Bergmann R, Johannsen B, Henle T (2003). Radiolabelling of isopeptide N-epsilon-(gamma-glutamyl)-L-lysine by conjugation with N-succinimidyl-4-[F-18]fluorobenzoate. *Applied Radiation and Isotopes* **59**, 43-48.

Yasuda S, Shohtsu A (1997). Cancer screening with whole-body ^{18}F-fluorodeoxyglucose positron-emission tomography. *Lancet* **350**, 1819.

Yuchi A, Tatebe A, Kani S, James TD (2001). Substituent and solvent effects on the reactions of organoboronic acids with fluoride. *Bulletin of the Chemical Society of Japan* **74**, 509-510.

Zalutsky MR, Narula AS (1988). Astatination of proteins using *N*-succinimidyl tri-normal-butylstannyl benzoate intermediate. *Applied Radiation and Isotopes* **39**, 227-232.

Analytical techniques and instrumentation

i) UV/visible spectrometry

The UV/visible spectra were measured using a UV 500 Spectronic Unicam Spectrophotometer with Vision Software. Quartz cuvettes were used with a pathlength of 1cm.

ii) IR Spectrometry

The IR Spectra were recorded using a Thermo Electron Corporation Nicolet 380 FTIR with a Smart Orbit Diamond ATR 30,000-200 cm^{-1} attachment. A small amount of dry solid (about 25-50mg) was placed on the sample disc and analysed directly.

iii) Elemental analysis

Elemental analysis for C, H, and N was provided as a service at UKC using a Carlo Erba 1106 CHN Elemental Analyzer with EMASyst Elemental Analysis Data System version 4.5.01 software. Acetanilide was used as a reference. Approximately 1.5mg of the compound was weighed accurately to a precision of 0.0001mg then heated with O_2 and catalysts to produce CO_2, $H_2O(g)$ and NO_X. The NO_X was then reduced to N_2 and the gases separated chromatographically. Detection and quantification were performed spectroscopically. The elemental analysis is given as an average of two readings.

iv) ^{13}C and ^{1}H NMR

1D ^{1}H NMR and ^{13}C NMR were recorded in 5mm NMR tubes using a JEOL GX-270FT at 270MHz. All NMR spectra on this spectrometer were recorded at 27°C. Spectra were interpreted using SpecNMR version 1.0 computer software.

2D ^{13}C and ^{1}H NMR was provided as a service at UKC using a Varian Unity INOVA 600MHz FT NMR Spectrometer with VNMR 6.1c software equipped with a 5 mm HCN z-pulse field gradient probe. ACDLABS 9.0 prediction software was used.

^{1}H NMR spectra in chapter 2 were referenced to the residual solvent signals DMSO-d_6 (δ 2.54 ppm downfield from Me_4Si), D_2O-d (4.76 ppm downfield from Me_4Si), or a mixture of D_2O-d and CD_3CN-d_3. CD_3CN-d_3 is 2.06 ppm downfield from Me_4Si.

^{13}C NMR spectra in chapter 2 were referenced to the residual solvent signal DMSO-d_6 (δ 40.45), or a mixture of D_2O-d and CD_3CN-d_3.

^{1}H NMR spectra in chapter 3 were referenced to the residual solvent signal DMSO-d_6 (δ 2.54 ppm downfield from Me_4Si).

^{13}C NMR spectra in chapter 3 were referenced to the residual solvent DMSO-d_6 (δ 40.45).

Coupling constants (J values) given in Hz.

To prepare the samples for NMR analysis, the sample was dissolved approximately 1mg/cm^3 in deuterated solvent.

The system used to number the atoms in the NMR assignments has been chosen for reasons of clarity and is used throughout this thesis.

v) HPLC

System A: RP HPLC was carried out on an Agilent 1100 system with Agilent 1100 software. A diode array detector was used using a standard flow cell with a pathlength of 10mm.

(HPLC / System A / Method 1 / Column 1 / A254, 280, 300 nm): Used for all HPLC analysis except where otherwise stated.

Flow rate: 1 ml / min, Injection volume: 5µl, Column temperature: 40°C, wavelengths recorded by diode Array: 254 nm, 280 nm, 300 nm.

Run time: 45 minutes in total (including 15 minutes for re-equilibration).

Solvent A: 0.1% trifluoroacetic acid in water. Solvent B: 0.1% trifluoroacetic acid in acetonitrile.

Column: C-18 Eclipse XDB, 5µm particle size, 4.6 internal diameter x 150 mm.

Gradient:

Time	**%A**	**%B**
0 min	95	5
5 min	95	5
20 min	0	100
25 min	0	100
30 min	95	5

Table 1

(HPLC / System A / Method 2 / Column 2 / A280nm): Used only for the reaction rate monitoring reactions in chapter 2.

Flow rate: 0.4 ml / min, Injection volume: 1µl, Column temperature: 50°C.

Run time: 12 minutes in total (5 minutes post time for re-equilibration).

Solvent A: 0.1% trifluoroacetic acid in water. Solvent B: 0.1% trifluoroacetic acid in acetonitrile.

Column: Synergi 2.5µ Hydro RP 100, 50 x 2mm, 2µ

Gradient:

Time	%A	%B
0 min	95	5
1 min	95	5
6 min	0	100
7 min	95	5

Table 2

vi) Mass spectrometry

High resolution electro-spray mass spectra (ES-MS) were obtained as a service from EPSRC Swansea Mass Spectrometry Centre. The instrument used was a Thermofisher LTQ Orbitrap XL. Resolution: up to 100,000 (FWHM), mass range: m/z 50-2000 or m/z 200-4000, mass accuracy: <3ppm RMS with external calibration or <2ppm with internal calibration.

Low resolution mass spectra were also obtained as a service from Swansea Mass Spectrometry Centre; the instrument used was a Waters ZQ4000 low resolution single quadrupole mass spectrometer, mass range: m/z 4000, unit mass resolution.

Chapter 2

An assessment of reactivity and specificity of conjugation reactions involving HYBA: Competition and monitoring reactions

2.0 Introduction

Chapter 1 deals with methods of site specific (or chemoselective) labelling of peptides for use in PET. This chapter examines the chemoselectivity between aldehydes and HYBA through the use of competition reactions. This labelling strategy is suitable for ^{18}F and other elements of use in PET, SPECT and radionuclide therapy, such as radioisotopes of iodine and bromine and also boron as a binding site for ^{18}F. An overview of the uses of these elements nuclear medicine has been given in chapter 1.

2.0.1 Formation of active esters

The active ester of 4-iodobenzoic acid is synthesised in this chapter for use in the competition reactions. In chapter 3 the active ester of HYBA-Boc and HYNIC-Boc are synthesised for the subsequent synthesis of Fmoc-Lys-HYBA-Boc and Fmoc-Lys-HYNIC-Boc. Active esters are used in chapter 4 as intermediates for solid phase peptide synthesis therefore a brief overview of active ester preparation will be given here. Active esters are prepared by the action of a dehydrating agent (D) on a ligand containing a free carboxylic acid and a hydroxyl moiety on a potential leaving group (L).

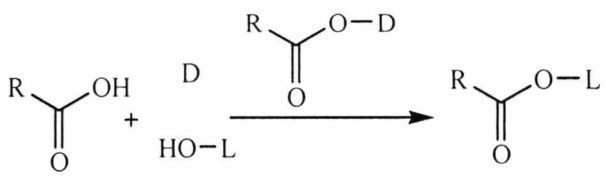

Scheme 2.0 Preparation of an active ester.

The active ester reacts cleanly with deprotonated primary amines to form a very stable amide bond (see scheme 2). The reaction can be carried out in aqueous conditions or using organic solvents.

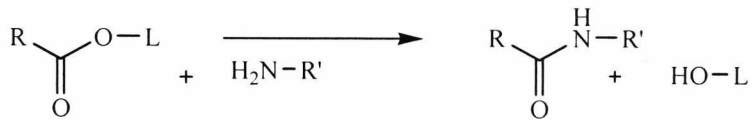

Scheme 2.1 Reaction of an active ester with a primary amine

DCC or 1,3-dicyclohexylcarbodiimide is a popular carbodiimide to use as a dehydrating agent. DCC is shown here with *N*-hydroxysuccinimide (NHS) as the leaving group. DCC leaves the insoluble waste product dicyclohexylurea, which is difficult to remove completely by filtration.

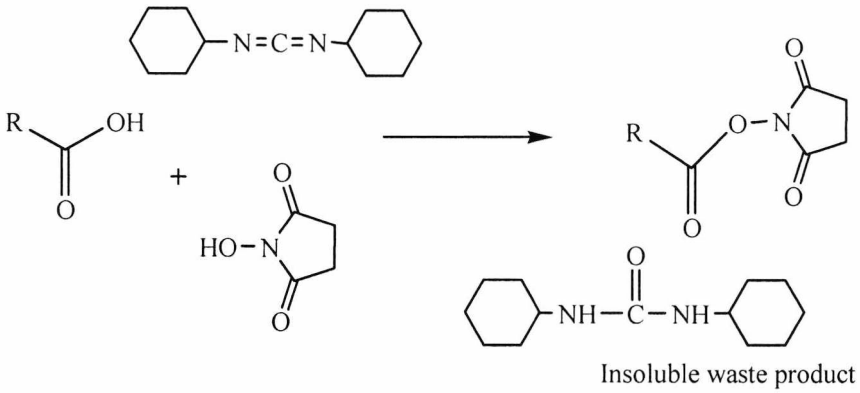

Scheme 2.2 Preparation of the DCC / NHS active ester

The waste product formed when using 1-ethyl-3(3-dimethylaminopropyl)carbodiimide HCl (EDC.HCl) is soluble in aqueous solvents and therefore is easily removed from the product. EDC.HCl has been used in preference to DCC for the synthesis of active esters in this thesis.

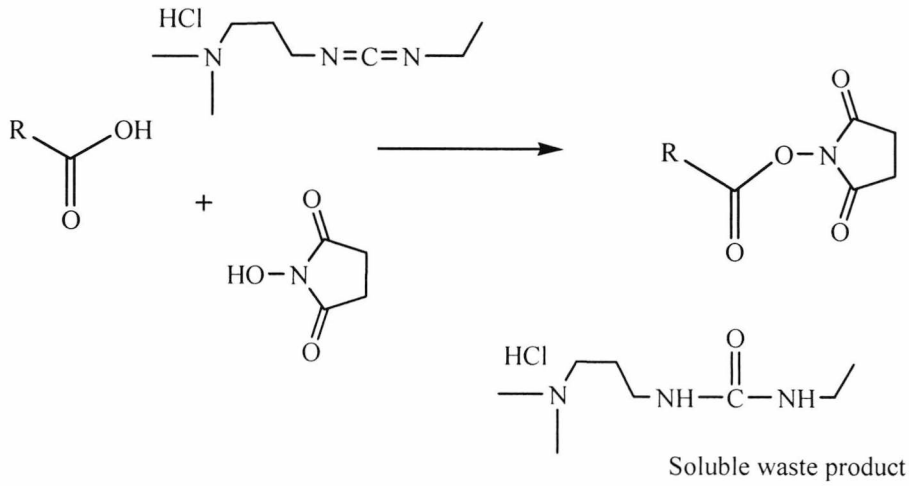

Scheme 2.3 Preparation of WSC.HCl / NHS active ester (Greenland 2002)

In this chapter, 4-iodobenzoic acid is synthesised by the Sandmeyer reaction. The Sandmeyer reaction enables substitution of an aromatic amino group via preparation of its diazonium salt and subsequent displacement with a nucleophile (Cl^-, I^-, RS^-, HO^-, CN^-). Many Sandmeyer reactions proceed under copper(I) catalysis (e.g. CN, Br, Cl, SO_3H). The reactions with thiols, water and potassium iodide do not require catalysis.

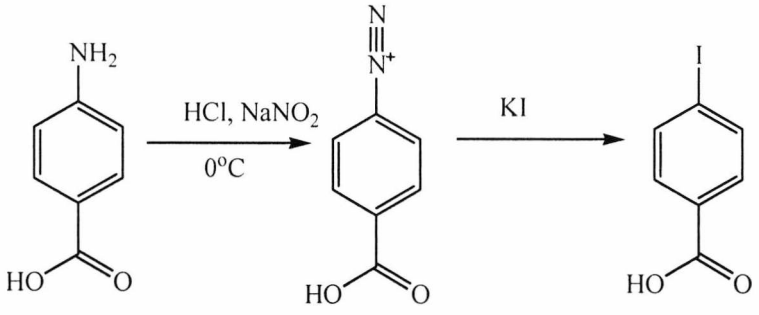

Scheme 2.4 The Sandmeyer reaction. Formation of a diazonium salt

2.1 Aims and objectives

In this chapter the aim is to determine the extent of selectivity in reactions between an aldehyde or active ester and HYBA when a competing amine (e.g. from lysine residue or *N*-terminal amino acid) is present. Ultimately this helps to develop a chemoselective labelling strategy to decrease the number of reaction steps needed to incorporate ^{18}F into peptides. This is because if the reaction is chemoselective, a peptide could have HYBA incorporated into it via solid phase synthesis and this would be a site specific binding site for a radiolabelled aldehyde or active ester. Chemoselectivity is important in radiolabelling as it is desirable to

know exactly where the radiolabel is on a labelled molecule and it is desirable to have a homogenous product to avoid extensive purification.

HYBA is a similar molecule to HYNIC, which is already extensively used for radiolabelling with technetium. HYBA has a hydrazine group which will react with an aldehyde to form a hydrazone and can be incorporated into a peptide initially then labelled as the last step.

The competition reactions were designed and carried out to test the selectivity of an aldehyde or active ester for the hydrazine group of HYBA rather than another amino group which, in this chapter takes the form of a competing amine and in radiolabelling would be any free NH_2 group on the peptide being labelled, for example a lysine side chain. This is based on the textbook assumption that hydrazine is more nucleophilic than the primary amine, and that the hydrazone product is more kinetically and thermodynamically stable than the imine product.

Experiments to assess the speed of the formation of the hydrazone under predetermined stable pH conditions were also carried out. This is an important factor in the potential usefulness of this conjugation reaction in radiolabelling.

2.2 Materials and methods

4-Aminobenzoic acid (99%) was bought from Acros Organics. Sodium nitrite was bought from Lancaster Synthesis. Potassium iodide (99%) was obtained from Aldrich. Hydrochloric acid (37% solution in water) was purchased from BDH Laboratory Supplies. Water (HPLC grade), methanol (HPLC grade), acetonitrile (HPLC grade), ethyl acetate (analytical reagent grade) and ethanol (absolute, analytical reagent grade) were purchased from Fisher Scientific. KI starch paper was purchased from Fischer Scientific. 4-Iodobenzoic acid was synthesised as described in section 2.2.1. EDC.HCl sold as WSC.HCl (water soluble carbodiimide hydrochloride) was purchased from Novabiochem. *N*-Hydroxysuccinimide (98+%) was bought from Acros Organics. Anhydrous sodium sulphate (analytical reagent grade) and dichloromethane (HPLC grade) were both purchased from Fisher Scientific. 4-fluorobenzaldehyde (98+%), 2-iodobenzaldehyde (98%), 4-formylphenyl boronic acid, 4-bromobenzaldehyde (99%) and 4-hydrazinobenzoic acid (98%) were purchased from Acros Organics. DMSO-d_6, acetonitrile -d_3 (99.8% D) and deuterium oxide (>99.9% D) were purchased from GOSS Scientific Instruments Ltd. 4-Aminobutryric acid (99%) was purchased from Acros Organics. Oxalyl chloride (99%) was bought from Avocado.

2.2.1 Synthesis of 4-iodobenzoic acid

4-Iodobenzoic acid was synthesised as described in Vogel (1978) following the method for synthesis of iodobenzene (using the Sandmeyer reaction). 4-Aminobenzoic acid (29.50 g, 0.22 mol) was dissolved in 55 cm^3 of a solution of concentrated HCl. A thermometer was placed in the solution and the round bottom flask was placed in an ice bath. The flask was cooled until the contents were below 5°C.

Sodium nitrite (16.0 g, 0.23 mol) was dissolved in 75 cm^3 of water and the solution was cooled in an ice bath.

The sodium nitrite solution was added a few drops at a time (slowly) to the 4-aminobenzoic acid solution while shaking, so that the temperature did not rise above 10°C. Sodium nitrite and HCl form nitrous acid. The last 5% of sodium nitrite solution was added more slowly still and then the resulting solution was shaken for 3-4 minutes.

A drop of the resulting solution (diluted with 3-4 drops of water) was tested for completeness of reaction with potassium iodide starch paper. A further amount of sodium nitrite was added dropwise until the KI starch paper turned blue (about 3 cm^3). This process was repeated until a slight excess of nitrous acid was present. KI starch paper is used to test for the presence of nitrite which oxidises KI to form elemental iodine that will react with starch. Once nitrite is found to be present, the reaction to form the diazonium salt is shown to be complete as the nitrite present is excess nitrite.

To the resulting solution KI (36.0 g, 0.22 mol in 40 cm^3 water) was added slowly while shaking. This was then allowed to stand for a few hours to allow nitrogen to evolve. When all nitrogen had evolved (overnight), the solution was placed in a separating funnel and the aqueous layer was extracted 3 times with ethyl acetate. The combined organic layers were kept and evaporated to dryness. The solid was recrystallised from water/ethanol and dried in the vacuum oven at 60°C for 24 h.

Yield: 10.50 g, 42.34 mmol, 20%. M.p.269-271°C, lit 272-274°C (Arcos Organics catalogue)

δ_H (270 MHz; DMSO) 7.7 (2H, d, *J* 8.6, 2CH, 2-H and 6-H), 7.9 (2H, d, *J* 8.6, 2CH, 3-H and 5-H), 8-H not observed.

δ_C (67.8 MHz; DMSO) 101.0 (C-4), 130.0 (C-1), 131.0 (C-2, C-6), 137.5 (C-3, C-5), 167.0 (C-7).

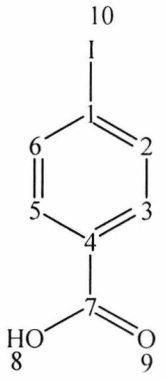

Figure 2.0 4-Iodobenzoic acid

ν_{max} cm^{-1} 2830 (m, OH *str* acid) 1933 (w, C-H, arene) 1675 (m, C=O *str* acid).

Analysis by RP HPLC: Eluted at 10.8 minutes. (HPLC / System A / Method 1 / Column 1 / A280nm). 98% by peak area percent.

$C_7H_5IO_2$ Molecular weight: 248.02, exact mass: 247.93.

m/z (ESI) (cone voltage 10V) Negative mode, molecular ion $[M - H]^-$: 246.8 100% intensity.

2.2.2 Synthesis of 4-iodobenzoic acid 2,5, dioxo-pyrrolidin-1-yl ester (active ester of iodobenzoic acid / IBAE)

4-Iodobenzoic acid (1.0 g, 4.0 mmol) was dissolved in dichloromethane (50 cm^3). WSC.HCl (1.15g, 6.0 mmol), hydroxysuccinimide (0.69 g, 6.0 mmol) and sodium sulphate (1-2g) (to absorb any water present) were then added. The reaction was stirred for 24 hours after which the reaction mixture was washed with saturated ammonium chloride solution (5 x 40 cm^3), dried over anhydrous sodium sulphate and filtered (Celite®). The solvent was removed *in vacuo*. A white solid was recovered and dried in the vacuum oven at 60°C for 24h. (Adapted from Parry 2003).

Yield: 0.51 g, 1.48 mmol, 67%. M.p.289-291°C.

δ_H (270 MHz; DMSO) 2.9 (4H, s, $2CH_2$, 9-H and 10-H), 7.85 (2H, d, *J* 8.8, 2CH, 2-H and 6-H), 8.08 (2H, d, *J* 8.8, 2CH, 3-H and 5-H).

δ_C (67.8 MHz; DMSO) 25.0 (C-9, C-10), 105.0 (C-4), 125.0 (C-1), 135.0 (C-2, C-6), 145.0 (C-3, C-5), 165.0 (C-8, C-11), 170.0 (C-7).

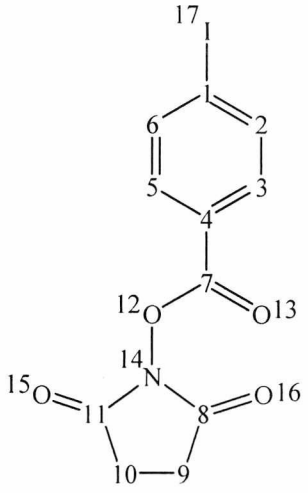

Figure 2.1 Active ester of 4-iodobenzoic acid

ν_{max} cm^{-1} 1767 (s, C=O *str,* ester), 1717 (s, C=O *str* ketone) 1202, 1013 (s, C-O, *str* ester).

Analysis by RP HPLC: Eluted at 12.2 minutes. (HPLC / System A / Method 1 / Column 1 / A280nm). 93% by peak area percent.

$C_{11}H_8INO_4$ Molecular weight: 345.09, exact mass: 344.95.

m/z (ESI)(cone voltage 10V) Negative mode, molecular ion $[M - H]^-$:343.9 100% intensity.

2.2.3 Synthesis of 4-aminobutyric acid methyl ester (ABAME)

4-Aminobutyric acid (5.0 g, 48.5 mmol) was added to methanol (150 cm^3) and cooled, with stirring, on an ice bath. Oxalyl chloride (5 cm^3, 57.3 mmol) was cautiously added while stirring. The reaction mixture was then stirred for 19 hours at room temperature. The solvent was removed *in vacuo*, washed with diethyl ether and the product (a white solid) was dried at 60°C for 24 hours in the vacuum oven (Adapated from Parry 2003).

Yield: 4.20 g, 35.85 mmol, 74%. M.p 120-123°C.

δ_H (270 MHz; D_2O) 2.28 (2H, quintet, *J* 10.8 CH_2, 2-H), 2.85 (2H, t, *J* 10.8 CH_2, 3-H), 3.32 (2H, t, *J* 10.8 CH_2, 1-H), 4.05 (3H, s, CH_3, 6-H).

δ_C (67.8 MHz; D_2O, ACN) 25.7 (C-2), 30.9 (C-3), 39.4 (C-1), 50.4 (C-6), 172.0 (C-4).

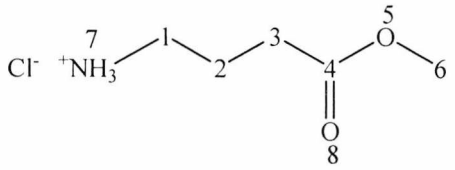

Figure 2.2 4-Aminobutyric acid methyl ester

ν_{max} cm^{-1} 3011 (m, N-H *str,* amine), 2951 (m C-H, *str*), 1724 (s, C=O *str,* ester), 1208, 1153 (s, C-O, *str* ester).

Analysis by RP HPLC: Eluted at 1.8 minutes. (HPLC / System A / Method 1 / Column 1 / A280nm). 97% pure by peak area percent.

$C_5H_{11}NO_2$ Molecular weight: 117.15, exact mass: 117.08.

m/z (ESI)(cone voltage 10V) Positive mode, molecular ion $[M + H]^+$:118.0 100% intensity.

2.2.4 Synthesis of standards for competition and monitoring reactions

2.2.4.1 Synthesis of 4-[*N*'-(2-iodobenzylidene)-hydrazino]-benzoic acid

2-Iodobenzaldehyde (0.20 g, 0.87 mmol) and 4-hydrazinobenzoic acid (0.13 g, 0.87 mmol) were dissolved in a mixture of acetonitrile and water (1:1) (20 cm^3 of each). The reaction mixture heated to reflux and left overnight. The reaction mixture was then concentrated under vacuum and left for a period of 24 hours after which a pale beige solid had formed. This was separated by filtration and the pale beige fluffy solid was kept for use as a standard after being dried in the vacuum oven for 24 hours at 60°C.

Yield 0.23 g, 0.63 mmol, 72% yield, m.p. 250-252°C.

δ_H (270 MHz; MeCN/D_2O) 7.15 (1H, t, *J* 1.7, 7.8 CH, 4-H), 7.25 (2H, d, *J* 8.9, 2CH, 11-H and 15-H), 7.50 (1H, t, *J* 7.8, CH, 3-H), 7.97 (1H, d, *J* 7.8, CH, 5-H), 7.98 (2H, d, *J* 8.9, 2CH, 12-H and 14-H), 8.05 (1H, d, *J* 1.7, 7.8, CH, 2-H), 8.20 (1H, s, CH, 7-H), 9-H and 17-H not observed.

δ_C (67.8 MHz; DMSO) 98.5 (C-4), 111.2 (C-11, C-15), 120.8 (C-3), 126.0 (C-1), 128.2 (C-5), 130.1 (C-13), 131.0 (C-12, C-14), 136.5 (C-2), 139.2 (C-6), 141.5 (C-10), 148.2 (C-7), 167.5 (C-16).

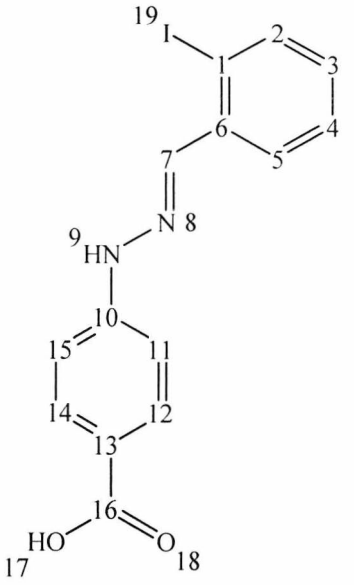

Figure 2.3 4-[*N*'-(2-Iodobenzylidene)-hydrazino]-benzoic acid

ν_{max} cm^{-1} 3323 (m, N-H *str,* amine), 2960 (m, OH *str* acid) 1668 (s, C=O *str* acid) 1603 (s, C=N *str* imine).

Analysis by RP HPLC: Eluted at 16.7 minutes. (HPLC / System A / Method 1 / Column 1 / A280nm). 100% by peak area percent.

$C_{14}H_{11}IN_2O_2$ Molecular weight: 366.15, exact mass: 365.99.

m/z (ESI)(cone voltage 20V) Positive mode, molecular ion $[M + H]^+$: 367.1 100% intensity, $[2M + H]^+$: 733.1 75% intensity.

Elemental analysis: Formula calculated from $C_{14}H_{11}IN_2O_2$

Expected: C 45.9%, H 3.0%, N 7.7%.

Found: C 45.7%, H 3.0%, N 7.6%.

2.2.4.2 Synthesis of 4-[*N*'-(4-fluorobenzylidene)-hydrazino]-benzoic acid

4-Fluorobenzaldehyde (0.11 g, 0.87 mmol) and 4-hydrazinobenzoic acid (0.13 g, 0.87 mmol) were dissolved in a mixture of acetonitrile and water (1:1) (20 cm^3 of each). The reaction mixture was heated to reflux and left overnight. The reaction mixture was then concentrated under vacuum and left for a period of 24 hours after which a yellow solid had formed. This was separated by filtration and the yellow solid was kept for use as a standard after being dried in the vacuum oven for 24 hours at 60°C.

Yield 0.10 g, 0.39 mmol, 45% yield, m.p. 249-252°C.

δ_H (270 MHz; MeCN/D_2O) 7.23 (4H, overlapping doublet and triplet, *J* 9.0, 5.9, 4CH, 2-H, 6-H, 11-H, 15-H), 7.80 (2H, m, 2CH, 3-H and 5-H), 7.96 (2H, d, *J* 9.0, 2CH, 12-H and 14-H), 7.98 (1H, s, CH, 7-H), 9-H and 17-H not observed.

δ_C (67.8 MHz; DMSO) 111.0 (C-11, C-15), 115.5 and 116.0 (C-2, C-6), 121.0 (C-4), 128.0 (C-13), 131.0 (C-3, C-5), 132.0 (C-10), 138.0 (C-7), 148.5 (C-12, C-14), 160.5 (C-1), 167.5 (C-16).

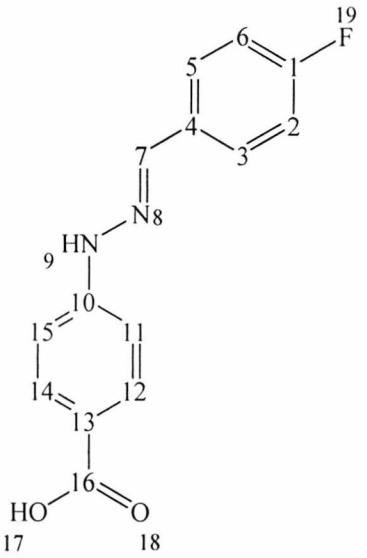

Figure 2.4 4-[*N*'-(4-Fluorobenzylidene)-hydrazino]-benzoic acid

ν_{max} cm^{-1} 3315 (m, N-H *str,* amine), 2971 (m, OH *str* acid), 1660 (s, C=O *str* acid) 1599 (s, C=N *str* imine).

Analysis by RP HPLC: Eluted at 15.3 minutes. (HPLC / System A / Method 1 / Column 1 / A280nm). 100% by peak area percent.

$C_{14}H_{11}FN_2O_2$ Molecular weight: 258.25, exact mass: 258.08.

m/z (ESI)(cone voltage 20V) Positive mode, molecular ion $[M + H]^+$: 259.2 100% intensity.

Elemental analysis: Formula calculated from $C_{14}H_{11}FN_2O_2$

Expected: C 65.1%, H 4.3%, N 10.9%.

Found: C 64.7%, H 4.3%, N 10.7%.

2.2.4.3 Synthesis of 4-[*N*'-(4-bromobenzylidene)-hydrazino]-benzoic acid

4-Bromobenzaldehyde (0.16 g, 0.87 mmol) and 4-hydrazinobenzoic acid (0.13 g, 0.87 mmol) were dissolved in a mixture of acetonitrile and water (1:1) (20 cm^3 of each). The reaction mixture was heated to reflux and left overnight. The reaction mixture was then concentrated under vacuum and left for a period of 24 hours after which a crystalline yellow solid had formed. This was separated by filtration and the yellow solid was kept for use as a standard after being dried in the vacuum oven for 24 hours at 60°C.

Yield 0.16 g, 0.50 mmol, 58% yield, m.p. 266-269°C.

δ_H (270 MHz; MeCN/D_2O) 7.22 (2H, d, *J* 8.9, 2CH, 11-H and 15-H), 7.63 (2H, d, *J* 8.9, 2CH, 3-H and 5-H), 7.69 (2H, d, *J* 8.9, 2CH, 2-H and 6-H), 7.97 (2H, d, *J* 8.9, 2CH, 12-H and 14-H), 7.99 (1H, s, 1CH, 7-H), H-9 and H-17 not observed.

δ_C (67.8 MHz; DMSO) 111.0 (C-11, C-15), 120.5 (C-13), 121.5 (C-4), 128.0 (C-3, C-5), 131.0 (C-2, C-6), 132.0 (C-12, C-14), 134.5 (C-1), 137.5 (C-10), 148.5 (C-7), 167.5 (C-16).

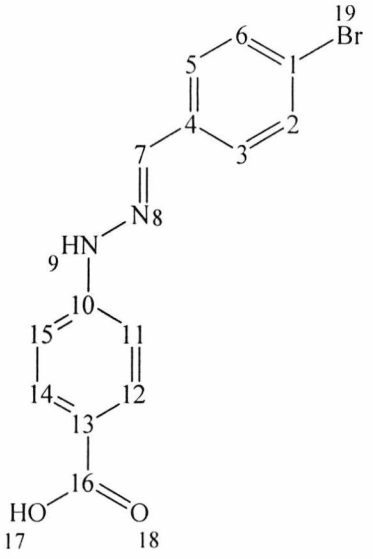

Figure 2.5 4-[*N*'-(4-Bromobenzylidene)-hydrazino]-benzoic acid

ν_{max} cm^{-1} 3280 (m, N-H *str,* amine), 2971 (m, OH *str* acid), 1651 (s, C=O *str* acid) 1591 (s, C=N *str* imine).

Analysis by RP HPLC: Eluted at 16.4 minutes. (HPLC / System A / Method 1 / Column 1 / A280nm). 100% by peak area percent.

$C_{14}H_{11}BrN_2O_2$ Molecular weight: 319.15, exact mass: 318.00.

m/z (ESI)(cone voltage 20V) Positive mode, molecular ion $[M + H]^+$: 319.1 98% intensity, 321.2 100% intensity.

Elemental analysis: Formula calculated from $C_{14}H_{11}BrN_2O_2$

Expected: C 52.7%, H 3.5%, N 8.8%.

Found: C 52.4%, H 3.4%, N 8.8%.

2.2.4.4 Synthesis of 4-[*N*'-(4-boronobenzylidene)hydrazino]-benzoic acid

4-Formylphenyl boronic acid (0.13 g, 0.87 mmol) and 4-hydrazinobenzoic acid (0.13 g, 0.87 mmol) were dissolved in a mixture of acetonitrile and water (1:1) (20 cm^3 of each). The reaction mixture was heated to reflux and left overnight. The reaction mixture was then concentrated under vacuum and left for a period of 24 hours after which a tan coloured solid had formed. This was separated by filtration and the tan coloured solid was kept for use as a standard after being dried in the vacuum oven for 24 hours at 60°C.

Yield: 0.18 g, 0.71 mmol, 82%, m.p. 198-201°C.

δ_H (270 MHz; MeCN/D_2O) 7.24 (2H, d, *J* 9.0, 2CH, 11-H and 15-H), 7.77 (2H, d, *J* 8.3, 2CH, 2-H and 6-H), 7.88 (2H, d, *J* 8.3, 2CH, 3-H and 5-H), 7.98 (2H, d, *J* 9.0, 2CH, 12-H and 14-H), 7.99 (1H, s, 1CH, 7-H), H-9, H-17, H-20 and H-21 not observed.

δ_C (67.8 MHz; DMSO) 112.0 (C-11, C-15), 121.5 (C-13), 125.8 (C-4), 125.9 (C-1), 132.2 (C-2, C-6), 135.5 (C-3, C-5), 137.8 (C-12, C-14), 140.0 (C-10), 149.5 (C-7), 167.5 (C-16).

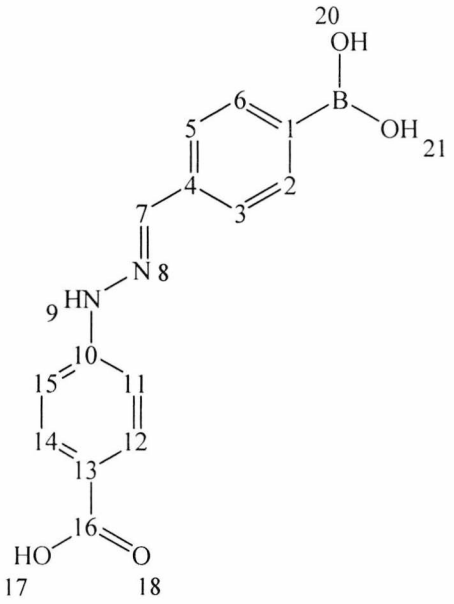

Figure 2.6 4-[*N*'-(4-Boronobenzylidene)hydrazino]-benzoic acid

ν_{max} cm^{-1} 3308 (m, N-H *str,* amine), 2972 (m, OH *str* acid), 1672 (s, C=O *str* acid), 1604, 1591 (s, C=N *str* imine).

Analysis by RP HPLC: Eluted at 13.8 minutes. (HPLC / System A / Method 1 / Column 1 / A280nm). 96% pure by peak area percent.

$C_{14}H_{13}BN_2O_4$ Molecular weight: 284.08, exact mass: 284.10.

m/z(ESI) Positive mode, molecular ion $[M + H]^+$: 285.1044 100% intensity.

Elemental analysis: Formula calculated from $C_{14}H_{13}BN_2O_4$

Expected: C 59.2%, H 4.6%, N 9.9%.

Found: C 59.5%, H 4.9%, N 9.0%.

2.3 Competition Reactions

The competition reactions were carried out at room temperature, left overnight then analysed by ^1H NMR. All reactions were analysed at a single time point (24 h). All reactions were carried out in deuterated solvents (ACN/H_2O 1:1 v/v, 100 cm^3 total volume) with no purification carried out before analysis by ^1H NMR. The weights and amount in moles of the reactants for each reaction are given below. HPLC analysis was also carried out on the reaction mixture. Samples were stored at -20°C before HPLC analysis for up to two weeks.

2.3.1.1 Competition reactions involving 4-aminobutyric acid methyl ester as the competing amine

2.3.1.1.1 Reaction between the active ester of 4-iodobenzoic acid and 4-aminobutyric acid methyl ester

The active ester of 4-iodobenzoic acid (0.05 g, 0.15 mmol) and 4-aminobutyric acid methyl ester (0.02 g, 0.15 mmol), TEA (20 µl, 0.02 g, 0.15 mmol) were weighed into a round bottom flask and treated as described above.

δ_H TEA (270 MHz; MeCN/D_20) 1.25 (9H, t, *J* 8.1, CH_3, 1-H), 3.15 (6H, quartet, *J* 8.1, CH_2, 2-H).

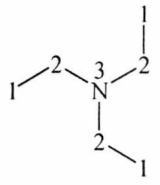

Figure 2.7 Triethylamine

δ_H 4-Aminobutyric acid methyl ester (270 MHz;MeCN /D_2O) 2.28 (2H, quintet, *J* 10.8, CH_2, 2-H), 2.85 (2H, t, *J* 10.8, CH_2, 3-H), 3.32 (2H, t, *J* 10.8, CH_2, 1-H), 4.05 (3H, s, CH_3, 6-H).

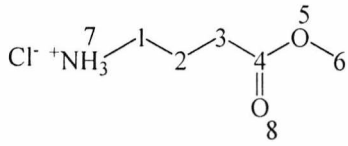

Figure 2.8 4-Aminobutyric acid methyl ester (ABAME)

δ_H 4-Iodobenzoic acid active ester (270 MHz; DMSO) 2.9 (4H, s, $2CH_2$, 9-H and 10-H), 7.85 (2H, d, *J* 8.8, 2CH, 2-H and 6-H), 8.08 (2H, d, *J* 8.8, 2CH, 3-H and 5-H).

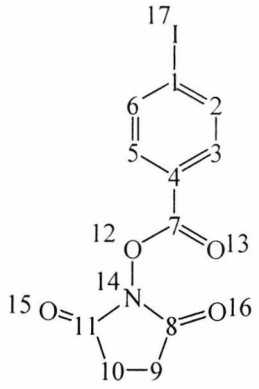

Figure 2.9 Active ester of 4-iodobenzoic acid (IBAE)

Analysis by RP HPLC: 4-Aminobutyric acid methyl ester eluted at 1.8 minutes. The unknown peaks eluted at 1.4 and 5.7 minutes. (HPLC / System A / Method 1 / Column 1 / A280nm).

2.3.1.1.2 Reaction between the active ester of 4-iodobenzoic acid and 4-hydrazinobenzoic acid

The active ester of 4-iodobenzoic acid (0.05 g, 0.15 mmol) and 4-hydrazinobenzoic acid (0.02 g, 0.15 mmol).

δ_H 4-(N'-[4-Iodobenzoyl)hydrazino]benzoic acid (270 MHz; MeCN/D_2O) 6.75 (2H, d, *J* 8.8, 2CH, 12-H and 16-H), 7.61 (2H, d, *J* 8.8, 2CH, 3-H and 5-H), 7.71 (2H, d, *J* 8.8, 2CH, 2-H and 6-H), 7.83 (2H, d, *J* 8.8, 2CH, 13-H and 15-H), 9-H, 10-H and 18-H not observed.

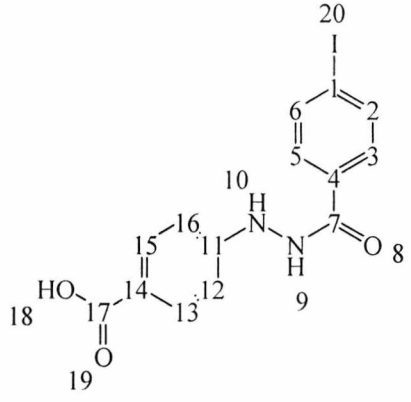

Figure 2.10 δ_H 4-[*N*'-(4-Iodobenzoyl)hydrazino]-benzoic acid

δ_H 4-Hydrazinobenzoic acid (HYBA) (270 MHz; MeCN/D_2O) 6.97 (2H, d, *J* 8.8, 2CH, 2-H and 6-H), 7.52 (1H, s, NH, 10-H), 7.99 (2H, d, *J* 8.8, 2CH, 3-H and 5-H) H-8 and H-11 not observed.

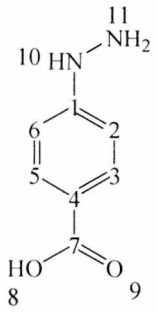

Figure 2.11 4-Hydrazinobenzoic acid (HYBA)

δ_H 4-Iodobenzoic acid active ester (270 MHz; DMSO) 2.9 (4H, s, $2CH_2$, 9-H and 10-H), 7.85 (2H, d, *J* 8.8, 2CH, 2-H and 6-H), 8.08 (2H, d, *J* 8.8, 2CH, 3-H and 5-H).

Analysis by RP HPLC: HYBA eluted at 9.0 minutes. The unknown peaks eluted at 13.6, 14.9, 15.4 and 16.3 minutes. (HPLC / System A / Method 1 / Column 1 / A280nm).

2.3.1.1.3 Competition reaction between 4-aminobutyric acid methyl ester and 4-hydrazinobenzoic acid for the active ester of 4-iodobenzoic acid

The active ester of 4-iodobenzoic acid (0.05 g, 0.15 mmol), 4-aminobutyric acid methyl ester (0.02 g, 0.15 mmol) and 4-hydrazinobenzoic acid (0.02 g, 0.15 mmol), TEA (20 µl, 0.02 g, 0.15 mmol).

Possibly formed: δ_H 4-(N'-[4-Iodobenzoyl)hydrazino]benzoic acid (270 MHz; MeCN/D_2O) 6.75 (2H, d, *J* 8.8, 2CH, 12-H and 16-H), 7.61 (2H, d, *J* 8.8, 2CH, 3-H and 5-H), 7.71 (2H, d, *J* 8.8, 2CH, 2-H and 6-H), 7.83 (2H, d, *J* 8.8, 2CH, 13-H and 15-H), 9-H, 10-H and 18-H not observed.

δ_H HYBA (270 MHz; MeCN/D_2O) 6.97 (2H, d, *J* 8.8, 2CH, 2-H and 6-H), 7.52 (1H, s, NH, 10-H), 7.99 (2H, d, *J* 8.8, 2CH, 3-H and 5-H) H-8 and H-11 not observed.

δ_H 4-Iodobenzoic acid active ester (270 MHz; DMSO) 2.9 (4H, s, $2CH_2$, 9-H and 10-H), 7.85 (2H, d, *J* 8.8, 2CH, 2-H and 6-H), 8.08 (2H, d, *J* 8.8, 2CH, 3-H and 5-H).

δ_H TEA (270 MHz; MeCN/D_20) 1.25 (9H, t, *J* 8.1, CH_3, 1-H), 3.15 (6H, quartet, *J* 8.1, CH_2, 2-H).

δ_H 4-Aminobutyric acid methyl ester (270 MHz;MeCN /D_2O) 2.28 (2H, quintet, *J* 10.8, CH_2, 2-H), 2.85 (2H, t, *J* 10.8, CH_2, 3-H), 3.32 (2H, t, *J* 10.8, CH_2, 1-H), 4.05 (3H, s, CH_3, 6-H).

Analysis by RP HPLC: HYBA eluted at 9.0 minutes, the active ester of iodobenzoic acid eluted at 12.2 minutes. The unknown peaks eluted at 12.8, 13.6 and 15.4 minutes. (HPLC / System A / Method 1 / Column 1 / A280nm).

2.3.1.1.4 Reaction between 4-aminobutyric acid methyl ester and 2-iodobenzaldehyde

2-Iodobenzaldehyde (0.05 g, 0.22 mmol) and 4-aminobutyric acid methyl ester (0.03 g, 0.22 mmol).

δ_H 2-Iodobenzaldehyde (270MHz; MeCN/D_20) 7.45 (1H, t, *J* 7.8, 1.7, CH, 5-H), 7.62 (1H, t, *J* 7.8, CH, 4-H), 7.90 (1H, d, *J* 7.8, 1.7, CH, 3-H), 8.15 (1H, d, *J* 7.8, CH, 6-H), 10.00 (1H, s, CHO, 9-H).

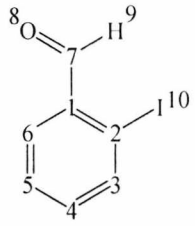

Figure 2.12.19 2-Iodobenzaldehyde

δ_H TEA (270 MHz; MeCN/D_20) 1.25 (9H, t, *J* 8.1, CH_3, 1-H), 3.15 (6H, quartet, *J* 8.1, CH_2, 2-H).

δ_H 4-Aminobutyric acid methyl ester (270 MHz;MeCN /D_2O) 2.28 (2H, quintet, *J* 10.8, CH_2, 2-H), 2.85 (2H, t, *J* 10.8, CH_2, 3-H), 3.32 (2H, t, *J* 10.8, CH_2, 1-H), 4.05 (3H, s, CH_3, 6-H).

Analysis by RP HPLC: 2-Iodobenzaldehyde eluted at 15.9 minutes, 4-aminobutyric acid methyl ester eluted at 1.8 minutes. The unknown peaks eluted at 12.9, 16.7 and 22.2 minutes. (HPLC / System A / Method 1 / Column 1 / A280nm).

2.3.1.1.5 Reaction between 2-iodobenzaldehyde and 4-hydrazinobenzoic acid

2-Iodobenzaldehyde (0.20 g, 0.87 mmol) and 4-hydrazinobenzoic acid (HYBA) (0.13 g, 0.87 mmol).

δ_H 4-[*N*'-(2-Iodobenzylidene)-hydrazino]-benzoic acid (270 MHz; MeCN/D_2O) 7.15 (1H, t, *J* 1.7, 7.8 CH, 4-H), 7.25 (2H, d, *J* 8.9, 2CH, 11-H and 15-H), 7.50 (1H, t, *J* 7.8, CH, 3-H), 7.97

(1H, d, *J* 7.8, CH, 5-H), 7.98 (2H, d, *J* 8.9, 2CH, 12-H and 14-H), 8.05 (1H, d, *J* 1.7, 7.8, CH, 2-H), 8.20 (1H, s, CH, 7-H), 9-H and 17-H not observed.

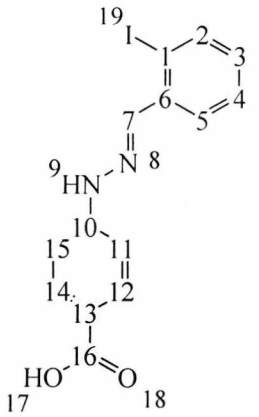

Figure 2.13 4-[*N*'-(2-Iodobenzylidene)-hydrazino]-benzoic acid

Analysis by RP HPLC: 4-[*N*'-(2-Iodobenzylidene)-hydrazino]-benzoic acid eluted at 16.7 minutes, HYBA eluted at 9.0 minutes. The unknown peak eluted at 14.9 minutes. (HPLC / System A / Method 1 / Column 1 / A280nm).

2.3.1.1.6 Competition reaction between 4-aminobutyric acid methyl ester and 4-hydrazinobenzoic acid for 2-iodobenzaldehyde

2-Iodobenzaldehyde (0.05g, 0.22 mmol), 4-aminobutyric acid methyl ester (0.03g, 0.22 mmol) and 4-hydrazinobenzoic acid (HYBA) (0.033g, 0.22 mmol), TEA (30 µl, 0.02 g, 0.22 mmol).

δ_H 4-[*N*'-(2-Iodobenzylidene)-hydrazino]-benzoic acid (270 MHz; MeCN/D_2O) 7.15 (1H, t, *J* 1.7, 7.8 CH, 4-H), 7.25 (2H, d, *J* 8.9, 2CH, 11-H and 15-H), 7.50 (1H, t, *J* 7.8, CH, 3-H), 7.97 (1H, d, *J* 7.8, CH, 5-H), 7.98 (2H, d, *J* 8.9, 2CH, 12-H and 14-H), 8.05 (1H, d, *J* 1.7, 7.8, CH, 2-H), 8.20 (1H, s, CH, 7-H), 9-H and 17-H not observed.

δ_H TEA (270 MHz; MeCN/D_20) 1.25 (9H, t, *J* 8.1, CH_3, 1-H), 3.15 (6H, quartet, *J* 8.1, CH_2, 2-H).

δ_H 4-Aminobutyric acid methyl ester (270 MHz;MeCN /D_2O) 2.28 (2H, quintet, *J* 10.8, CH_2, 2-H), 2.85 (2H, t, *J* 10.8, CH_2, 3-H), 3.32 (2H, t, *J* 10.8, CH_2, 1-H), 4.05 (3H, s, CH_3, 6-H).

Analysis by RP HPLC: 4-[*N*'-(2-Iodobenzylidene)-hydrazino]-benzoic acid eluted at 16.7 minutes, HYBA eluted at 9.0 minutes. The unknown peak eluted at 14.9 minutes. (HPLC / System A / Method 1 / Column 1 / A280nm).

2.3.1.1.7 Reaction between 4-aminobutyric acid methyl ester and 4-fluorobenzaldehyde

4-Fluorobenzaldehyde (4.61 µl, 0.005 g, 0.04 mmol) and 4-aminobutyric acid methyl ester (0.005 g, 0.04 mmol), TEA (5.98 µl, 0.04 mmol).

δ_H 4-Fluorobenzaldehyde (270 MHz; MeCN/D_20) 7.20 (2H, t, *J* 8.8, 2CH, 2-H and 6-H), 7.88 (2H, quartet, *J* 3.0, 8.8, 2CH, 3-H and 5-H), 10.00 (1H, s, CHO, 8-H).

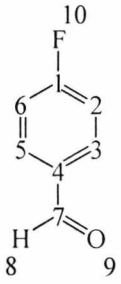

Figure 2.14 4-Fluorobenzaldehyde

δ_H TEA (270 MHz; MeCN/D_20) 1.25 (9H, t, *J* 8.1, CH_3, 1-H), 3.15 (6H, quartet, *J* 8.1, CH_2, 2-H).

δ_H 4-Aminobutyric acid methyl ester (270 MHz;MeCN /D_2O) 2.28 (2H, quintet, *J* 10.8, CH_2, 2-H), 2.85 (2H, t, *J* 10.8, CH_2, 3-H), 3.32 (2H, t, *J* 10.8, CH_2, 1-H), 4.05 (3H, s, CH_3, 6-H).

Analysis by RP HPLC: 4-Fluorobenzaldehyde eluted at 13.2 minutes. (HPLC / System A / Method 1 / Column 1 / A280nm).

2.3.1.1.8 Reaction between 4-hydrazinobenzoic acid and 4-fluorobenzaldehyde

4-Fluorobenzaldehyde (0.11 g, 0.87 mmol) and 4-hydrazinobenzoic acid (0.13 g, 0.87 mmol).

δ_H 4-[*N*'-(4-Fluorobenzylidene)-hydrazino]-benzoic acid (270 MHz; MeCN/D_2O) 7.23 (4H, overlapping doublet and triplet, *J* 9.0, 5.9, 4CH, 2-H, 6-H, 11-H, 15-H), 7.80 (2H, m, 2CH, 3-H and 5-H), 7.96 (2H, d, *J* 9.0, 2CH, 12-H and 14-H), 7.98 (1H, s, CH, 7-H), 9-H and 17-H not observed.

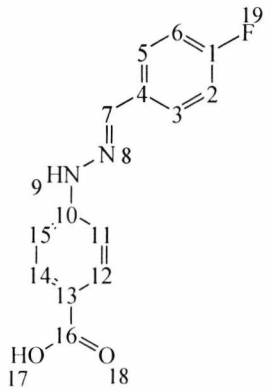

Figure 2.15 4-[*N*'-(4-Fluorobenzylidene)-hydrazino]-benzoic acid

Analysis by RP HPLC: 4-[*N*'-(4-Fluorobenzylidene)-hydrazino]-benzoic acid eluted at 15.3 minutes and HYBA eluted at 9.0 minutes. 4-[*N*'-(4-fluorobenzylidene)-hydrazino]-benzoic acid: 70% by peak area percent. (HPLC / System A / Method 1 / Column 1 / A280nm).

2.3.1.1.9 Competition reaction between 4-aminobutryric acid methyl ester and 4-hydrazinobenzoic acid for 4-fluorobenzaldehyde

4-Fluorobenzaldehyde (4.61 µl, 0.0053 g, 0.04 mmol), 4-aminobutyric acid methyl ester (0.005 g, 0.04 mmol) and 4-hydrazinobenzoic acid (0.0065 g, 0.04 mmol), TEA (5.98 µl, 0.015 g, 0.04 mmol).

δ_H 4-[*N*'-(4-Fluorobenzylidene)-hydrazino]-benzoic acid (270 MHz; MeCN/D_2O) 7.23 (4H, overlapping doublet and triplet, *J* 9.0, 5.9, 4CH, 2-H, 6-H, 11-H, 15-H), 7.80 (2H, m, 2CH, 3-H and 5-H), 7.96 (2H, d, *J* 9.0, 2CH, 12-H and 14-H), 7.98 (1H, s, CH, 7-H), 9-H and 17-H not observed.

δ_H TEA (270 MHz; MeCN/D_20) 1.25 (9H, t, *J* 8.1, CH_3, 1-H), 3.15 (6H, quartet, *J* 8.1, CH_2, 2-H).

δ_H 4-Aminobutyric acid methyl ester (270 MHz;MeCN /D_2O) 2.28 (2H, quintet, *J* 10.8, CH_2, 2-H), 2.85 (2H, t, *J* 10.8, CH_2, 3-H), 3.32 (2H, t, *J* 10.8, CH_2, 1-H), 4.05 (3H, s, CH_3, 6-H).

Analysis by RP HPLC: 4-[*N*'-(4-Fluorobenzylidene)-hydrazino]-benzoic acid eluted at 15.3 minutes, 4-fluorobenzaldehyde eluted at 13.2 minutes. The unknown peak present in HPLC eluted at 16.4 minutes. (HPLC / System A / Method 1 / Column 1 / A280nm).

2.3.1.2.0 Reaction between 4-aminobutyric acid methyl ester and 4-bromobenzaldehyde

4-Bromobenzaldehyde (0.008 g, 0.04 mmol) and 4-aminobutyric acid methyl ester (0.005 g, 0.04 mmol), TEA (5.98 µl, 0.04 mmol).

δ_H 4-Bromobenzaldehyde (270 MHz; MeCN/D_2O) 7.80 (2H, d, *J* 8.6, 2CH, 2-H and 6-H), 7.90 (2H, d, *J* 8.6, 2CH, 3-H and 5-H), 10.0 (1H, s, CHO, 8-H).

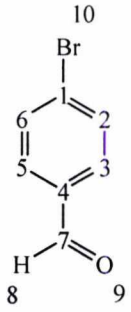

Figure 2.16 4-Bromobenzaldehyde

δ_H TEA (270 MHz; MeCN/D_20) 1.25 (9H, t, *J* 8.1, CH_3, 1-H), 3.15 (6H, quartet, *J* 8.1, CH_2, 2-H).

δ_H 4-Aminobutyric acid methyl ester (270 MHz;MeCN /D_2O) 2.28 (2H, quintet, *J* 10.8, CH_2, 2-H), 2.85 (2H, t, *J* 10.8, CH_2, 3-H), 3.32 (2H, t, *J* 10.8, CH_2, 1-H), 4.05 (3H, s, CH_3, 6-H).

(HPLC / System A / Method 1 / Column 1 / A280nm).Analysis by RP HPLC: 4-Bromobenzaldehyde eluted at 15.2 minutes, 4-aminobutyric acid methyl ester eluted 1.8 minutes. The unknown peaks present in the HPLC eluted at 5.2, 13.9, 16.3 and 16.7 minutes.

2.3.1.2.1 Reaction between 4-hydrazinobenzoic acid and 4-bromobenzaldehyde

4-Bromobenzaldehyde (0.16 g, 0.87 mmol) and 4-hydrazinobenzoic acid (0.13 g, 0.87 mmol).

δ_H 4-[*N*'-(4-Bromobenzylidene)-hydrazino]-benzoic acid (270 MHz; MeCN/D_2O) 7.22 (2H, d, *J* 8.9, 2CH, 11-H and 15-H), 7.63 (2H, d, *J* 8.9, 2CH, 3-H and 5-H), 7.69 (2H, d, *J* 8.9, 2CH, 2-H and 6-H), 7.97 (2H, d, *J* 8.9, 2CH, 12-H and 14-H), 7.99 (1H, s, 1CH, 7-H), H-9 and H-17 not observed.

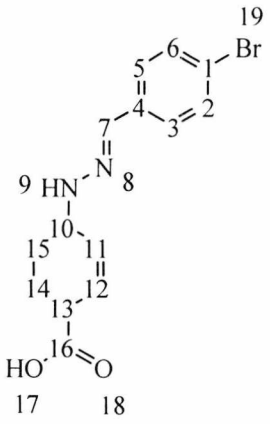

Figure 2.17 4-[*N*'-(4-Bromobenzylidene)-hydrazino]-benzoic acid

Analysis by RP HPLC: 4-[*N*'-(4-Bromobenzylidene)-hydrazino]-benzoic acid eluted at 16.4 minutes, HYBA eluted at 9.0 minutes and 4-bromobenzaldehyde eluted at 15.2 minutes. 4-[*N*'-(4-Bromobenzylidene)-hydrazino]-benzoic acid: 67% by peak area percent (HPLC / System A / Method 1 / Column 1 / A280nm).

2.3.1.2.2 Competition reaction between 4-aminobutyric acid methyl ester and 4-hydrazinobenzoic acid for 4-bromobenzaldehyde

4-Bromobenzaldehyde (0.008 g, 0.04 mmol), 4-aminobutyric acid methyl ester (0.005 g, 0.04 mmol) and 4-hydrazinobenzoic acid (HYBA) (0.0065 g, 0.04 mmol), TEA (5.98 µl, 0.02 g, 0.04 mmol).

δ_H 4-[*N*'-(4-Bromobenzylidene)-hydrazino]-benzoic acid (270 MHz; MeCN/D_2O) 7.22 (2H, d, *J* 8.9, 2CH, 11-H and 15-H), 7.63 (2H, d, *J* 8.9, 2CH, 3-H and 5-H), 7.69 (2H, d, *J* 8.9, 2CH, 2-H and 6-H), 7.97 (2H, d, *J* 8.9, 2CH, 12-H and 14-H), 7.99 (1H, s, 1CH, 7-H), H-9 and H-17 not observed.

δ_H TEA (270 MHz; MeCN/D_20) 1.25 (9H, t, *J* 8.1, CH_3, 1-H), 3.15 (6H, quartet, *J* 8.1, CH_2, 2-H).

δ_H 4-Aminobutyric acid methyl ester (270 MHz;MeCN /D_2O) 2.28 (2H, quintet, *J* 10.8, CH_2, 2-H), 2.85 (2H, t, *J* 10.8, CH_2, 3-H), 3.32 (2H, t, *J* 10.8, CH_2, 1-H), 4.05 (3H, s, CH_3, 6-H).

Analysis by RP HPLC: 4-[*N*'-(4-Bromobenzylidene)-hydrazino]-benzoic acid eluted at 16.4 minutes, HYBA eluted at 9.0 minutes, 4-bromobenzaldehyde eluted at 15.1 minutes. The unknown peaks present eluted at 11.3 and 11.8 minutes. (HPLC / System A / Method 1 / Column 1 / A280nm).

2.3.1.2.3 Reaction between 4-aminobutyric acid methyl ester and 4-formylphenyl boronic acid

4-Formylphenyl boronic acid (0.006 g, 0.04 mmol) and 4-aminobutyric acid methyl ester (0.005 g, 0.04 mmol), TEA (5.98 µl, 0.02 g, 0.04 mmol).

δ_H TEA (270 MHz; MeCN/D_20) 1.25 (9H, t, *J* 8.1, CH_3, 1-H), 3.15 (6H, quartet, *J* 8.1, CH_2, 2-H).

δ_H 4-Aminobutyric acid methyl ester (270 MHz;MeCN /D_2O) 2.28 (2H, quintet, *J* 10.8, CH_2, 2-H), 2.85 (2H, t, *J* 10.8, CH_2, 3-H), 3.32 (2H, t, *J* 10.8, CH_2, 1-H), 4.05 (3H, s, CH_3, 6-H).

Analysis by RP HPLC: An unknown peak eluted at 13.9 minutes. (HPLC / System A / Method 1 / Column 1 / A280nm).

2.3.1.2.4 Reaction between 4-hydrazinobenzoic acid and 4-formylphenyl boronic acid

4-Formylphenyl boronic acid (0.13 g, 0.87 mmol) and 4-hydrazinobenzoic acid (0.132 g, 0.87 mmol).

δ_H 4-[N'-(4-Boronobenzylidene)hydrazino]-benzoic acid (270 MHz; MeCN/D_2O) 7.24 (2H, d, *J* 9.0, 2CH, 11-H and 15-H), 7.77 (2H, d, *J* 8.3, 2CH, 2-H and 6-H), 7.88 (2H, d, *J* 8.3, 2CH, 3-H and 5-H), 7.98 (2H, d, *J* 9.0, 2CH, 12-H and 14-H), 7.99 (1H, s, 1CH, 7-H), H-9, H-17, H-20 and H-21 not observed.

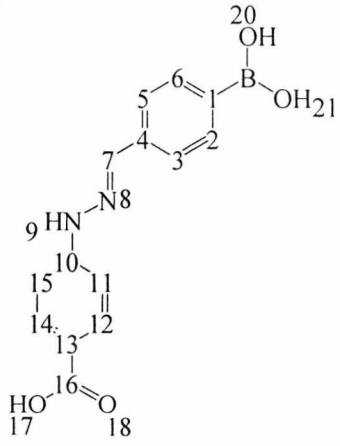

Figure 2.18 4-[N'-(4-Boronobenzylidene)hydrazino]-benzoic acid

δ_H HYBA (270 MHz; MeCN/D_2O) 6.97 (2H, d, *J* 8.8, 2CH, 2-H and 6-H), 7.52 (1H, s, NH, 10-H), 7.99 (2H, d, *J* 8.8, 2CH, 3-H and 5-H), H-8 and H-11 not observed.

δ_H 4-Formylphenyl boronic acid (270 MHz;MeCN/D_20) 7.98 (2H, d, J 8.6, 2CH, 2-H and 6-H), 8.03 (2H, d, J 8.6, 2CH, 3-H and 5-H), 10.07 (1H, s, CHO, 8-H), H-11 and H-12 not observed.

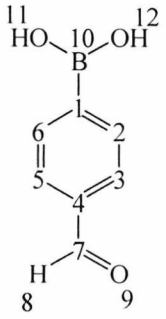

Figure 2.19 4-Formylphenyl boronic acid

Analysis by RP HPLC: 4-[N'-(4-Boronobenzylidene)hydrazino]-benzoic acid eluted at 13.8 minutes, HYBA eluted at 9.0 minutes and 4 formylphenyl boronic acid eluted at 10.1 minutes. (HPLC / System A / Method 1 / Column 1 / A280nm). Product 48% by peak area percent.

2.3.1.2.5 Competition reaction between 4-aminobutyric acid methyl ester and 4-hydrazinobenzoic acid for 4-formylphenyl boronic acid

4-Formylphenyl boronic acid (0.006 g, 0.04 mmol), 4-aminobutyric acid methyl ester (0.005 g, 0.04 mmol) and 4-hydrazinobenzoic acid (0.007 g, 0.04 mmol), TEA (5.98 µl, 0.02 g, 0.04 mmol).

δ_H 4-[N'-(4-Boronobenzylidene)hydrazino]-benzoic acid (270 MHz; MeCN/D_2O) 7.24 (2H, d, *J* 9.0, 2CH, 11-H and 15-H), 7.77 (2H, d, *J* 8.3, 2CH, 2-H and 6-H), 7.88 (2H, d, *J* 8.3, 2CH, 3-H and 5-H), 7.98 (2H, d, *J* 9.0, 2CH, 12-H and 14-H), 7.99 (1H, s, 1CH, 7-H), H-9, H-17, H-20 and H-21 not observed.

δ_H HYBA (270 MHz; MeCN/D_2O) 6.97 (2H, d, *J* 8.8, 2CH, 2-H and 6-H), 7.52 (1H, s, NH, 10-H), 7.99 (2H, d, *J* 8.8, 2CH, 3-H and 5-H) H-8 and H-11 not observed.

δ_H 4-Formylphenyl boronic acid (270 MHz;MeCN/D_20) 7.98 (2H, d, J 8.6, 2CH, 2-H and 6-H), 8.03 (2H, d, J 8.6, 2CH, 3-H and 5-H), 10.07 (1H, s, CHO, 8-H), H-11 and H-12 not observed.

δ_H TEA (270 MHz; MeCN/D_20) 1.25 (9H, t, *J* 8.1, CH_3, 1-H), 3.15 (6H, quartet, *J* 8.1, CH_2, 2-H).

δ_H 4-Aminobutyric acid methyl ester (270 MHz;MeCN /D_2O) 2.28 (2H, quintet, *J* 10.8, CH_2, 2-H), 2.85 (2H, t, *J* 10.8, CH_2, 3-H), 3.32 (2H, t, *J* 10.8, CH_2, 1-H), 4.05 (3H, s, CH_3, 6-H).

Analysis by RP HPLC: 4-[N'-(4-Boronobenzylidene)hydrazino]-benzoic acid eluted at 13.9 minutes, the unknown peaks present in the HPLC chromatogram eluted at 10.5, 13.2 and 14.4 minutes. (HPLC / System A / Method 1 / Column 1 / A280nm).

2.3.1.3 Competition reactions involving benzylamine as the competing amine

2.3.1.3.1 Reaction between benzylamine and the active ester of 4-iodobenzoic acid

The active ester of 4-iodobenzoic acid (0.01 g, 0.03 mmol) and benzylamine (3.17 µl, 0.003 g, 0.03 mmol).

δ_H Benzylamine (270 MHz; MeCN/D_2O) 3.80 (2H, s, CH_2, 7-H), 7.28-7.49 (5H, m, 5CH, 2, 3, 4, 5, 6-H).

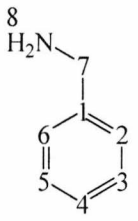

Figure 2.20 Benzylamine

δ_H 4-Iodobenzoic acid active ester (270 MHz; DMSO) 2.9 (4H, s, $2CH_2$, 9-H and 10-H), 7.64 (2H, d, *J* 8.8, 2CH, 2-H and 6-H), 7.96 (2H, d, *J* 8.8, 2CH, 3-H and 5-H).

Analysis by RP HPLC: Benzylamine eluted at 5.8 minutes. (HPLC / System A / Method 1 / Column 1 / A280nm).

2.3.1.3.2 Competition reaction between benzylamine and 4-hydrazinobenzoic acid for the active ester of 4-iodobenzoic acid

The active ester of 4-iodobenzoic acid (0.01 g, 0.03 mmol), benzylamine (3.17 µl, 0.003 g, 0.03 mmol) and 4-hydrazinobenzoic acid (HYBA) (0.005 g, 0.03 mmol).

δ_H 4-Iodobenzoic acid active ester (270 MHz; DMSO) 2.9 (4H, s, $2CH_2$, 9-H and 10-H), 7.64 (2H, d, *J* 8.8, 2CH, 2-H and 6-H), 7.96 (2H, d, *J* 8.8, 2CH, 3-H and 5-H).

δ_H 4-(N'-[4-Iodobenzoyl)hydrazino]benzoic acid (270 MHz; MeCN/D_2O) 6.75 (2H, d, *J* 8.8, 2CH, 12-H and 16-H), 7.61 (2H, d, *J* 8.8, 2CH, 3-H and 5-H), 7.71 (2H, d, *J* 8.8, 2CH, 2-H and 6-H), 7.83 (2H, d, *J* 8.8, 2CH, 13-H and 15-H), 9-H, 10-H and 18-H not observed.

δ_H Benzylamine (270 MHz; MeCN/D_2O) 3.80 (2H, s, CH_2, 7-H), 7.28-7.49 (5H, m, 5CH, 2, 3, 4, 5, 6-H).

Analysis by RP HPLC: HYBA eluted at 9.0 minutes, benzylamine eluted at 5.8 minutes, The unknown peaks eluted at 11.7, 6.3 and 2.5 minutes. (HPLC / System A / Method 1 / Column 1 / A280nm).

2.3.1.3.3 Reaction between 2-iodobenzaldehyde and benzylamine

2-Iodobenzaldehyde (0.01 g, 0.04 mmol) and benzylamine (4.69 µl, 0.005 g, 0.04 mmol).

δ_H Benzyl-(2-iodobenzylidene)-amine (270 MHz; MeCN/D_2O) 4.93 (2H, s, CH_2, 9-H), 7.18 (1H, t, *J* 8.3, 1CH, 3-H), 7.30 (1H, t, *J* 8.3, 1CH, 13-H), 7.32-7.58 (6H, m, 6CH, 4, 5, 11, 12, 14, 15-H), 8.18 (1H, d, *J* 8.3 1CH, 2-H), 8.69 (1H, s, 1CH, 7-H).

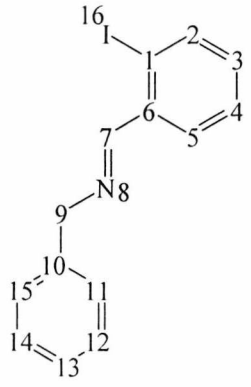

Figure 2.21 Benzyl-(2-iodobenzylidene)-amine

δ_H Benzylamine (270 MHz; MeCN/D_2O) 3.80 (2H, s, CH_2, 7-H), 7.28-7.49 (5H, m, 5CH, 2, 3, 4, 5, 6-H).

δ_H 2-Iodobenzaldehyde (270MHz; MeCN/D_20) 7.45 (1H, t, *J* 7.8, 1.7, CH, 5-H), 7.62 (1H, t, *J* 7.8, CH, 4-H), 7.90 (1H, d, *J* 7.8, 1.7, CH, 3-H), 8.15 (1H, d, *J* 7.8, CH, 6-H), 10.00 (1H, s, CHO, 9-H).

Analysis by RP HPLC: Benzyl-(2-iodobenzylidene)-amine eluted at 16.7 minutes, 2-iodobenzaldehyde eluted at 15.8 minutes. The unknown peaks present in HPLC eluted at 11.8, 12.8 and 14.4 minutes. (HPLC / System A / Method 1 / Column 1 / A280nm).

2.3.1.3.4 Competition reaction between benzylamine and 4-hydrazinobenzoic acid for 2-iodobenzaldehyde

2-Iodobenzaldehyde (0.01 g, 0.04 mmol), benzylamine (4.69 µl, 0.004 g, 0.04 mmol) and 4-hydrazinobenzoic acid (0.007 g, 0.04 mmol).

δ_H 4-[*N*'-(2-Iodobenzylidene)-hydrazino]-benzoic acid (270 MHz; MeCN/D_2O) 7.15 (1H, ovddd, *J* 1.7, 8.3 CH, 4-H), 7.20 (2H, d, *J* 8.9, 2CH, 11-H and 15-H), 7.50 (1H, ovdd, *J* 7.8, CH, 3-H) (behind benzylamine peak), 7.93 (2H, d, *J* 9.1, 2CH, 12-H and 14-H), 7.97 (1H, d, *J* 8.3 CH, 5-H), 8.18 (1H, dd, *J* 1.6, 7.8, CH, 2-H), 8.20 (1H, s, CH, 7-H), 9-H and 17-H not observed.

δ_H Benzylamine (270 MHz; MeCN/D_2O) 3.80 (2H, s, CH_2, 7-H), 7.28-7.49 (5H, m, 5CH, 2, 3, 4, 5, 6-H).

Analysis by RP HPLC: 4-[*N*'-(2-Iodobenzylidene)-hydrazino]-benzoic acid eluted at 16.7 minutes, HYBA eluted at 9.0 minutes and 2-iodobenzaldehyde eluted at 15.8 minutes. Several other unknown peaks were present by HPLC analysis. (HPLC / System A / Method 1 / Column 1 / A280nm).

2.3.1.3.5 Reaction between benzylamine and 4-fluorobenzaldehyde

4-Fluorobenzaldehyde (4.6 µl, 0.005 g, 0.04 mmol) and benzylamine (4.69 µl, 0.005 g, 0.04 mmol).

δ_H Benzyl-(4-fluorobenzylidene)-amine (270 MHz; MeCN/D_2O) 4.80 (2H, s, CH_2, 9-H), 7.30 (1H, t, *J* 8.6, CH, 13-H), 7.35-7.50 (6H, m, 6CH, 2, 6, 11, 12, 14, 15-H), 7.85 (2H, quartet, *J* 2.9, 8.6, 2CH, 3-H and 5-H), 8.52 (1H, s, CH, 7-H).

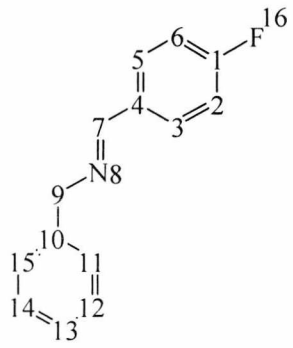

Figure 2.22 Benzyl-(4-fluorobenzylidene)-amine

δ_H 4-Fluorobenzaldehyde (270 MHz; MeCN/D_20) 7.40 (2H, t, *J* 8.8, 2CH, 2-H and 6-H), 8.10 (2H, quartet, *J* 3.0, 8.8, 2CH, 3-H and 5-H), 10.00 (1H, s, CHO, 8-H).

δ_H Benzylamine (270 MHz; MeCN/D_2O) 3.80 (2H, s, CH_2, 7-H), 7.28-7.49 (5H, m, 5CH, 2, 3, 4, 5, 6-H).

Analysis by RP HPLC: Benzyl-(4-fluorobenzylidene)-amine eluted at 16.1 minutes, benzylamine eluted at 5.8 minutes and 4-fluorobenzaldehyde eluted at 13.1 minute. (HPLC / System A / Method 1 / Column 1 / A280nm).

2.3.1.3.6 Competition reaction between benzylamine and 4-hydrazinobenzoic acid for 4-fluorobenzaldehyde

4-Fluorobenzaldehyde (4.61 µl, 0.04 mmol), benzylamine 4.69 µl, 0.04 mmol) and 4-hydrazinobenzoic acid (HYBA) (0.07 g, 0.04 mmol).

δ_H 4-[*N*'-(4-Fluorobenzylidene)-hydrazino]-benzoic acid (270 MHz; MeCN/D_2O) 7.23 (4H, overlapping doublet and triplet, *J* 9.0, 5.9, 4CH, 2-H, 6-H, 11-H, 15-H), 7.8 (2H, m, 2CH, 3-H and 5-H), 7.96 (2H, d, *J* 9.0, 2CH, 12-H and 14-H), 7.98 (1H, s, CH, 7-H), 9-H and 17-H not observed.

δ_H Benzylamine (270 MHz; MeCN/D_2O) 3.80 (2H, s, CH_2, 7-H), 7.28-7.49 (5H, m, 5CH, 2, 3, 4, 5, 6-H).

Analysis by RP HPLC: 4-[*N*'-(4-Fluorobenzylidene)-hydrazino]-benzoic acid eluted at 15.2 minutes, 4-fluorobenzaldehyde 13.1 minute, HYBA eluted at 9.0 minutes. The unknown peaks eluted at 11.3, 11.8 and 15.5 minutes. (HPLC / System A / Method 1 / Column 1 / A280nm).

2.3.1.3.7 Reaction between benzylamine and 4-bromobenzaldehyde

4-Bromobenzaldehyde (0.008 g, 0.04 mmol) and benzylamine (4.69 µl, 0.04 mmol).

δ_H Benzyl-(4-bromobenzylidene)-amine (270 MHz; MeCN/D_2O) 4.80 (2H, s,CH_2, 9-H), 7.32-7.50 (7H, m, 7CH, 3, 5, 11, 12, 13, 14, 15-H), 7.72 (2H, d, *J* 2.8, 2CH, 2-H and 6-H), 8.50 (1H, s, CH, 7-H).

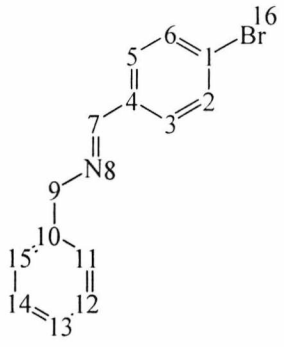

Figure 2.23 Benzyl-(4-bromobenzylidene)-amine

δ_H Benzylamine (270 MHz; MeCN/D_2O) 3.80 (2H, s, CH_2, 7-H), 7.28-7.49 (5H, m, 5CH, 2, 3, 4, 5, 6-H).

δ_H 4-Bromobenzaldehyde (270 MHz; MeCN/D_2O) 7.80 (2H, d, *J* 8.6, 2CH, 2-H and 6-H), 7.90 (2H, d, *J* 8.6, 2CH, 3-H and 5-H), 10.0 (1H, s, CHO, 8-H).

Analysis by RP HPLC: 4-Bromobenzaldehyde eluted at 15.2 minutes. The unknown peak present eluted at 13.9 minutes. This peak was also present in HPLC analysis of 4-bromobenzaldehyde starting material. (HPLC / System A / Method 1 / Column 1 / A280nm).

2.3.1.3.8 Competition reaction between benzylamine and 4-hydrazinobenzoic acid for 4-bromobenzaldehyde

4-Bromobenzaldehyde (0.008 g, 0.04 mmol), benzylamine (4.69 µl, 0.04 mmol) and 4-hydrazinobenzoic acid (HYBA) (0.07 g, 0.04 mmol).

δ_H 4-[*N*'-(4-Bromobenzylidene)-hydrazino]-benzoic acid (270 MHz; MeCN/D_2O) 7.22 (2H, d, *J* 8.9, 2CH, 11-H and 15-H), 7.63 (2H, d, *J* 8.9, 2CH, 3-H and 5-H), 7.69 (2H, d, *J* 8.9, 2CH, 2-H and 6-H), 7.97 (2H, d, *J* 8.9, 2CH, 12-H and 14-H), 7.99 (1H, s, 1CH, 7-H), H-9 and H-17 not observed.

δ_H Benzylamine (270 MHz; MeCN/D_2O) 3.80 (2H, s, CH_2, 7-H), 7.28-7.49 (5H, m, 5CH, 2, 3, 4, 5, 6-H).

Analysis by RP HPLC: 4-[*N*'-(4-Bromobenzylidene)-hydrazino]-benzoic acid eluted at 16.4 minutes, 4-bromobenzaldehyde eluted at 15.2 minutes. The unknown peak eluted at 13.9 minutes (possibly from 4-bromobenzaldehyde, see earlier discussion). (HPLC / System A / Method 1 / Column 1 / A280nm).

2.3.1.3.9 Reaction between benzylamine and 4-formylphenyl boronic acid

4-Formylphenyl boronic acid (0.006 g, 0.04 mmol) and benzylamine (4.69 µl, 0.04 mmol).

δ_H (Benzyl-(4-boronobenzylidene)-amine) (270 MHz; MeCN/D_2O) 4.80 (2H, s, CH_2, 9-H), 7.30–7.50 (5H, m, 5CH, 11, 12, 13, 14, 15-H), 7.80 (2H, d, *J* 8.8, 2CH, 2-H and 6-H), 7.90 (2H, d, *J* 8.8, 2CH, 3-H and 5-H), 8.57 (1H, s, CH, 7-H).

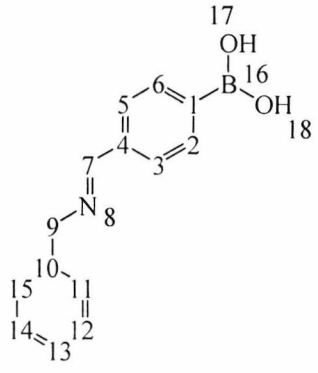

Figure 2.24 Benzyl-(4-boronobenzylidene)-amine

δ_H Benzylamine (270 MHz; MeCN/D_2O) 3.80 (2H, s, CH_2, 7-H), 7.28-7.49 (5H, m, 5CH, 2, 3, 4, 5, 6-H).

δ_H 4-Formylphenyl boronic acid (270 MHz;MeCN/D_20) 7.98 (2H, d, J 8.6, 2CH, 2-H and 6-H), 8.03 (2H, d, J 8.6, 2CH, 3-H and 5-H), 10.07 (1H, s, CHO, 8-H), H-11 and H-12 not observed.

Analysis by RP HPLC: Benzyl-(4-boronobenzylidene)-amine eluted at 13.8 minutes, 4-formylphenyl boronic acid eluted at 10.2 minutes. Benzyl-(4-bromobenzylidene)-amine was present 18% by peak area percent. (HPLC / System A / Method 1 / Column 1 / A280nm).

2.3.1.4.0 Competition reaction between benzylamine and 4-hydrazinobenzoic acid for 4-formylphenyl boronic acid

4-Formylphenyl boronic acid (0.006 g, 0.04 mmol), benzylamine (4.69 µl, 0.04 mmol) and 4-hydrazinobenzoic acid (HYBA) (0.007 g, 0.04 mmol).

δ_H 4-[N'-(4-Boronobenzylidene)hydrazino]-benzoic acid (270 MHz; MeCN/D_2O) 7.24 (2H, d, *J* 9.0, 2CH, 11-H and 15-H), 7.77 (2H, d, *J* 8.3, 2CH, 2-H and 6-H), 7.88 (2H, d, *J* 8.3, 2CH, 3-H and 5-H), 7.98 (2H, d, *J* 9.0, 2CH, 12-H and 14-H), 7.99 (1H, s, 1CH, 7-H), H-9, H-17, H-20 and H-21 not observed.

δ_H 4-Formylphenyl boronic acid (270 MHz;MeCN/D_20) 7.98 (2H, d, J 8.6, 2CH, 2-H and 6-H), 8.03 (2H, d, J 8.6, 2CH, 3-H and 5-H), 10.07 (1H, s, CHO, 8-H), H-11 and H-12 not observed.

δ_H Benzylamine (270 MHz; MeCN/D_2O) 3.80 (2H, s, CH_2, 7-H), 7.28-7.49 (5H, m, 5CH, 2, 3, 4, 5, 6-H).

δ_H HYBA (270 MHz; MeCN/D_2O) 6.97 (2H, d, *J* 8.8, 2CH, 2-H and 6-H), 7.52 (1H, s, NH, 10-H), 7.99 (2H, d, *J* 8.8, 2CH, 3-H and 5-H), H-8 and H-11 not observed.

Analysis by RP HPLC: 4-[N'-(4-Boronobenzylidene)hydrazino]-benzoic acid eluted at 13.9 minutes, 4-formylphenyl boronic acid eluted at 10.5 minutes. The unknown peaks eluted at 11.0, 11.4 and 14.4 minutes. (HPLC / System A / Method 1 / Column 1 / A280nm).

2.3.1.5 Competition reactions involving Fmoc-Lys-OH as the competing amine

The active ester of 4-iodobenzoic acid was not used in the competitions reactions involving Fmoc-Lys-OH as the competing amine.

2.3.1.5.1 Reaction between Fmoc-lysine-OH (Fmoc-Lys-OH) and 2-iodobenzaldehyde

2-Iodobenzaldehyde (0.01 g, 0.04 mmol) and Fmoc-Lys-OH (0.016 g, 0.04 mmol).

δ_H Fmoc-Lys-OH (270MHz; MeCN/D_20) 1.37 (2H, m, CH_2, 21-H), 1.68 (2H, m, CH_2 22-H), 2.05 under ACN peak (2H, m, CH_2, 20-H), 2.97 (2H, t, *J* 7.5, CH_2, 23-H), 3.97 (1H, t, *J* 7.5, CH, 1-H or 19-H), 4.32 under D_2O peak (1H, t, *J* 7.5, CH, 19-H or 1-H), 4.42 (2H, d, *J* 7.5, CH_2, 14-H), 7.44 (2H, t, *J* 1.3, 7.4, 2CH, 7-H and 11-H), 7.52 (2H, t, *J* 7.4, 2CH, 8-H and 12-H), 7.75 (2H, t, *J* 7.4, 2CH, 6-H and 10-H), 7.92 (2H, d, *J* 7.4, 2CH, 9-H and 13-H).

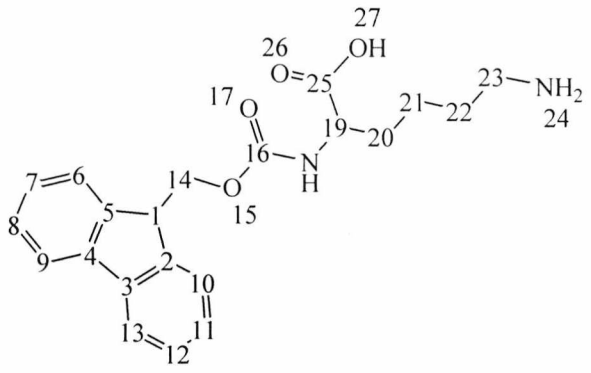

Figure 2.25 Fmoc-Lys-OH

δ_H 2-Iodobenzaldehyde (270MHz; MeCN/D_20) 7.45 (1H, t, *J* 7.8, 1.7, CH, 5-H), 7.62 (1H, t, *J* 7.8, CH, 4-H), 7.90 (1H, d, *J* 7.8, 1.7, CH, 3-H), 8.15 (1H, d, *J* 7.8, CH, 6-H), 10.00 (1H, s, CHO, 9-H).

Analysis by RP HPLC: Fmoc-Lys-OH eluted at 12.8 minutes and 2-iodobenzaldehyde eluted at 15.9 minutes. (HPLC / System A / Method 1 / Column 1 / A280nm).

2.3.1.5.2 Competition reaction between Fmoc-Lys-OH and 4-hydrazinobenzoic acid for 2-iodobenzaldehyde

2-Iodobenzaldehyde (0.01 g, 0.04 mmol), 4-hydrazinobenzoic acid (0.007 g, 0.04 mmol) and Fmoc-Lys-OH (0.016 g, 0.04 mmol).

δ_H 4-[*N*'-(2-Iodobenzylidene)-hydrazino]-benzoic acid (270 MHz; MeCN/D_2O) 7.15 (1H, ovddd, *J* 1.7, 7.8, CH, 4-H), 7.25 (2H, d, *J* 8.9, 2CH, 11-H and 15-H), 7.50 (1H, ovdd, *J* 7.8, CH, 3-H), 7.97 (1H, d, *J* 7.8, CH, 5-H), 7.98 (2H, d, *J* 8.9, 2CH, 12-H and 14-H), 8.05 (1H, dd, *J* 1.7, 7.8, CH, 2-H), 8.20 (1H, s, CH, 7-H), 9-H and 17-H not observed.

δ_H Fmoc-Lys-OH (270MHz; MeCN/D_20) 1.37 (2H, m, CH_2, 21-H), 1.68 (2H, m, CH_2 22-H), 2.05 under ACN peak (2H, m, CH_2, 20-H), 2.97 (2H, t, *J* 7.5, CH_2, 23-H), 3.97 (1H, t, *J* 7.5, CH, 1-H or 19-H), 4.32 under D_2O peak (1H, t, *J* 7.5, CH, 19-H or 1-H), 4.42 (2H, d, *J* 7.5, CH_2, 14-H), 7.44 (2H, t, *J* 1.3, 7.4, 2CH, 7-H and 11-H), 7.52 (2H, t, *J* 7.4, 2CH, 8-H and 12-H), 7.75 (2H, t, *J* 7.4, 2CH, 6-H and 10-H), 7.92 (2H, d, *J* 7.4, 2CH, 9-H and 13-H).

Analysis by RP HPLC: 4-[*N*'-(2-Iodobenzylidene)-hydrazino]-benzoic acid eluted at 16.7 minutes and Fmoc-Lys-OH eluted at 12.8 minutes. (HPLC / System A / Method 1 / Column 1 / A280nm). Product 27% by peak area percent.

2.3.1.5.3 Reaction between Fmoc-Lys-OH and 4-fluorobenzaldehyde

4-Fluorobenzaldehyde (4.61 µl, 0.04 mmol) and Fmoc-Lys-OH (0.016 g, 0.04 mmol).

δ_H 4-Fluorobenzaldehyde (270 MHz; MeCN/D_20) 7.40 (2H, t, *J* 8.8, 2CH, 2-H and 6-H), 8.10 (2H, quartet, *J* 3.0, 8.8, 2CH, 3-H and 5-H), 10.00 (1H, s, CHO, 8-H).

δ_H Fmoc-Lys-OH (270MHz; MeCN/D_20) 1.37 (2H, m, CH_2, 21-H), 1.68 (2H, m, CH_2 22-H), 2.05 under ACN peak (2H, m, CH_2, 20-H), 2.97 (2H, t, *J* 7.5, CH_2, 23-H), 3.97 (1H, t, *J* 7.5, CH, 1-H or 19-H), 4.32 under D_2O peak (1H, t, *J* 7.5, CH, 19-H or 1-H), 4.42 (2H, d, *J* 7.5, CH_2, 14-H), 7.44 (2H, t, *J* 1.3, 7.4, 2CH, 7-H and 11-H), 7.52 (2H, t, *J* 7.4, 2CH, 8-H and 12-H), 7.75 (2H, t, *J* 7.4, 2CH, 6-H and 10-H), 7.92 (2H, d, *J* 7.4, 2CH, 9-H and 13-H).

Analysis by RP HPLC: Fmoc-Lys-OH eluted at 12.8 minutes and 4-fluorobenzaldehyde eluted at 13.2 minutes. (HPLC / System A / Method 1 / Column 1 / A280nm).

2.3.1.5.4 Competition reaction between Fmoc-Lys-OH and 4-hydrazinobenzoic acid for 4-fluorobenzaldehyde

4-Fluorobenzaldehyde (4.61 µl, 0.04 mmol), 4-hydrazinobenzoic acid (0.007 g, 0.04 mmol) and Fmoc-Lys-OH (0.016 g, 0.04 mmol).

δ_H 4-[*N*'-(4-Fluorobenzylidene)-hydrazino]-benzoic acid (270 MHz; MeCN/D_2O) 7.23 (4H, overlapping doublet and triplet, *J* 9.0, 5.9, 4CH, 2-H, 6-H, 11-H, 15-H), 7.80 (2H, m, 2CH, 3-H and 5-H), 7.96 (2H, d, *J* 9.0, 2CH, 12-H and 14-H), 7.98 (1H, s, CH, 7-H), 9-H and 17-H not observed.

δ_H Fmoc-Lys-OH (270MHz; MeCN/D_20) 1.37 (2H, m, CH_2, 21-H), 1.68 (2H, m, CH_2 22-H), 2.05 under ACN peak (2H, m, CH_2, 20-H), 2.97 (2H, t, *J* 7.5, CH_2, 23-H), 3.97 (1H, t, *J* 7.5, CH, 1-H or 19-H), 4.32 under D_2O peak (1H, t, *J* 7.5, CH, 19-H or 1-H), 4.42 (2H, d, *J* 7.5, CH_2, 14-H), 7.44 (2H, t, *J* 1.3, 7.4, 2CH, 7-H and 11-H), 7.52 (2H, t, *J* 7.4, 2CH, 8-H and 12-H), 7.75 (2H, t, *J* 7.4, 2CH, 6-H and 10-H), 7.92 (2H, d, *J* 7.4, 2CH, 9-H and 13-H).

Analysis by RP HPLC: 4-[*N*'-(4-Fluorobenzylidene)-hydrazino]-benzoic acid eluted at 15.3 minutes and Fmoc-Lys-OH eluted at 12.8 minutes. (HPLC / System A / Method 1 / Column 1 / A280nm). Product 11% by peak area percent.

2.3.1.5.5 Reaction between Fmoc-Lys-OH and 4-bromobenzaldehyde

4-Bromobenzaldehyde (0.008 g, 0.04 mmol) and Fmoc-Lys-OH (0.016 g, 0.04 mmol).

δ_H 4-Bromobenzaldehyde (270 MHz; MeCN/D_2O) 7.80 (2H, d, *J* 8.6, 2CH, 2-H and 6-H), 7.90 (2H, d, *J* 8.6, 2CH, 3-H and 5-H), 10.0 (1H, s, CHO, 8-H).

δ_H Fmoc-Lys-OH (270MHz; MeCN/D_20) 1.37 (2H, m, CH_2, 21-H), 1.68 (2H, m, CH_2 22-H), 2.05 under ACN peak (2H, m, CH_2, 20-H), 2.97 (2H, t, *J* 7.5, CH_2, 23-H), 3.97 (1H, t, *J* 7.5, CH, 1-H or 19-H), 4.32 under D_2O peak (1H, t, *J* 7.5, CH, 19-H or 1-H), 4.42 (2H, d, *J* 7.5, CH_2, 14-H), 7.44 (2H, t, *J* 1.3, 7.4, 2CH, 7-H and 11-H), 7.52 (2H, t, *J* 7.4, 2CH, 8-H and 12-H), 7.75 (2H, t, *J* 7.4, 2CH, 6-H and 10-H), 7.92 (2H, d, *J* 7.4, 2CH, 9-H and 13-H).

Analysis by RP HPLC: Fmoc-Lys-OH Eluted at 12.8 minutes and 4-bromrobenzaldehyde eluted at 15.2 minutes. (HPLC / System A / Method 1 / Column 1 / A280nm).

2.3.1.5.6 Competition reaction between Fmoc-Lys-OH and 4-hydrazinobenzoic acid for 4-bromobenzaldehyde

4-Bromobenzaldehyde (0.008 g, 0.04 mmol), 4-hydrazinobenzoic acid (0.007 g, 0.04 mmol) and Fmoc-Lys-OH (0.016 g, 0.04 mmol).

δ_H 4-[*N*'-(4-Bromobenzylidene)-hydrazino]-benzoic acid (270 MHz; MeCN/D_2O) 7.22 (2H, d, *J* 8.9, 2CH, 11-H and 15-H), 7.63 (2H, d, *J* 8.9, 2CH, 3-H and 5-H), 7.69 (2H, d, *J* 8.9, 2CH, 2-H and 6-H), 7.97 (2H, d, *J* 8.9, 2CH, 12-H and 14-H), 7.99 (1H, s, 1CH, 7-H), H-9 and H-17 not observed.

δ_H Fmoc-Lys-OH (270MHz; MeCN/D_20) 1.37 (2H, m, CH_2, 21-H), 1.68 (2H, m, CH_2 22-H), 2.05 under ACN peak (2H, m, CH_2, 20-H), 2.97 (2H, t, *J* 7.5, CH_2, 23-H), 3.97 (1H, t, *J* 7.5, CH, 1-H or 19-H), 4.32 under D_2O peak (1H, t, *J* 7.5, CH, 19-H or 1-H), 4.42 (2H, d, *J* 7.5, CH_2, 14-H), 7.44 (2H, t, *J* 1.3, 7.4, 2CH, 7-H and 11-H), 7.52 (2H, t, *J* 7.4, 2CH, 8-H and 12-H), 7.75 (2H, t, *J* 7.4, 2CH, 6-H and 10-H), 7.92 (2H, d, *J* 7.4, 2CH, 9-H and 13-H).

Analysis by RP HPLC: Fmoc-Lys-OH eluted at 12.8 minutes. (HPLC / System A / Method 1 / Column 1 / A280nm).

2.3.1.5.7 Reaction between Fmoc-Lys-OH and 4-formylphenyl boronic acid

4-Formylphenyl boronic acid (0.006 g, 0.04 mmol) and Fmoc-Lys-OH (0.016 g, 0.04 mmol).

δ_H 4-Formylphenyl boronic acid (270 MHz;MeCN/$D_2$0) 7.98 (2H, d, J 8.6, 2CH, 2-H and 6-H), 8.03 (2H, d, J 8.6, 2CH, 3-H and 5-H), 10.07 (1H, s, CHO, 8-H), H-11 and H-12 not observed.

δ_H Fmoc-Lys-OH (270MHz; MeCN/$D_2$0) 1.37 (2H, m, CH_2, 21-H), 1.68 (2H, m, CH_2 22-H), 2.05 under ACN peak (2H, m, CH_2, 20-H), 2.97 (2H, t, *J* 7.5, CH_2, 23-H), 3.97 (1H, t, *J* 7.5, CH, 1-H or 19-H), 4.32 under D_2O peak (1H, t, *J* 7.5, CH, 19-H or 1-H), 4.42 (2H, d, *J* 7.5, CH_2, 14-H), 7.44 (2H, t, *J* 1.3, 7.4, 2CH, 7-H and 11-H), 7.52 (2H, t, *J* 7.4, 2CH, 8-H and 12-H), 7.75 (2H, t, *J* 7.4, 2CH, 6-H and 10-H), 7.92 (2H, d, *J* 7.4, 2CH, 9-H and 13-H).

Analysis by RP HPLC: Fmoc-Lys-OH eluted at 12.8 minutes and 4-formylphenyl boronic acid eluted at 9.9 minutes. (HPLC / System A / Method 1 / Column 1 / A280nm).

2.3.1.5.8 Competition reaction between 4-formylphenyl boronic acid, Fmoc-Lys-OH and 4-hydrazinobenzoic acid

4-Formylphenyl boronic acid (0.006 g, 0.04 mmol), 4-hydrazinobenzoic acid (0.007 g, 0.04 mmol) and Fmoc-Lys-OH (0.016 g, 0.04 mmol).

δ_H 4-[N'-(4-Boronobenzylidene)hydrazino]-benzoic acid (270 MHz; MeCN/D_2O) 7.24 (2H, d, *J* 9.0, 2CH, 11-H and 15-H), 7.77 (2H, d, *J* 8.3, 2CH, 2-H and 6-H), 7.88 (2H, d, *J* 8.3, 2CH, 3-H and 5-H), 7.98 (2H, d, *J* 9.0, 2CH, 12-H and 14-H), 7.99 (1H, s, 1CH, 7-H), H-9, H-17, H-20 and H-21 not observed.

δ_H Fmoc-Lys-OH (270MHz; MeCN/$D_2$0) 1.37 (2H, m, CH_2, 21-H), 1.68 (2H, m, CH_2 22-H), 2.05 under ACN peak (2H, m, CH_2, 20-H), 2.97 (2H, t, *J* 7.5, CH_2, 23-H), 3.97 (1H, t, *J* 7.5, CH, 1-H or 19-H), 4.32 under D_2O peak (1H, t, *J* 7.5, CH, 19-H or 1-H), 4.42 (2H, d, *J* 7.5, CH_2, 14-H), 7.44 (2H, t, *J* 1.3, 7.4, 2CH, 7-H and 11-H), 7.52 (2H, t, *J* 7.4, 2CH, 8-H and 12-H), 7.75 (2H, t, *J* 7.4, 2CH, 6-H and 10-H), 7.92 (2H, d, *J* 7.4, 2CH, 9-H and 13-H).

Analysis by RP HPLC: Fmoc-Lys-OH eluted at 12.8 minutes. (HPLC / System A / Method 1 / Column 1 / A280nm).

2.4 Reactions monitoring the rate of formation of the hydrazone

Reactions monitoring the rate of reaction between 2-iodobenzaldehyde or 4-fluorobenzaldehyde and HYBA in the presence of the competing amine benzylamine were carried out to assess the speed of the reaction between the aromatic aldehyde and HYBA. The reactions were carried out in 0.5 M ammonium formate buffer pH 4.5/acetonitrile (1:1 v/v, 100 cm^3 total volume) at room temperature and at 50°C.

The samples were prepared for HPLC analysis by taking approximately 0.5 ml from the reaction mixture and diluting this with approximately 1.5 mls of an ACN/H_2O mix (1:1 v/v). Samples were taken and analysed (immediately) every fifteen minutes for 2 hours.

2.4.1 Rate-monitoring competition reaction between HYBA and benzylamine for 4-fluorobenzaldehyde

At room temperature and 50°C: 4-fluorobenzaldehyde (93 µl, 0.87 mmol), benzylamine (94.8 µl, 0.87 mmol) and HYBA (0.13 g, 0.87 mmol) were added to a round bottom flask and treated as described above.

2.4.2 Rate-monitoring competition reaction between HYBA and benzylamine for 2-iodobenzaldehyde

At room temperature and 50°C: 2-iodobenzaldehyde (0.20 g, 0.87 mmol), benzylamine (94.8 µl, 0.87 mmol) and HYBA (0.13 g, 0.87 mmol) were added to a round bottom flask and treated as described above.

2.5 Results and discussion

2.5.1 Synthesis

During the synthesis of 4-iodobenzoic acid, reaction mixture was spilt at the nitrogen evolution stage, causing the low yield of 20%. As the reaction was carried out on a large scale, there was enough product formed for the next reaction despite the low yield.

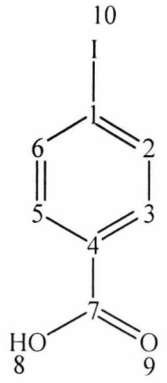

Figure 2.26 4-Iodobenzoic acid

In the ^{1}HNMR spectrum of 4-iodobenzoic acid, protons 2 and 6 are in the same chemical environment because the benzene ring is a symmetrical *para*-substituted ring. There is one doublet peak for the protons in the 2 and 6 positions. The same is true for the protons in the 3 and 5 positions. The iodine and the carboxylic acid substituents on the ring are both electronegative and take electron density away from the benzene ring. This has the effect of moving the peaks for the protons 2, 6, 3 and 5 to a higher chemical shift than protons in an unsubstituted benzene ring would appear. The coupling constants for 2 and 6 are the same as those for 3 and 5 (both 8.6) demonstrating that these protons are coupled to each other i.e. 5 to 6 and 2 to 3. The carboxylic acid group is more electron withdrawing than iodine and so the protons 2 and 6 are at a lower chemical shift (7.7 ppm) than protons 3 and 5 (7.9 ppm). The carboxylic acid proton did not appear in the ^{1}H NMR spectrum. Protons in carboxylic acids, hydroxyls, primary or secondary amines do not always give a good signal due to exchange with trace amounts of water in the deuterated solvent, which has the effect of broadening the peak. Delta values are concentration dependent.

The ^{13}C NMR spectrum shows the protons 2 and 6 at a lower chemical shift (131 ppm) than 3 and 5 (137.5 ppm) for the reasons stated above. The ipso carbon at position 1 comes at a higher chemical shift than that of C-4 (130 ppm and 101 ppm respectively) as the carboxylic acid group has the effect of withdrawing electron density away from the *ortho-* and *para-* positions as shown in the diagram below illustrating resonance structures.

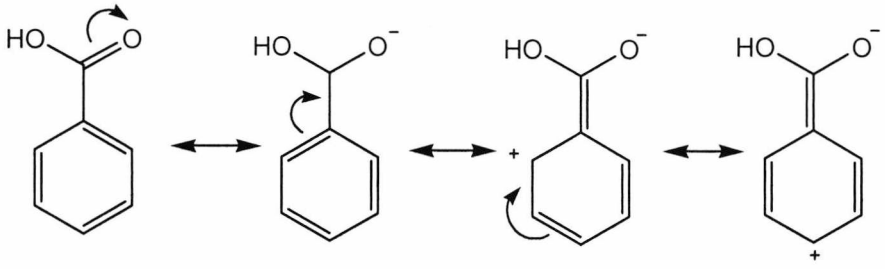

Figure 2.27 Mesomeric effects of an electron withdrawing group; resonance structures

The carboxylic acid carbon at position 7 (167 ppm) comes at the highest chemical shift as it is near two oxygen atoms which are electron withdrawing.

As with all the IR spectra discussed in this chapter, not every peak present in the IR spectra have been noted, rather enough peaks to be sure the correct functional groups were present in the spectrum for each compound. The IR spectrum showed a peak at 2830 cm^{-1} characteristic of an OH stretch, a peak at 1933 cm^{-1} assigned as the C-H stretch of an aryl compound and a carbonyl stretch at 1675 cm^{-1} typical of an acid. The exact mass of the 4-iodobenzoic acid is 247.93. In the mass spectrum, the molecular ion $[M - H]^-$ gave a peak at 246.8. Purity according to HPLC analysis was 98% by peak area percent.

4-Iodobenzoic acid 2,5, dioxo-pyrrolidin-1-yl ester (active ester of 4-iodobenzoic acid referred to as IBAE) was synthesised with a yield of 67%. The ^1H NMR spectrum for IBAE shows the succinimidyl CH_2 protons gave rise to a peak at 2.9 ppm. The 2 CH_2 groups are in an identical chemical environment and give rise to one peak; a singlet. The protons in the 2 and 6 positions and those in the 3 and 5 positions are at similar chemical shifts to the same protons discussed above for the ^1H NMR spectrum of 4-iodobenzoic acid (7.85 ppm and 8.08 ppm respectively).

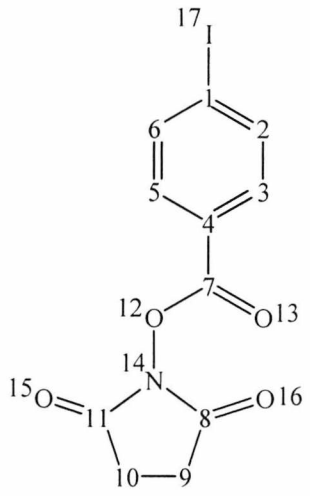

Figure 2.28 Active ester of 4-iodobenzoic acid (IBAE)

In the ^{13}C NMR spectrum, the protons in the positions 2, 6, 3 and 5 give peaks at similar chemical shifts to those found for 4-iodobenzoic acid (C-2 and 6 are found at 135 ppm and C-3 and 5 at 145 ppm). The ipso carbons 1 and 4 are again found at very similar chemical shifts to those for 4-iodobenzoic acid for the same reasons as given above (105 ppm for C-4 and 125 ppm for C-1). C-7 is also at a similar chemical shift to C-7 in the ^{13}C NMR spectrum of 4-iodobenzoic acid (170 ppm). The two succinimidyl CH_2 (C- 9 and 10) carbons come at a low chemical shift of 25 ppm. The two succinimidyl C=O carbons give a singlet at 165 ppm, as they are carbonyl carbons and so are deshielded.

The IR spectrum showed functional groups at 1767 cm^{-1} for an C=O ester stretch, 1717 cm^{-1} for a ketone stretch and at 1202 cm^{-1} and 1013 cm^{-1} for a C-O ester stretch. The mass spectrum showed the expected ion of 343.9 for $[M - H]^-$. Purity according to HPLC analysis was 93% by peak area percent. The purity was considered high enough to use the product IBAE in the competition reactions. Purifying IBAE further would have meant using preparative HPLC, which was considered unnecessary for the purposes for which it was to be used.

4-Amino butyric acid methyl ester (ABAME) was synthesised with a yield of 74%.

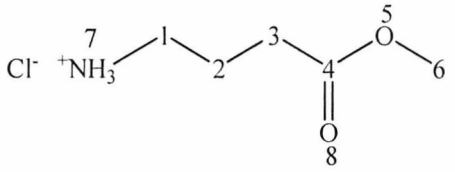

Figure 2.29 4-Aminobutyric acid methyl ester (ABAME)

In the ^{1}H NMR spectrum, the methylene group in position 2 is at the lowest chemical shift at 2.28 ppm. This CH_2 is in the middle of two other CH_2 groups, whereas the CH_2 in position 3 is next to an ester group and so is found at a higher chemical shift (2.85 ppm) as the carbonyl group is electronegative and so draws electron density away from the CH_2 group. The CH_2 protons in position 1 are next to the amine. The nitrogen in the amine is positively charged and therefore has no lone pair, meaning the nitrogen (an electronegative atom), draws away electron density. The methyl group is next to the oxygen and so is shifted to a higher chemical shift as the electronegative oxygen pulls electron density towards itself. This causes a large shift to a higher chemical shift for the methyl group due to the strongly electronegative oxygen atom. Typically a methyl group next to a CH_2 or CH may be found at around 1 ppm, this CH_3 group is at 4.05 ppm because of the effect of the oxygen atom.

In the ^{13}C NMR spectrum, the carbons give peaks in the same order as the corresponding protons for the same reasons. The carbonyl carbon is found at 172 ppm. This carbon is next to an oxygen atom, but has no protons attached to it and therefore less electron density than the carbon at position 6. It feels more of the magnetic field and so is present at a very high chemical shift. D_2O was used as a ^{1}HNMR solvent as ABAME would not dissolve in DMSO. ACN/D_2O was used as a ^{13}CNMR solvent to carry out the NMR to give a solvent reference peak as tetramethylsilane (TMS) is not soluble in D_2O.

The IR spectrum showed the functional groups 3011 cm^{-1} for an amine stretch, 2951 cm^{-1} for a C-H stretch, 1724 cm^{-1} for a C=O ester stretch with 1208 and 1153 cm^{-1} being typical of a C-O ester stretch. The mass spectrum gave a molecular ion peak $[M + H]^{+}$ of 118.0. The exact mass for ABAME is 117.08 therefore the correct molecular ion was present. HPLC analysis showed one peak representing 97% of the total area.

4-[*N*'-(2-Iodobenzylidene)-hydrazino]-benzoic acid was synthesised with a yield of 72%. The ^{1}H NMR spectrum shows the *para-* substituted benzene ring from the HYBA moiety in a typical pattern of two doublets representing two hydrogens each. *Para*-substituted benzene rings have a plane of symmetry and atoms on either side of this plane are in identical chemical environments and give rise to one peak only. The peak is a doublet because of the adjacent hydrogen atom causing splitting of the peak. The *ortho*-substituted benzene ring has no plane of symmetry and so individual signals are seen for each of the four hydrogens in the ring.

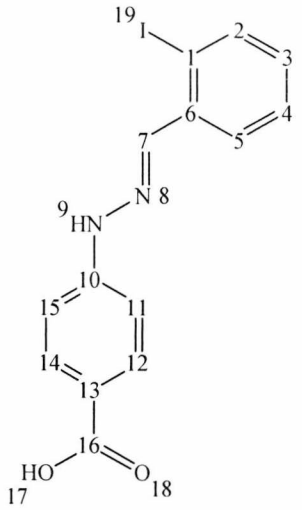

Figure 2.30 4-[*N*'-(2-Iodobenzylidene)-hydrazino]-benzoic acid

In the ^{1}H NMR spectrum, at 7.25 ppm protons 11 and 15 give rise to a doublet, at 7.98 ppm protons 12 and 14 also give rise to a doublet. The protons nearest the amine (15 and 11) are shielded by electron donation into the ring by the nitrogen lone pair as shown in the diagram below.

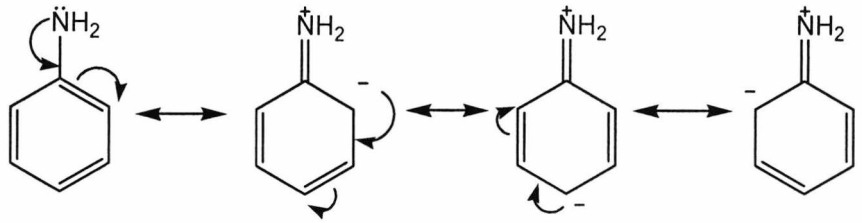

Figure 2.31 Mesomeric effects of an electron donating group; resonance structures

In contrast, the protons nearest to the carboxylic acid (12 and 14) have electron density taken away by the carboxylic acid group. Protons 3 and 4 are next to each other and to CH groups on the other side and so are more shielded than the protons 2 and 5 that are next to carbon atoms with no hydrogens attached. H-3 and H-4 are therefore at a lower chemical shift in the ^{1}H NMR spectrum (7.50 ppm and 7.15 ppm respectively) than H-2 and H-5 (8.05 ppm and 7.97 ppm respectively). The N-H and O-H protons are not seen. The proton in position 7 has a double bond with an electronegative nitrogen and this has the effect of making that proton come into resonance at a higher frequency. The double bond produces local inductive effects that cause π electrons in double bonds to circulate creating an induced magnetic field that reinforces the external magnetic field The protons will therefore have a higher chemical shift as the magnetic field felt by them is larger. This effect is called diamagnetic anisotropy and is the reason hydrogen atoms in aromatic rings are found at such high chemical shifts.

In the ^{13}C NMR spectrum, the carbon atoms with attached hydrogens mirror the ^{1}H spectrum for the reasons stated above. The ipso carbon (quaternary carbon) C-1 is next to an iodine atom, which is electronegative. The carbon C-13 is in a *para-* position to the amine in the benzene ring derived from HYBA. The amine group will donate electron density causing the carbon atom to have a lower chemical shift (130.1ppm) than for the C-10 (141.5 ppm) which is in a *para-* position to the carboxylic acid and so has electron density removed from it causing it to appear at a higher chemical shift. The carbon in position 6 is next to the HC=N carbon and so appears at a high chemical shift (139.2 ppm), but not as high as C-7 which therefore appears at a higher chemical shift than C-6 (C-7 148.2 ppm). C-10, as it is para to the carboxylic acid which has an electron withdrawing effect, is highly shifted. The electronegativity of the carboxylic acid group means that the carbon in position 16 is the most highly shifted of all the carbon atoms in the molecule (167.5ppm).

The IR spectrum showed the functional groups. 3323 cm^{-1} for an N-H stretch, 2960 cm^{-1} for an OH stretch typical of an acid, 1668 cm^{-1} for an acid carbonyl stretch and 1603 cm^{-1} for an imine C=N stretch. The exact mass is 365.99. The mass spectrum showed the molecular ion $[M + H]^{+}$ 367.1 100% intensity and a dimer ion at 75% of the intensity. A dimer is two molecules joined together in a complex. HPLC analysis gave a single peak which shows that the product 4-[*N*'-(2-iodobenzylidene)-hydrazino]-benzoic acid is analytically pure (>98%). The elemental analysis results are within 0.3% of the expected results which is the accepted standard imposed by Royal Society of Chemistry (RSC) journals for demonstration of purity.

4-[*N*'-(4-Fluorobenzylidene)-hydrazino]-benzoic acid was synthesised with a yield of 45%. In the ^{1}H spectrum, the protons in positions 11 and 15 (at 7.23 ppm) are seen as a doublet as expected for reasons already discussed.

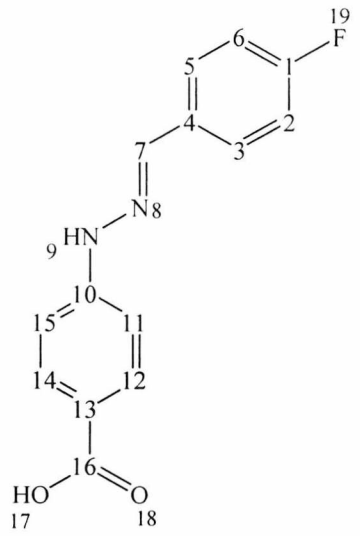

Figure 2.32 4-[*N*'-(4-Fluorobenzylidene)-hydrazino]-benzoic acid

Protons 2 and 6 are split further into a triplet. This is due to the effect of the fluorine causing further splitting of what would otherwise be expected to be a doublet peak. All nuclei with an odd number of protons (e.g. ^{1}H, ^{2}H, ^{14}N, ^{19}F, ^{31}P) and all nuclei with an odd number of neutrons (^{13}C) show magnetic properties. ^{19}F has a spin of ½ and so is NMR active. Nuclei with an even number of protons and neutrons do not have magnetic properties so are NMR inactive. Protons 3 and 5 are at a higher frequency of 7.80 ppm. The proximity of the CH=N proton causes electron density to be withdrawn from the protons 3 and 5, but this is seen to greater effect with protons 12 and 14 (at 7.96 ppm) that have a higher chemical shift than 3-H and 5-H shift due to the proximity of the carboxylic acid group. As for 4-[*N*'-(2-iodobenzylidene)-hydrazino]-benzoic acid, proton 7 comes at around 8 ppm (7.98 ppm). Protons 9 and 17 were not observed.

Carbon atoms 10 and 13 follow the explanation given above for 4-[*N*'-(2-iodobenzylidene)-hydrazino]-benzoic acid. The carbons with attached hydrogens, as for 4-[*N*'-(2-iodobenzylidene)-hydrazino]-benzoic acid, replicate the ^{1}H spectrum in explanation of position on the ^{13}C spectrum. C-4 is at 121 ppm and C-1 at 160.5 ppm. C-1 is para to the CH=N carbon and the effect is that electron density is withdrawn from C-1. C-4 therefore appears at a lower chemical shift.

The IR spectrum showed the functional groups at 3315cm^{-1} for an N-H stretch, 2971 cm^{-1} for the OH stretch of an acid, 1660 cm^{-1} for the carbonyl stretch of an acid and 1599 cm^{-1} for an imine C=N stretch. The mass spectrum showed the molecular ion $[M + H]^{+}$ 259.2 which is in agreement with the exact mass of 258.08. HPLC analysis gave a single peak which shows that

the product 4-[*N*'-(4-fluorobenzylidene)-hydrazino]-benzoic acid is analytically pure (>98%). The elemental analysis results were not quite within 0.3% of the expected results as the % carbon differed from the expected result by 0.4%.

4-[*N*'-(4-Bromobenzylidene)-hydrazino]-benzoic acid was synthesised with a yield of 58%. The protons 11 and 15 are at the lowest chemical shift in the ^{1}H NMR spectrum, this is for reasons explained in the discussion for 4-[*N*'-(2-iodobenzylidene)-hydrazino]-benzoic acid.

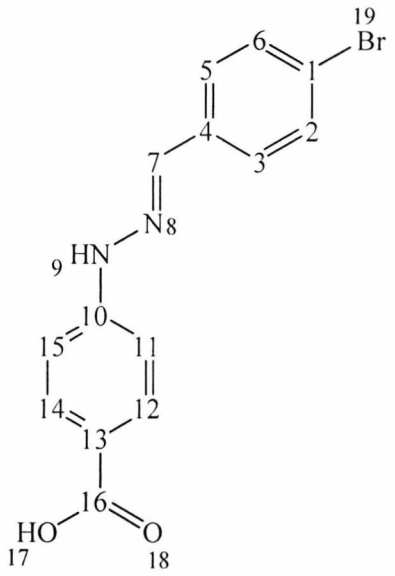

Figure 2.33 4-[*N*'-(4-Bromobenzylidene)-hydrazino]-benzoic acid

The protons 2 and 6 near the bromine atom come at a higher chemical (7.69 ppm) shift than 3 and 5 (7.63 ppm). The electronegative inductve effect of the bromine is the same as for other electronegative groups or atoms (e.g. F, I) and it has the effect of drawing electron density away from the ring in the *ortho-* and *para-* positions, due to mesomeric effects. The electronegative mesomeric effect of the bromine atom is greater than for the HC=N on the opposite side of the ring meaning that the protons 5 and 3 come at a lower frequency than 2 and 6. Protons in positions 12 and 14 (7.97 ppm) are affected by the carboxylic acid moiety as demonstrated in the figure 2.21. This effect is greater in the strongly electron withdrawing carboxylic acid group than for the bromine or the HC=N, the protons in positions 12 and 14 are at the highest chemical shift of all the aromatic protons. The proton in position 7 is again at the highest chemical shift (7.99 ppm). Protons 9 and 17 were not observed.

In the ^{13}CNMR spectrum, the carbon atoms with hydrogen atoms attached are positioned in the same order and their positioning within the spectrum is explained in the same way as the

^{1}H NMR spectrum. Carbon atoms 10, 13, 7 and 16 follow the explanation given above for 4-[*N*'-(2-iodobenzylidene)-hydrazino]-benzoic acid. C1 and C-4 although the chemical shifts are different (C-4 121.5 ppm, C-1 134.5 ppm), follow the explanation given for 4-[*N*'-(4-fluorobenzylidene)-hydrazino]-benzoic acid above.

The IR spectrum showed the following functional groups 3280 cm^{-1} N-H stretch, 2971 cm-1 OH stretch of an acid, 1651 cm-1 C=O stretch of an acid and 1591 cm-1 corresponding to an imine C=N stretch. The mass spectrum showed the expected mass. Bromine has two stable isotopes, ^{79}Br and ^{81}Br. These two isotopes have a natural abundance of approximately 50:50. The exact mass is 318.0. In the mass spectrum two molecular ions are seen [M + H] $^{+}$ 319.1 and 321.2, 98% intensity and 100% intensity respectively. These two molecular ions are two mass units apart. This is typical of a mass spectrum of a molecule containing a bromine atom. HPLC analysis gave a single peak which shows that the product 4-[*N*'-(4-bromobenzylidene)-hydrazino]-benzoic acid is analytically pure (>98%). The elemental analysis results are within 0.3% of the expected results which is a good demonstration of purity.

4-[N'-(4-Boronobenzylidene)hydrazino]-benzoic acid was synthesised with a yield of 82%.

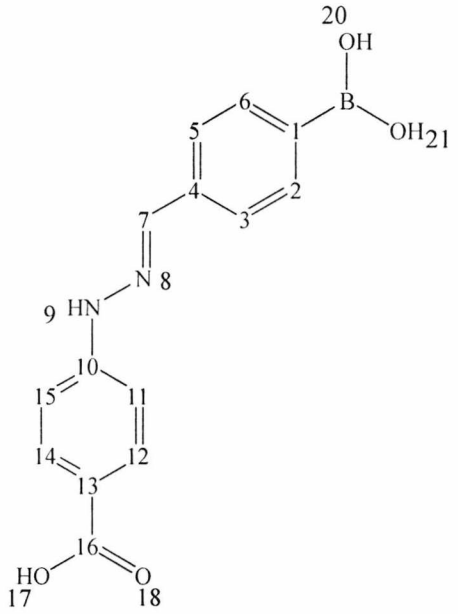

Figure 2.34 4-[N'-(4-Boronobenzylidene)hydrazino]-benzoic acid

Protons in positions 11 and 15 come at the lowest chemical shift (7.24 ppm). Protons 2 and 6, as the boronic acid group is not quite as electron withdrawing as the HC=N group, come at 7.77 ppm. Protons 3 and 5 are found at a higher chemical shift (7.88 ppm) due to their proximity of the HC=N which is electron withdrawing by the same mechanism shown for a

carboxylic acid group, although not as strongly. Protons 12 and 14 have the highest chemical shift of 7.98 ppm. Protons 9, 17, 20 and 21 were not observed.

In the ^{13}C NMR spectrum, the carbon atoms with hydrogens attached are positioned in the same order and their positioning within the spectrum is explained in the same way as the ^{1}H NMR spectrum. Carbon atoms 10, 13, 7 and 16 follow the explanation given above for 4-[*N*'-(2-iodobenzylidene)-hydrazino]-benzoic acid. C1 and C4 come very close together in the ^{13}C spectrum at 128.5 ppm and 129.5 ppm respectively.

The IR spectrum showed the following functional groups at 3308 cm^{-1} relating to an N-H stretch, at 2972 cm^{-1} the OH stretch of an acid, 1672 cm^{-1} the C=O stretch of an acid and at 1604 cm^{-1} and 1591 cm^{-1} the C=N stretch of an imine. The HPLC analysis showed 4-[N'-(4-boronobenzylidene)hydrazino]-benzoic acid to be analytically pure (>98%), although the elemental analysis did not show a pure compound as the nitrogen was 0.9% from the expected result. It has been noted that occasionally samples subjected to elemental analysis show a marked difference between the duplicates (up to 1% difference has been seen) and therefore, generally speaking, although good results have been obtained for the other compounds subjected to elemental analysis in this chapter, it is difficult to know how much weight to put on elemental analysis results. In this case, the HPLC analysis result was taken as evidence for the 4-[N'-(4-boronobenzylidene)hydrazino]-benzoic acid to be pure enough for use as a standard. The exact mass is 284.10 is and the mass spectra showed the expected molecular ion $[M + H]^{+}$ 285.1044 at 100% intensity.

2.6 Competition Reactions

2.6.1 Competition reactions with ABAME as the competing amine

The reactions carried out were as follows:

i) Aromatic aldehyde* or IBAE + HYBA

ii) Aromatic aldehyde or IBAE + ABAME

iii) Aromatic aldehyde or IBAE + HYBA + ABAME

iv) Aromatic aldehyde or IBAE + HYBA + ABAME (3 equivalents)

*Where aromatic aldehyde is 2-iodobenzaldehyde, 4-fluorobenzaldehyde, 4-bromobenzaldehyde or 4-formylphenylboronic acid.

In reaction iv) ten equivalents of ABAME would have ideally been used to show chemoselectivity relevant to a clinical setting. ABAME was not soluble enough to allow this quantity to be used, therefore three equivalents were used.

2.6.2 Competition reactions with benzylamine (BA) as the competing amine

The reactions carried out were as follows:

i) Aromatic aldehyde* or IBAE + HYBA

ii) Aromatic aldehyde or IBAE + BA

iii) Aromatic aldehyde or IBAE + HYBA + BA

iv) Aromatic aldehyde or IBAE + HYBA + BA (10 equivalents)

*Where aromatic aldehyde is 2-iodobenzaldehyde, 4-fluorobenzaldehyde, 4-bromobenzaldehyde or 4-formylphenylboronic acid.

In reaction iv) ten equivalents of BA were used to show chemoselectivity relevant to a clinical setting.

2.6.3 Competition reactions with 2-(((9H-fluoren-9-yl)methoxy)carbonylamino)-6-aminohexanoic acid (Fmoc-Lys-OH) as the competing amine

The reactions carried out were as follows:

i) Aromatic aldehyde* + HYBA

ii) Aromatic aldehyde + Fmoc-Lys-OH

iii) Aromatic aldehyde + HYBA + Fmoc-Lys-OH

*Where aromatic aldehyde is 2-iodobenzaldehyde, 4-fluorobenzaldehyde, 4-bromobenzaldehyde or 4-formylphenylboronic acid.

Excess equivalents of Fmoc-Lys-OH were not used in this instance as this Fmoc-Lys-OH was insoluble in greater concentrations than those used. The active ester of 4-iodobenzoic acid was not used in the competition reactions involving Fmoc-Lys-OH as the work carried out up until this point shows that it does not have the same reactivity with HYBA that the aromatic aldehydes have.

All reactions were carried out in deuterated solvents (ACN/H_2O 1:1 v/v) with no purification carried out before analysis by ^1H NMR to ensure the analysis was carried out on the whole reaction mixture. This was to avoid the possibility that any components of the reaction mixture were inadvertently removed before the ^1H NMR analysis was performed. ^1H NMR spectra shown in this chapter show the aromatic peaks only because it was judged that this was the clearest way to present the most diagnostic peaks in the ^1H NMR data.

4-Aminobutyric acid methyl ester (ABAME) was introduced as an aliphatic amino acid model. This procedure was repeated replacing 4-aminobutyric acid methyl ester with benzylamine. Benzylamine was used as a model for an aromatic amino acid. Fmoc-Lys-OH was used as another competing amine as the NH_2 on the lysine side chain of a peptide would compete with the hydrazine group on the HYBA or HYNIC in a clinical setting when radiolabelling peptides with [^{18}F]fluorobenzaldehyde.

2.7 Results and discussion of competition reactions

In all spectra, the aromatic region only is shown.

2.7.1.1 Competition reactions with 4-aminobutyric acid methyl ester as the competing amine

2.7.1.1.1 Reaction between the active ester of 4-iodobenzoic acid and 4-aminobutyric acid methyl ester

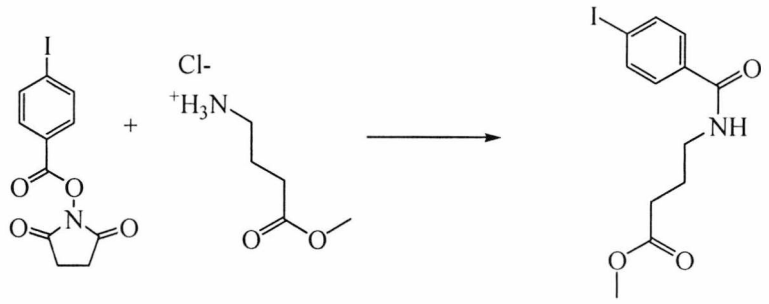

Scheme 2.5

The ^{1}H spectrum showed mainly active ester of 4-iodobenzoic acid. There were other small peaks present in the spectrum which may be due to product formation, however as some of the peaks are behind the IBAE peaks and are small, it difficult to tell whether any product formation has occurred and identify the peaks. The HPLC analysis showed a peak for ABAME only. IBAE did not show very strong absorption in UV light; the extinction coefficient (ε) was calculated as 0.4 which is extremely low.

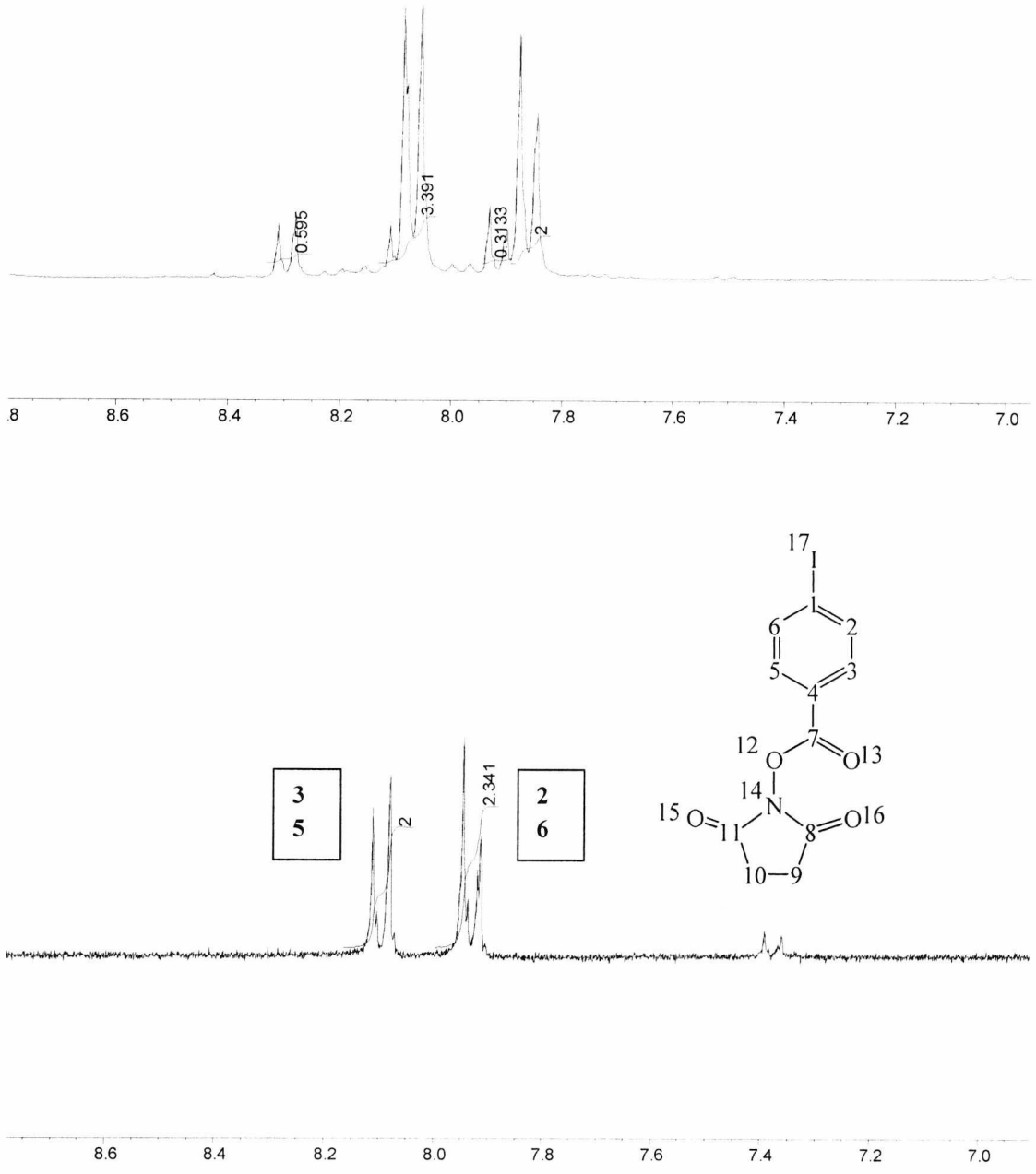

Figure 2.35 The top spectrum is the of the reaction mixture from the reaction between ABAME and IBAE. The bottom spectrum is of IBAE

2.7.1.1.2 Reaction between the active ester of 4-iodobenzoic acid and 4-hydrazinobenzoic acid

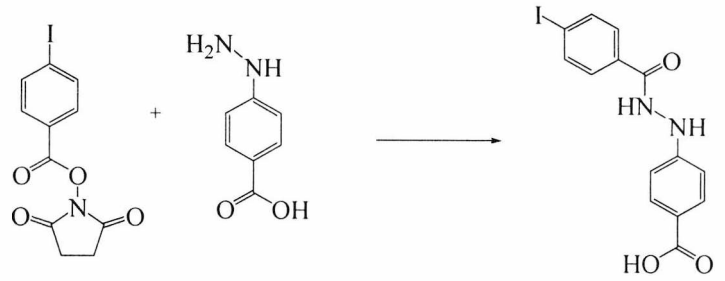

Scheme 2.6

From the ^{1}H spectrum, it can be seen that there was a small amount of product formation (20%) with more starting material than 4-(*N*'-[4-iodobenzoyl)hydrazino]-benzoic acid present (80% starting material). The active ester of 4-iodobenzoic acid (IBAE) did not react with HYBA completely, but a reaction did occur. There is no IBAE present in the HPLC chromatogram. As mentioned above, the IBAE did not show strong UV light absorbtion explaining its absence in the HPLC chromatogram. As 4-(*N*'-[4-iodobenzoyl)hydrazino]-benzoic acid was never isolated, the retention time is not known.

2.7.1.1.3 Competition reaction between 4-aminobutryric acid methyl ester and 4-hydrazinobenzoic acid for the active ester of 4-iodobenzoic acid

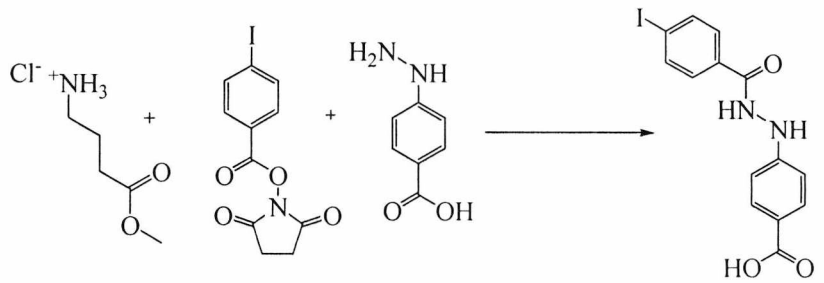

Scheme 2.7

The ^{1}H spectrum shows some starting material. It is possible that some 4-(*N*'-[4-iodobenzoyl)hydrazino]benzoic acid has formed, but it is not clear as there are many peaks in the spectrum. As already mentioned, it is not known what the product retention time for 4-

(*N*'-[4-iodobenzoyl)hydrazino]benzoic acid is as this product was never isolated. However there are peaks in the HPLC chromatogram at 13.6 minutes and 15.4 minutes which are also present in the HPLC analysis of the reaction between HYBA and IBAE.

It was not thought necessary to carry out a competition reaction with increased equivalents of the competing amine as, unlike 2-iodobenzaldehyde, the active ester reacted only to a small degree with HYBA and was not considered reactive enough to justify using increased equivalents of ABAME.

Summary of competition reactions between 4-aminobutyric acid methyl ester and 4-hydrazinobenzoic acid for the active ester of 4-iodobenzoic acid

The reaction between ABAME and IBAE and the reaction between HYBA and IBAE showed the presence of mainly starting material in the spectra with some product formation. The competition reaction showed a mixture of starting materials and possibly some 4-(*N*'-[4-iodobenzoyl)hydrazino]benzoic acid although due to there being many peaks in the spectrum, it is difficult to interpret. The reactions carried out in this section show a selectivity of HYBA for IBAE but are probably not reactive enough to be useful for labelling.

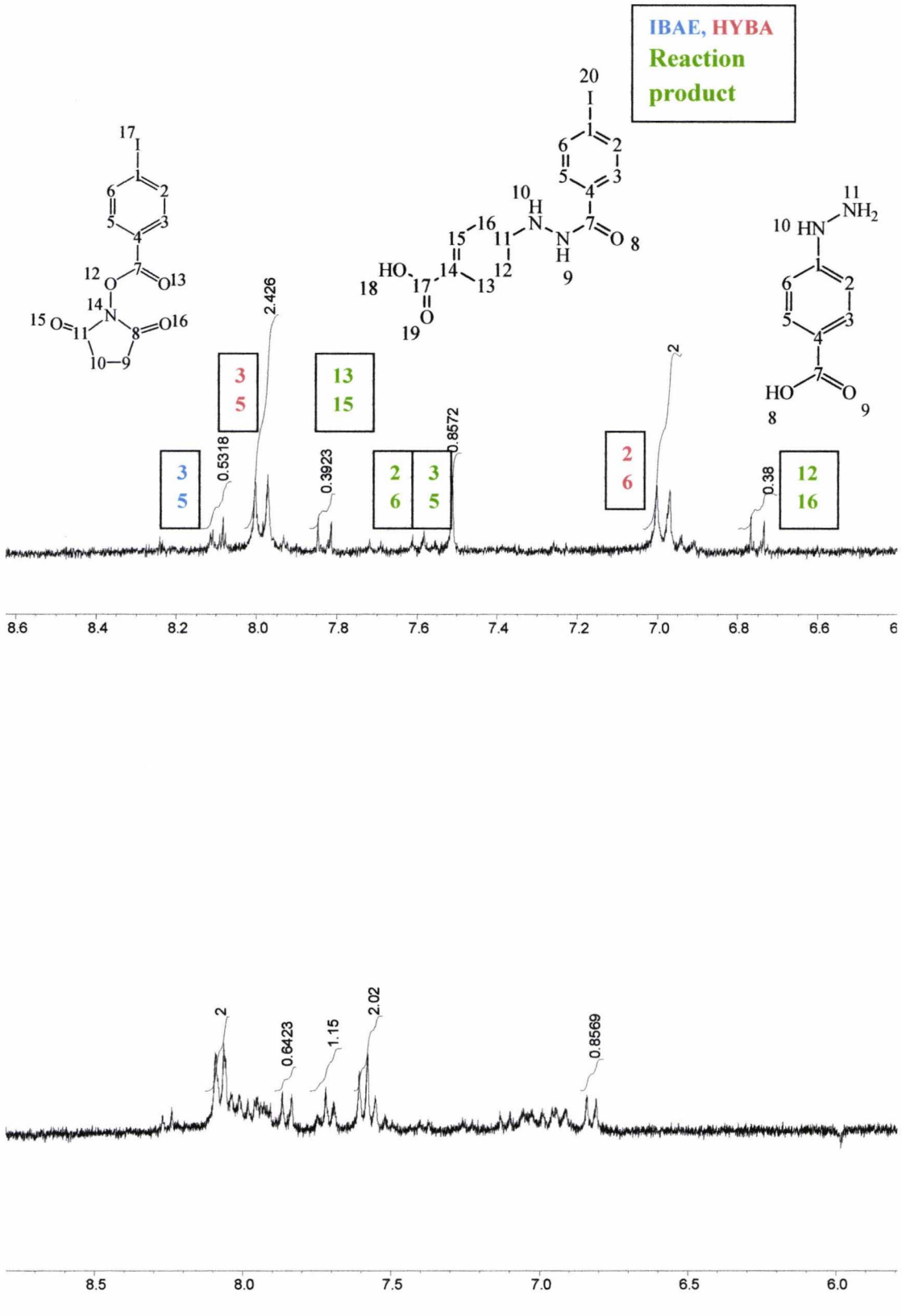

Figure 2.36 The top spectrum of the reaction mixture from the reaction between HYBA and IBAE. The bottom spectrum is the reaction mixture from the competition reaction between HYBA and ABAME for IBAE

2.7.1.1.4 Reaction between 4-aminobutyric acid methyl ester and 2-iodobenzaldehyde

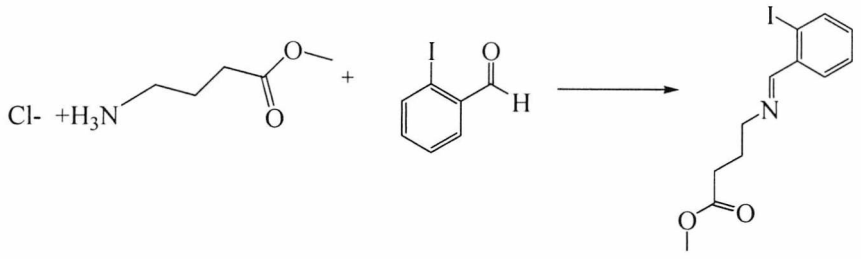

Scheme 2.8

The ^{1}H spectrum showed starting material only. 2-iodobenzaldehyde can be seen in the ^{1}H NMR spectrum shown in figure 2.37. The ^{1}H spectrum also showed 4-aminobutyric acid methyl ester (ABAME) and triethylamine (TEA) as the HCl salt. TEA was added to the reactions with ABAME as ABAME was synthesised as a salt. TEA is a base and deprotonates the ABAME to allow it to take part in the reaction. Starting material was present in the HPLC chromatogram, along with some unknown peaks, which are likely to be present because of storage before analysis rather than being product peaks, as there was no product formed according to NMR analysis.

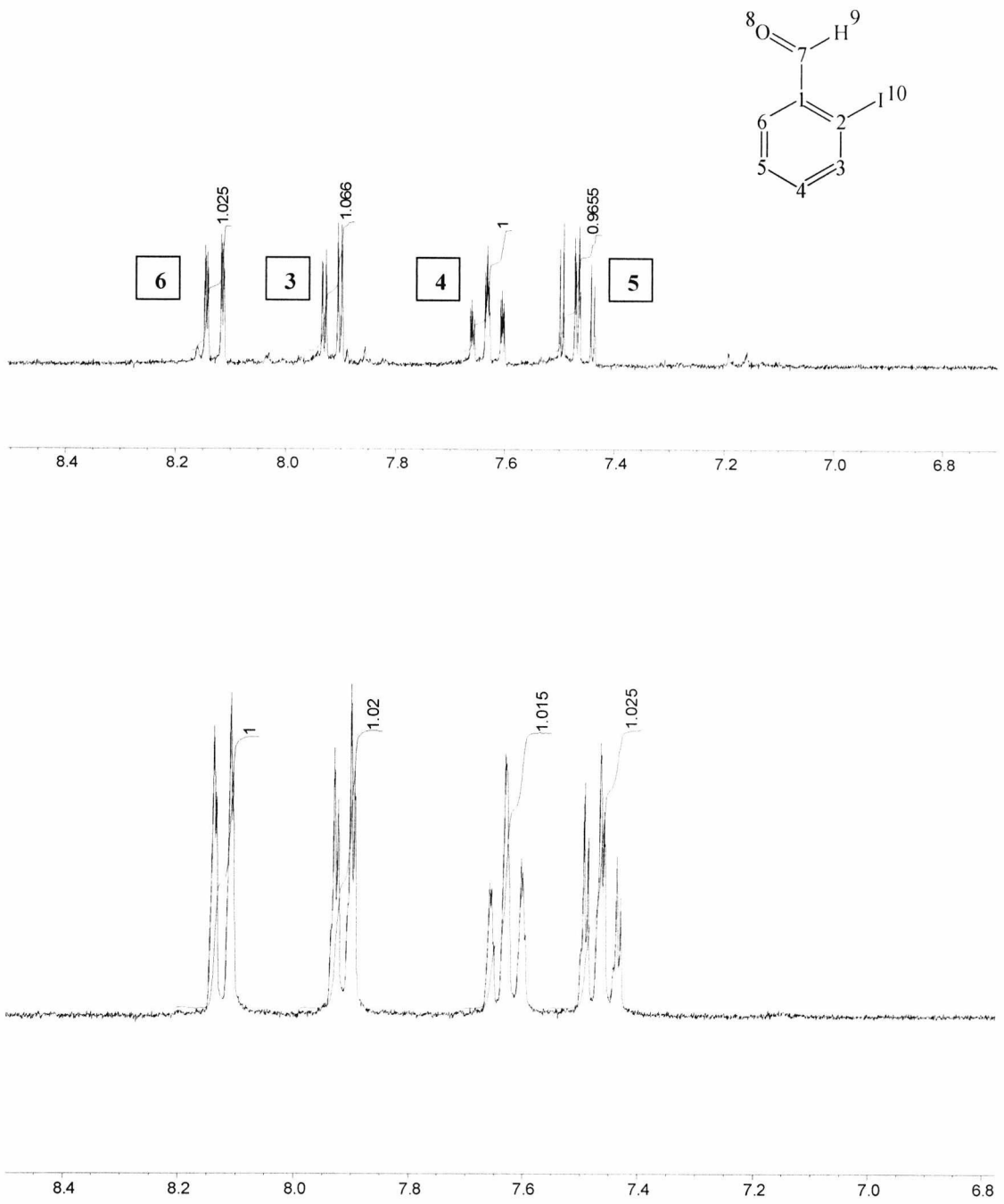

Figure 2.37 The top spectrum shows the reaction mixture from the reaction between 2-iodobenzaldehyde and ABAME. The bottom spectrum shows 2-iodobenzaldehyde starting material

2.7.1.1.5 Reaction between 2-iodobenzaldehyde and 4-hydrazinobenzoic acid

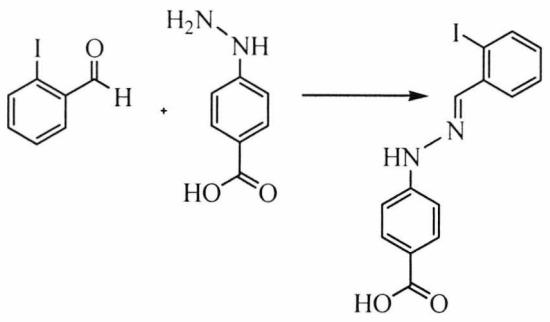

Scheme 2.9

The ^{1}H NMR spectrum showed only the formation of the product 4-[*N*'-(2-iodobenzylidene)-hydrazino]-benzoic acid. HYBA was present in the HPLC chromatogram as well as the above product, most likely because a slight excess was added in error at the start of the reaction. This was the only other compound in the HPLC chromatogram. However, it is worth noting that the λ_{max} for HYBA is 272nm which is very near the wavelength used for the monitoring reactions 280nm). Therefore very little excess HYBA would give rise to a relatively large peak in the HPLC chromatogram. (The λ_{max} for iodobenzaldehyde is 224nm). The unknown peaks present in this chromatogram and in others is likely to be due to having to store the samples for up to 2 weeks (at - 20°C) before HPLC analysis due to heavy use of the instrument. All unknown peaks in all chromatograms were small peaks.

2.7.1.1.6 Competition reaction between 4-aminobutryric acid methyl ester and 4-hydrazinobenzoic acid for 2-iodobenzaldehyde

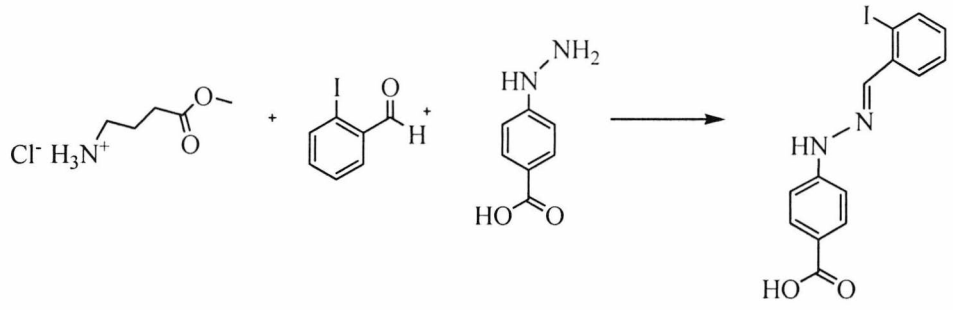

Scheme 2.10

The ^{1}H spectrum shows that 2-iodobenzaldehyde reacted selectively with the HYBA and not at all with ABAME. A couple of the peaks are in a slightly different position to those in the reaction between HYBA and 2-iodobenzaldehyde only. Peak 5 was shifted to the left in the ^{1}H spectrum so that it is clearly visible and the doublet corresponding to 11 and 15 have moved slightly to the right. The chemical environment the molecule is in has changed with the addition of ABAME and this has an effect on chemical shift. This is the same effect as using different solvents for NMR analysis which leads to changes in peak position and slight variations in chemical shift. The identity of the product formed in the reaction is the same; 4-[*N*'-(2-iodobenzylidene)-hydrazino]-benzoic acid, despite a couple of the peaks having changed position slightly. The HPLC chromatogram shows there is some unreacted HYBA in the reaction mixture.

This reaction was also carried out as above but using three times the amount of ABAME. The ^{1}H NMR results showed formation of the same product as when one equivalent of the competing amine only was added.

Summary of competition reactions between 4-aminobutyric acid methyl ester and 4-hydrazinobenzoic acid for 2-iodobenzaldehyde

2-Iodobenzaldehyde and HYBA reacted to yield 4-[*N*'-(2-iodobenzylidene)-hydrazino]-benzoic acid even in the presence of the competing amine, ABAME. This occurs even when a threefold excess of ABAME is present. The reaction between HYBA and 2-iodobenzaldehyde proceeded to completion as shown in figure 2.38 in a summary of the ^{1}H NMR spectra shown in this section. The competition reaction therefore shows selectivity between HYBA and 2-iodobenzaldehyde in the presence of an excess of a competing amine.

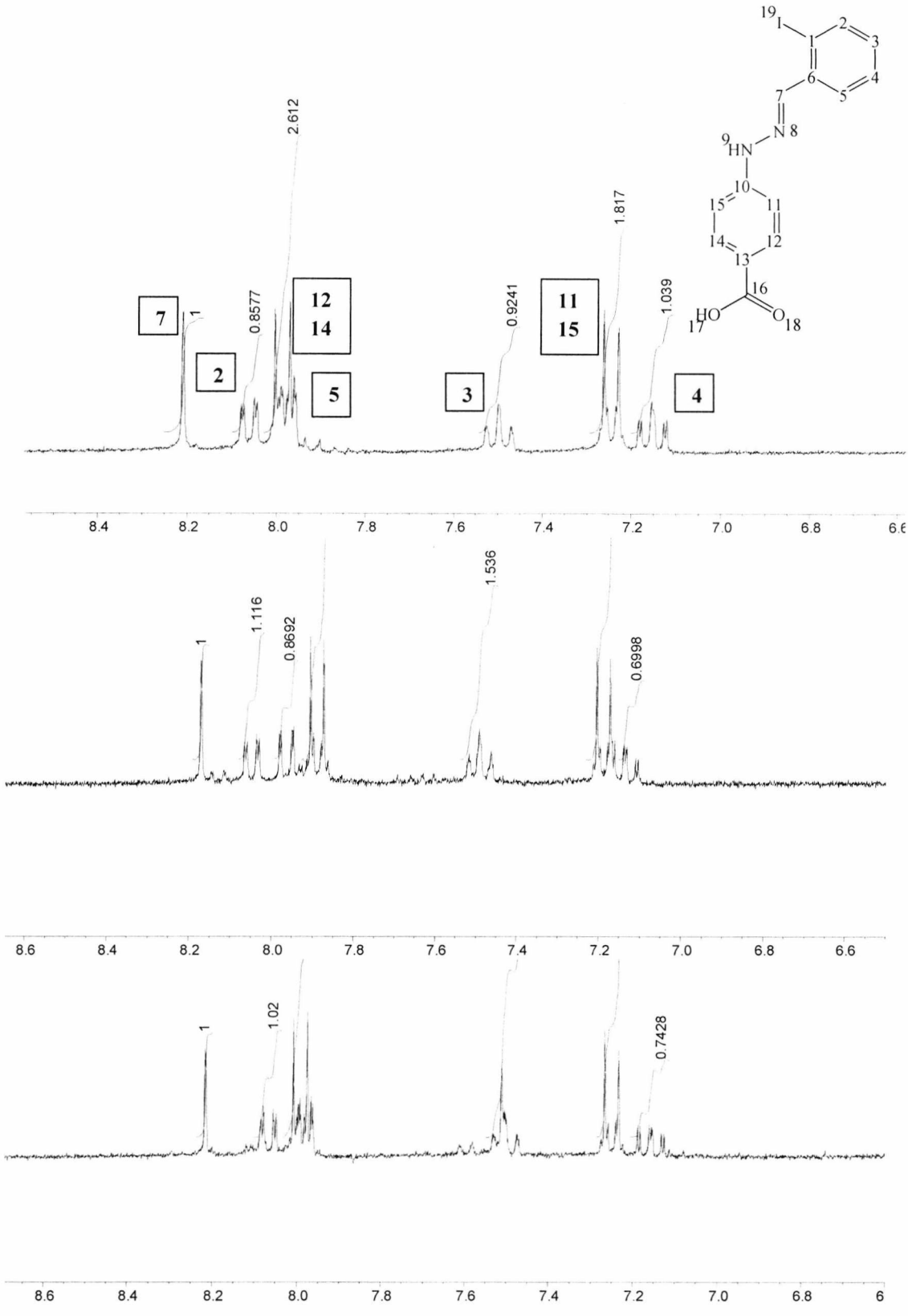

Figure 2.38 The top ^{1}H spectrum is the 'clean' reaction between HYBA and 2-iodobenzaldehyde. The middle spectrum shows the competition reaction with one equivalent of ABAME. The bottom spectrum shows the competition reaction with three equivalents of ABAME

2.7.1.1.7 Reaction between 4-aminobutyric acid methyl ester and 4-fluorobenzaldehyde

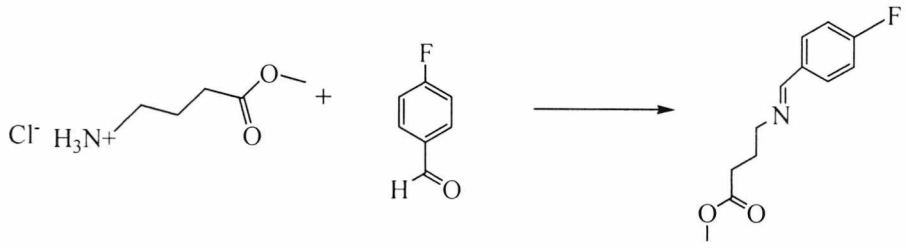

Scheme 2.11

The ^{1}H spectrum showed very small peaks in the aromatic region. The peaks present are difficult to interpret as they are so small but are likely to be 4-fluorobenzaldehyde. It is possible that the product is forming and precipitating out of solution, however from the ^{1}H spectrum, no evidence of new product formation is visible. HPLC analysis was in agreement with this.

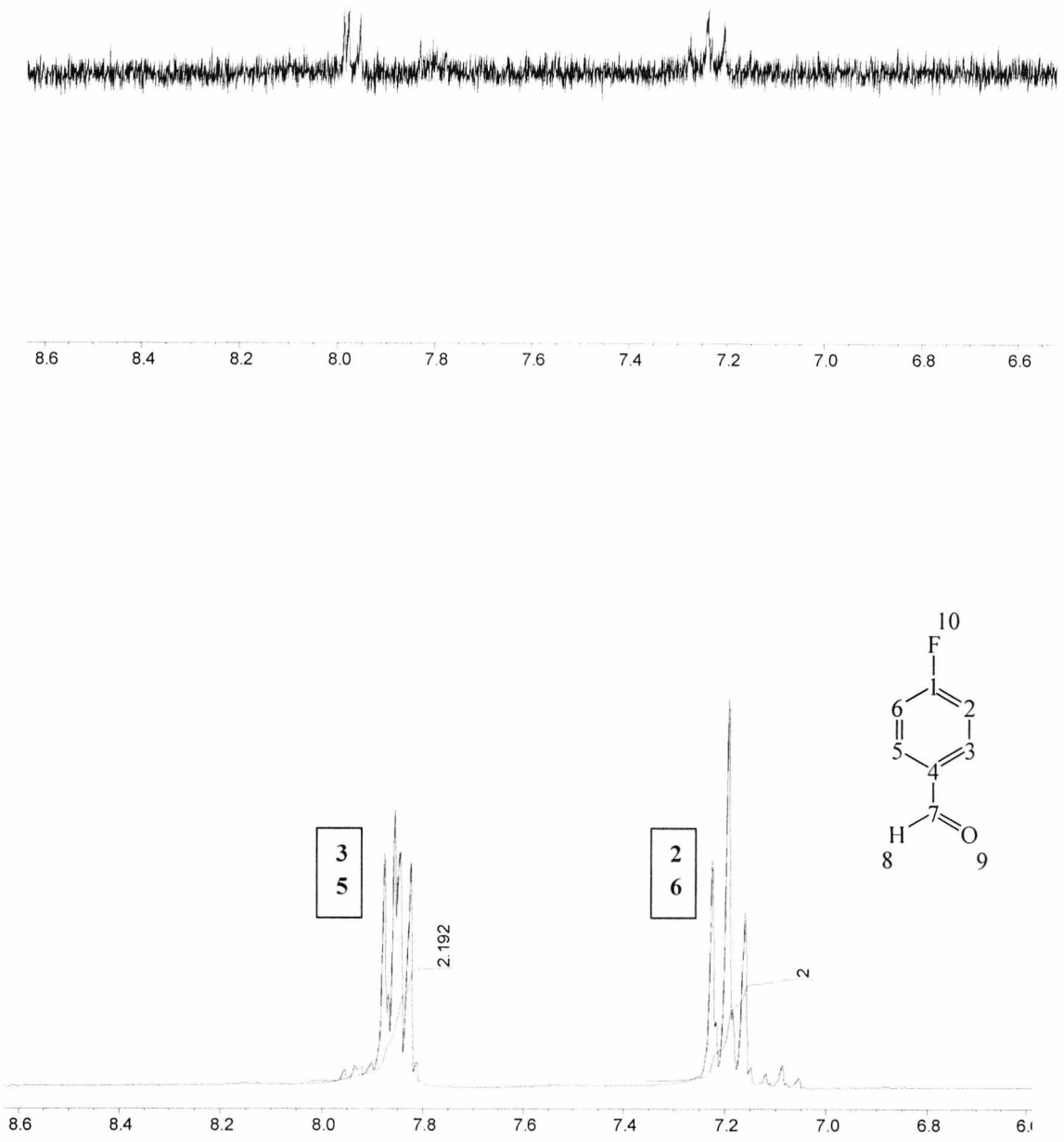

Figure 2.39 The top spectrum is of the reaction mixture from the reaction between ABAME and 4-fluorobenzaldehyde. The bottom spectrum is of 4-fluorobenzaldehyde starting material

2.7.1.1.8 Reaction between 4-hydrazinobenzoic acid and 4-fluorobenzaldehyde

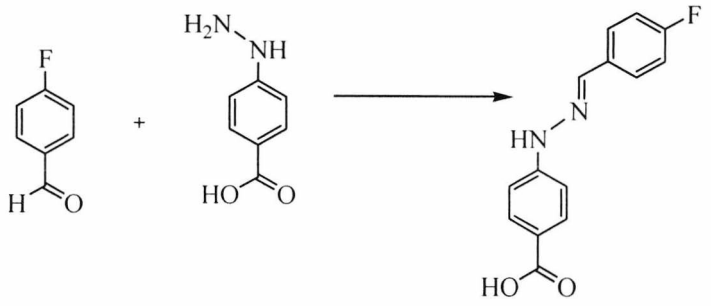

Scheme 2.12

The ^1H spectrum showed the presence of 4-[*N*'-(4-fluorobenzylidene)-hydrazino]-benzoic acid only with no starting material. HPLC analysis showed the presence of HYBA as well as 4-[N'-(4-fluorobenzylidene)-hydrazino]-benzoic acid. 4-[*N*'-(4-fluorobenzylidene)-hydrazino]-benzoic acid was present as 70% of the total peak area. No other products were formed.

2.7.1.1.9 Competition reaction between 4-aminobutyric acid methyl ester and 4-hydrazinobenzoic acid for 4-fluorobenzaldehyde

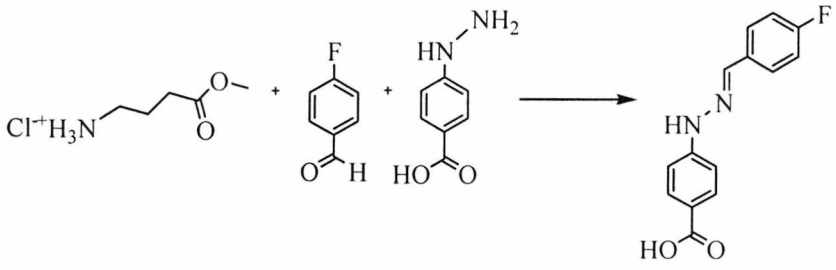

Scheme 2.13

The ^1H spectrum showed the presence of the same product (4-[*N*'-(4-fluorobenzylidene)-hydrazino]-benzoic acid) that was formed when HYBA and 4-fluorobenzaldehyde reacted together on their own. This was confirmed by the HPLC analysis. No other product was formed. 4-fluorobenzaldehyde was present in the HPLC chromatogram.

This reaction was also carried out as above but using three times the amount of 4-aminobutyric acid methyl ester. The ^{1}H NMR spectrum showed the formation of the same product as for when one equivalent only of the competing amine was present.

Summary of competition reactions between 4-aminobutryric acid methyl ester and 4-hydrazinobenzoic acid for 4-fluorobenzaldehyde

4-fluorobenzaldehyde and HYBA reacted chemoselectively with each other, giving the product 4-[*N*'-(4-fluorobenzylidene)-hydrazino]-benzoic acid. This shows that 4-fluorobenzaldehyde has reacted with HYBA in preference to the competing amine, 4-aminobutyric acid methyl ester. This occurs even when an excess of competing amine is present. The reaction between HYBA and 4-fluorobenzaldehyde proceeded to completion in a selective manner. Below is a summary of the NMR results for the reactions in this section.

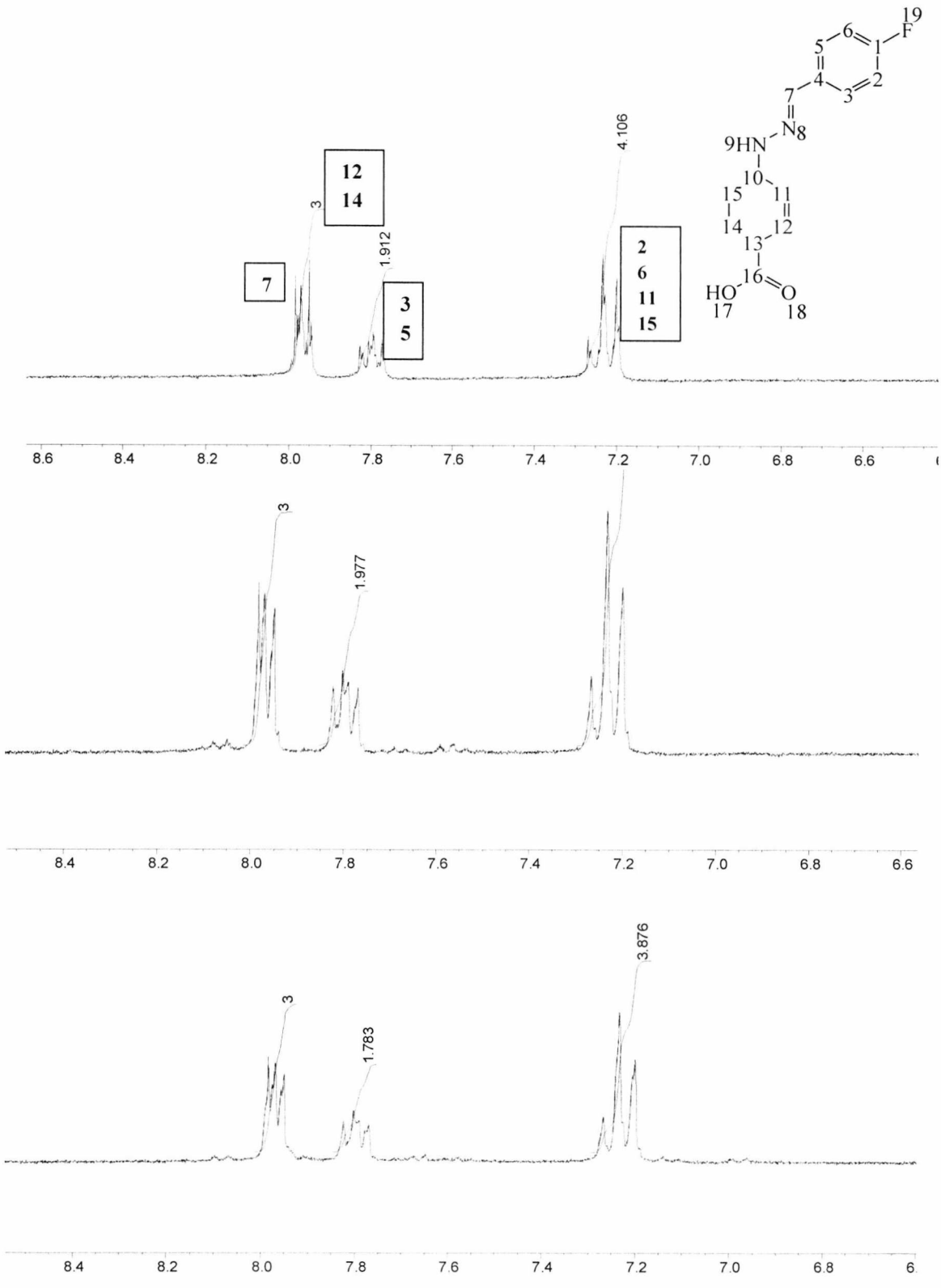
12
14
7
3
5
2
6
11
15
4.106
1.912
3
1.977
3.876
1.783
8.6
8.4
8.2
8.0
7.8
7.6
7.4
7.2
7.0
6.8
6.6

Figure 2.40 The top spectrum is the reaction between HYBA and 4-fluorobenzaldehyde. In the middle is the spectrum of the competition reaction with one equivalent of ABAME and at the bottom the spectrum of the competition reaction with three equivalents of ABAME

2.7.1.2.0 Reaction between 4-aminobutyric acid methyl ester and 4-bromobenzaldehyde

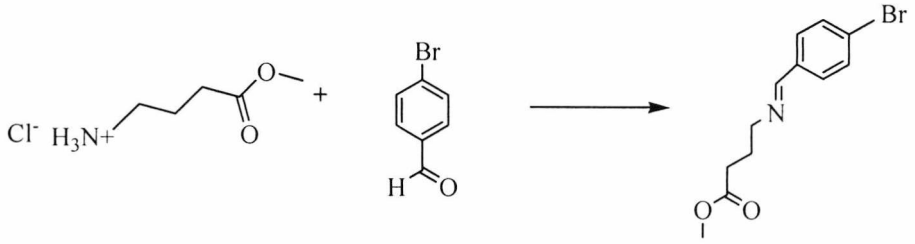

Scheme 2.14

The ^{1}H spectrum possibly showed the presence of a small amount of 4-bromobenzaldehyde but as with the reaction between 4-fluorobenzaldehyde and ABAME, the peaks are so small that it is difficult to tell if any product has formed and whether starting material is present. The small peaks may be due to an insoluble product forming and precipitating out of solution, although no precipitate was noted in the reaction mixture. The HPLC analysis also showed unknown peaks. The peak at 13.9 minutes was also present in chromatogram of 4-bromobenzaldehyde starting material and is likely to be an impurity from synthesis. The peak at 16.3 minutes is possibly due to carry over from the previous sample as this is the retention time for 4-[*N*'-(4-bromobenzylidene)-hydrazino]-benzoic acid.

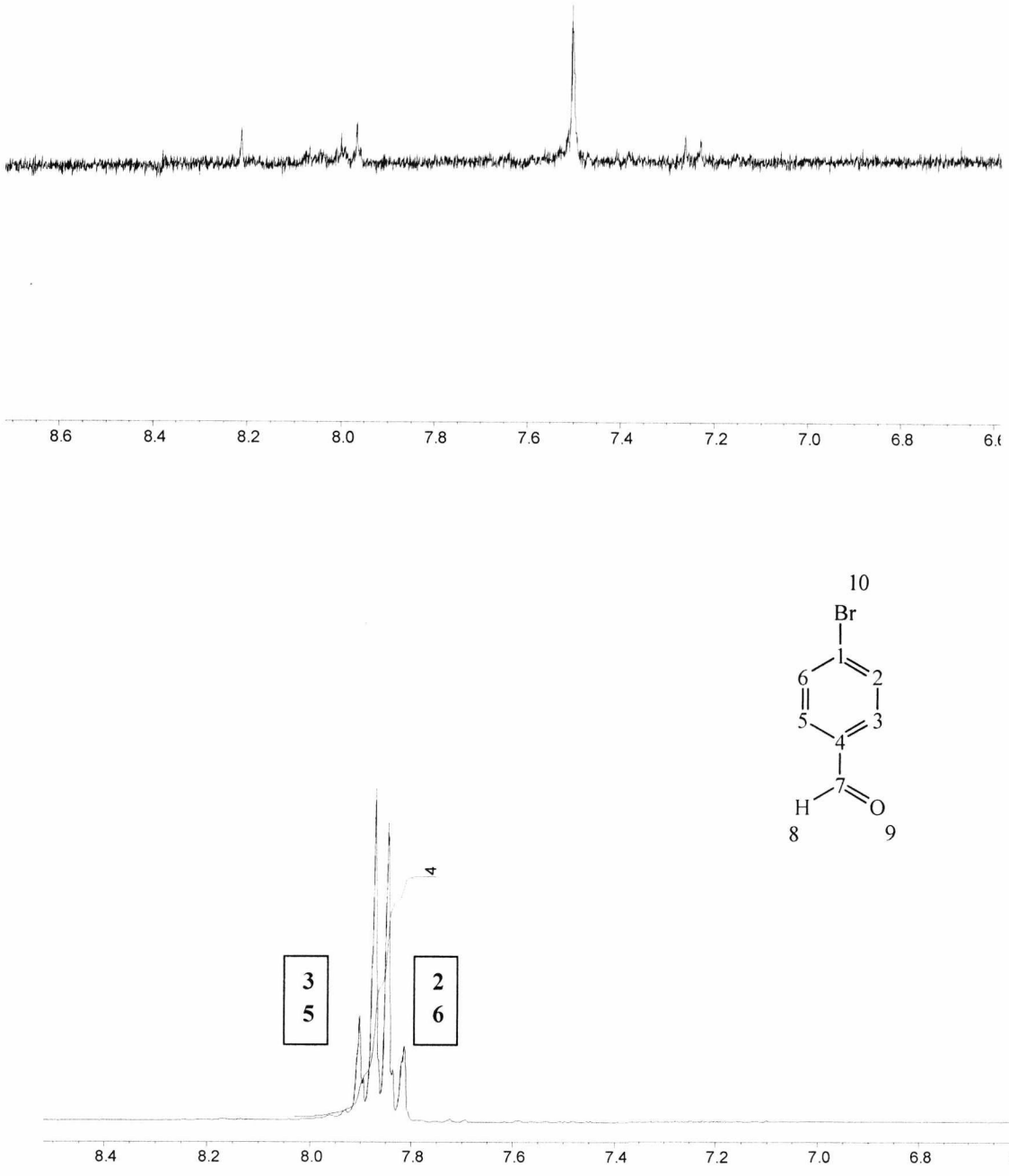

Figure 2.41 The top spectrum was obtained from the reaction between 4-bromobenzaldehyde and ABAME. The bottom spectrum shows the starting material 4-brombenzaldehyde for comparison purposes

2.7.1.2.1 Reaction between 4-hydrazinobenzoic acid and 4-bromobenzaldehyde

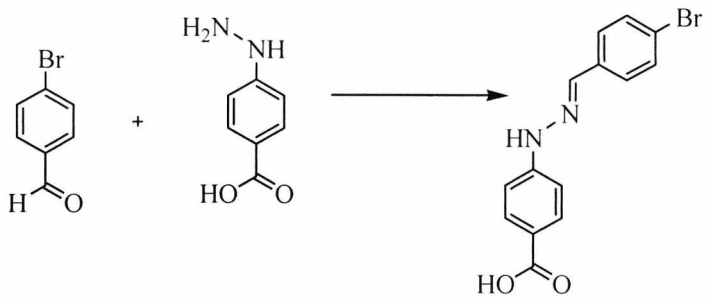

Scheme 2.15

The ^1H spectrum showed the presence of 4-[N'-(4-bromobenzylidene)-hydrazino]-benzoic acid as the only product formed with no starting material present. HPLC analysis showed the presence of starting material present as 33% of the total peak area. It is possible that storage of the sample before HPLC analysis lead to hydrolysis of the sample.

2.7.1.2.2 Competition reaction between 4-aminobutyric acid methyl ester and 4-hydrazinobenzoic acid for 4-bromobenzaldehyde

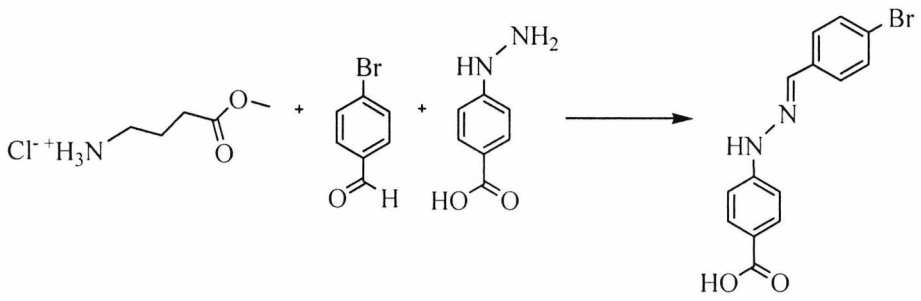

Scheme 2.16

The ^1H spectrum shows the formation of the product 4-[N'-(4-bromobenzylidene)-hydrazino]-benzoic acid. The reaction occurred between 4-bromobenzaldehyde and HYBA in a selective way, even in the presence of a competing amine. There were some starting materials in the HPLC chromatogram and in the ^1H spectrum (15% starting material in the ^1H spectrum). Both HYBA and 4-bromobenzaldehyde are present, showing that the reaction did not go quite to completion or hydrolysis occurred.

This reaction was also carried out as above but using three times the amount of ABAME. The reaction went to completion with no starting material remaining in the spectrum.

Summary of competition reactions between 4-aminobutyric acid methyl ester and 4-hydrazinobenzoic acid for 4-bromobenzaldehyde

4-Bromobenzaldehyde and HYBA reacted giving the product 4-[N'-(4-bromobenzylidene)-hydrazino]-benzoic acid in the presence of the competing amine. This shows that 4-bromobenzaldehyde has reacted with HYBA in preference to the competing amine, ABAME. This occurs even when a threefold excess of competing amine is present. The reaction between HYBA and bromobenzaldehyde proceeded to completion. A summary of the NMR results in this section are shown below.

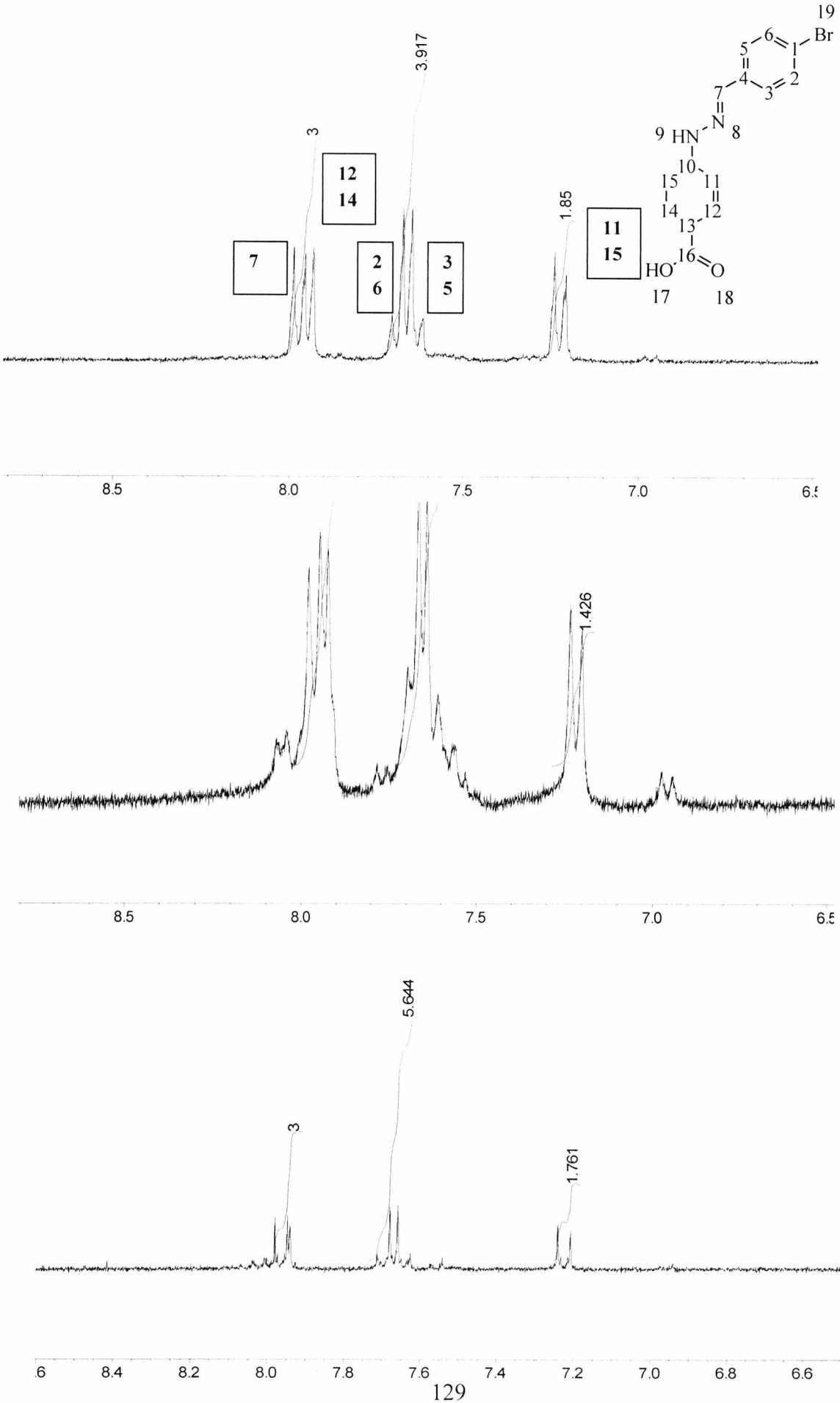
19
Br
6
5
1
4
2
3
7
N
8
9 HN
10
15
11
14
12
13
16
O
HO
17
18
3.917
3
1.85
12
14
7
2
6
3
5
11
15
8.5
8.0
7.5
7.0
1.426
5.644
1.761

Figure 2.42 The top ^{1}H spectrum shows the reaction between HYBA and 4-bromobenzaldehyde only. The middle spectrum shows the competition reaction with one equivalent of ABAME and the bottom spectrum shows the competition reaction with three equivalents of ABAME

2.7.1.2.3 Reaction between 4-aminobutyric acid methyl ester and 4-formylphenyl boronic acid

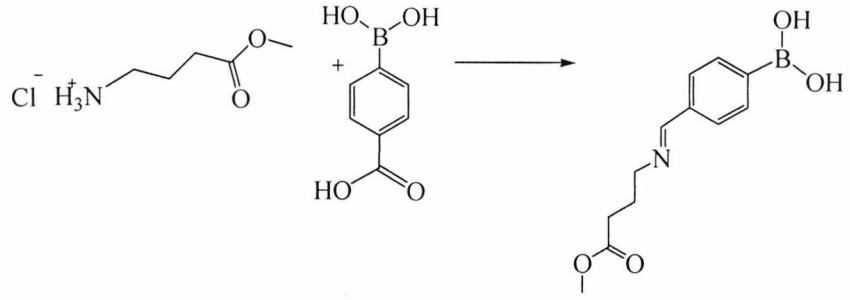

Scheme 2.17

The ^{1}H spectrum showed starting material only (TEA and 4-aminobutyric acid methyl ester only) with no evidence of any product formation. There was no evidence product formation and no 4-formylphenyl boronic acid present by either NMR or HPLC analysis. This reaction was repeated and the results obtained were consistent with the data presented here. It is possible that a reaction occurred between ABAME and 4-formylphenyl boronic acid but that the resulting product precipitated out of solution. However, no precipitate was noted in the reaction mixture. As analysis was carried out on the reaction mixture any precipitated solid in the reaction mixture would not show up by NMR or HPLC analysis. Similar results were obtained when the aldehydes 4-fluorobenzaldehyde and 4-bromobenzaldehyde were reacted with ABAME.

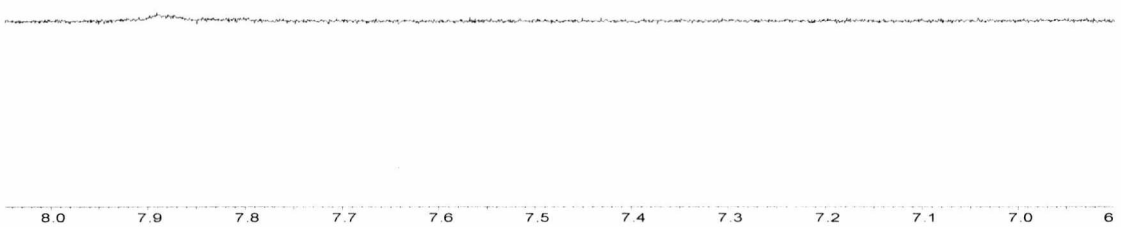

Figure 2.43 Aromatic region of the ^1H spectrum from the reaction between 4-formylphenyl boronic acid and ABAME

2.7.1.2.4 Reaction between 4-hydrazinobenzoic acid and 4-formylphenyl boronic acid

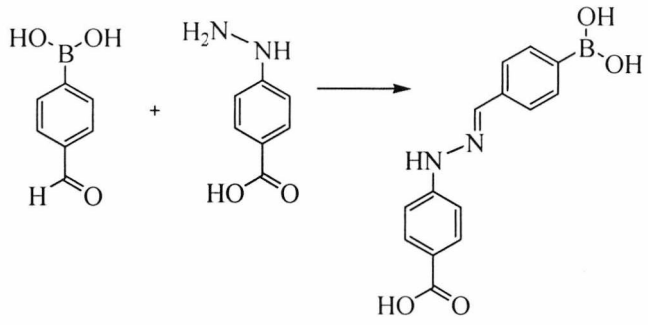

Scheme 2.18

This reaction did not proceed to completion as the other reactions between the aromatic aldehyde and HYBA did. A significant amount of starting material was present in the ^1H spectrum (25%). The reaction between 4-formylphenyl boronic acid and HYBA occurred, but not as quickly as for the other aldehydes above and did not proceed to completion. Starting material and 4-[N'-(4-boronobenzylidene)hydrazino]-benzoic acid (48% by peak area percent) were present by HPLC analysis.

2.7.1.2.5 Competition reaction between 4-aminobutyric acid methyl ester and 4-hydrazinobenzoic acid for 4-formylphenyl boronic acid

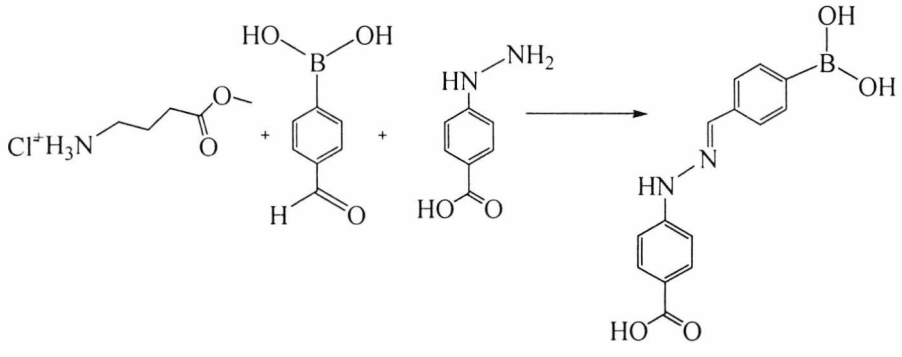

Scheme 2.19

The ^1H spectrum had significant amounts of all starting materials but also showed the formation of 4-[N'-(4-boronobenzylidene)hydrazino]-benzoic acid (50% by NMR analysis). HYBA and 4-formylphenyl boronic acid reacted preferentially with one another to form 4-

[N'-(4-boronobenzylidene)hydrazino]-benzoic acid, but the reaction did not go to completion. The reaction above was carried out using three times the amount of ABAME. When an excess of competing amine was present, the results became difficult to interpret as there were so many peaks present in the ^{1}H spectrum. In the reaction between ABAME and 4-formylphenyl boronic acid, the expectation would be that the same results as those for the reaction between ABAME and 4-formylphenyl boronic acid, i.e. no product formation would be seen in the NMR spectrum, however it may be that the product did not precipitate out of solution to the same degree in the competition reaction and therefore some product formation from the reaction between ABAME and 4-formylphenyl boronic acid occurred and was present in the reaction mixture. A summary of the NMR results in this section are shown below.

Summary of competition reactions between 4-aminobutyric acid methyl ester and 4-hydrazinobenzoic acid for 4-formylphenyl boronic acid

4-Formylphenyl boronic acid reacted specifically with HYBA even in the presence of a competing amine, but the reaction did not go to completion, unlike the other aldehydes discussed above. It is not clear from the results whether 4-formylphenyl boronic acid reacts with ABAME but it seems likely a reaction does occur. However, the reaction of 4-formylphenyl boronic acid with HYBA is favoured over the reaction of 4-formylphenyl boronic acid with ABAME.

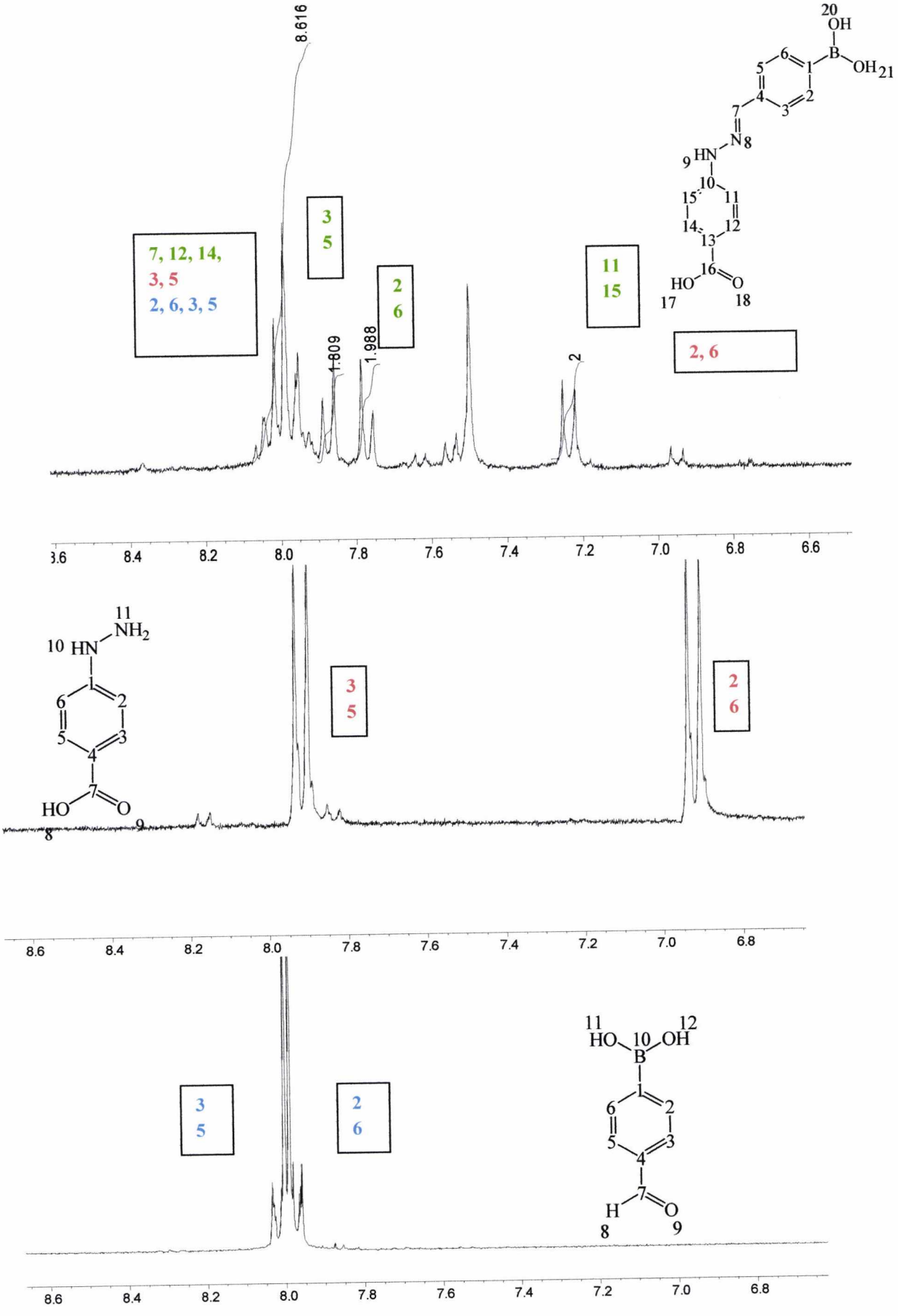
8.616
1.809
1.988
2
7, 12, 14,
3, 5
2, 6, 3, 5
3
5
2
6
11
15
2, 6
20
OH
B
OH 21
HN
N 8
HO
O
17
18
8.6
8.4
8.2
8.0
7.8
7.6
7.4
7.2
7.0
6.8
6.6
11
NH2
10 HN
HO
O
3
5
2
6
H
8
9

Figure 2.44 The top spectrum is of the reaction mixture from the reaction between HYBA and 4-formylphenyl boronic acid (4-FPB). The middle spectrum is of HYBA and the bottom spectrum shows 4-formylphenyl boronic acid for comparison

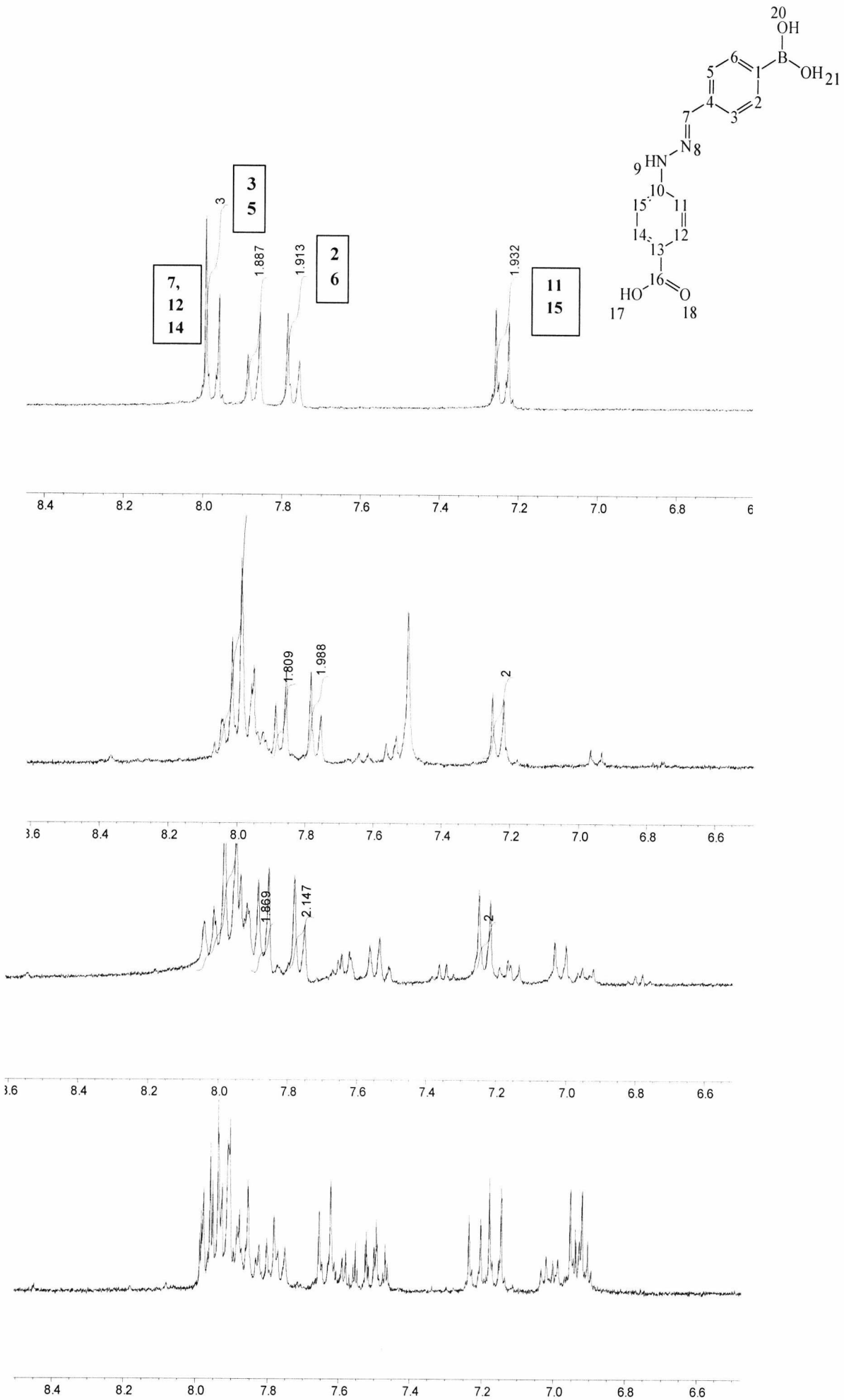
20
OH
B
OH 21
6
1
5
2
4
3
7
N 8
9 HN
10
15
11
14
12
13
16
HO
O
17
18
7,
12
14
3
5
1.887
1.913
2
6
1.932
11
15
8.4
8.2
8.0
7.8
7.6
7.4
7.2
7.0
6.8
1.809
1.988
2
1.869
2.147
2
3.6
8.4
8.2
8.0
7.8
7.6
7.4
7.2
7.0
6.8
6.6

Figure 2.45 The top ^{1}H spectrum shows the standard (inserted here for comparison purposes). The second to top ^{1}H spectrum is from the reaction between HYBA and 4-formylphenyl boronic acid. The third from top spectrum is from the competition reaction with one equivalent of ABAME. The bottom spectrum is from the competition reaction with three equivalents of ABAME

2.7.1.3 Competition reactions with benzylamine as the competing amine

2.7.1.3.1 Reaction between benzylamine and the active ester of 4-iodobenzoic acid

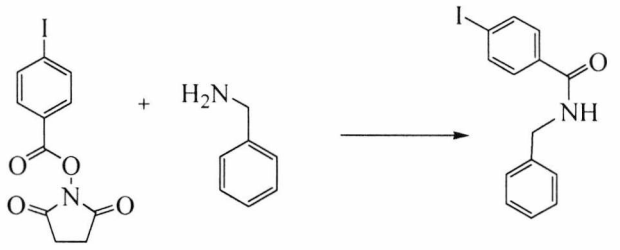

Scheme 2.20

NMR and HPLC analysis showed the reaction mixture contained unreacted starting material only showing that benzylamine did not react with IBAE. IBAE was not present in the HPLC chromatogram, although benzylamine was present. As previously referred to, the active ester of 4-iodobenzoic acid did not strongly absord UV light when subjected to UV/visible spectrophotometric analysis. This would explain the absence of IBAE from the HPLC chromatogram. It is possible that IBAE hydrolysed during storage, although no peak equivalent to 4-iodobenzoic acid was present in the chromatogram (10.8 mins). Benzylamine has the effect of shifting some the peaks of IBAE compared to a ^{1}H NMR spectrum of IBAE without benzylamine present. This effect of benzylamine was consistently noted and was investigated more thoroughly with 4-fluorobenzaldehyde and benzylamine.

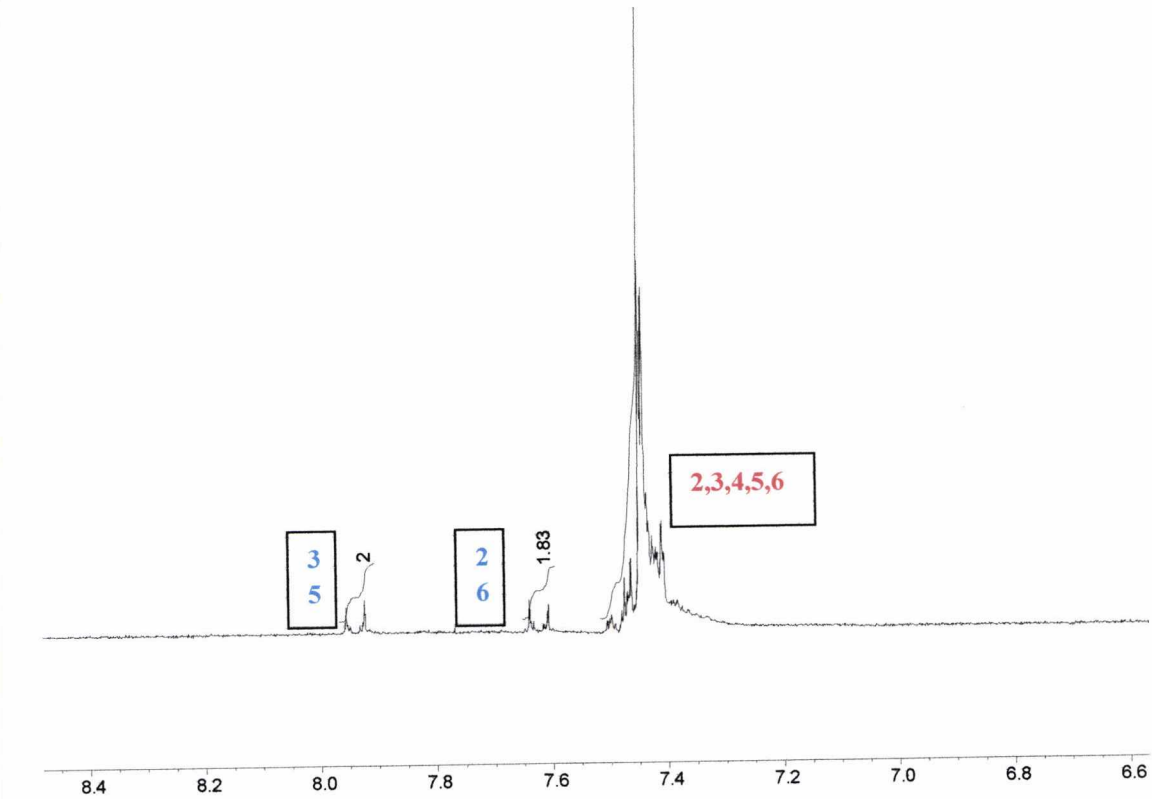
3
5
2
2
6
1.83
2,3,4,5,6
8.4
8.2
8.0
7.8
7.6
7.4
7.2
7.0
6.8
6.6

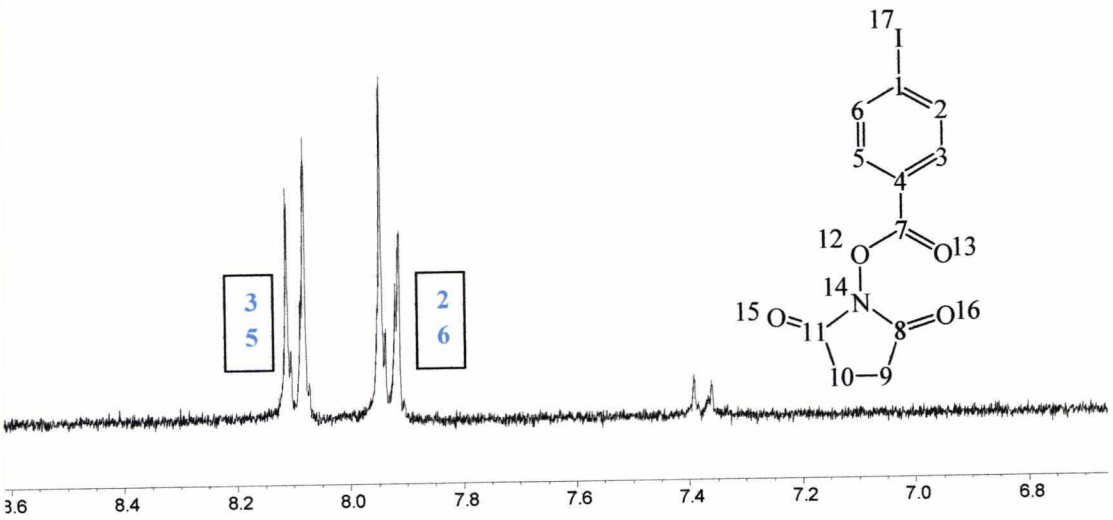
3
5
2
6
17
I
1
2
3
4
5
6
7
12
O
13
O
14
N
15
O
11
8
16
O
10
9
3.6
8.4
8.2
8.0
7.8
7.6
7.4
7.2
7.0
6.8

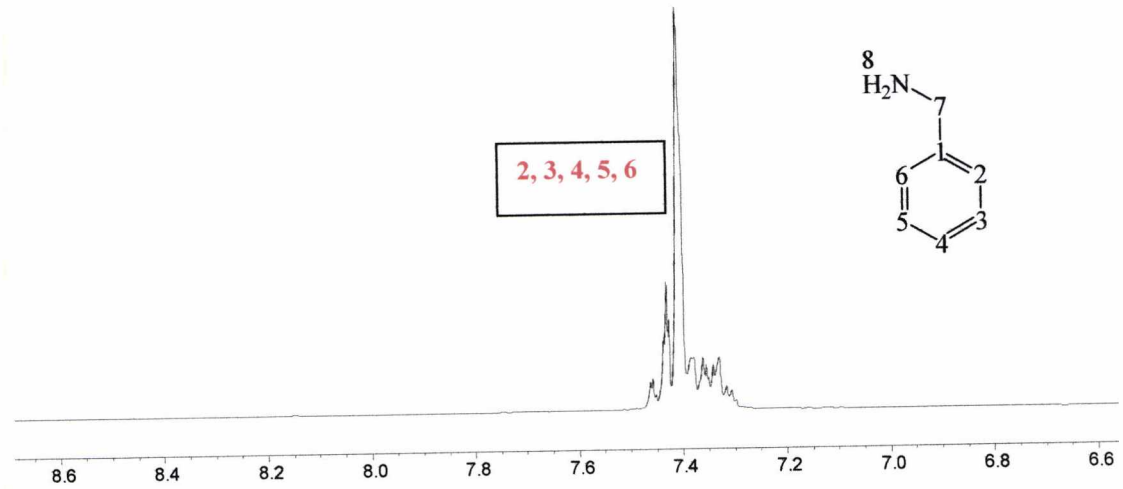
2, 3, 4, 5, 6
8
H2N
7
1
2
3
4
5
6
8.6
8.4
8.2
8.0
7.8
7.6
7.4
7.2
7.0
6.8
6.6

Figure 2.46 The top spectrum is of the reaction mixture from the reaction between IBAE and benzylamine. The middle spectrum shows a spectrum of IBAE and the bottom spectrum shows benzylamine for comparison

2.7.1.3.2 Competition reaction between benzylamine and 4-hydrazinobenzoic acid for the active ester of 4-iodobenzoic acid

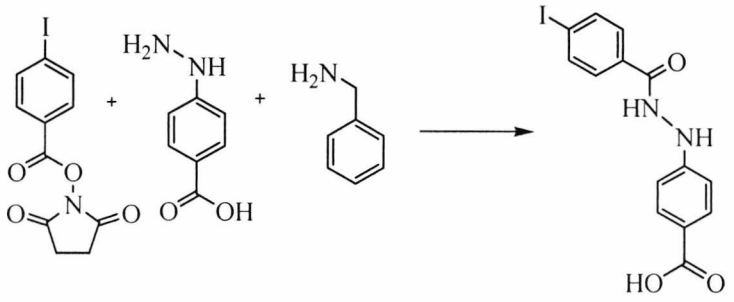

Scheme 2.21

4-[*N*'-(4-Iodobenzoyl)hydrazinyl]-benzoic acid was possibly present in the NMR spectrum. No HYBA was present. It is difficult to accurately assign all peaks for 4-[*N*'-(4-iodobenzoyl)hydrazinyl]-benzoic acid as benzylamine has the effect of shifting some the peaks slightly. However, an attempt as been made to assign the peaks. HPLC analysis showed HYBA and benzylamine only. There was no evidence of product formation from the HPLC results. It is possible that due to storage before HPLC analysis degradation of the sample occurred.

It was not thought necessary to carry out a competition reaction with increased equivalents of the competing amine as, unlike the aldehydes, the active ester essentially does not show enough reactivity with HYBA to make radiolabelling in this way a viable option.

Summary of competition reactions between benzylamine and 4-hydrazinobenzoic acid for the active ester of 4-iodobenzoic acid

The reactions carried out in this section demonstrate a lack of reactivity between IBAE and HYBA that was clearly seen with the aldehydes. There was possible evidence of some product formation between IBAE and HYBA in the competition reaction; however, it was difficult to assign peaks accurately.

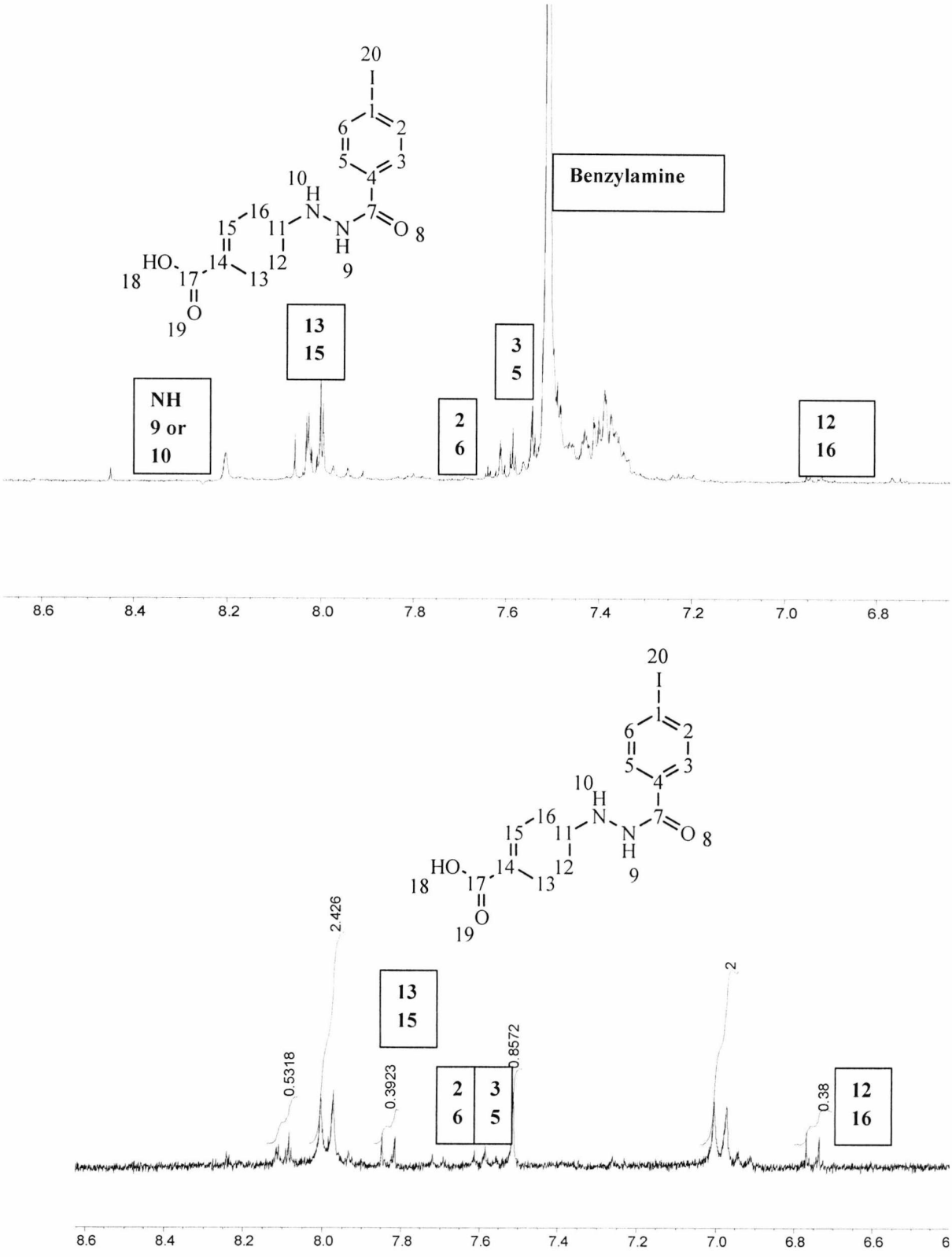

Figure 2.47 The top ^{1}H spectrum shows the competition reaction between HYBA and benzylamine for IBAE. The bottom ^{1}H spectrum shows the reaction between HYBA and IBAE

2.7.1.3.3 Reaction between 2-iodobenzaldehyde and benzylamine

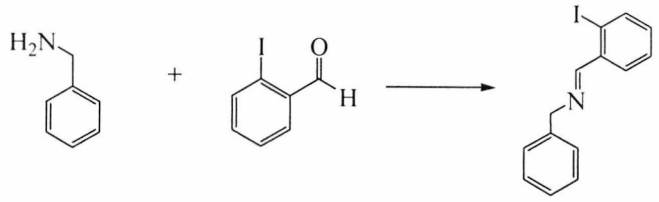

Scheme 2.22

The ^{1}H NMR spectrum showed the presence of both product (benzyl-(2-iodobenzylidene)-amine) and starting material (about 50% of each). A reaction occurred, but it did not go to completion. The equilibrium constants for hydrazone formation are high, even in aqueous media, whereas the equilibrium constant for imine formation is lower, although imine formation can be driven forwards by dehydration. The difference between the stability of imines and hydrazones in aqueous solution may be due to that, for hydrazone formation, the reduction in lone pair repulsion present in hydrazine reactants may be more important (Carey and Sundberg 2007). In the HPLC analysis the peak at 16.7 minutes for the product is the same retention time as for 4-[*N*'-(2-iodobenzylidene)-hydrazino]-benzoic acid. This is not expected as it is likely that due to the carboxylic acid group, 4-[*N*'-(2-iodobenzylidene)-hydrazino]-benzoic acid would be more polar than benzyl-(2-iodobenzylidene)-amine and therefore have a shorter retention time.

Benzylamine does not absorb UV light strongly even at its λ_{max} of 248nm, (extinction coefficient (ε) measured as 0.1) this would explain its absence from the HPLC analysis, especially if not present in large quantities.

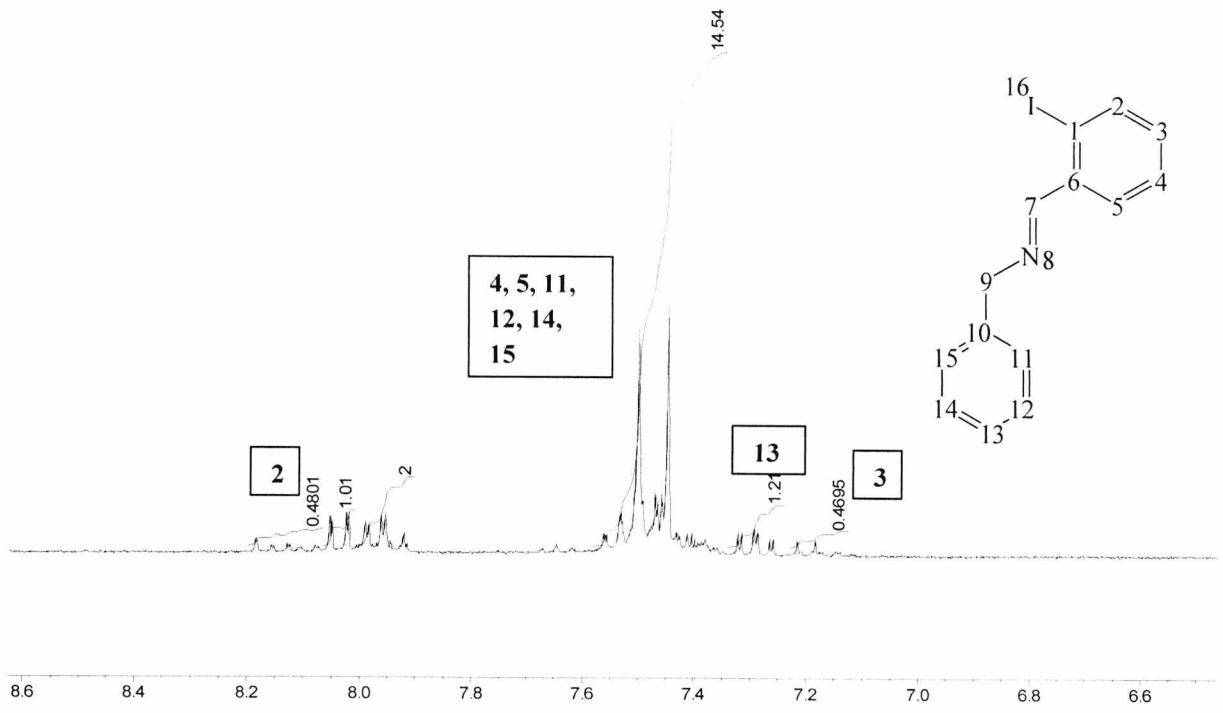
14.54
4, 5, 11, 12, 14, 15
2
0.4801
1.01
2
13
1.21
3
0.4695
16
I
1
2
3
4
5
6
7
N
8
9
10
11
12
13
14
15
8.6
8.4
8.2
8.0
7.8
7.6
7.4
7.2
7.0
6.8
6.6

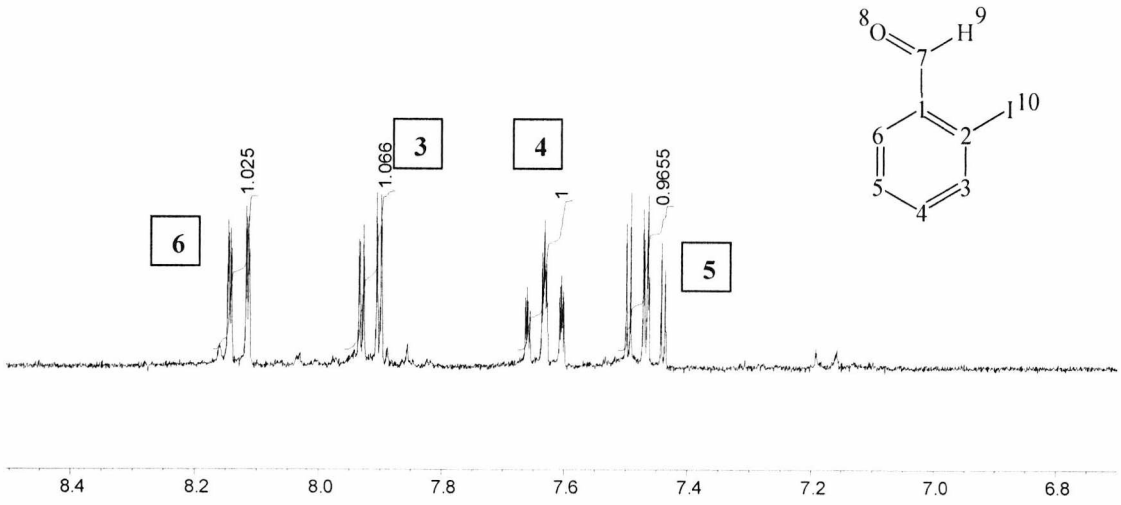
6
1.025
3
1.066
4
1
0.9655
5
8
O
H
9
7
1
2
I
10
3
4
5
6
8.4
8.2
8.0
7.8
7.6
7.4
7.2
7.0
6.8

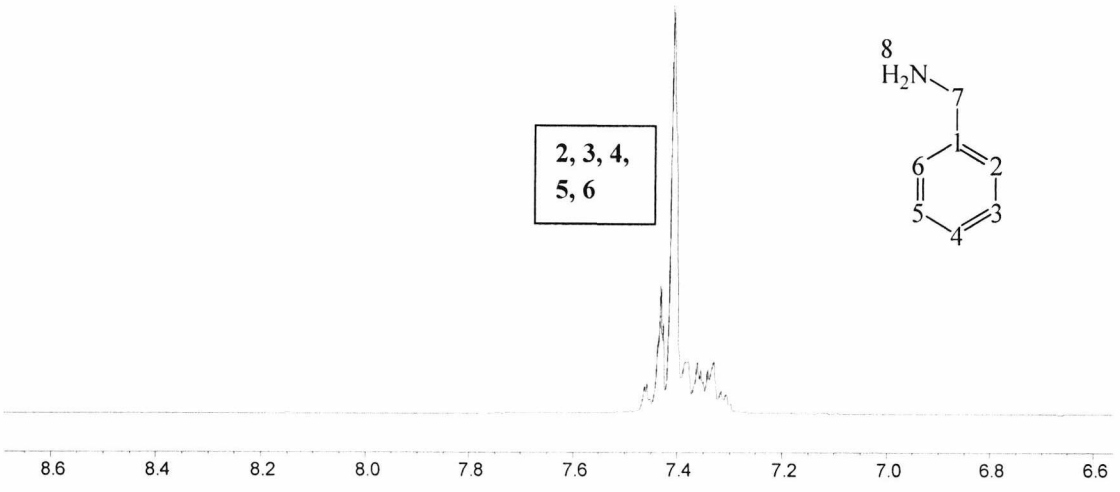
2, 3, 4, 5, 6
8
H2N
7
1
2
3
4
5
6
8.6
8.4
8.2
8.0
7.8
7.6
7.4
7.2
7.0
6.8
6.6

Figure 2.48 The top spectrum is of the reaction mixture from the reaction between 2-iodobenzaldehyde and benzylamine. The middle spectrum shows a spectrum of 2-iodobenzaldehyde and the bottom spectrum shows benzylamine for comparison

2.7.1.3.4 Competition reaction between benzylamine and 4-hydrazinobenzoic acid for 2-iodobenzaldehyde

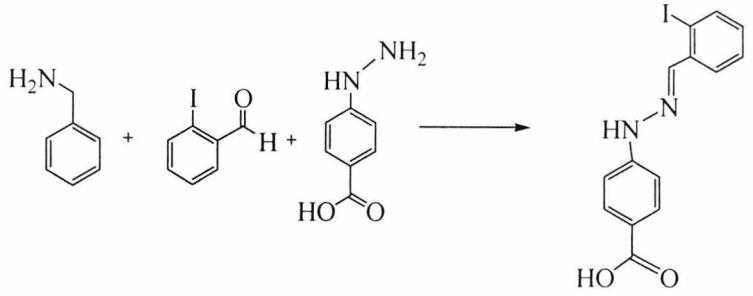

Scheme 2.23

Benzylamine had the effect of shifting slightly some of the peaks in the ^{1}H spectrum of the reaction mixture containing the product 4-[*N*'-(2-iodobenzylidene)-hydrazino]-benzoic acid in comparison to a spectrum of 4-[*N*'-(2-iodobenzylidene)-hydrazino]-benzoic acid without benzylamine present. A ^{1}H spectrum of the standard of 4-[*N*'-(4-fluorobenzylidene)-hydrazino]-benzoic acid with benzylamine added was carried out to verify that the same product was actually being formed in the reaction and the shift of the peaks was due to the benzyamine and not a different product being formed. This was found to be the case. This is also true of the reactions with the other aromatic aldehydes. This is likely to be a similar effect as changing the NMR solvent can have on peak position in the spectrum as changing the chemical environment the protons are in can have an effect on chemical shift. See section 2.7.1.3.6 for the results of the investigation of this phenomenon. The HPLC analysis showed 4-[*N*'-(2-iodobenzylidene)-hydrazino]-benzoic acid and the starting materials 2-iodobenzaldehyde and HYBA, indicating the reaction between HYBA and 2-iodobenzaldehyde did not quite proceed to completion, however no evidence of starting materials could be seen in the ^{1}H spectrum. It may be that storage of the sample before HPLC analysis has caused degradation of the sample.

This reaction was also carried out as above but using ten times the amount of benzylamine. Results obtained again demonstrated that HYBA reacted preferentially with the aldehyde as judged by ^{1}H NMR analysis.

Summary of the competition reactions between benzylamine and 4-hydrazinobenzoic acid for 2-iodobenzaldehyde

2-Iodobenzaldehyde and HYBA reacted to yield 4-[*N*'-(2-iodobenzylidene)-hydrazino]-benzoic acid. 2-Iodobenzaldehyde therefore reacted with HYBA in preference to the competing amine, benzylamine. This occured even when a tenfold excess of competing amine benzylamine was present. The reaction proceeded to completion with no starting material remaining in the ^{1}H spectrum. The NMR results are shown below in a summary of the ^{1}H NMR spectra shown in this section.

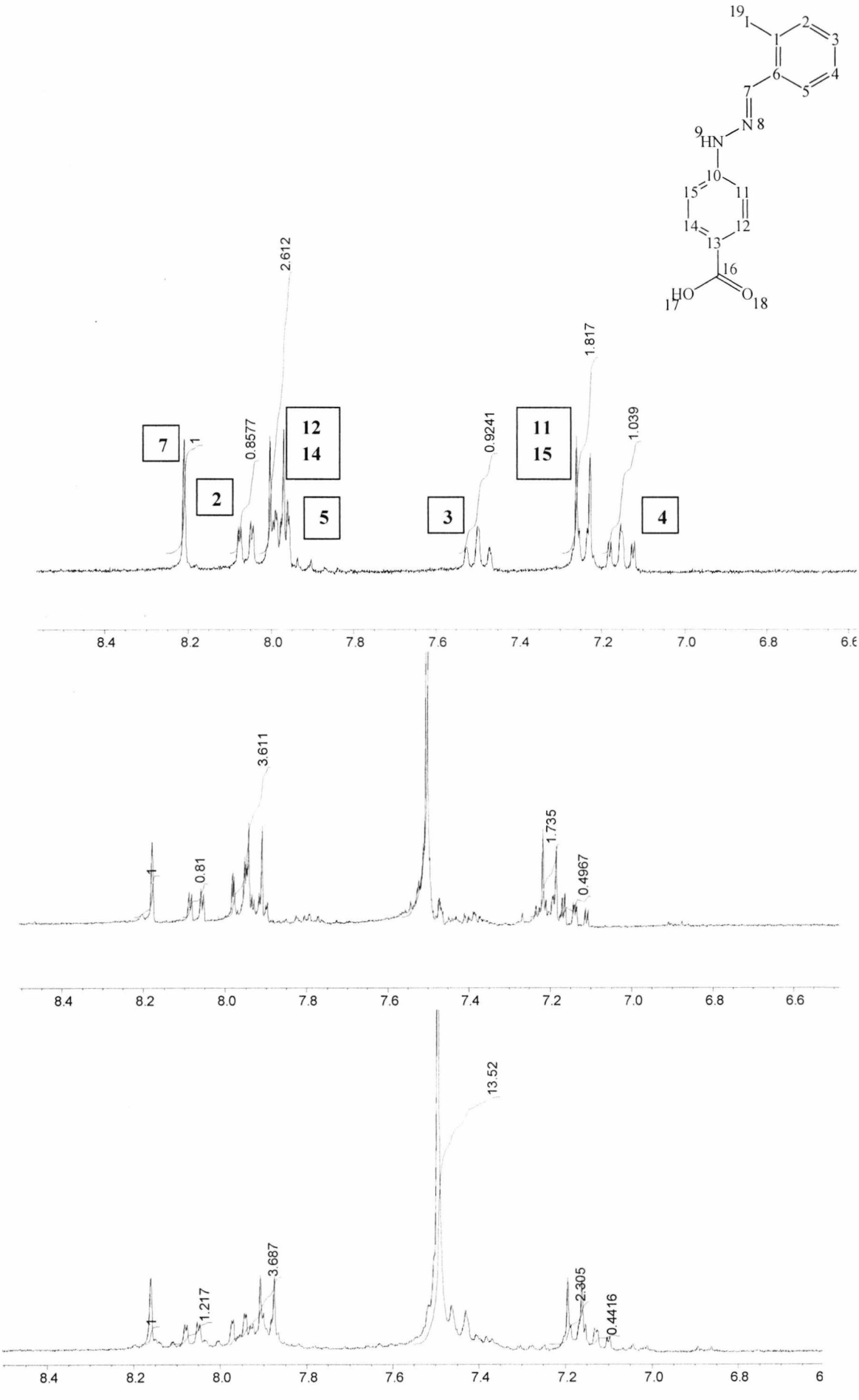
19
1
2
3
4
5
6
7
8
9
HN
10
11
12
13
14
15
16
17
HO
18
2.612
1.817
0.8577
0.9241
1.039
7
1
2
12
14
5
3
11
15
4
8.4
8.2
8.0
7.8
7.6
7.4
7.2
7.0
6.8
3.611
1.735
0.81
0.4967
13.52
3.687
1.217
2.305
0.4416

Figure 2.49 The top ^{1}H specrum is the reaction between HYBA and 2-iodobenzaldehyde. The middle spectrum shows the competition reaction with one equivalent of benzylamine. The bottom spectrum shows the competition reaction with ten equivalents of benzylamine

2.7.1.3.5 Reaction between benzylamine and 4-fluorobenzaldehyde

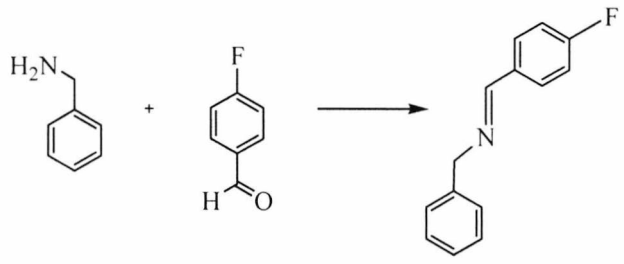

Scheme 2.24

The ^{1}H spectrum showed product formation (80%) of benzyl-(4-fluorobenzylidene)-amine that can be seen from the peak at 8.52 ppm (the proton in position 7-H) with both starting materials also found (20%). 4-fluorobenzaldehyde reacted with the benzylamine, but the reaction did not proceed to completion.

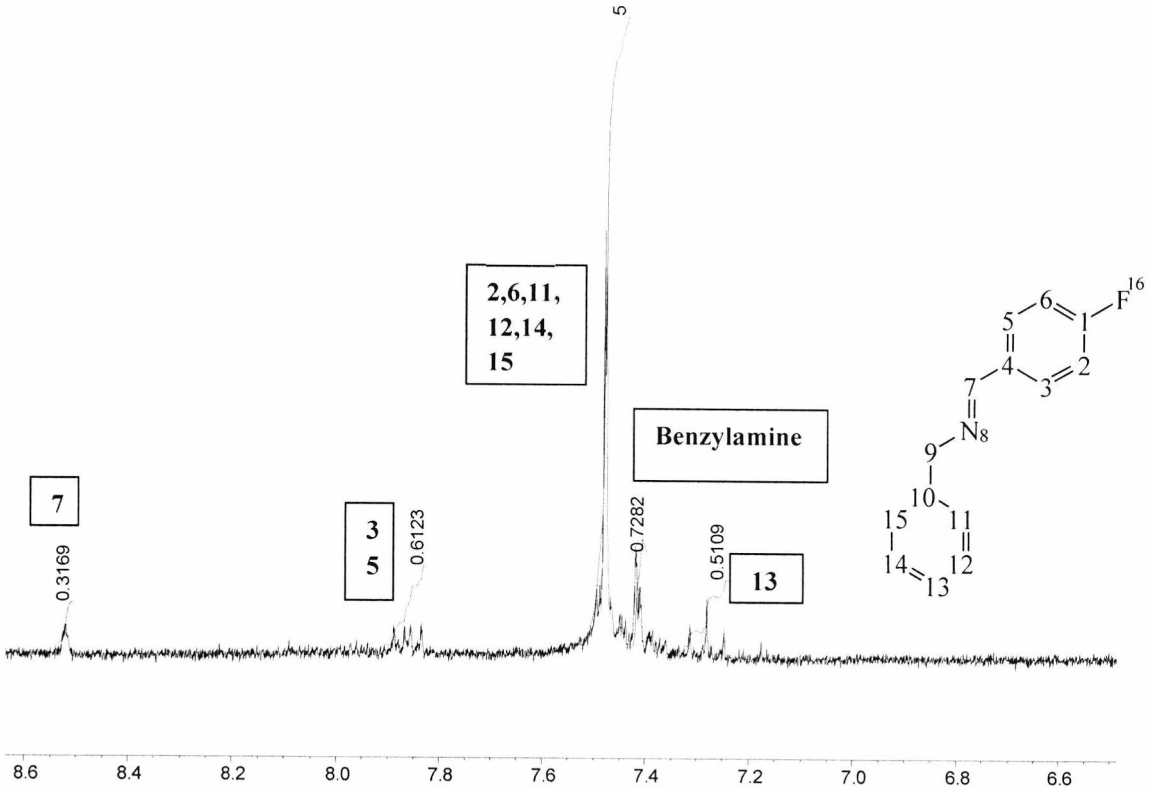
2,6,11,
12,14,
15
Benzylamine
7
3
5
13
0.3169
0.6123
0.7282
0.5109
F16
N8
8.6
8.4
8.2
8.0
7.8
7.6
7.4
7.2
7.0
6.8
6.6

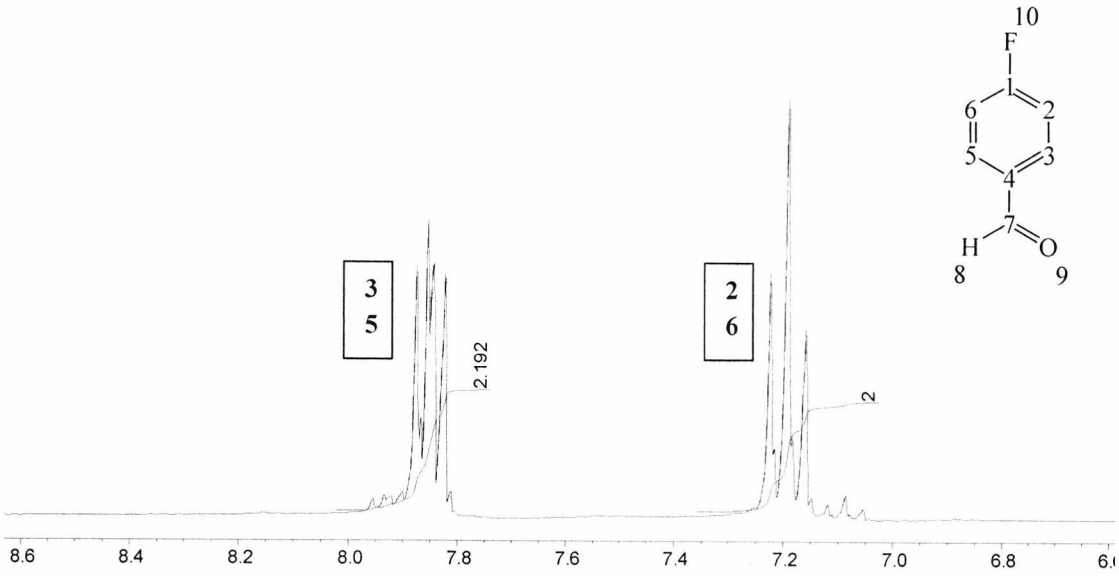
3
5
2
6
2.192
F10
O9
H8
8.6
8.4
8.2
8.0
7.8
7.6
7.4
7.2
7.0
6.8

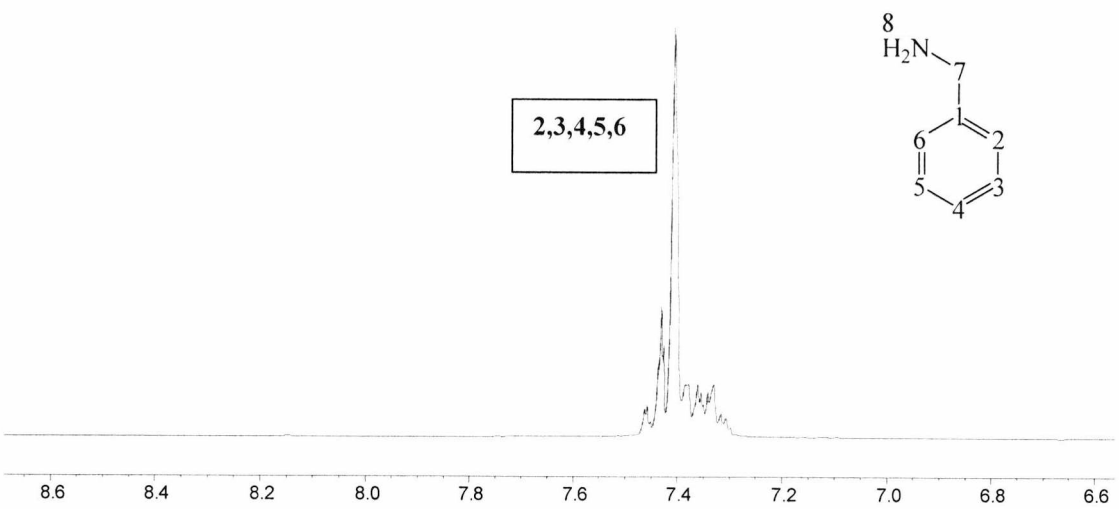
2,3,4,5,6
H2N8
8.6
8.4
8.2
8.0
7.8
7.6
7.4
7.2
7.0
6.8
6.6

Figure 2.50 The top spectrum is of the reaction mixture from the reaction between 4-fluorobenzaldehyde and benzylamine. The middle spectrum shows a spectrum of 4-fluorobenzaldehyde and the bottom spectrum shows benzylamine for comparison

2.7.1.3.6 Competition reaction between benzylamine and 4-hydrazinobenzoic acid for 4-fluorobenzaldehyde

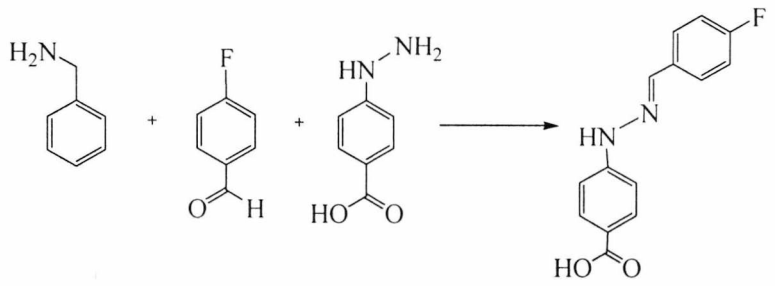

Scheme 2.25

The ^{1}H spectrum shows that upon addition of benzylamine to a pure solution of 4-[*N*'-(4-fluorobenzylidene)-hydrazino]-benzoic acid, the chemical shift of some of the peaks in the ^{1}H spectrum corresponding to 4-[*N*'-(4-fluorobenzylidene)-hydrazino]-benzoic acid changes. This is due to the change in the chemical environment induced by addition of benzylamine to the sample in the same way changing the ^{1}H NMR solvent has an effect on chemical shift. Benzylamine did not show strong UV absorbance, even at its λ_{max}. It needs to be present in large quantities to show a peak by HPLC analysis as discussed already. This is probably the reason for its absence from the HPLC chromatogram.

The competition reaction above was carried out again using ten times the amount of benzylamine. The ^{1}H NMR results showed formation of 4-[*N*'-(4-fluorobenzylidene)-hydrazino]-benzoic acid from the reaction of HYBA with 4-fluorobenzaldehyde and no reaction of 4-fluorobenzaldehyde with benzylamine.

Summary of competition reactions between benzylamine and 4-hydrazinobenzoic acid for 4-fluorobenzaldehyde

4-fluorobenzaldehyde and HYBA reacted giving 4-[*N*'-(4-fluorobenzylidene)-hydrazino]-benzoic acid. This shows that 4-fluorobenzaldehyde reacted with HYBA in preference to the competing amine, benzylamine. This occured even when a tenfold excess of competing amine

benzylamine was present. The reaction between HYBA and 4-fluorobenzaldehyde proceeded nearly to completion in both competition reactions (90% product formation by NMR) as shown below in a summary of the ^{1}H NMR spectra shown in this section.

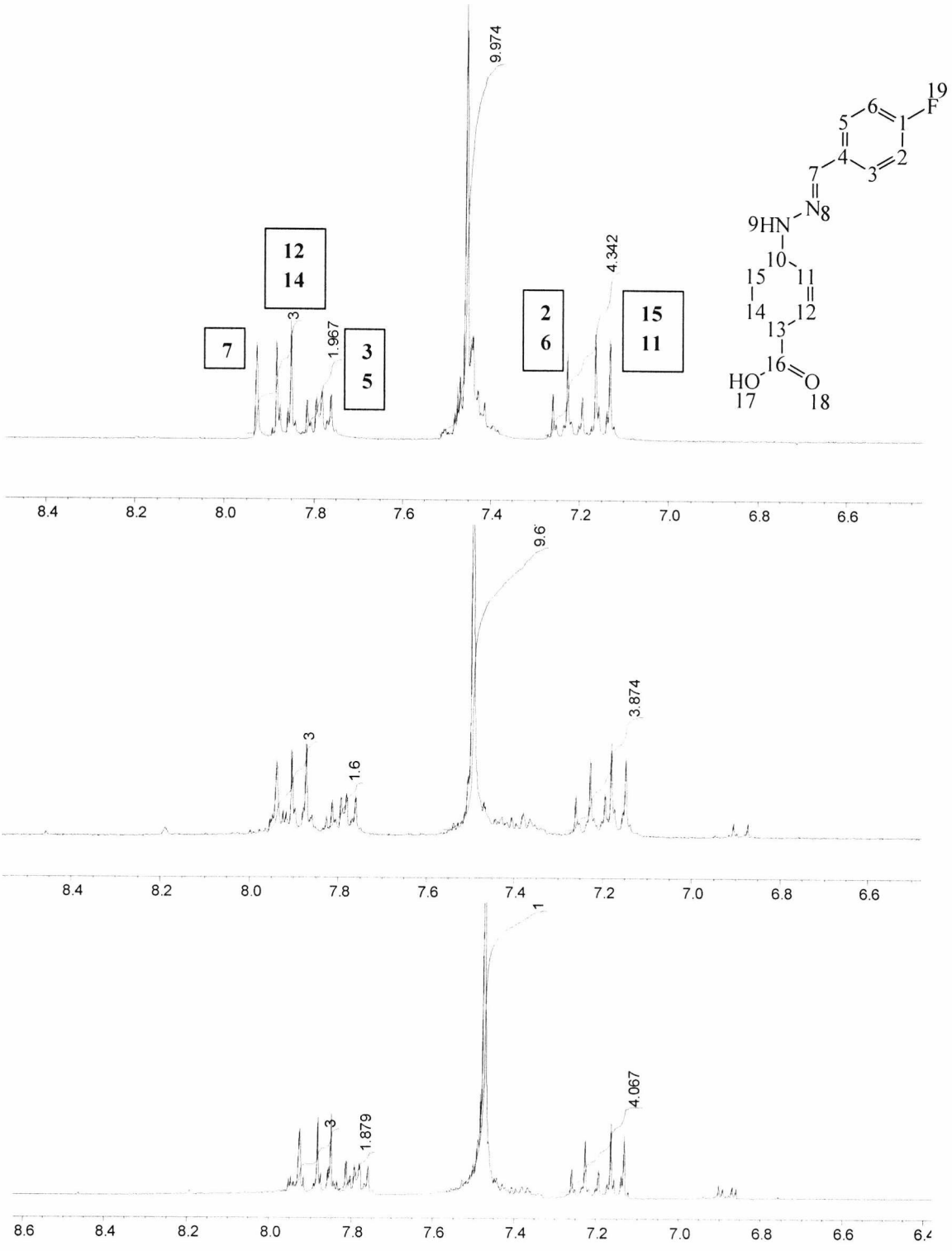
9.974
4.342
1.967
3
12
14
7
3
5
2
6
15
11
19
F
6
1
5
2
4
3
7
N8
9HN
10
15
11
14
12
13
16
HO
17
O
18
8.4
8.2
8.0
7.8
7.6
7.4
7.2
7.0
6.8
6.6
9.6
3.874
3
1.6
8.4
8.2
8.0
7.8
7.6
7.4
7.2
7.0
6.8
6.6
1
4.067
3
1.879
8.6
8.4
8.2
8.0
7.8
7.6
7.4
7.2
7.0
6.8
6.6

Figure 2.51 The top spectrum is of 4-[*N*'-(4-fluorobenzylidene)-hydrazino]-benzoic acid standard. Benylamine was added just before the NMR analysis was carried out. In the middle is the spectrum of the reaction mixture from the competition reaction with one equivalent of benzylamine added. At the bottom is the spectrum of the reaction mixture from competition reaction with ten equivalents of benzylamine added

2.7.1.3.7 Reaction between benzylamine and 4-bromobenzaldehyde

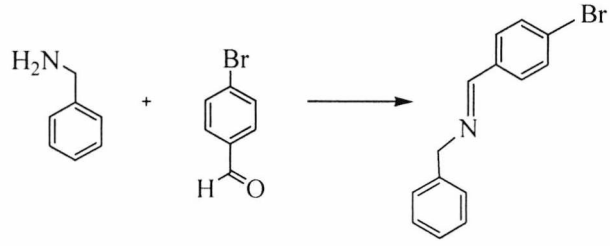

Scheme 2.26

Both starting material and product were present in the ^{1}H spectrum (40% starting material, 60% product). HPLC analysis showed the presence of 4-bromobenzaldehyde but not benzylamine. 4-Bromobenzaldehyde reacted with benzylamine, although the reaction did not proceed to completion.

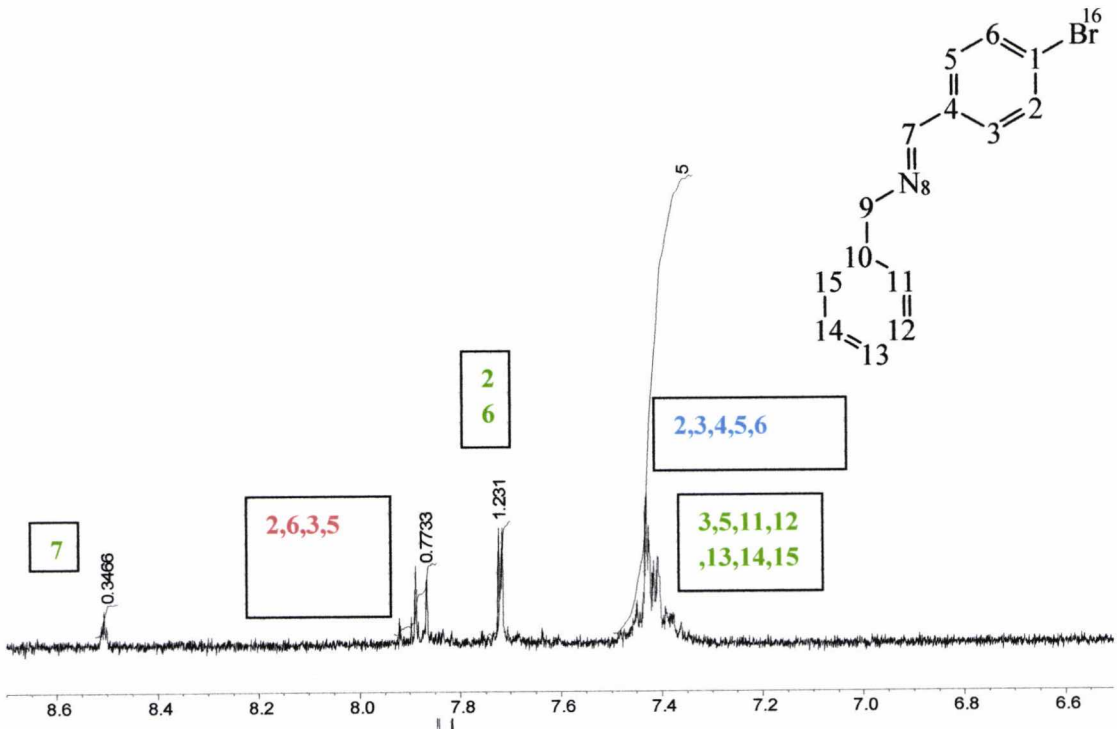
7
0.3466
2,6,3,5
0.7733
1.231
2
6
2,3,4,5,6
3,5,11,12
,13,14,15
8.6
8.4
8.2
8.0
7.8
7.6
7.4
7.2
7.0
6.8
6.6

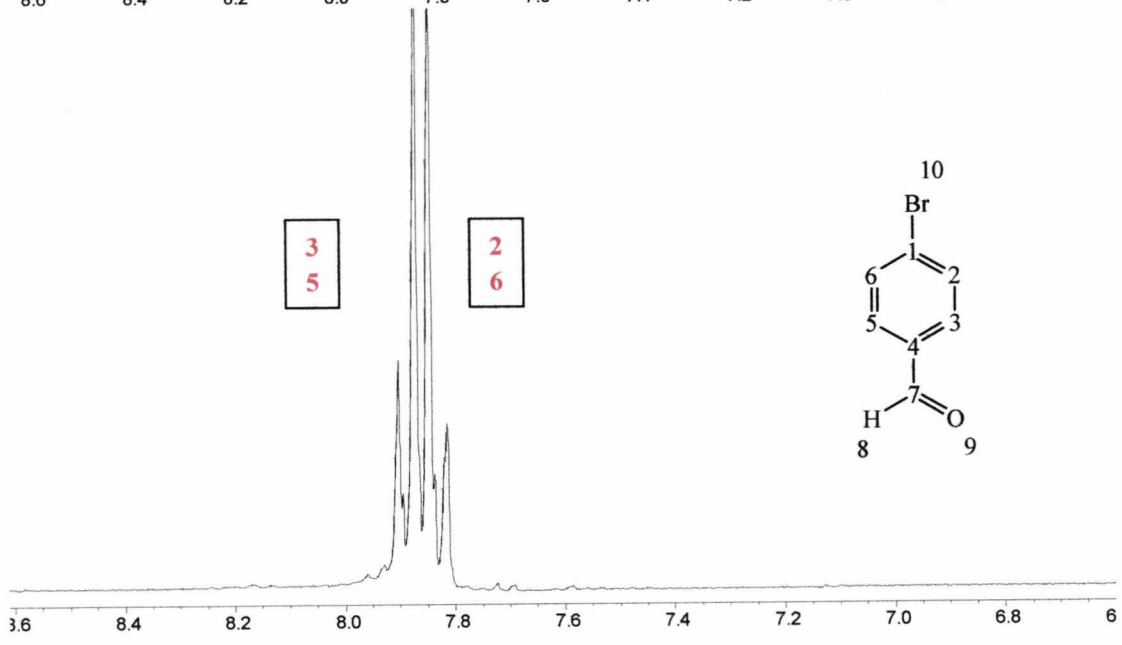
3
5
2
6
8.4
8.2
8.0
7.8
7.6
7.4
7.2
7.0
6.8

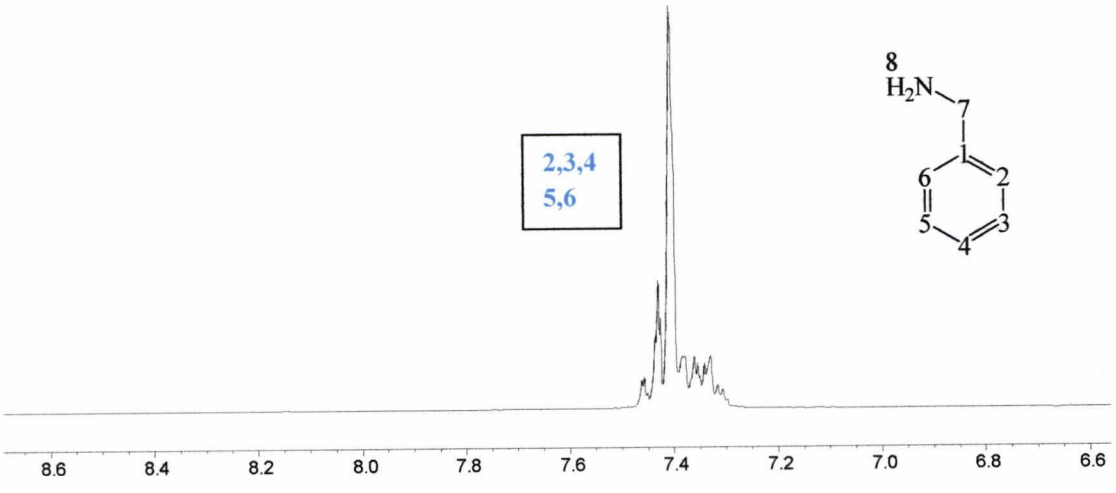
2,3,4
5,6
8.6
8.4
8.2
8.0
7.8
7.6
7.4
7.2
7.0
6.8
6.6

Figure 2.52 The top spectrum is of the reaction mixture from the reaction between 4-bromobenzaldehye (4-BB) and benzylamine. The middle spectrum is of 4-bromobenzaldehyde and the bottom spectrum shows benzylamine for comparison

2.7.1.3.8 Competition reaction between benzylamine and 4-hydrazinobenzoic acid for 4-bromobenzaldehyde

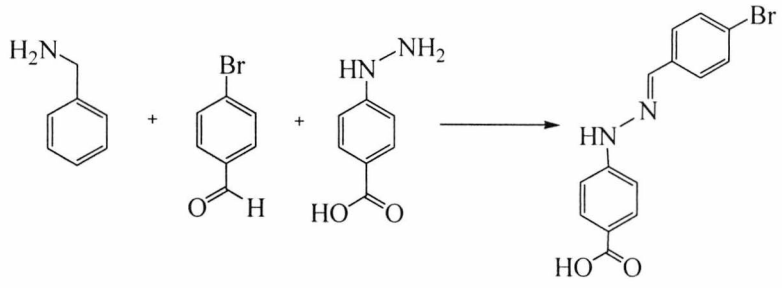

Scheme 2.27

No benzylamine was present by HPLC analysis. 4-[*N*'-(4-Bromobenzylidene)-hydrazino]-benzoic acid was present according to HPLC and NMR analysis. A small amount of unreacted 4-bromobenzaldehyde was present in the chromatogram (10%). This is possibly due to a slight excess being added to the reaction mixture initially (as there is no HYBA present in the ^{1}H spectrum or HPLC chromatogram) or storage of the sample before analysis leading to degradation. HYBA and 4-bromobenzaldehyde reacted together in the presence of benzylamine, with 4-bromobenzaldehyde reacting preferentially with HYBA and not at all with benzylamine. The presence of benzylamine has shifted the peaks in the ^{1}H spectrum. This is likely to be an effect similar to the effect of using a different deuterated NMR solvent for dissolving a sample; the peaks are shifted a small amount due to the changing chemical environment of the molecule in solution.

This reaction was also carried out as above but using ten times the amount of benzylamine. Results obtained showed that 4-bromobenzaldehyde reacted preferentially with HYBA even in the presence of a tenfold excess of the competing amine.

Summary of competition reactions with 4-bromobenzaldehyde, HYBA and benzylamine

4-Bromobenzaldehyde and HYBA reacted giving the product 4-[*N*'-(4-bromobenzylidene)-hydrazino]-benzoic acid. This shows that 4-bromobenzaldehyde reacted with HYBA in preference to the competing amine, benzylamine. This occurred even when a tenfold excess of

competing amine benzylamine was present. The reaction between HYBA and 4-bromobenzaldehyde proceeded almost to completion with 90% product formation.

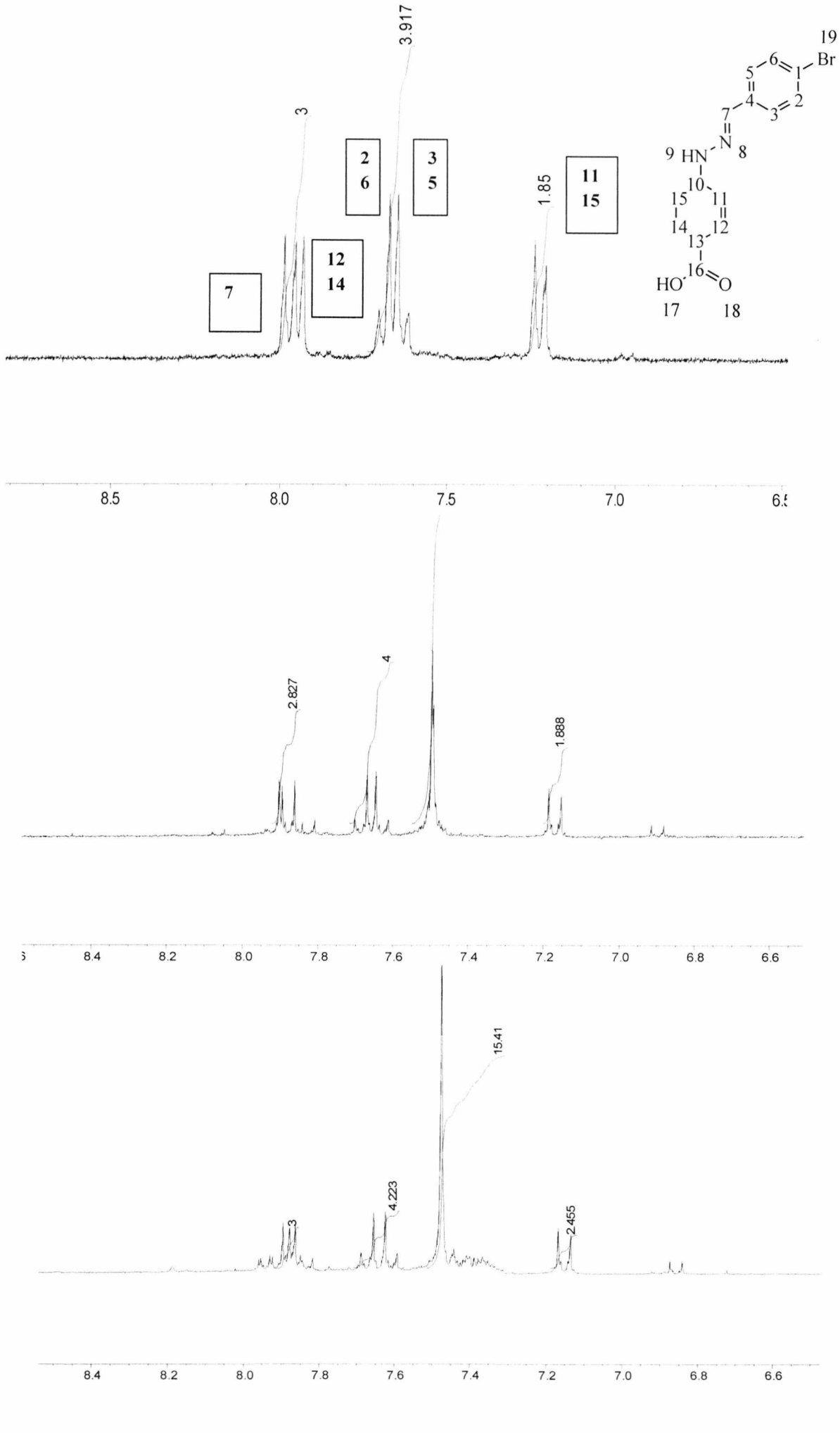
3.917
3
2
6
3
5
1.85
11
15
12
14
7
19
Br
9 HN
N 8
HO
O
17
18
8.5
8.0
7.5
7.0
2.827
4
1.888
8.4
8.2
8.0
7.8
7.6
7.4
7.2
7.0
6.8
6.6
15.41
4.223
3
2.455

Figure 2.53 The top spectrum is shows the reaction between HYBA and 4-bromobenzaldehyde only. The middle spectrum shows the reaction mixture from the competition reaction with one equivalent of benzylamine added. At the bottom the spectrum shows the reaction mixture from the competition reaction with ten equivalents of benzylamine added

2.7.1.3.9 Reaction between benzylamine and 4-formylphenyl boronic acid

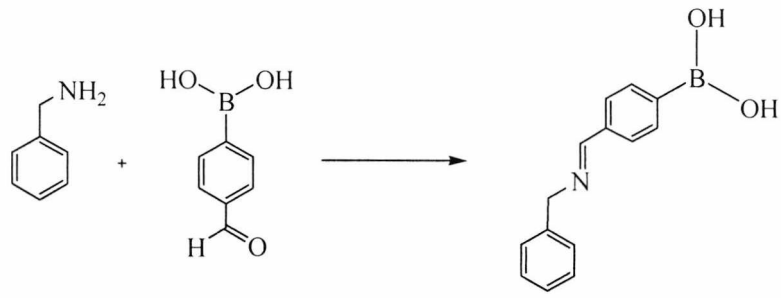

Scheme 2.28

Benzlyamine and 4-formylphenyl boronic acid reacted together to give the product shown in the NMR spectrum. Benzylamine and 4-formylphenyl boronic acid were present in the ^{1}H spectrum (spectrum showed 40% product formation) with HPLC analysis showing 4-formylphenyl boronic acid to be present but no benzylamine. The reaction occurred, but the unreacted starting materials present show that they have only partially reacted.

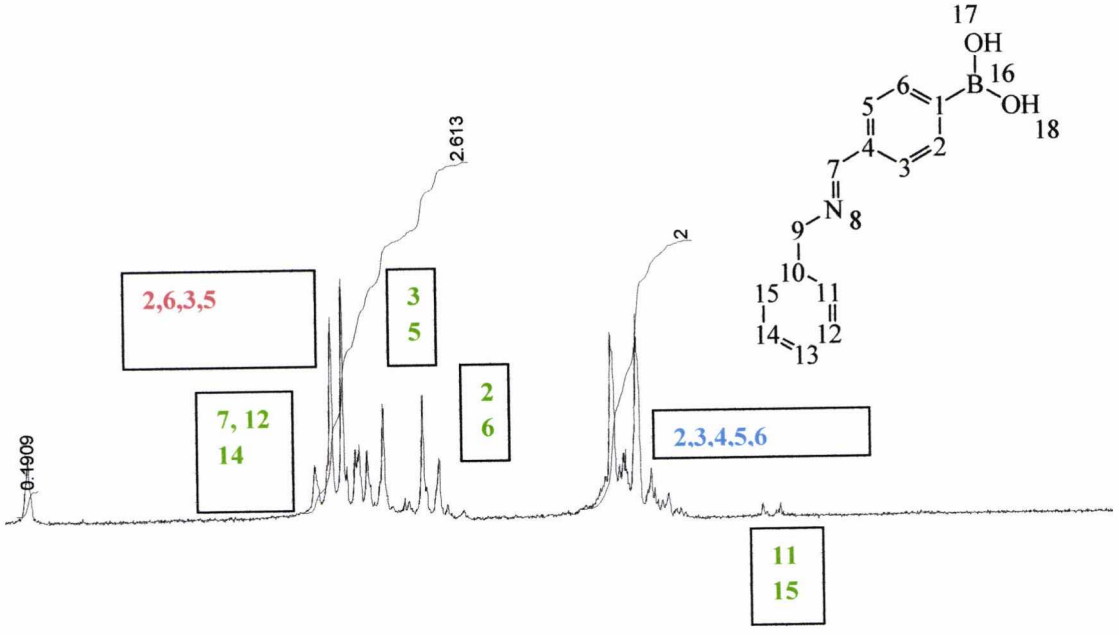
2,6,3,5
3
5
2
6
7, 12
14
2,3,4,5,6
11
15
0.4909
2.613

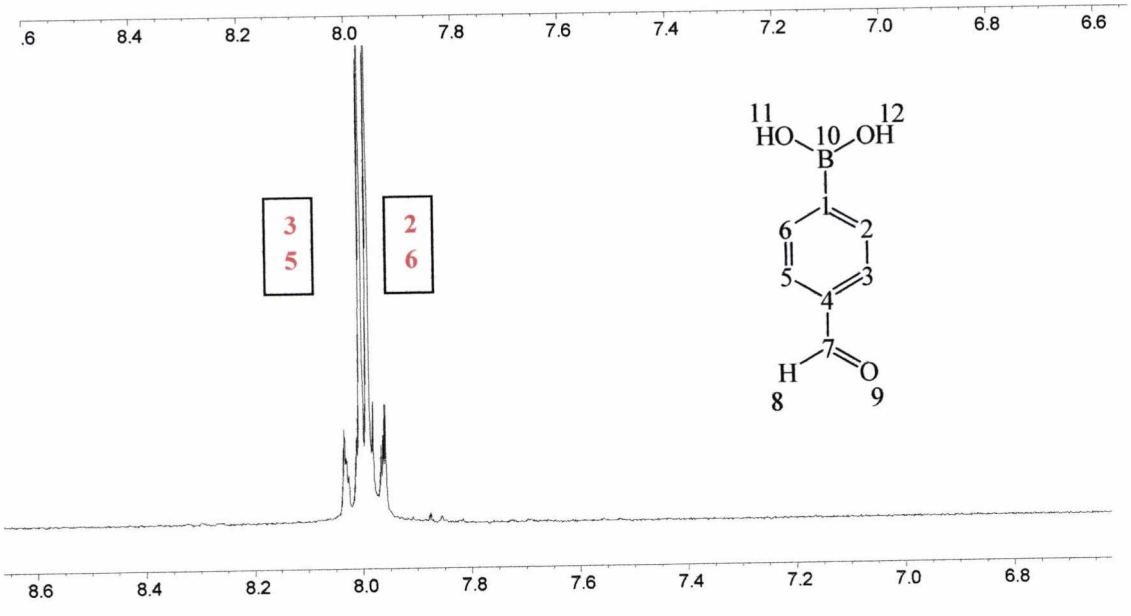
3
5
2
6

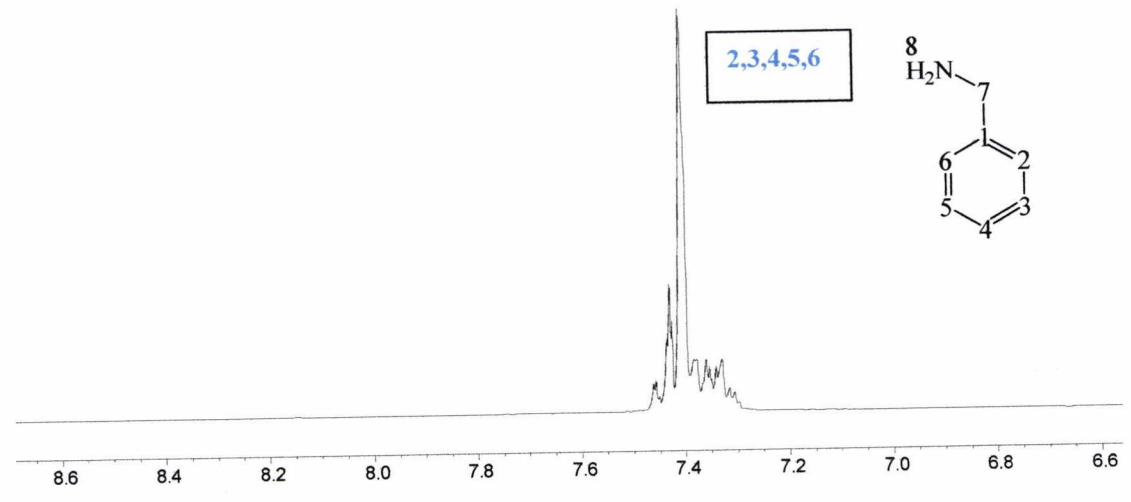
2,3,4,5,6

Figure 2.54 The top spectrum is of the reaction mixture from the reaction between 4-formylphenyl boronic acid and benzylamine. The middle spectrum is of 4-formylphenyl boronic acid and the bottom spectrum shows benzylamine for comparison

2.7.1.4.0 Competition reaction between benzylamine and 4-hydrazinobenzoic acid for 4-formylphenyl boronic acid

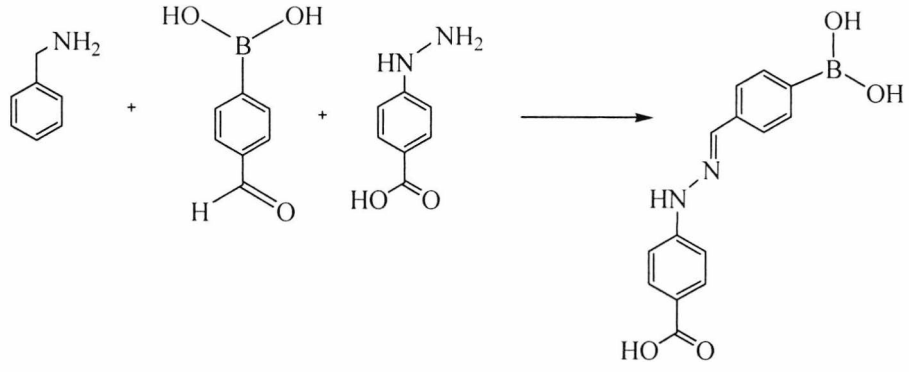

Scheme 2.29

From the NMR spectrum, it can be seen that 4-formylphenyl boronic acid reacted with HYBA to yield 4-[N'-(4-boronobenzylidene)hydrazino]-benzoic acid. The reaction was incomplete when one equivalent of benzylamine was added (60% product formation by NMR) and the number of peaks in the spectrum makes it difficult to assign peaks accurately. The reaction was repeated using a tenfold excess of benzylamine. This reaction went to completion. No HYBA or benzylamine peaks were present according to HPLC analysis.

Summary of competition reactions between benzylamine and 4-hydrazinobenzoic acid for 4-formylphenyl boronic acid

4-Formylphenylboronic acid and HYBA reacted giving the product 4-[N'-(4-boronobenzylidene)hydrazino]-benzoic acid. This shows that 4-formylphenyl boronic acid reacted with HYBA in preference to the competing amine benzylamine, when an excess was present. This occurred even when a tenfold excess of competing amine benzylamine is present.

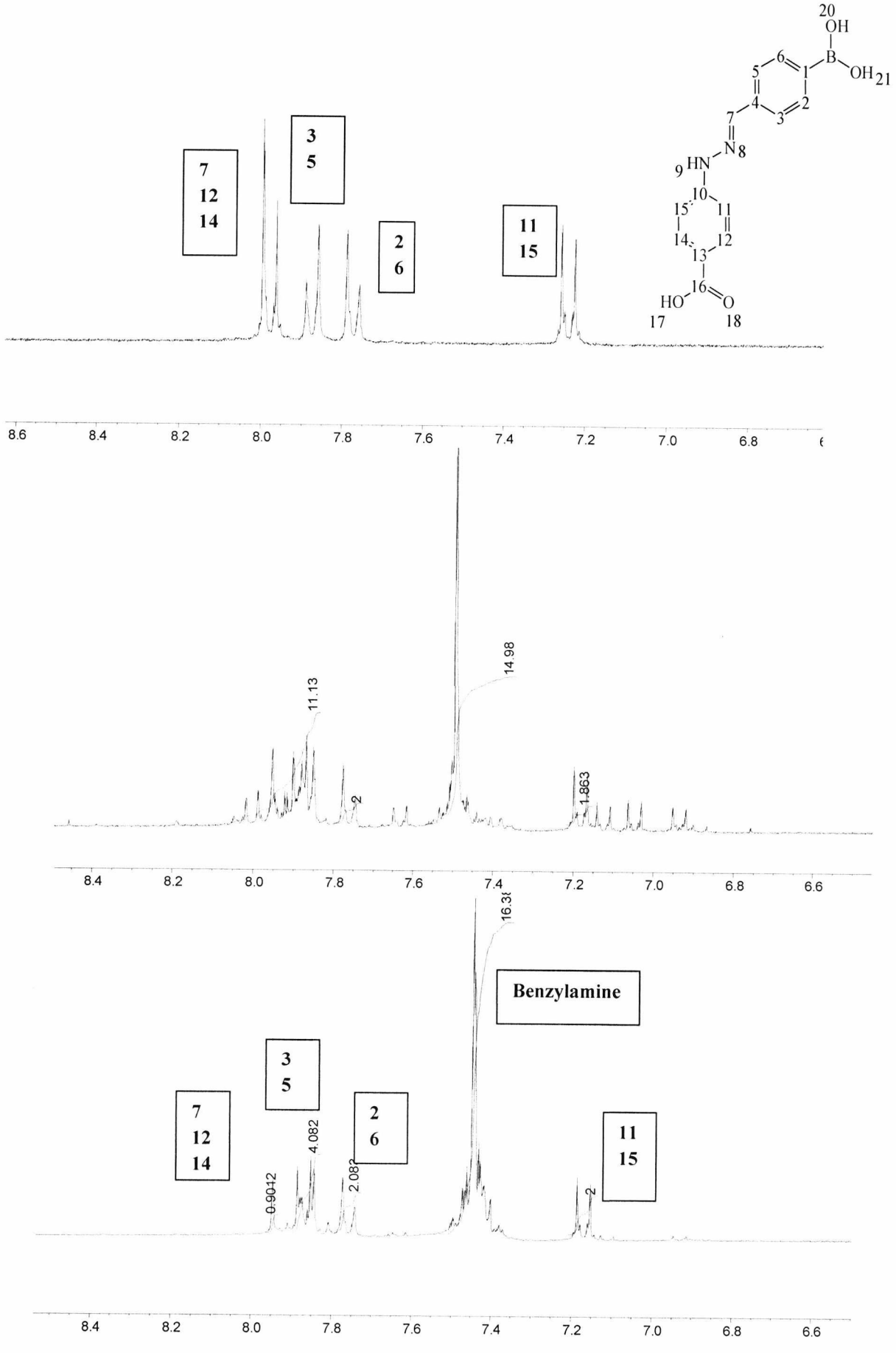
7
12
14
3
5
2
6
11
15
20
OH
B
OH
21
HN
HO
O
17
18
8.6
8.4
8.2
8.0
7.8
7.6
7.4
7.2
7.0
6.8
11.13
14.98
1.863
8.4
8.2
8.0
7.8
7.6
7.4
7.2
7.0
6.8
6.6
16.31
Benzylamine
3
5
7
12
14
2
6
11
15
4.082
2.082
0.9012
8.4
8.2
8.0
7.8
7.6
7.4
7.2
7.0
6.8
6.6

Figure 2.55 The top ^{1}H spectrum the standard of 4-[N'-(4-boronobenzylidene)hydrazino]-benzoic acid. The middle spectrum is the reaction mixture of the competition reaction with one equivalent of benzylamine added and at the bottom, the spectrum is the reaction mixture for the competition reaction with ten equivalents of benzylamine added

2.7.1.5 Competition reactions with Fmoc-Lys-OH as the competing amine

2.7.1.5.1 Reaction between Fmoc-lysine-OH (Fmoc-Lys-OH) and 2-iodobenzaldehyde

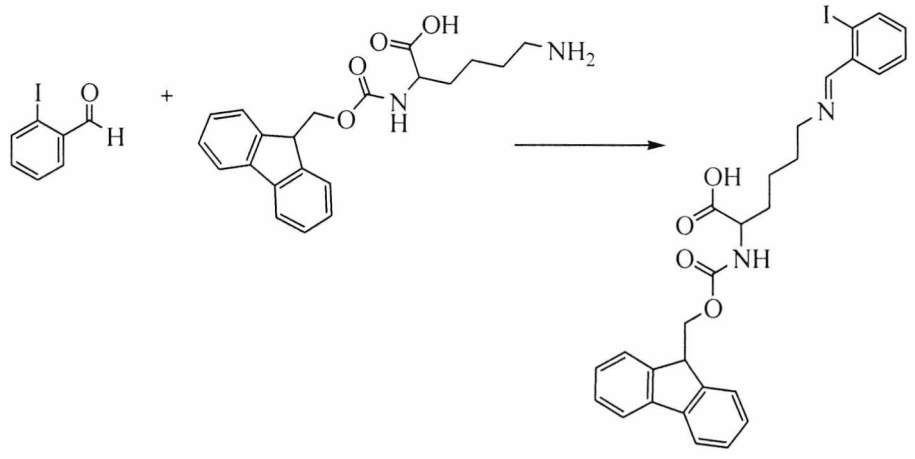

Scheme 2.30

There was no reaction between Fmoc-Lys-OH and 2-iodobenzaldehyde. NMR and HPLC analysis showed the presence of unreacted starting material only.

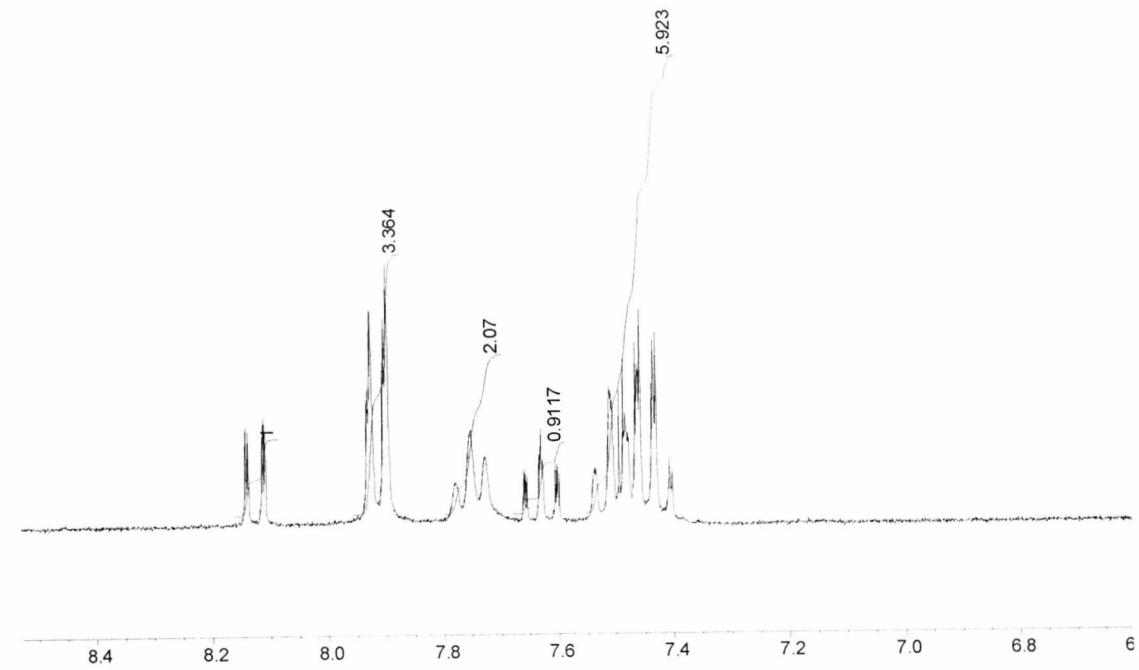
5.923
3.364
2.07
0.9117
8.4
8.2
8.0
7.8
7.6
7.4
7.2
7.0
6.8
6

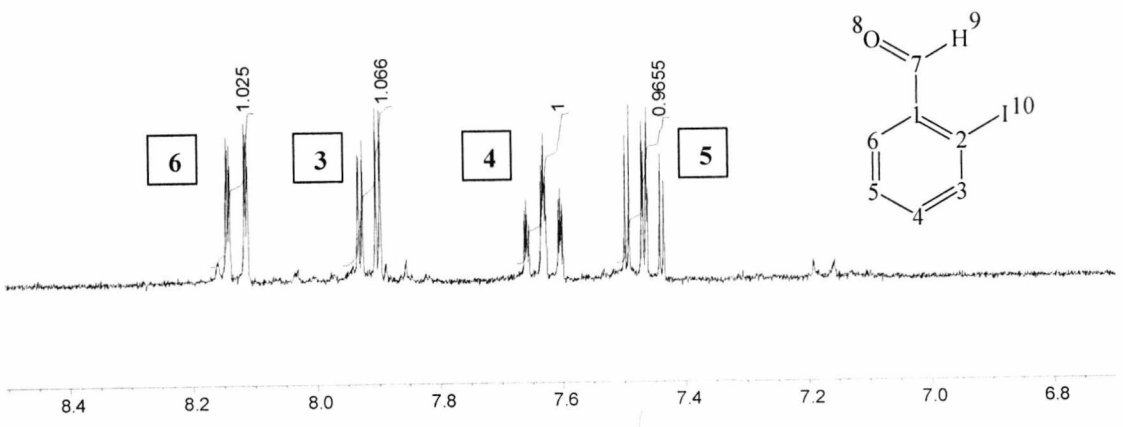
1.025
1.066
1
0.9655
6
3
4
5
8
O
H
9
7
1
I
10
2
6
3
5
4
8.4
8.2
8.0
7.8
7.6
7.4
7.2
7.0
6.8

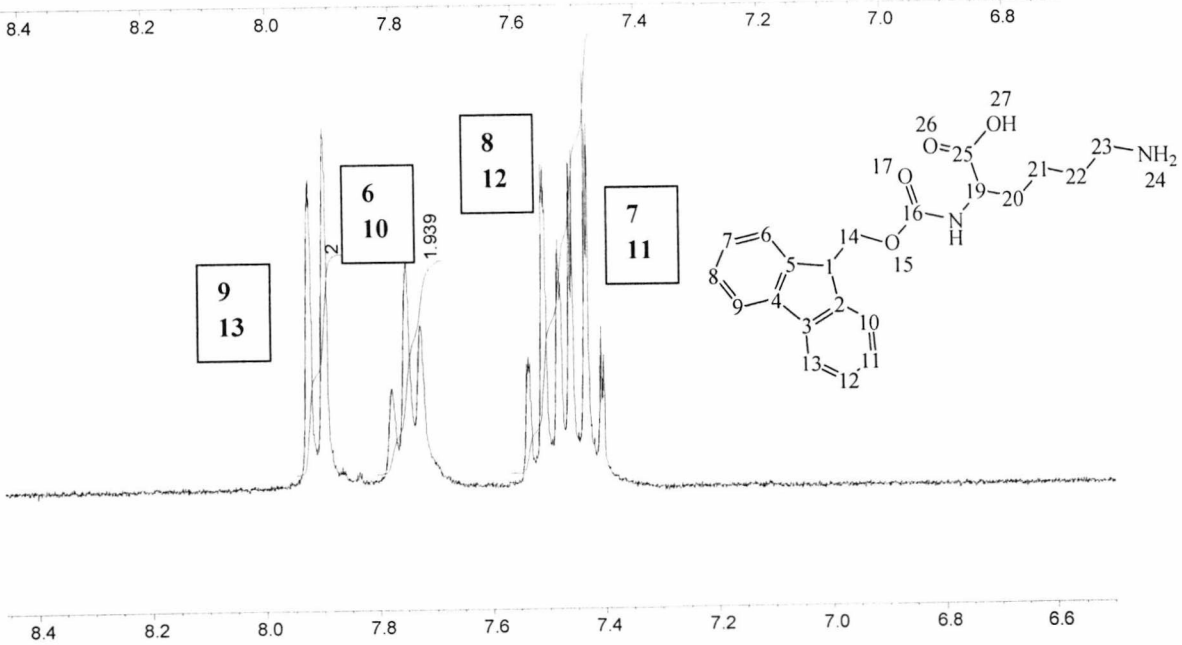
2
1.939
9
13
6
10
8
12
7
11
27
OH
26
O
25
23
NH2
24
17
O
21
22
19
20
16
N
H
14
O
15
7
6
5
1
8
9
4
2
3
10
13
12
11
8.4
8.2
8.0
7.8
7.6
7.4
7.2
7.0
6.8
6.6

Figure 2.56 The top spectrum is the ^{1}H spectrum of the reaction mixture from the reaction between 2-iodobenzaldeyhde and Fmoc-Lys-OH. In the middle is a ^{1}H spectrum of 2-iodobenzaldehyde. The bottom spectrum is a spectrum of Fmoc-Lys-OH only

2.7.1.5.2 Competition reaction between Fmoc-Lys-OH and 4-hydrazinobenzoic acid for 2-iodobenzaldehyde

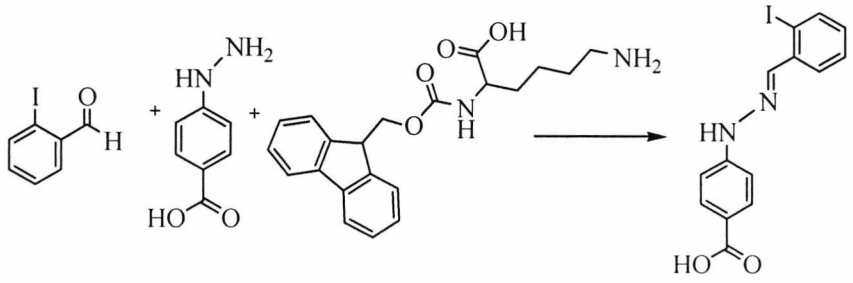

Scheme 2.31

NMR and HPLC results showed that HYBA reacted with 2-iodobenzaldehyde to yield 4-[*N*'-(2-iodobenzylidene)-hydrazino]-benzoic acid. Fmoc-Lys-OH did not react at all. The NMR spectrum showed the presence of unreacted HYBA (10%). HYBA was not present by HPLC analysis.

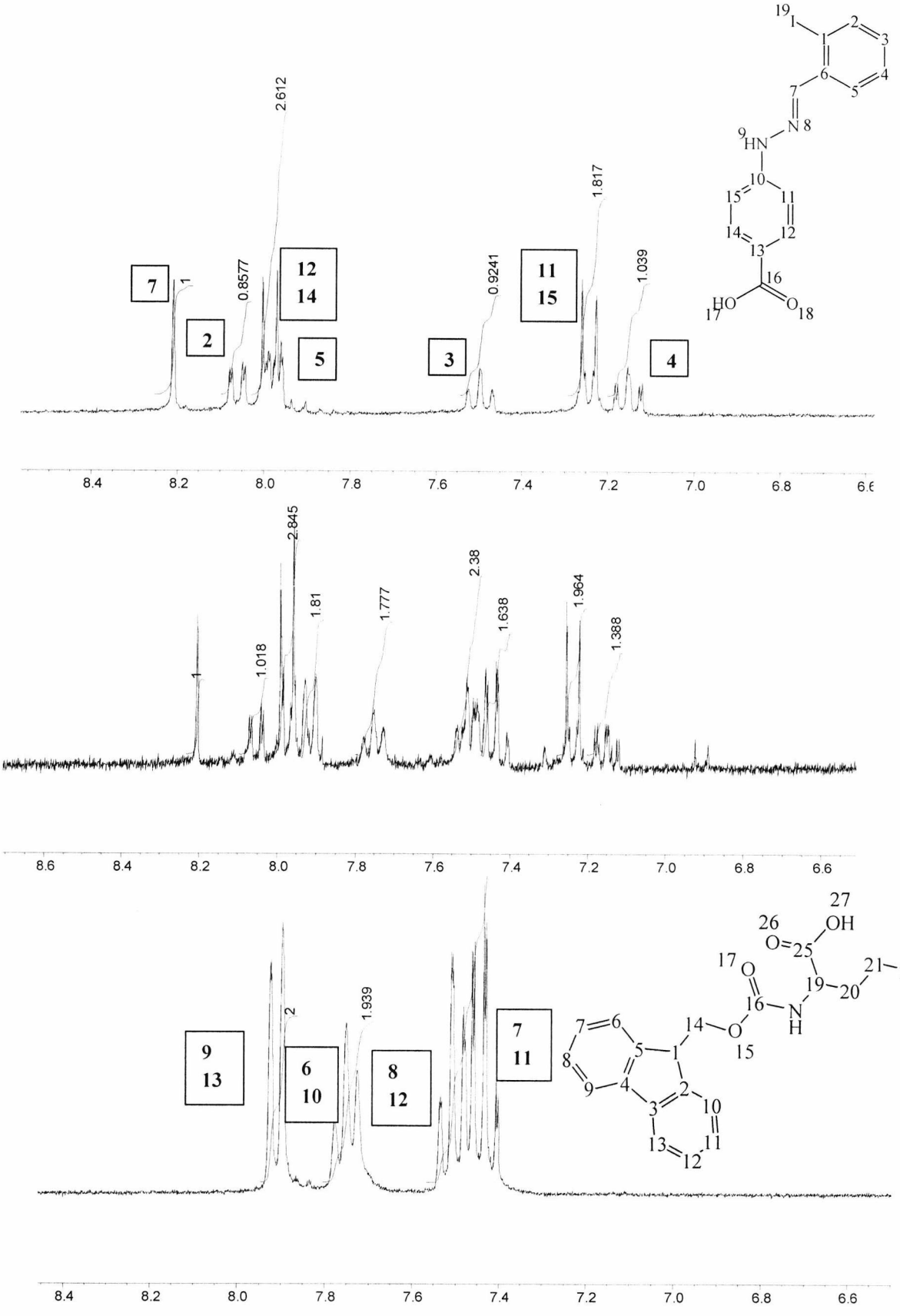
7
2
12
14
5
3
11
15
4
2.612
0.8577
0.9241
1.817
1.039
8.4
8.2
8.0
7.8
7.6
7.4
7.2
7.0
6.8
2.845
1.018
1.81
1.777
2.38
1.638
1.964
1.388
8.6
8.4
8.2
8.0
7.8
7.6
7.4
7.2
7.0
6.8
6.6
9
13
6
10
8
12
7
11
1.939
8.4
8.2
8.0
7.8
7.6
7.4
7.2
7.0
6.8
6.6

Figure 2.57 The top spectrum is the ^1H spectrum of the reaction between 2-iodobenzaldeyhde and HYBA. In the middle is a ^1H spectrum of the competition reaction between Fmoc-Lys-OH and HYBA for 2-iodobenzaldehyde. The bottom spectrum is a spectrum of Fmoc-Lys-OH only

2.7.1.5.3 Reaction between Fmoc-Lys-OH and 4-fluorobenzaldehyde

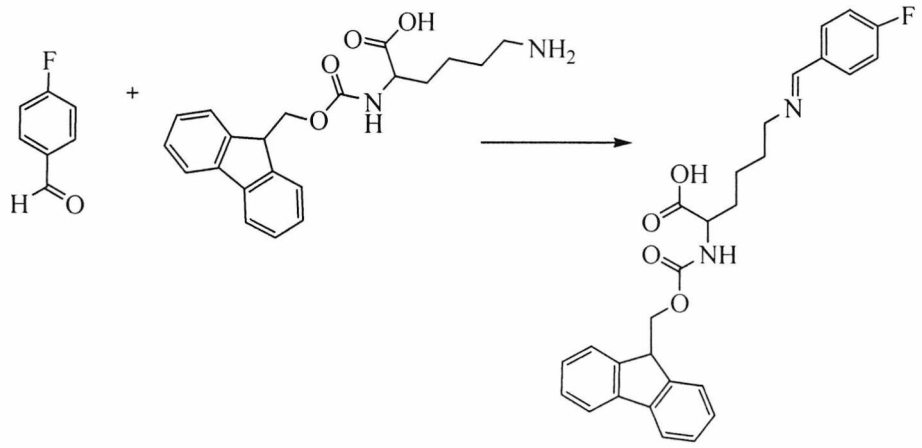

Scheme 2.32

There was no reaction between Fmoc-Lys-OH and 4-fluorobenzaldehyde. NMR and HPLC analysis showed the presence of unreacted starting material only.

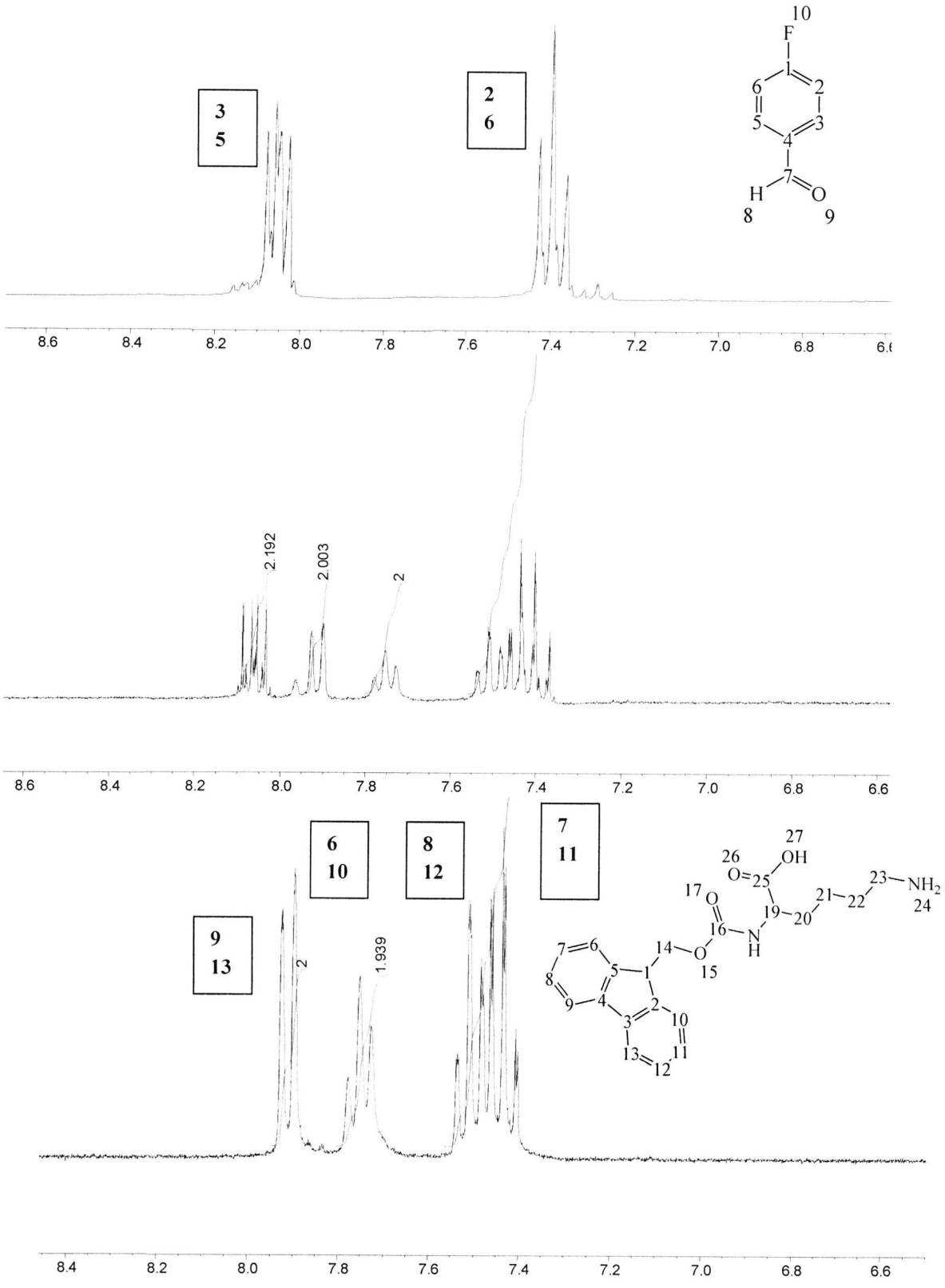
3
5
2
6
10
F
1
2
3
4
5
6
7
H
O
8
9
8.6
8.4
8.2
8.0
7.8
7.6
7.4
7.2
7.0
6.8
2.192
2.003
2
9
13
6
10
8
12
7
11
1.939
27
OH
26
O
25
17
O
16
N
H
14
O
15
23
NH2
24
21
22
19
20

Figure 2.58 The top spectrum is a ^{1}H spectrum of 4-fluorobenzaldehyde. The middle spectrum is the ^{1}H spectrum of the reaction mixture from the reaction between 4-fluorbenzaldeyhde and Fmoc-Lys-OH. The bottom spectrum is a spectrum of Fmoc-Lys-OH only

2.7.1.5.4 Competition reaction between Fmoc-Lys-OH and 4-hydrazinobenzoic acid for 4-fluorobenzaldehyde

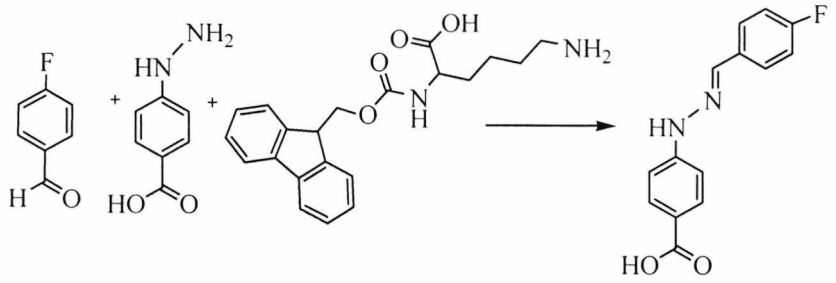

Scheme 2.33

HYBA and 4-flurobenzaldehyde reacted together completely. Fmoc-Lys-OH did not react. Both the NMR and the HPLC results showed the presence of unreacted Fmoc-Lys-OH and 4-[*N*'-(4-fluorobenzylidene)-hydrazino]-benzoic acid only.

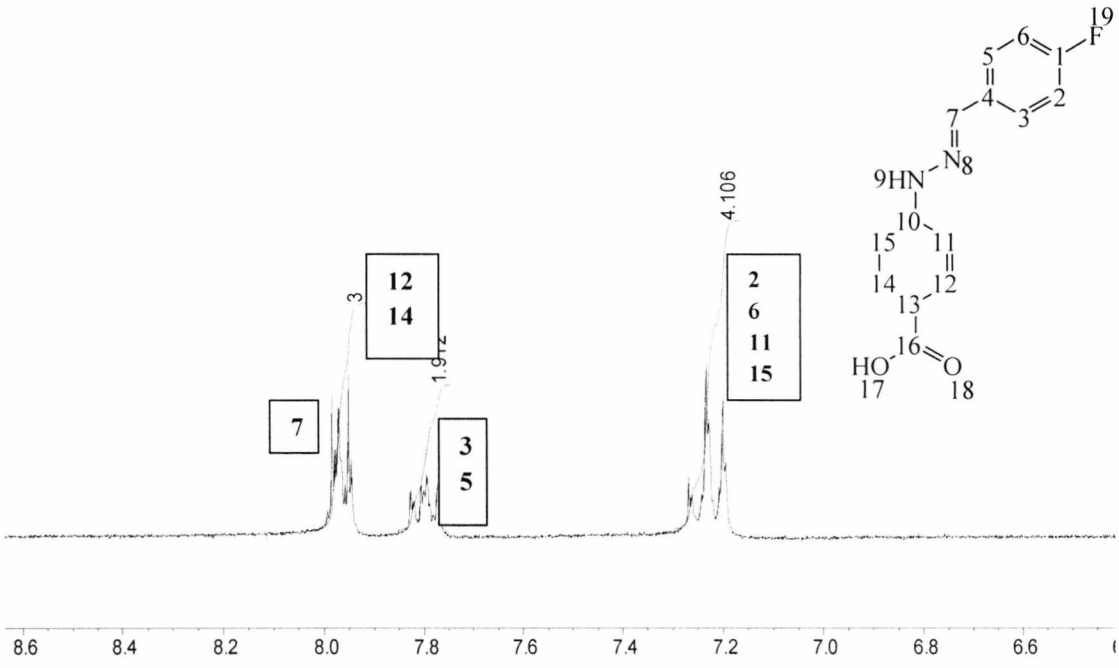
4.106
3
1.912
12
14
2
6
11
15
7
3
5
8.6
8.4
8.2
8.0
7.8
7.6
7.4
7.2
7.0
6.8
6.6

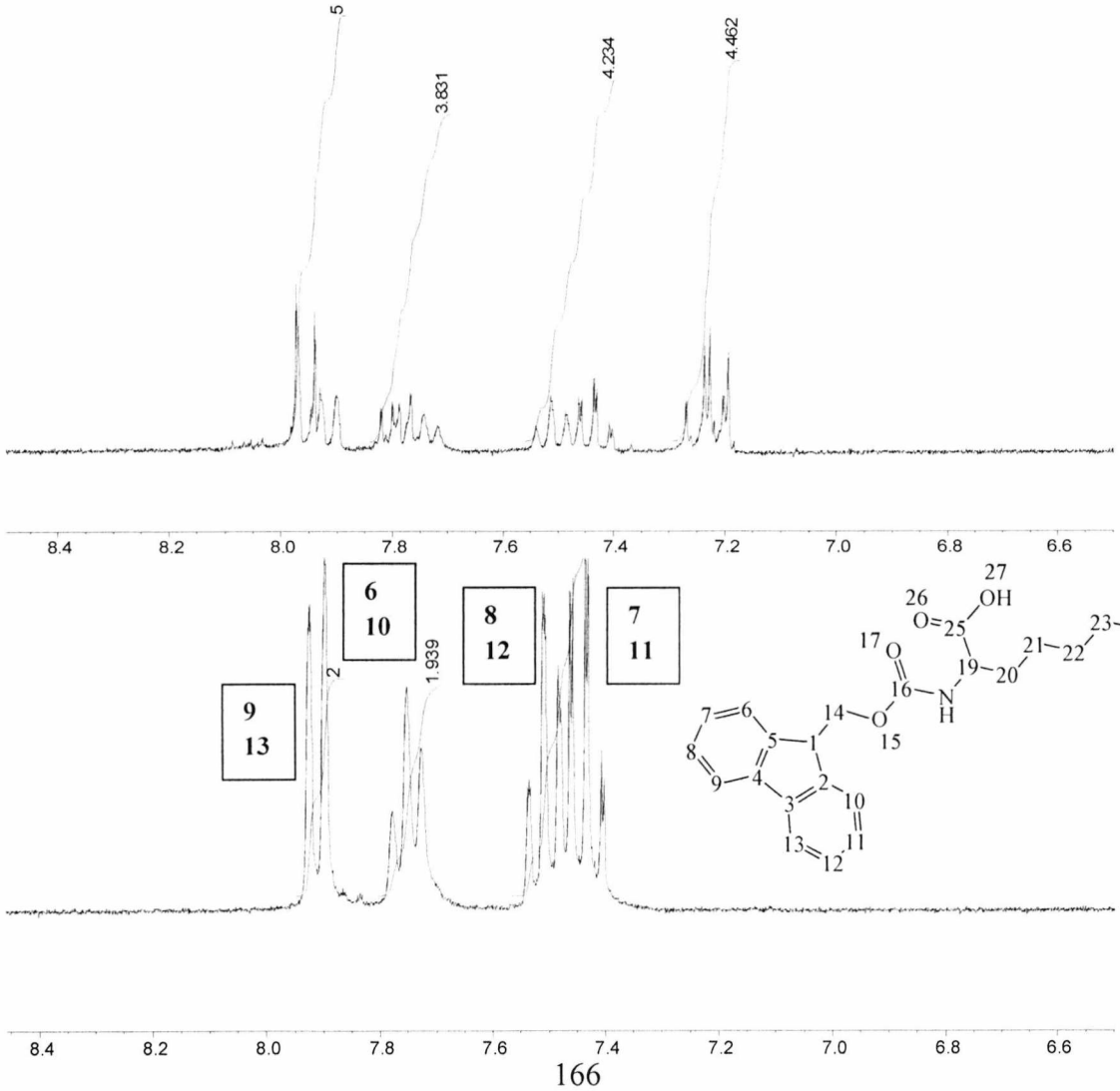
5
3.831
4.234
4.462
8.4
8.2
8.0
7.8
7.6
7.4
7.2
7.0
6.8
6.6

2
1.939
6
10
8
12
7
11
9
13
8.4
8.2
8.0
7.8
7.6
7.4
7.2
7.0
6.8
6.6

Figure 2.59 The top ^{1}H spectrum is from the reaction between 4-fluorobenzaldehyde and HYBA only. In the middle is the spectrum from the competition reaction between HYBA and Fmoc-Lys-OH for 4-fluorobenzaldehyde. At the bottom a spectrum of Fmoc-Lys-OH is shown

2.7.1.5.5 Reaction between Fmoc-Lys-OH and 4-bromobenzaldehyde

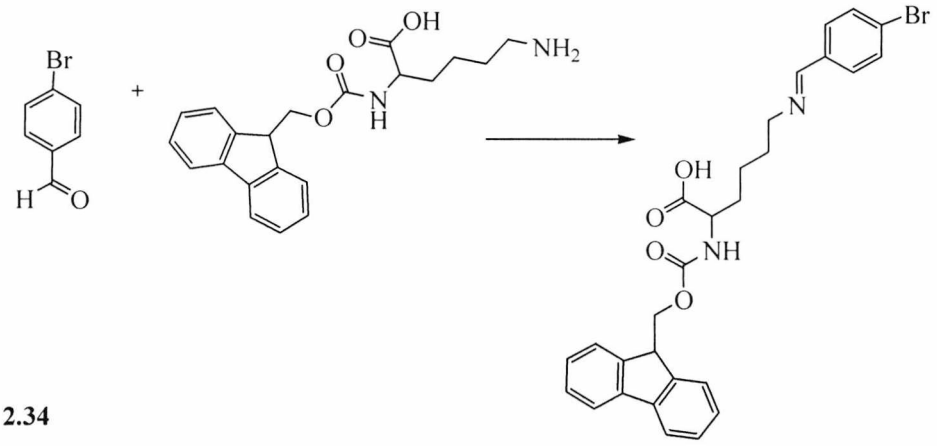

Scheme 2.34

There was no reaction between Fmoc-Lys-OH and 4-bromobenzaldehyde. NMR and HPLC analysis showed the presence of unreacted starting material only.

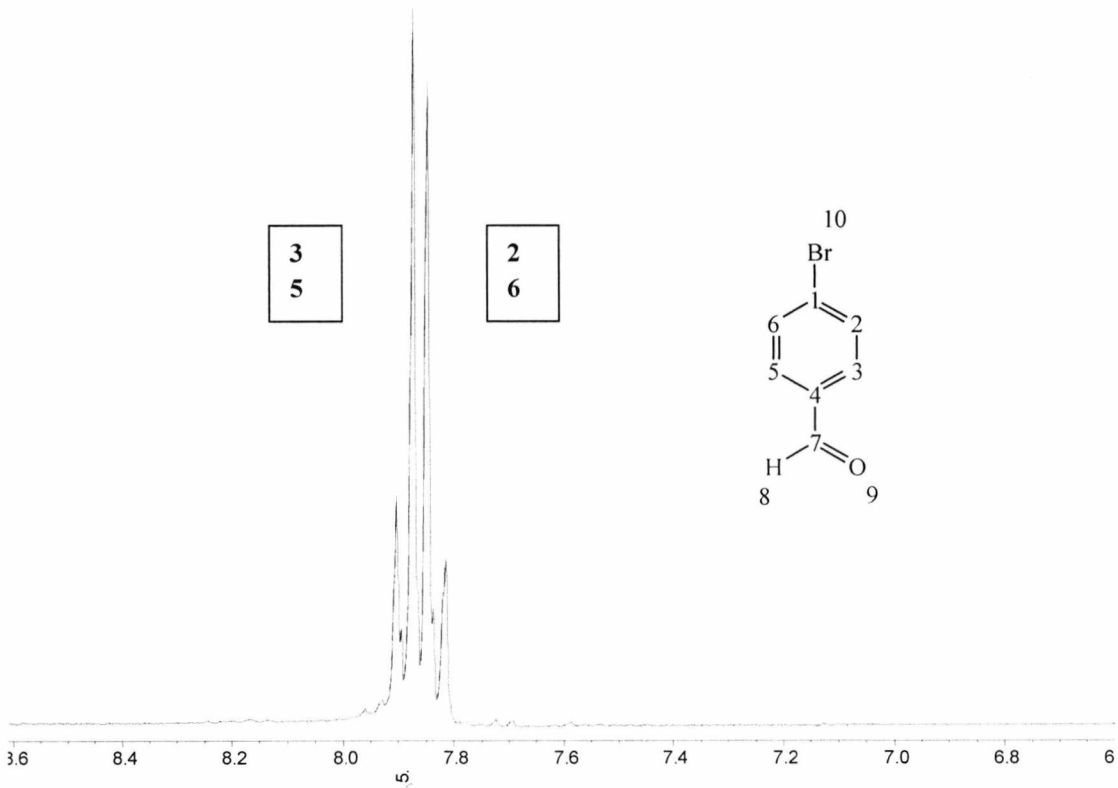
3
5
2
6
10
Br
1
2
3
4
5
6
7
H
O
8
9
3.6
8.4
8.2
8.0
7.8
7.6
7.4
7.2
7.0
6.8
6

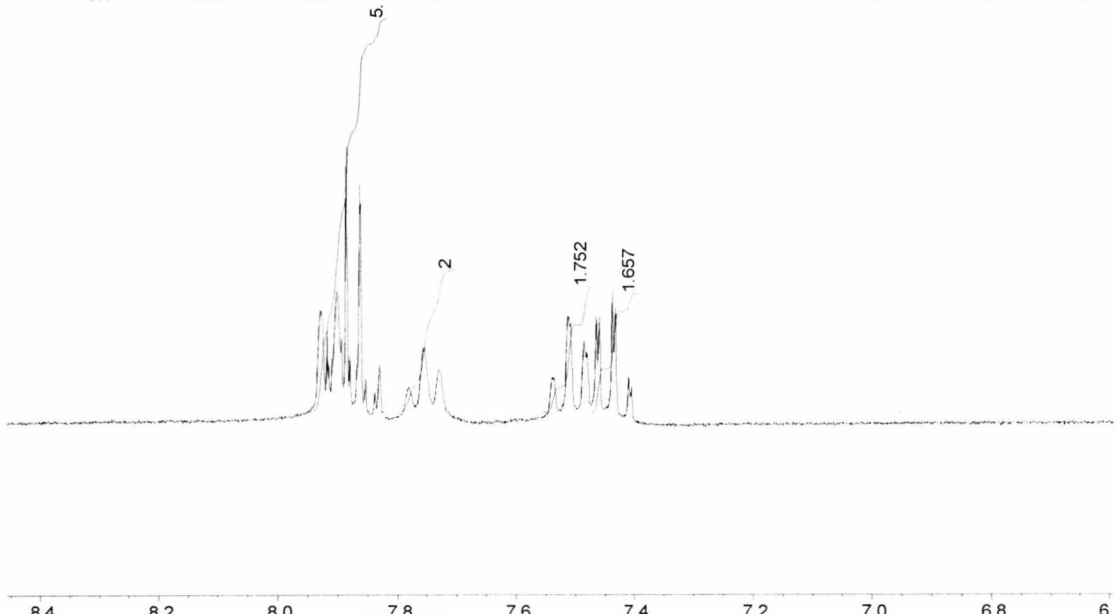
5.
2
1.752
1.657
8.4
8.2
8.0
7.8
7.6
7.4
7.2
7.0
6.8
6.

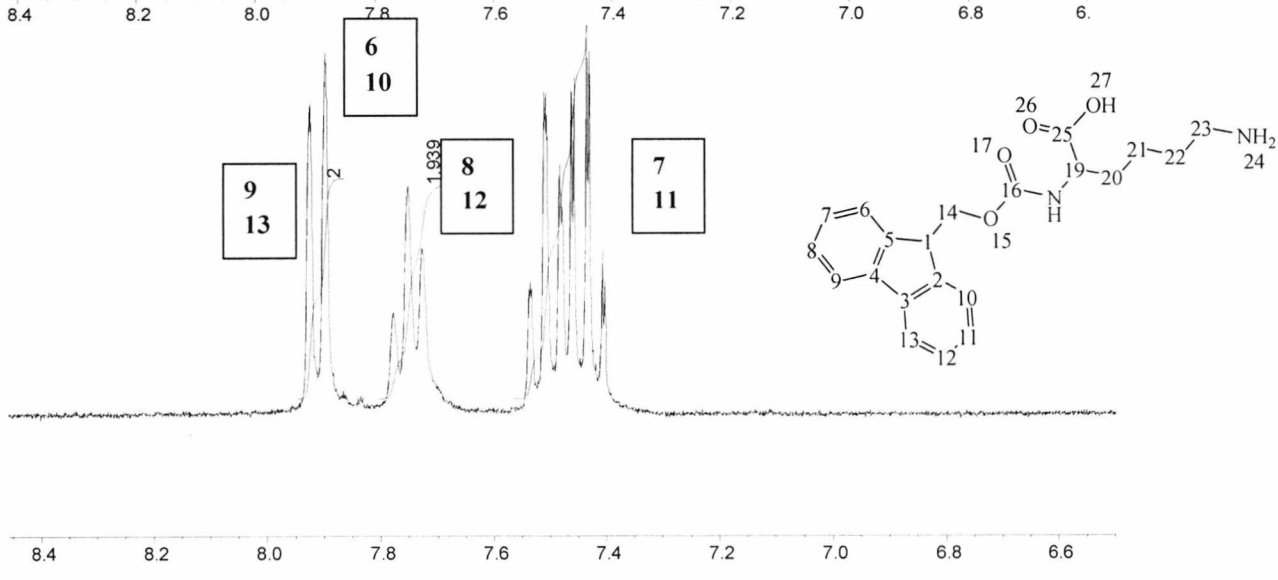
6
10
9
13
2
1.939
8
12
7
11
27
OH
26
O
25
17
O
16
N
H
14
O
15
19
20
21
22
23
NH2
24
8.4
8.2
8.0
7.8
7.6
7.4
7.2
7.0
6.8
6.6

Figure 2.60 The top spectrum is of 4-bromobenzaldehyde The middle spectrum is of the reaction mixture from the reaction between 4-bromobenzaldehye and Fmoc-Lys-OH. The bottom spectrum shows a spectrum of Fmoc-Lys-OH for comparison

2.7.1.5.6 Competition reaction between Fmoc-Lys-OH and 4-hydrazinobenzoic acid for 4-bromobenzaldehyde

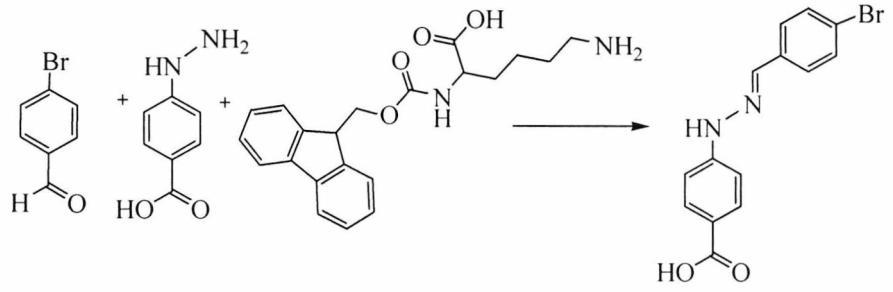

Scheme 2.35

4-[*N*'-(4-Bromobenzylidene)-hydrazino]-benzoic acid was present in the ^{1}H spectrum. A small amount of unreacted HYBA was also present (10% by NMR analysis). 4-[*N*'-(4-Bromobenzylidene)-hydrazino]-benzoic acid was not present by HPLC analysis. It is possible that some degradation of the sample occurred before HPLC analysis. The samples were stored at -20°C for up to two weeks before HPLC analysis.

Only one equivalent of the competing amine Fmoc-Lys-OH was used due to its insolubility.

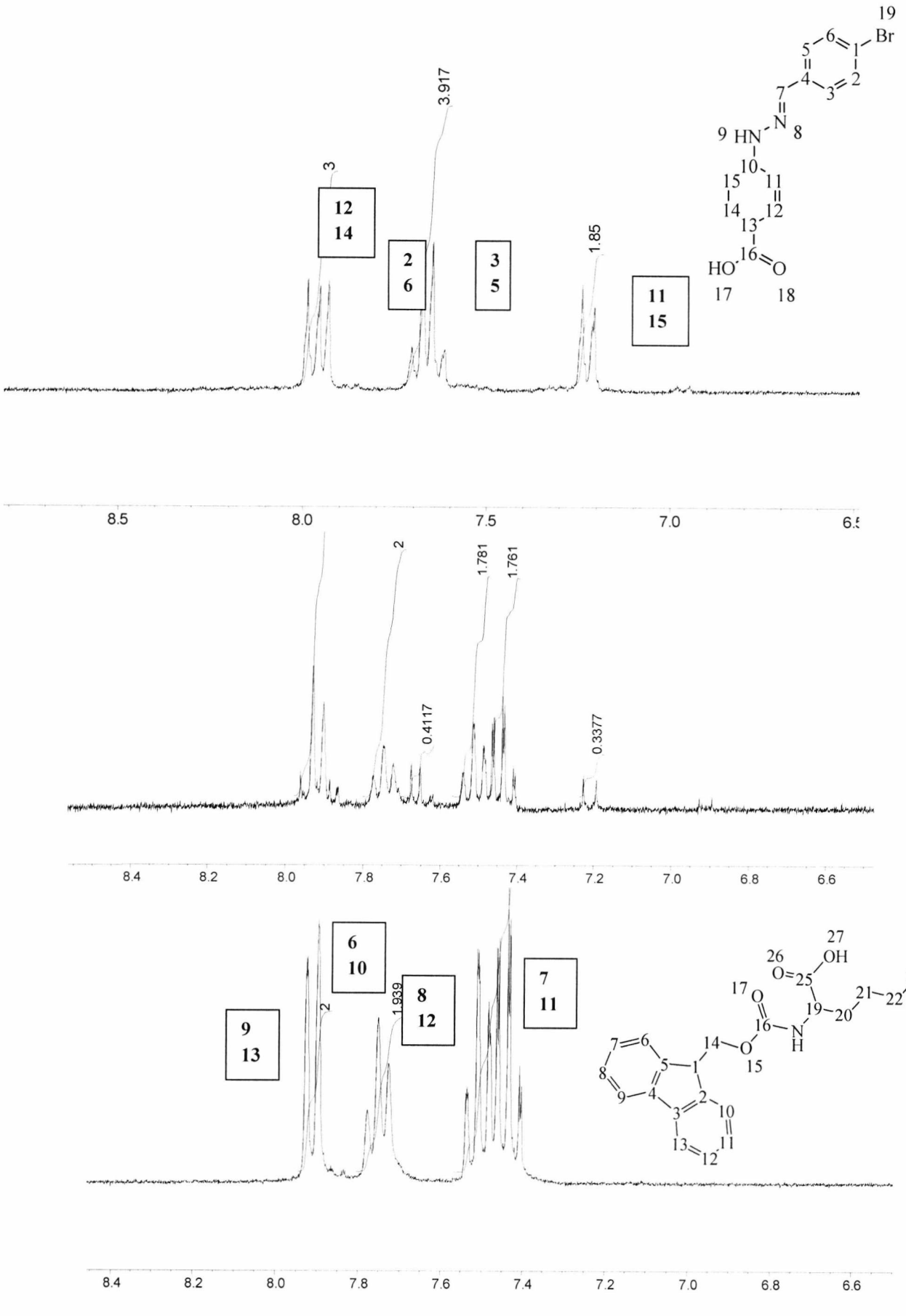
3.917
3
1.85
12
14
2
6
3
5
11
15
19
Br
HN
HO
O
8.5
8.0
7.5
7.0
2
1.781
1.761
0.4117
0.3377
8.4
8.2
8.0
7.8
7.6
7.4
7.2
7.0
6.8
6.6
6
10
1.939
8
12
7
11
9
13
27
OH
NH2
24
8.4
8.2
8.0
7.8
7.6
7.4
7.2
7.0
6.8
6.6

Figure 2.61 The top spectrum is a ^{1}H spectrum of the reaction between 4-bromobenzaldehyde and HYBA. The middle spectrum is of the competition reaction between Fmoc-Lys-OH and HYBA for 4-bromobenzaldehyde. At the bottom a ^{1}H spectrum of Fmoc-Lys-OH is shown

2.7.1.5.7 Reaction between Fmoc-Lys-OH and 4-formylphenyl boronic acid

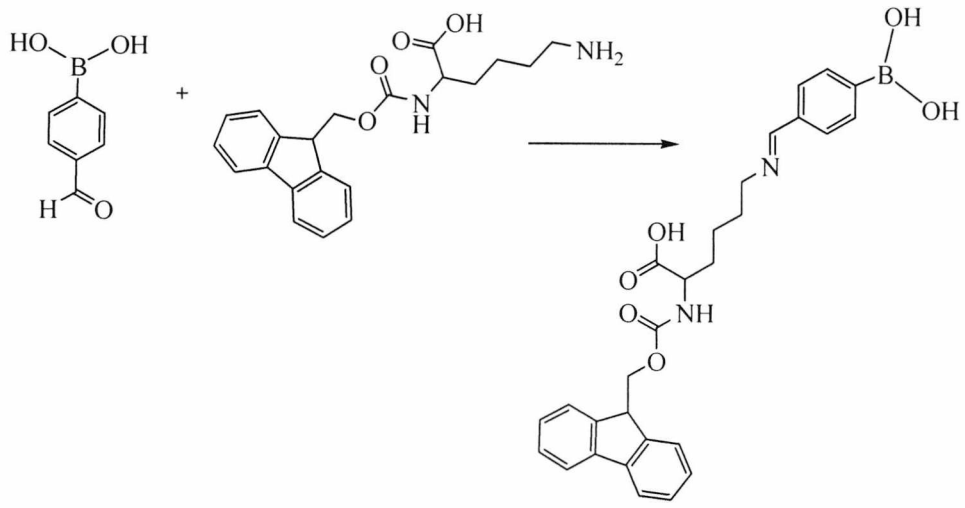

Scheme 2.36

There was no reaction between Fmoc-Lys-OH and 4-formylphenyl boronic acid. NMR and HPLC analysis showed the presence of unreacted starting material only.

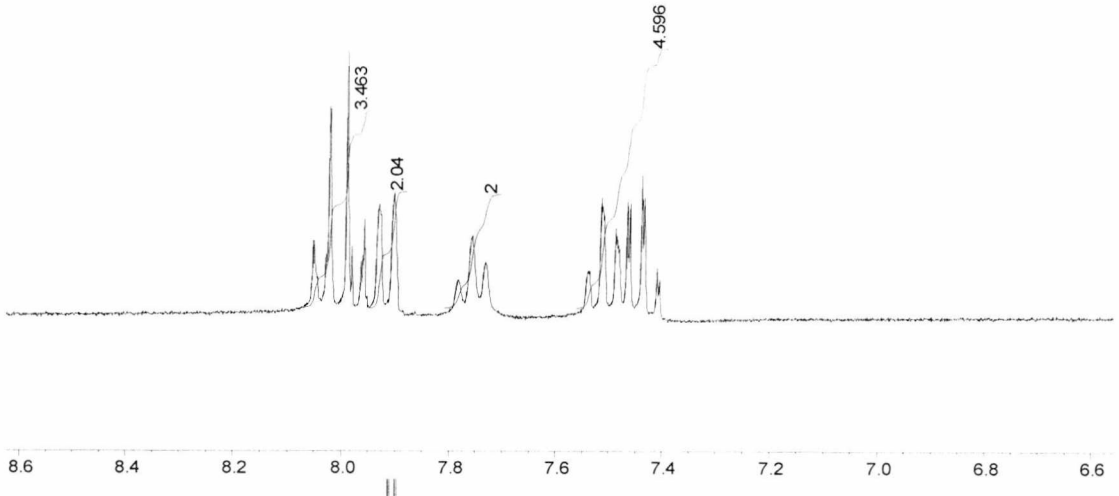
4.596
3.463
2.04
2
8.6
8.4
8.2
8.0
7.8
7.6
7.4
7.2
7.0
6.8
6.6

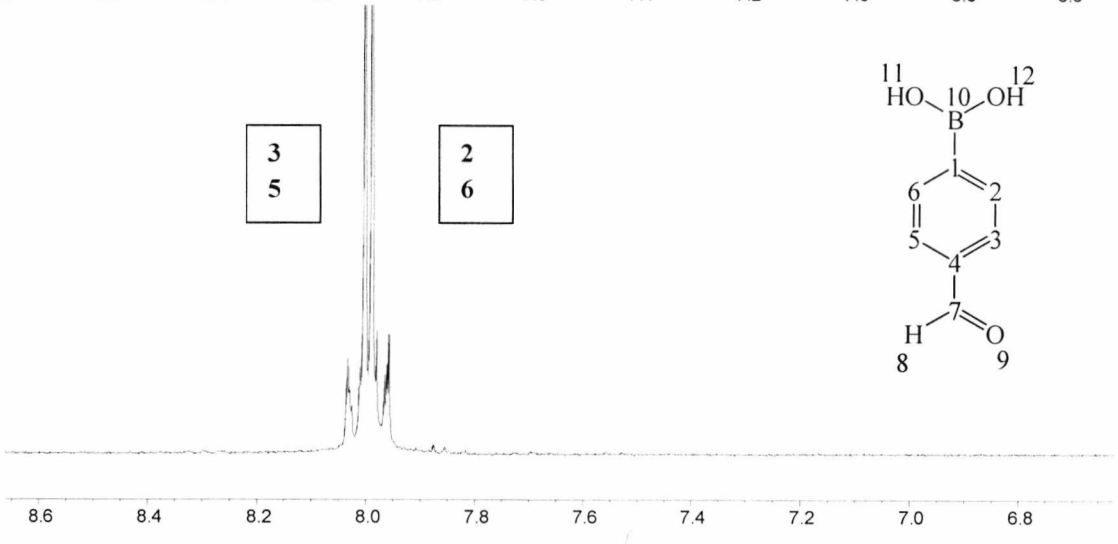
3
5
2
6
11
HO
10
B
OH
12
1
2
3
4
5
6
7
H
8
O
9
8.6
8.4
8.2
8.0
7.8
7.6
7.4
7.2
7.0
6.8

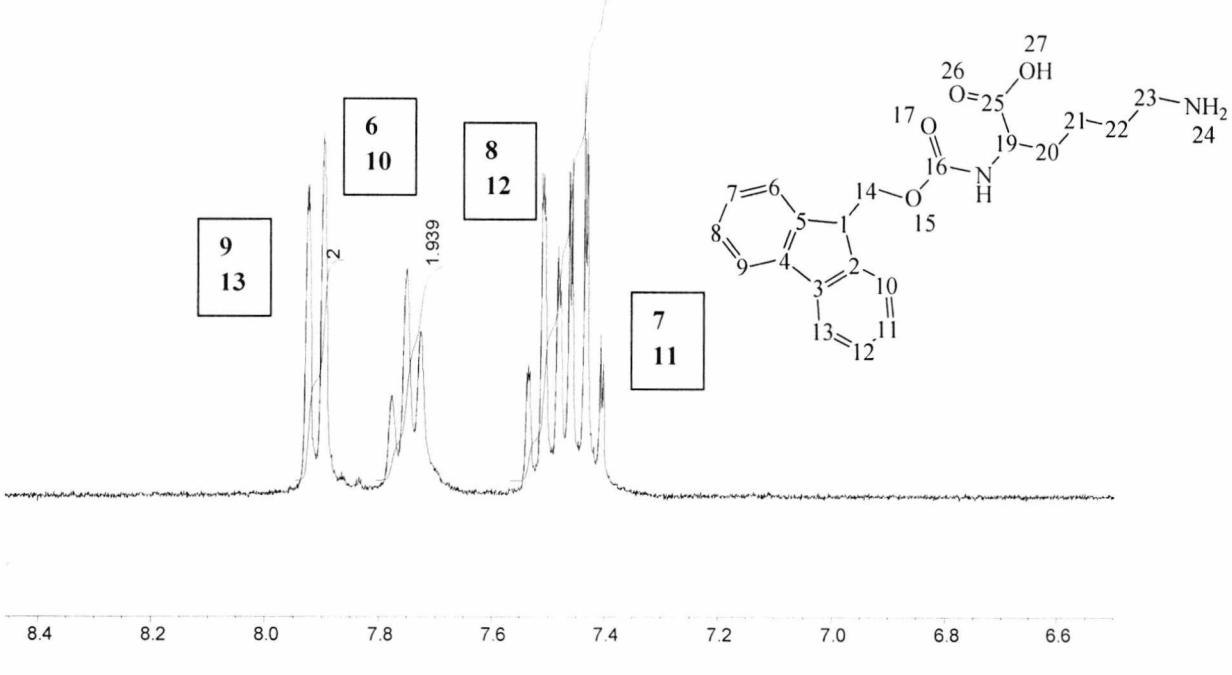
9
13
2
1.939
6
10
8
12
7
11
27
OH
26
O
25
17
O
16
N
H
14
O
15
19
20
21
22
23
NH2
24
1
2
3
4
5
6
7
8
9
10
11
12
13
8.4
8.2
8.0
7.8
7.6
7.4
7.2
7.0
6.8
6.6

Figure 2.62 The top spectrum is of the reaction mixture from the reaction between 4-formylphenyl boronic acid and Fmoc-Lys-OH. The middle spectrum is of 4-formylphenyl boronic acid and the bottom spectrum shows Fmoc-Lys-OH for comparison

2.7.1.5.8 Competition reaction between Fmoc-Lys-OH and 4-hydrazinobenzoic acid for 4-formylphenyl boronic acid

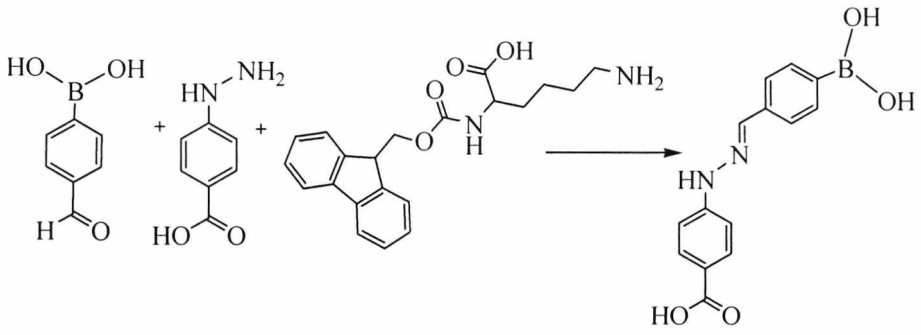

Scheme 2.37

HYBA and 4-formylphenyl boronic acid reacted together completely and exclusively to yield 4-[N'-(4-boronobenzylidene)hydrazino]-benzoic acid. Fmoc-Lys-OH did not react. 4-[N'-(4-Boronobenzylidene)hydrazino]-benzoic acid is not present in HPLC chromatogram, possibly due to sample degradation before the HPLC analysis.

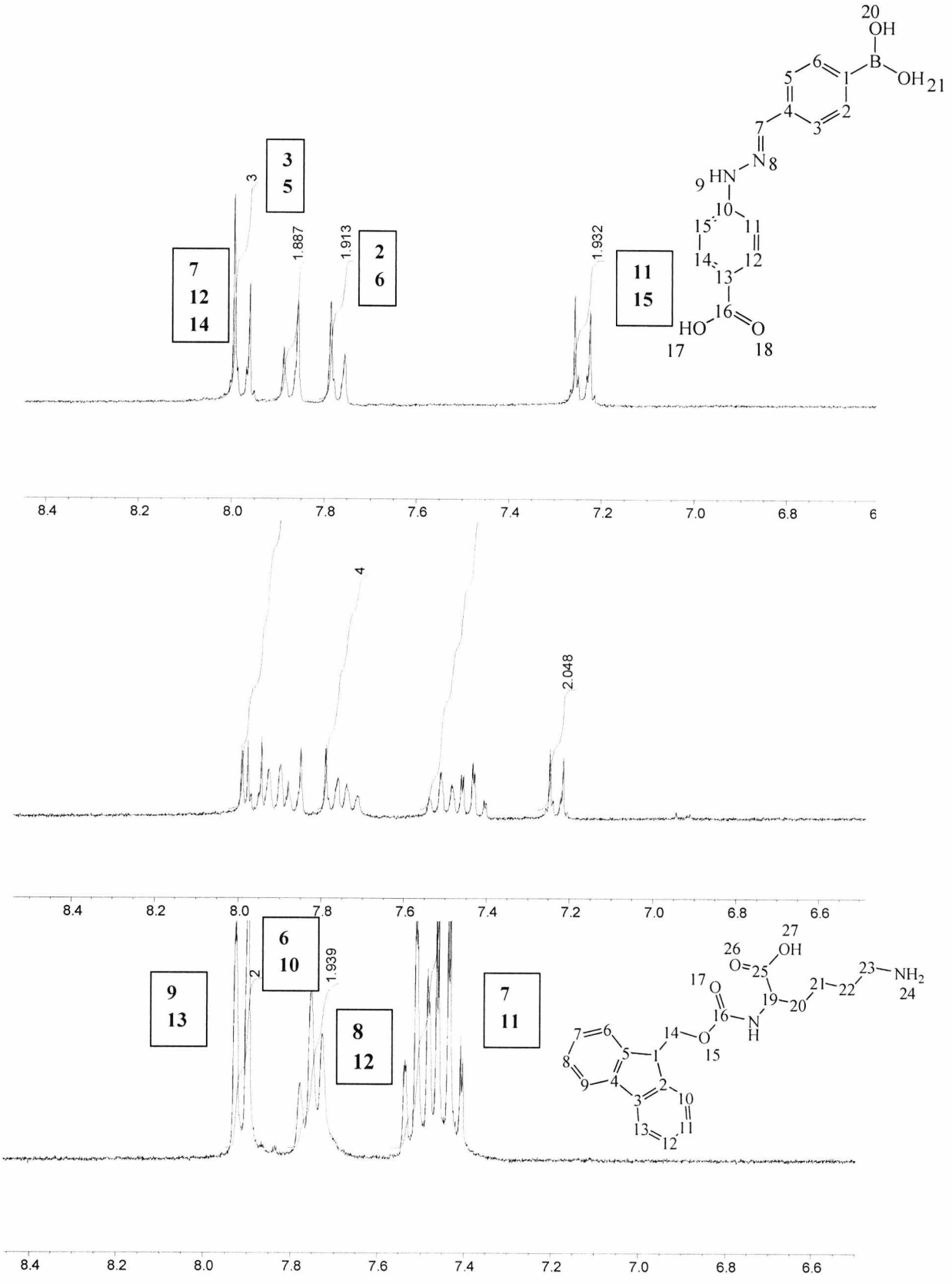
7
12
14
3
5
1.887
1.913
2
6
1.932
11
15
20
OH
B
OH 21
HN
N
HO
O
17
18
8.4
8.2
8.0
7.8
7.6
7.4
7.2
7.0
6.8
4
2.048
9
13
6
10
2
1.939
8
12
7
11
27
OH
26
O=25
23
NH2
24
21
22
19
20
16
N
H
14
O
15
17
O

Figure 2.63 The top ^{1}H spectrum is the from the reaction between 4-formylphenyl boronic acid and HYBA. The middle spectrum is from the competition reaction between Fmoc-Lys-OH and HYBA for 4-formylphenyl boronic acid. At the bottom a ^{1}H spectrum of Fmoc-Lys-OH is shown

2.7.2 General discussion of competition reactions

The results of the HPLC analysis were not always so straight-forward to interpret as the NMR results as they did not always have the expected peaks and often had peaks that were not expected. The samples were analysed by NMR spectroscopy immediately whereas the same samples were stored before HPLC analysis for up to two weeks. This was because the HPLC system was in constant use and was not always available at the time the samples were first collected. The HPLC analysis was carried out to back up the NMR results and so where the HPLC analysis disagrees with the NMR analysis, the NMR results are taken into account in preference to the HPLC results. It was found when running the starting materials, in order to record retention times, that both benzylamine and IBAE did not give very big peaks in the HPLC chromatograms, even when present in large quantities. When UV/visible spectroscopy was carried out on benzylamine and IBAE, only a very small peak was recorded as a λ_{max} for both these chemicals ($\varepsilon = 0.1$ for benzylamine and 0.4 for IBAE). This was unexpected as due to both compounds having an aromatic ring and therefore a system of conjugated double bonds, strong UV absorbance would be expected. The starting materials, products and other compounds present in the chromatograms all have different molar extinction coefficients and therefore a quantitative representation of the amounts of each compound by HPLC is not available from the data here, although qualitatively, the area under the peak is proportional to the mass of material and so gives relative amounts of each compound. The molar extinction coefficient is a measurement of how strongly a chemical absorbs light at a given wavelength. The actual absorbance of a sample is dependent on the pathlength and the concentration of the molecule, where the pathlength is the distance UV or visible light travels through a sample in an analytical cell. Different molecules absorb maximally (λ_{max}) at different wavelengths and therefore absolute values present cannot be calculated by peak area percent except when corrected for by molar absorptivity (ε). However the peak area percent of the product with respect to the total peak area percent of the all peaks in the chromatogram can be used to show relative amount of product present and is representative of what has occurred in a reaction as long as no unknown peaks are present due to storage and decomposition of the sample analysed. In other words, only if analysed before sample decomposition are the peak

area percent results for each compound meaningful. The amount of a product present by peak area percent was therefore not calculated other than when no extra peaks due to decomposition were present in a chromatogram. None of the reactions in this chapter gave more than one product. The samples were analysed by HPLC as a back up to the NMR analysis and the NMR results obtained more accurately show what has occurred in each reaction for the reasons outlined.

For the aldehydes, the competition reactions involving ABAME as the amine competitor showed that all the aldehydes reacted specifically with HYBA when the competing amine was present, even when it was present at three times the concentration over the other reactants. 4-Formylphenyl boronic acid did not react as as completely as the other aldehydes did.

When ABAME was used as the amine competitor, the active ester of 4-iodobenzoic acid reacted with HYBA in the 'clean' reaction, although the reaction did not go to completion. However in the presence of ABAME (the competition reaction), it did not appear to react with HYBA or ABAME, as all starting materials were present in the ^{1}H spectrum. It is possible some product formed, but it is very difficult to tell as there are many peaks present in the spectrum.

There was no evidence that any reaction occurred between any of the aldehydes or IBAE with ABAME.

With benzylamine as the competing amine, the main difference is that reactions occurred between the aldehydes and benzylamine. Other than this, as before, all the aldehydes reacted specifically with HYBA even in the presence of up to ten equivalents of benzylamine.

When benzylamine was used as the amine competitior, IBAE did not react with it. In the competition reaction between IBAE, benzylamine and HYBA, there was possibly some of the product 4-[*N*'-(4-iodobenzoyl)hydrazinyl]-benzoic acid formed but it was difficult to tell due to the many peaks present and the effect of benzylamine shifting some of the peaks.

With Fmoc-Lys-OH as the competing amine, all aldehydes reacted specifically with HYBA in the competition reactions and no reaction occurred with Fmoc-Lys-OH. It was noted that when 2-iodobenzaldehyde was reacted with HYBA in the presence of Fmoc-Lys-OH as the competing amine, a very small amount of HYBA starting material (10%) was present in the ^{1}H spectrum (although not by HPLC analysis). This was also true for 4-bromobenzaldehyde

but 4-fluorobenzaldehyde and 4-formylphenyl boronic acid reacted completely with HYBA. It is possible that a slight excess of HYBA was present in the reactions with 2-iodobenzaldehyde and 4-bromobenzaldehyde, accounting for the HYBA seen in the NMR spectra.

The NMR spectra mainly showed the expected results. A few of the ^{1}H spectra were difficult to interpret due to the presence of many peaks, but these were reactions without HYBA. One of the ^{1}H spectra had no peaks in the aromatic region at all (the reaction between 4-formylphenyl boronic acid and ABAME). The competing amine benzylamine reacted with the aldehydes when no HYBA was present, whereas the other competing amines (4-aminobutyric acid methyl ester and Fmoc-Lysine-OH) did not. However, once HYBA was added, the aldehydes reacted preferentially with it over the benzylamine.

When HYBA reacts with IBAE instead of an aldehyde, there is very little reactivity between HYBA and IBAE, whereas, it can be clearly seen in all the competition reactions involving the aldehydes that they react very specifically and cleanly with HYBA in preference to the competing amines. Therefore, using HYBA or its heterocyclic analogue, HYNIC, any peptide can be labelled specifically with [^{18}F]fluorobenzaldehyde.

Labelled aldehydes will be better prosthetic groups than labelled active esters for reaction with HYBA-containing molecules.

2.8 Results and discussion of the reactions monitoring the rate of formation of the hydrazone

Below are shown some example chromatograms. The top chromatogram is of the rate monitoring competition reaction between HYBA and benzylamine for 2-iodobenzaldehyde at 50°C and was taken 15 minutes after the start of the reaction. The two small peaks correspond to HYBA and 2-iodobenzaldehyde and the large peak is of the product 4-[*N*'-(2-iodobenzylidene)-hydrazino]-benzoic acid. The bottom chromatogram shows the same reaction but taken after one hour. The starting material is gone.

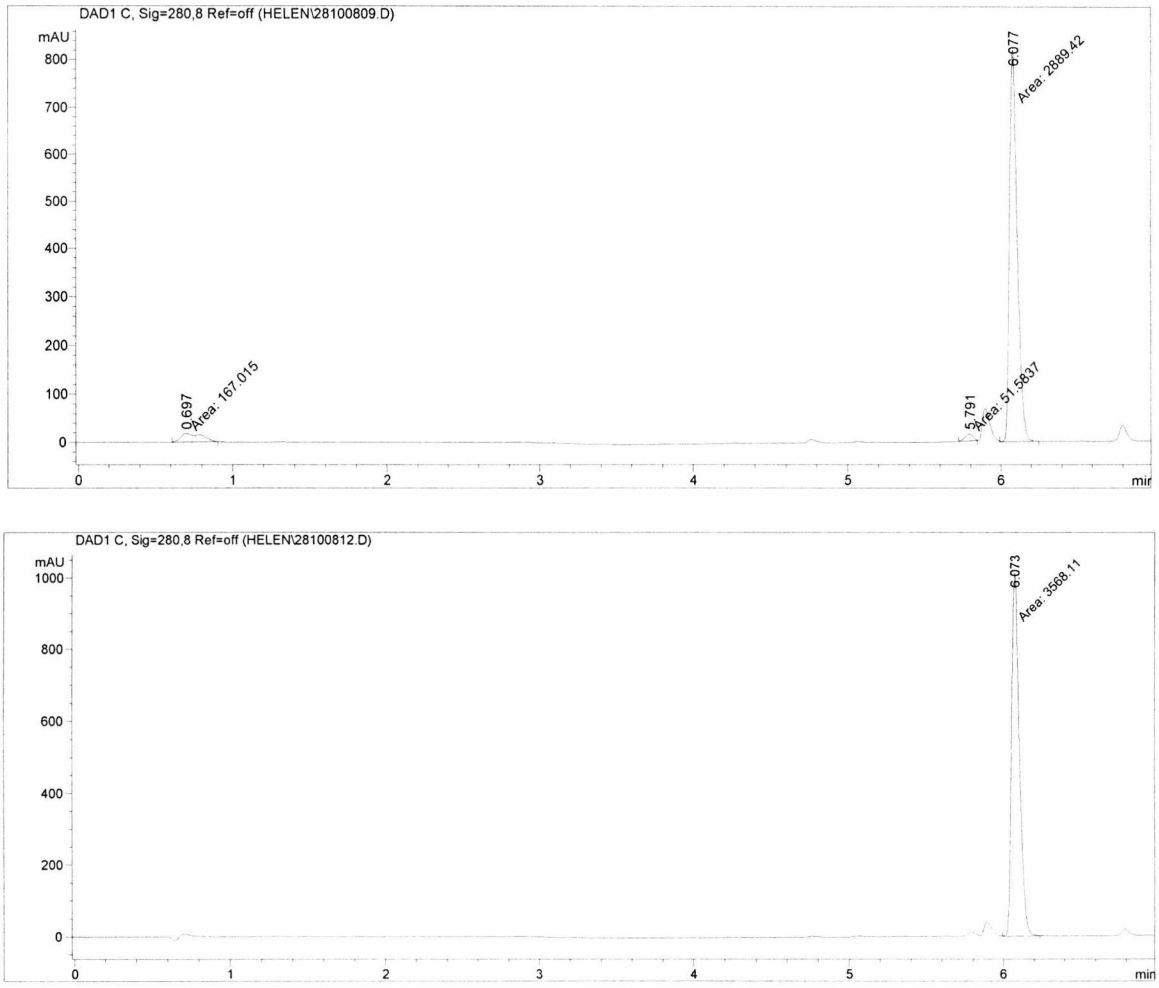

Figure 2.64 Example HPLC chromatograms

2.8.1 Rate of reaction between HYBA and benzylamine for 4-fluorobenzaldehyde at RT

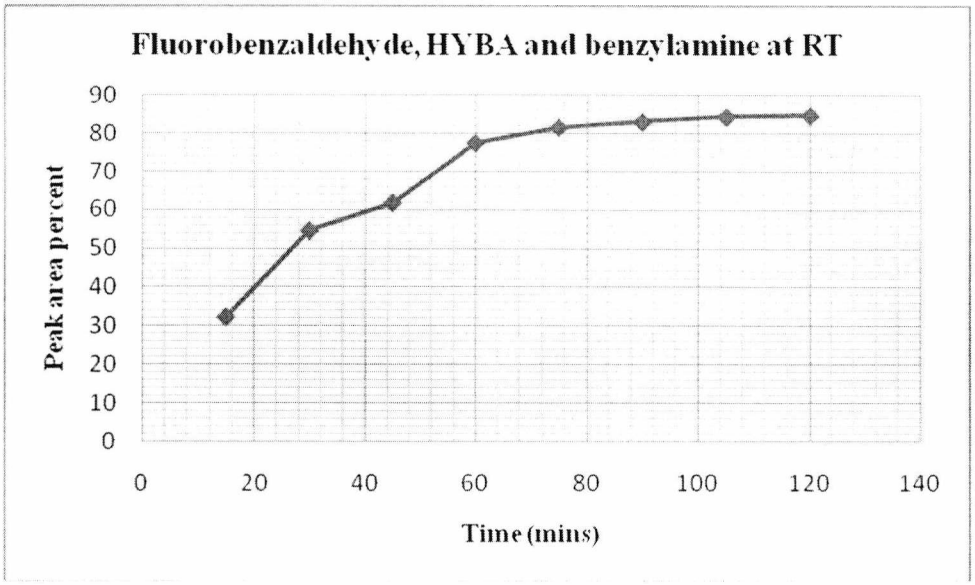

Figure 2.65

The graph above shows the reaction between 4-fluorobenzaldehyde, HYBA and benzylamine at room temperature. HYBA was also present in the HPLC chromatogram as well as the product 4-[*N*'-(4-fluorobenzylidene)-hydrazino]-benzoic acid. It is possible that a slight excess of HYBA was added in error at the start of the reaction. If the reaction had not gone to completion, there would be 4-fluorobenzaldehyde present in the chromatogram as well as HYBA and there was not. However the λ_{max} for HYBA is 272 nm which is very near the wavelength used for the monitoring reactions 280 nm. Therefore very little excess HYBA would give rise to a relatively large peak in the HPLC chromatogram. (The λ_{max} for 4-fluorobenzaldehyde is 248 nm). The graph shows that at room temperature the expected product 4-[N'-(4-fluorobenzylidene)-hydrazino]-benzoic acid is formed quickly and the reaction is almost complete within 1 hour with no heating. The last time point showed the presence of HYBA as 15.7% of the total peak area. Benzylamine was not present in any of the chromatograms. 4-[*N*'-(4-Fluorobenzylidene)-hydrazino]-benzoic acid was the only product formed, assuming no other products were formed that precipitated out of solution, were retained on the column, or had little UV absorption. Therefore, the yield was assumed to be 100%.

2.8.2 Rate of reaction between, HYBA and benzylamine for 2-iodobenzaldehyde at RT

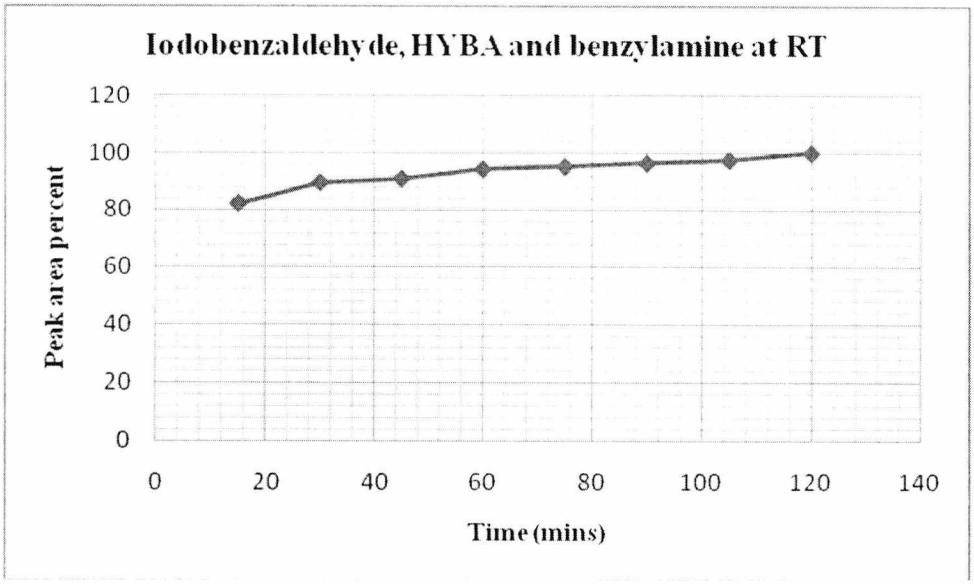

Figure 2.66

This graph shows the reaction between 2-iodobenzaldehyde, HYBA and benzylamine and formation of the expected product over a two hour period at room temperature. It can again be seen that the product is formed rapidly at room temperature. 4-[N'-(2-Iodobenzylidene)-hydrazino]-benzoic acid was the only product formed. The product is present as 100% of the peak area after 2 hours.

2.8.3 Rate of reaction between HYBA and benzylamine for 4-fluorobenzaldehyde at 50°C

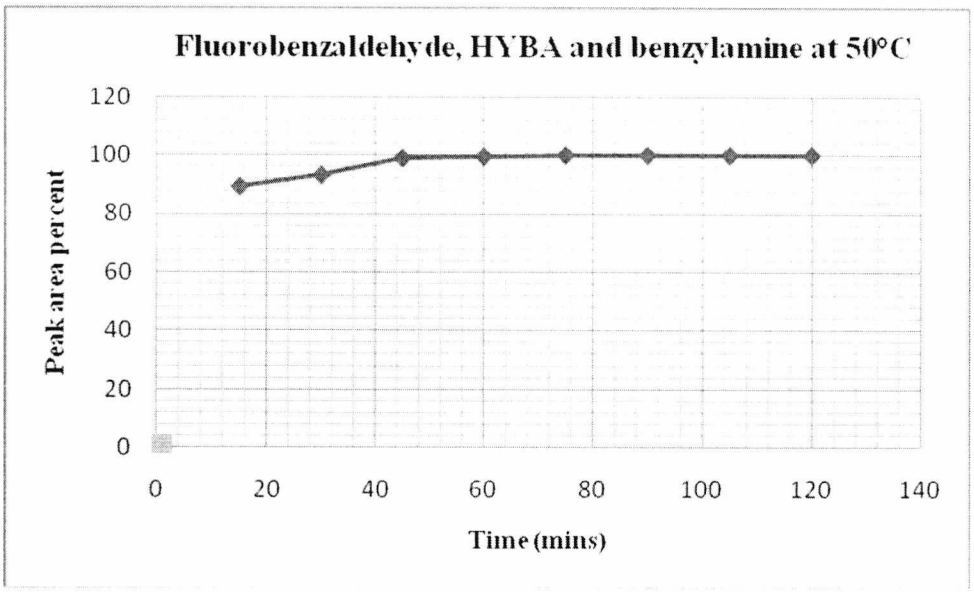

Figure 2.67

The reaction proceeds more quickly at 50°C than room temperature. 4-[*N*'-(4-Fluorobenzylidene)-hydrazino]-benzoic acid is present as 100% of the peak area after 1 hour.

2.8.4 Rate of reaction between HYBA and benzylamine for 2-iodobenzaldehyde at 50°C

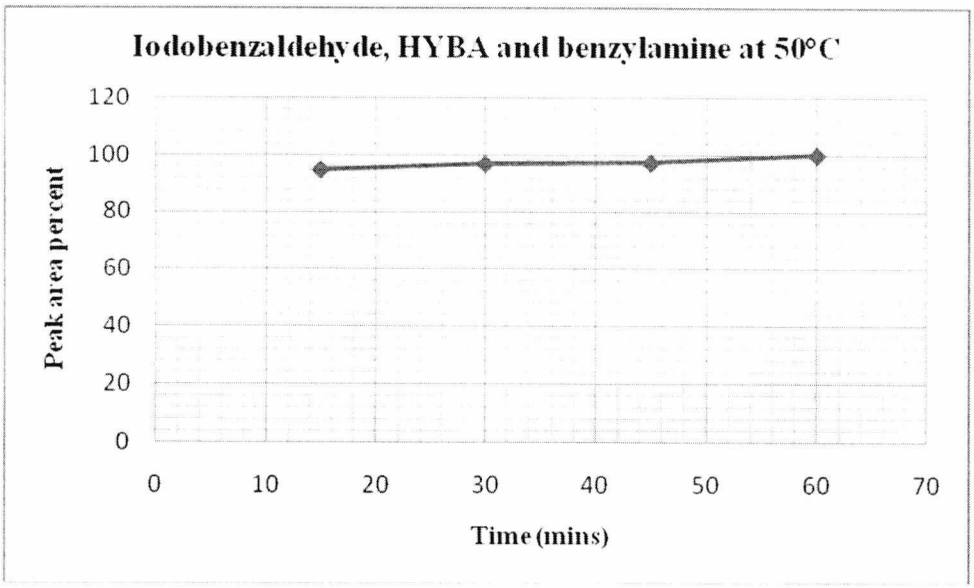

Figure 2.68

The reaction proceeded very quickly, going to nearly 100% complete at 15 minutes after the start of the reaction. This reaction was stopped after 1 hour as the product was precipitating out of solution and therefore there was a risk of damage to the HPLC system. The reaction at 50°C, as expected, proceeds more quickly than at room temperature. The reactions with 2-iodobenzaldehyde occurred more quickly at both temperatures than the same reactions with 4-fluorobenzaldehyde. It is possible that 4-fluorobenzaldehyde forms a hydrated species, slowing the reaction. 2-Iodobenzaldehyde would be less likely to form a hydrated species due to iodine being a bigger atom than fluorine and in an ortho rather than para position. Fluorine is highly electron withdrawing, encouraging hydration. The possible hydrated species is shown in scheme 2.24.

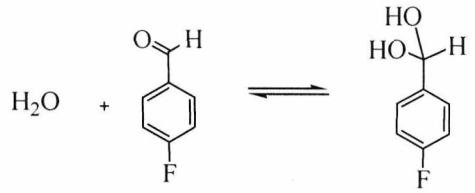

Scheme 2.38 Formation of hydrated species of 4-fluorobenzaldehyde

The product 4-[*N*'-(2-iodobenzylidene)-hydrazino]-benzoic acid was present as 100% of the peak area after 1 hour.

2.8.5 General discussion of rate monitoring reactions

In all reactions only one HPLC-detectable product was formed; 4-[*N*'-(4-fluorobenzylidene)-hydrazino]-benzoic acid and 4-[*N*'-(2-iodobenzylidene)-hydrazino]-benzoic acid which were the products expected from the competition reactions. The use of the peak area percent corrects for any slight differences in amount taken from the reaction mixture at different time points.

Samples were analysed for two hours only for hydrazone formation as any longer than this and the relevance of this reaction to [^{18}F] labelling of biomolecules in a clinical setting declines due to to large a loss in specific activity of the radiopharmaceutical. In any case the reactions were essentially complete within this time.

Initially conditions for monitoring and competition reactions were adapted from Y-S Lee et al. (2006). The use of sodium acetate and acetic acid for the buffer was rejected because initially the aim was to monitor the reactions by NMR analysis and it was found that acetic acid was too difficult to remove quickly from the sample prior to analysis. Formic acid and ammonium formate were chosen instead as formic acid is more volatile than acetic acid. However, due to the fact that rapid removal of formic acid was still problematic, it was decided that monitoring the reactions by HPLC analysis would be quicker than NMR analysis and therefore more accurate. It meant that removal of the (undeuterated) solvent and buffers used for the reactions was not necessary. A pH of 4.5 was chosen for the buffer to provide optimal conditions for formation of hydrazones, which are formed and cleaved under acidic conditions. A pH of 4.5 was also chosen because the pKa of formic acid is 3.77, therefore for it to function efficiently as a buffer, it needs to be within two pH units of its pKa value. 2-Iodobenzaldehyde and 4-fluorobenzaldehyde were used in the monitoring reactions. Benzylamine was chosen as the competing amine, as it has the greatest solubility and reactivity. Fluorine-18 is the most commonly used radioisotope in PET and iodine is also

more commonly used in nuclear medicine than bromine (or boron as a binding site for fluorine - see chapter 1 for more information about the use of these elements in PET). These reactions show that even at room temperature, the reactions involving 2-iodobenzaldehyde are extremely rapid at a concentration of 8.7 mmol/l. This would be ideal for radiolabelling as the more rapidly a molecule can be radiolabelled, the higher the specific activity of the radiopharmaceutical. The reactions with 4-fluorobenzaldehyde are slower, possibly due to the formation of a hydrated species of 4-fluorobenzaldehyde. At room temperature, after 1 hour, 77% of the peak area percent was 4-[*N*'-(4-fluorobenzylidene)-hydrazino]-benzoic acid, whereas with gentle heating to 50°C, more than 80% was synthesised after 15 minutes. Gentle heating would not cause a problem with decomposition of the molecules being heated, or denaturation of the peptide, therefore this would represent a viable way of radiolabelling quickly a molecule with [^{18}F]fluorobenzaldehyde. The method is also chemoselective and so likely that the end product would not require much purification.

Shao and Tam (1995) found that the oxime bond was more stable in aqueous media than the hydrazone bond. The oxime bond was stable in the pH range 3-7 over 24 hours and was only slightly degraded at pH 9 (21% of compound degraded) (Shao and Tam 1995). Shao and Tam (1995) found that the hydrazone bond containing peptide [^{18}F] FB-CH=N-HYNIC-TOCam showed rapid release of [^{18}F]fluorobenzaldehyde. At pH4 65% and at pH7 87% of the intact peptide was detected after 5 hours. The results obtained and presented in this thesis show the hydrazone bond to be very stable in aqueous media over 24 hours and stable at acidic pH in aqueous media for a least 2 hours at the concentration used (the duration of the rate-monitoring reactions). No instability of the hydrazone bond at the pH and concentration used in the rate monitoring reactions (pH 4.5) was noted. Bruus-Jensen et al. (2006) noted that the hydrazone bond of a HYNIC derivative was not as stable at low pH levels as at pH > 5.5. It is possible that the HYNIC hydrazone is less stable than the HYBA hydrazone. The pyridyl N could act as a nucleophilic catalyst and accelerate hydrolysis or the protonated pyridine could act as an acid catalyst. This requires further research to establish whether the HYBA hydrazone would indeed be more stable than the HYNIC hydrazone.

To summarise, when HYBA reacts with either 2-iodobenzaldehyde or 4-fluorobenzaldehyde, only one product is formed rapidly, with little or no heating. This is the case even in the presence of the competing amine, benzylamine.

2.8.6 Conclusion

Aldehydes react with HYBA with complete specificity over amines. This reaction occurs rapidly even at room temperature.

Active esters are less reactive with HYBA and less selective than aldehydes.

If a peptide or protein is derivatised with HYBA, radiolabelled aldehydes would be better prosthetic groups than active esters.

References

Carey FA, Sundberg RJ (2007). Advanced Organic Chemistry: Structure and Mechanisms Part A, 5th Edition, Springer.

Lee Y-S, Jeong JM, Kim HW, Chang YS, Kim YJ, Hong MK, Rai GB, Chi DY, Kang WJ, Kang HK, Lee DS, Chung J-K, Lee MC, Suh Y-G (2006). An improved method of 18F peptide labelling: hydrazone formation with HYNIC-conjugated c(RGDyK). *Nuclear Medicine and Biology* **33**, 677-683.

Parry A (2003). The synthesis and characterisation of novel bio-active norborenyl derived peptide esters and their subsequent ring-opening metathesis polymerisation. MSc Thesis.

Vogel A (1978). Vogel's textbook of organic chemistry including qualitative organic chemistry. 4th Edition, Longman Group Limited, London, UK

Chapter 3

Synthesis of hydrazine-containing amino acids for peptide synthesis

3.0 Introduction

3.1 HYNIC and ^{99m}Tc

The hydrazine group containing compound HYNIC or 6-hydrazinonicotinic acid (6-hydrazinopyridine-3-carboxylic acid) is already used routinely as a bifunctional chelating agent in nuclear medicine to label peptides with ^{99m}Tc for SPECT (Babich et al. 1993). It has also been used for labelling peptides and other biomolecules with ^{18}F (Bruus-Jensen et al. 2006, Chang et al. 2005, Lee et al.2006, Rennen et al. 2007, Shao and Tam 1995). However no commercial products incorporating HYNIC conjugation are licensed as radiopharmaceuticals.

The first example using HYNIC as a bifunctional chelating agent for the synthesis of a radiopharmaceutical was the labelling of human polyclonal immunoglobulin G (IgG) with ^{99m}Tc and ^{111}In in 1990 (Abrams et al.) In this study, ^{99m}Tc hydrazine nicotinamide IgG was demonstrated to have high *in vivo* stability in serum.

Technetium is used in about 85% of all diagnostic applications (Fichna and Janecka 2003). ^{99m}Tc is the radionuclide of choice in scintigraphic imaging (SPECT) because it has favourable characteristics, such as low cost of production, gives a low radiation dose to the patient, optimum gamma-energy profile (γ = 142.7 keV) and wide commercial availability via ^{99m}Tc generators (Banerjee et al. 2001). High specific activity is obtainable using HYNIC as a chelating agent (Babich et al. 1993). HYNIC can be added to the peptide during its solid phase synthesis, which allows greater flexibility and control of the positioning of the HYNIC within the peptide. The finished peptide can be easily and specifically labelled with ^{99m}Tc using a number of different co-ligand systems. However, the way in which ^{99m}Tc is bound to HYNIC and the co-ligand in these complexes is still unclear. It is thought that ^{99m}Tc binds the hydrazine group through its terminal nitrogen and the other coordination sites are occupied by

atoms from one or more co-ligands. It has been demonstrated that the binding of a technetium atom to HYNIC peptides and co-ligands is accompanied by the loss of $5H^+$ which implies an oxidation state of (V) (King et al. 2007).

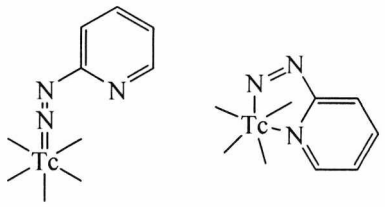

Figure 3.0 Two possible structures of 99mTc-HYNIC-peptide complexes showing monodentate and bidentate binding of HYNIC to technetium (chelating mode) (King et al. 2007)

Three commonly used co-ligands involved in labelling a peptide with ^{99m}Tc are EDDA, tricine and nicotinic acid, the structures of which are shown below. The co-ligands assist the HYNIC in forming a stable complex with technetium.

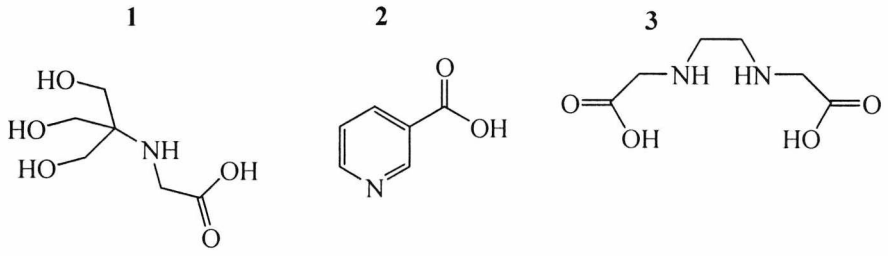

Figure 3.1 (**1**) Tricine, (**2**) nicotinic acid and (**3**) EDDA (King et al. 2007)

The potential mono- or bi-denticity of HYNIC leaves co-ordination sites free on the Tc atom to be completed by different co-ligands. This may be beneficial for fine-tuning biodistribution of the radiopharmaceutical. HYNIC has been used successfully to label octreotide to give the conjugate [HYNIC-D-Phe^1,Tyr^3]-octreotide which has been shown to have good receptor binding and tumour uptake in an animal model (Heppeler et al. 2000). The uptake was very similar to the commercially available OctreoScan ([DTPA-D-Phe^1]-octreotide). A kit formulation of [HYNIC-D-Phe^1,Tyr^3]-octreotide was studied in seven patients. The biodistribution was comparable to OctreoScan with high tumour uptake, excretion by the kidneys plus low liver uptake with the ^{99m}Tc labelled compound demonstrating better image quality (Bangard et al 1998).

It can be seen from the above the impact HYNIC has had for binding ^{99m}Tc to peptides already in nuclear medicine for use in SPECT. This project evaluates the potential use of HYNIC and HYBA to specifically label peptides with ^{18}F via a hydrazone bond to synthesise radiolabelled compounds for use in PET.

Chemical solid phase peptide synthesis (SPPS) usually starts at the *C*-terminus of a peptide. The general principle of SPPS is one of coupling and deprotection. The free *N*-terminal amine of a solid phase attached peptide is coupled to a new amino acid. The incoming amino acid has the *N*-terminal amine protected by Fmoc (9-fluorenylmethoxycarbonyl) and couples with the free *N*-terminal amine of the attached amino acid via its *C*-terminal. The amino acid is deprotected by removal of the Fmoc group, revealing a new *N*-terminal amine. This chapter addresses the synthesis of hydrazine-containing amino acids to be incorporated into the small peptide 'nanogastrin', a truncated form of gastrin comprising the *C*-terminal domain of the peptide, during solid phase synthesis. Nanogastrin is discussed in more detail along with solid-phase peptide synthesis in Chapter 4. Before incorporation into peptides, HYBA and HYNIC must be in a suitably protected form; they must have their hydrazine groups protected by a Boc (butoxycarbonyl) group. This prevents the hydrazine group, which is highly nucleophilic, undergoing unwanted side reactions with electrophiles. Boc-HYBA and Boc-HYNIC were therefore to be synthesised initially from HYBA and HYNIC. In this form they were to be incorporated (separately) into the peptide nanogastrin via the carboxylic acid group in the same way a new amino acid would be via the *C*-terminal. As there is no *N*-terminal amine to protect, Fmoc protection is not needed as it is with natural amino acids. An additional two hydrazine containing amino acids were also to be synthesised from the Boc protected forms of HYBA and HYNIC. Boc-HYBA and Boc-HYNIC were first to be converted to the active esters and then reacted with Fmoc-Lys-OH to give Fmoc-Lys-HYNIC-Boc and Fmoc-Lys-HYBA-Boc which were then to be incorporated (separately) into the nanogastrin. The lysine of Fmoc-Lys-HYBA-Boc and Fmoc-Lys-HYNIC-Boc is a natural amino acid and therefore, as the incoming amino acid, lysine has its *N*-terminal protected with an Fmoc group that is then removed once incorporated into the peptide chain. The Boc group is removed at the same time as the finished peptide is cleaved from the resin, this is covered in more detail in Chapter 4.

3.2 Aims and objectives

From the competition and monitoring reactions described in the previous chapter, the specificity of HYBA for aromatic aldehydes has been demonstrated. The next step is to incorporate HYBA and its heterocyclic analogue HYNIC, into a peptide and use these HYBA and HYNIC containing peptides to provide a specific binding site for [^{18}F]FB-CHO on the peptide. The aim of this project was to decrease the number of reaction steps needed to incorporate fluorine (and the other elements discussed in chapters 1 and 2) into a peptide. The method developed should also be chemoselective meaning the exact position of the fluorine (or other element) in the molecule is completely predictable and therefore produces a homogenous radiopharmaceutical. This strategy keeps the chemistry simple, as it is not necessary to incorporate protecting groups to ensure the radiolabel is added to the correct position on the molecule and this saves time with respect to removal of protecting groups and purification before the end product is ready for use in the clinic. As has been discussed, the hydrazone bond formed between the hydrazine group of HYBA and HYNIC and [^{18}F]FB-CHO fits these requirements. Boc-HYBA, Boc-HYNIC, Fmoc-Lys-HYBA-Boc and Fmoc-Lys-HYNIC-Boc were synthesised to be incorporated into the peptide nanogastrin.

In this strategy, ^{18}F is not added as the last step but the radiolabelling of trimethylammonium triflate with ^{18}F is quick and easy (see schemes 3.0 and 3.1). Secondly, attachment of the [^{18}F]fluorobenzaldehyde to the peptide is rapid and chemoselective using HYBA or HYNIC. Attachment of the HYBA or HYNIC to the peptide is carried out beforehand, as part of the peptide synthesis and this can be freeze-dried and stored at -20°C until needed. This would be viable in a clinical setting while being a big improvement on current labelling technology.

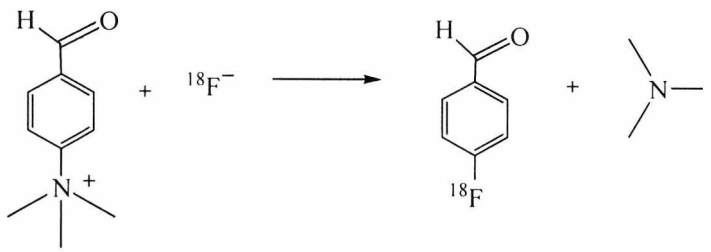

Scheme 3.0 Formation of [^{18}F]fluorobenzaldehyde

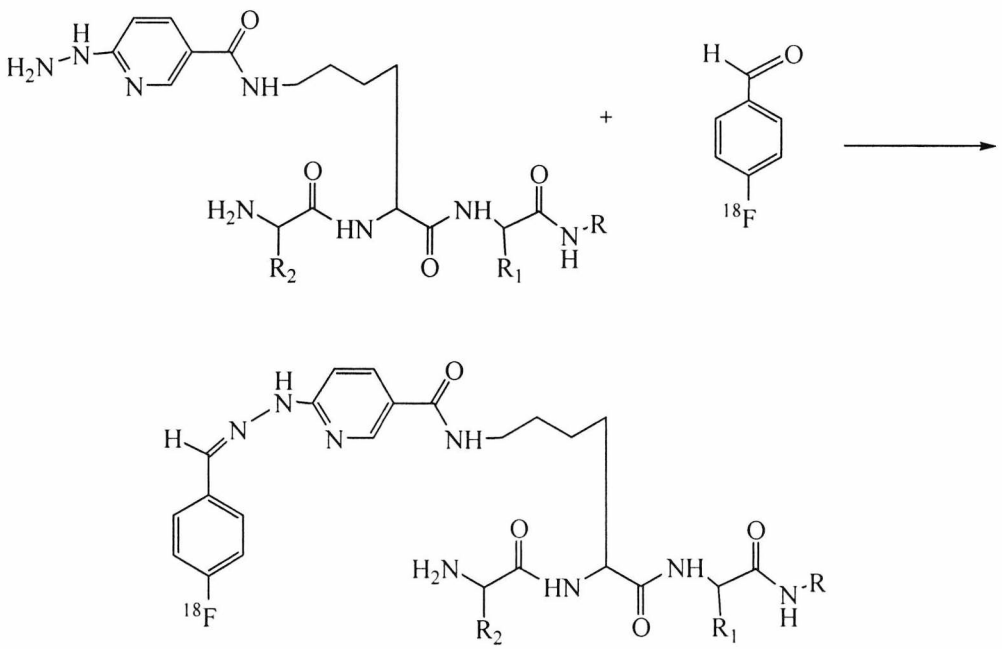

Scheme 3.1 1 + 1 labelling strategy via pre-synthesised hydrazine amino acid containing peptides for [^{18}F]fluorobenzaldehyde

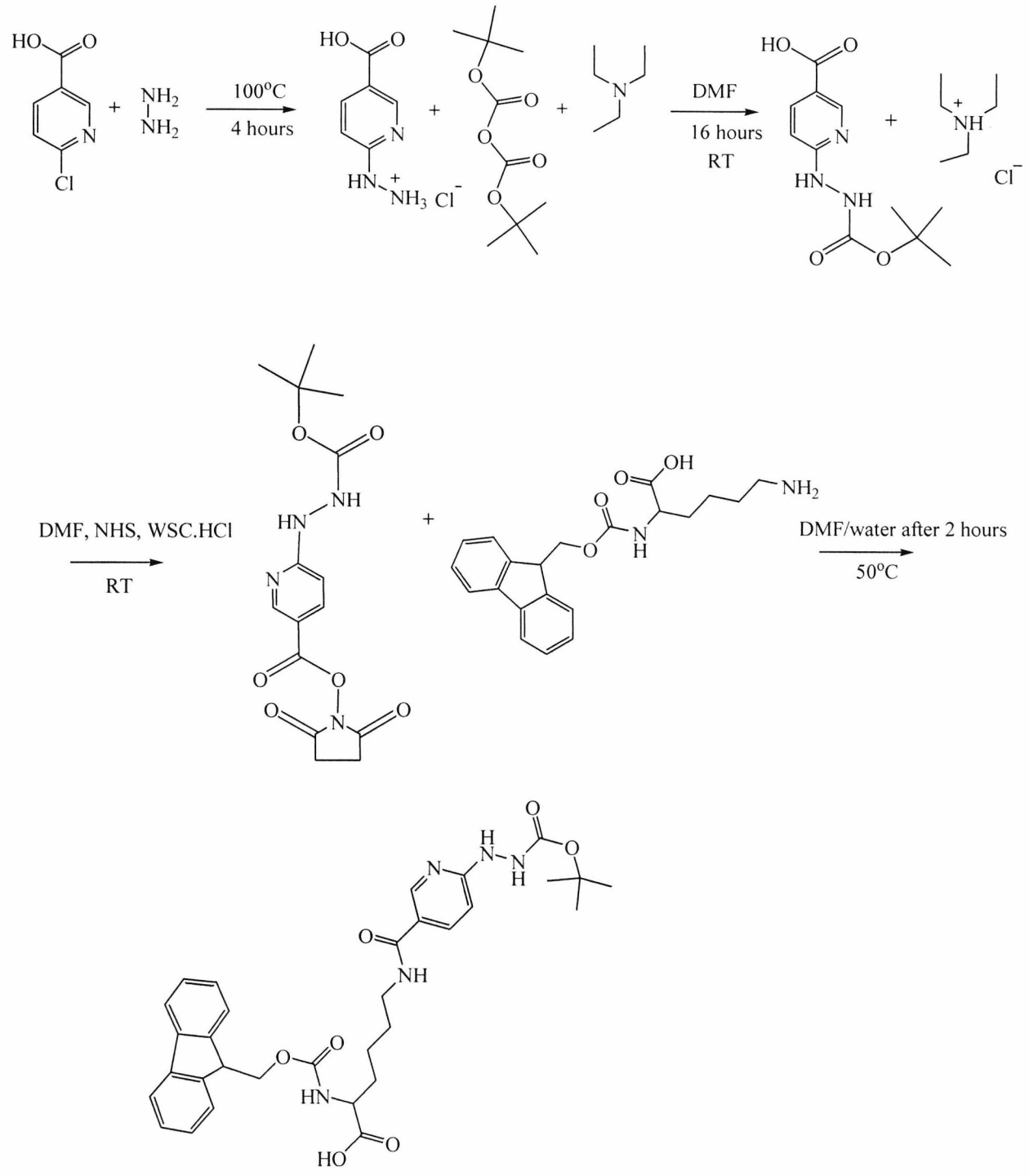

Scheme 3.2 Reaction scheme showing synthesis of Fmoc-Lys-HYNIC-Boc. Fmoc-Lys-HYBA-Boc was synthesised in the same way, except the starting material was (purchased) HYBA

3.3 Materials and methods

Anhydrous sodium sulphate, ammonium chloride (99.6%), 6-chloronicotinic acid (99%) 4-hydrazinobenzoic acid (98%) and hydrazine hydrate (80%, hydrazine 51%) were bought from Acros Organics. Concentrated hydrochloric acid (37%) was obtained from BDH chemicals. Water (HPLC grade), Acetonitrile (HPLC grade), absolute ethanol (analytical reagent grade) and diethyl ether (analytical reagent grade) were bought from Fisher Scientific. Triethylamine (99%) was purchased from Avocado. Di-tert-butyl dicarbonate (97+%) was purchased from Alfa Aesar. Fmoc-lysine-OH and WSC.HCl (water soluble carbodiimide hydrochloride) were bought from Novabiochem. Anhydrous *N,N*-dimethylformamide (99.5%) was obtained from Fluka. DMSO-d_6 was purchased from Goss Scientific Instruments Ltd.

3.3.1 Synthesis of N-α- Fmoc-Lysine-HYNIC-Boc

3.3.1.1 Synthesis of 6-hydrazinonicotinic acid (6-hydrazinopyridine-3-carboxylic acid); 'HYNIC'

Hydrazine hydrate 80% (4.57 g, 4.45 cm^3, 114.12 mmol) and 6-chloronicotinic acid (1.00 g, 6.34 mmol) were heated to reflux in a round bottom flask at 100°C for 4 hours to give a clear light tan solution. The reaction mixture was cooled to room temperature and concentrated to dryness to give a yellow paste. The yellow paste was dissolved in a minimal amount of H_2O to give a light tan solution and then acidified to pH 5.5 with concentrated hydrochloric acid. At pH 5.5 a yellow precipitate formed which was isolated by filtration and then washed with ethanol (3 x 100 cm^3 aliquots) and dried with diethyl ether. The product was dried in the vacuum oven (60°C 24 h) to yield a pale yellow solid which was used without further purification. (Abrams et al. 1990, Greenland 2002).

Yield: 0.70 g, 4.57 mmol, 72% (lit 77%), m.p. 268-271°C (lit 292-293°C).

δ_H from literature (270 MHz; DMSO): 6.69 (1H, d, *J* 8), 7.84 (1H, dd, *J* 2.4, 8.8), 8.51 (1H, d, *J* 2.4).

δ_H (270 MHz; DMSO) 6.75 (1H, d, *J* 8.8, CH, 3-H), 7.90 (1H, dd, *J* 2.2, 8.8, CH, 4-H), 8.35 (1H, s, NH, 7-H), 8.65 (1H, d, *J* 2.2, CH, 6-H), 8-H and 11-H not observed.

δ_C (67.8 MHz; DMSO) 106.0 (C-3), 115.0 (C-5), 138 (C-4), 152 (C-6), 164 (C-2), 167 (C-9).

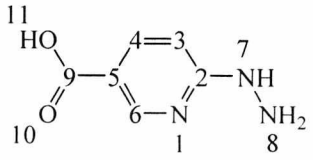

Figure 3.2 HYNIC Structure: ^{1}H and ^{13}C NMR assignments

ν_{max} cm^{-1} 3315 (m, N-H *str,* secondary amine), 3226 (m, N-H_2 *str*, primary amine), 2726 (m, O-H *str*, carboxylic acid), 1683 (s, C=O *str* carboxylic acid).

Analysis by RP HPLC: Eluted at 1.8 minutes. (HPLC / System A / Method 1 / Column 1 / A254, 280, 300 nm). 72% by peak area percent.

$C_6H_7N_3O_2$ Molecular weight: 153.14, exact mass: 153.05

m/z (ESI) (cone voltage 10V) Positive mode, molecular ion $[M + H]^+$:154.1 100% intensity.

3.3.1.2 Synthesis of 6-Boc-hydrazinopyridine-3-carboxylic acid; 'Boc-HYNIC'

To a solution of HYNIC (0.938 g, 6.13 mmol) and triethylamine (0.852 cm^3, 6.13 mmol) in anhydrous DMF (10 cm^3) di-tert-butyl dicarbonate (1.34 g, 6.13 mmol) was added. The reaction mixture became homogenous over 1 hour and stirring was continued for 16 hours at room temperature. The yellow suspension turned into a clear pale yellow solution. The reaction mixture was concentrated to remove as much DMF as possible under reduced pressure to give a yellow solid. The resulting yellow paste was dissolved in a minimum amount of ethyl acetate and shaken in a separating funnel with 8 consecutive aliquots of saturated ammonium chloride solution (100 cm^3 each). The organic layer was dried with sodium sulphate and vacuum filtered to give a clear yellow solution. This was concentrated to dryness and dried in the vacuum oven (60°C 24 h) to yield an off-white solid which was used without further purification. (Abrams et al. 1990, Greenland 2002).

Yield: 1.02 g, 4.03 mmol, 66%, (lit 94%), m.p. 144-150°C, (lit not reported).

δ_H from literature (270 MHz; DMSO): 1.40 (9H, s), 6.52 (1H, d, *J* 8.8), 7.97 (1H, dd, *J* 2.4, 8.8), 8.58 (1H, d, *J* 2.4).

δ_H (270 MHz; DMSO) 1.46 (9H, s, 3(-CH_3), 12, 16, 17-H), 6.75 (1H, d, *J* 8.9, CH, 3-H), 8.0 (1H, dd, *J* 2.2, 8.9, CH, 4-H), 8.62 (1H, d, *J* 2.2 CH, 6-H), 8.93 (1H, s, NH, 7-H), 9.02 (1H, s, NH, 8-H), 18-H not observed.

δ_C (67.8 MHz; DMSO) 29.0 (C-12, 16, 17), 80.0 (C-11), 105.0 (C-5), 118.0 (C-3), 139.0 (C-4), 151.0 (C-6), 156.0 (C-9), 164.0 (C-2), 168.0 (C-13).

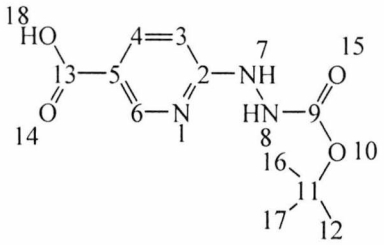

Figure 3.3 HYNIC-Boc Structure: ^{1}H and ^{13}C NMR assignments

ν_{max} cm^{-1} 3255 (m, N-H *str,* secondary amine), 2978 (m, C-H *str*), 1721, 1712, 1693 (s, C=O *str* acid), 1246, 1150 (s, C-O *str*, ester).

Analysis by RP HPLC: Eluted at 9.8 minutes. (HPLC / System A / Method 1 / Column 1 / A254, 280, 300 nm). 94% by peak area percent.

$C_{11}H_{15}N_3O_4$ Molecular weight: 253.25, exact mass: 253.11

m/z (ESI) (cone voltage 10V) Negative mode, molecular ion $[M - H]^-$:252.0 100% intensity, $[2M - H]^-$:505.2 15% intensity, $[3M - H]^-$:758.3 5% intensity.

3.3.1.3 Synthesis of succinimidyl 6-Boc-hydrazinopyridine-3-carboxylic acid; 'NHS-HYNIC-Boc'

HYNIC-Boc (0.730 g, 2.88 mmol), *N*-hydroxysuccinimide (NHS) (0.398 g, 3.46 mmol) and WSC.HCl (water soluble carbodiimide hydrochloride) (0.663 g, 3.46 mmol) were dissolved in anhydrous DMF (20 cm^3) under an atmosphere of nitrogen gas. The reaction mixture was stirred for eighteen hours at room temperature and resulted in an orange coloured solution. As much DMF as possible was removed under vacuum. The orange/pink paste remaining was dissolved in a minimal amount of ethyl acetate and shaken in a separating funnel with 8 consecutive aliquots of saturated ammonium chloride (100 cm^3 each). The organic layer was dried with sodium sulphate and vacuum filtered to give a clear pinkish orange solution. This

was concentrated to dryness and dried in the vacuum oven (60°C 24 h) to yield a beige coloured solid which was used without further purification (Abrams et al. 1990, K. Bruus-Jensen et al. 2006, Greenland 2002).

Yield: 0.49 g, 1.41 mmol, 49%, (lit 60 %), m.p. 164-165°C, (lit 169.5-172°C).

δ_H from literature (270 MHz; DMSO) 1.41 (9H, s), 2.87 (4H, s), 6.64 (1H, d, *J* 8.8), 8.08 (1H, dd, *J* 2.4, 8.8) 8.73 (1H, d, *J* 2.4)

δ_H (270 MHz; DMSO) 1.46 (9H, s, 3(-CH_3), 12, 16, 17-H), 2.91 (4H, s, 2(-CH_2) 22-H and 23-H), 6.67 (1H, d, *J* 8.8, CH, 3-H), 8.15 (1H, d, *J* 8.8, CH, 4-H), 8.78 (1H, d, *J* 2.3, CH, 6-H), 9.21 (1H, s, NH, 8-H), 9.5 (1H, s, NH, 7-H).

δ_C (67.8 MHz; DMSO) 26.5 (C-22 and 23), 28.0 (C-12, 16, 17), 80.0 (C-11), 110.0 (C-3), 117.0 (C-5), 128.0 (C-2), 153.0 (C-6), 157.0 (C-4), 162.0 (C-18 and 19), 172.0 (C-9).

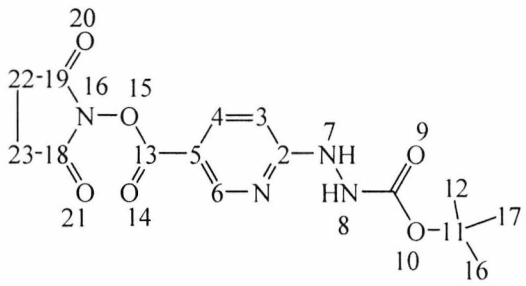

Figure 3.4 NHS-HYNIC-Boc Structure: ^{1}H and ^{13}C NMR assignments

ν_{max} cm^{-1} 3323 (m, N-H *str,* secondary amine), 2978 (m, C-H *str*), 1765, 1730 (s C=O *str* ester), 1719, 1715, 1601 (s, C=O *str* amide), 1239, 1201, 1153 (s, C-O *str* ester).

Analysis by RP HPLC: Eluted at 12.4 minutes. (HPLC / System A / Method 1 / Column 1 / A254, 280, 300 nm). 93% by peak area percent.

$C_{15}H_{18}N_4O_6$ Molecular weight: 350.33, exact mass: 350.12, measured mass of ion: 351.1306.

m/z (ESI) Positive mode, molecular ion $[M + H]^+$: 351.1302 100% intensity, 253.1298 15% intensity, loss of NHS, $[2M + H]^+$:701.2523 45% intensity, 603.2518 22% intensity, loss of NHS.

3.3.1.4 Synthesis of N-α- Fmoc-Lysine-HYNIC-Boc

NHS-HYNIC-Boc (0.250 g, 0.714 mmol) was added to a round bottom flask along with Fmoc-Lys-OH (0.316 g, 0.857 mmol). Anhydrous DMF was then added to the flask (25 cm^3). The reaction mixture was stirred for 2 hours at 50°C and then water (approx 20 cm^3) was added slowly until the reaction mixture turned from a cloudy suspension to a clear liquid. The solution was stirred overnight at 50°C. The resulting solution was a pale yellow colour. The reaction mixture was concentrated to remove water and as much DMF as possible under reduced pressure to give a yellow solid. The resulting yellow paste was dissolved in 30 cm^3 of ethyl acetate and shaken in a separating funnel with 8 consecutive aliquots of saturated ammonium chloride (100 cm^3 each). The product was dried with sodium sulphate and vacuum filtered to give a clear pale yellow solution. This was concentrated to dryness and dried in the vacuum oven (60°C 24 h) to yield an off- white solid (Greenland et al. 2003, Greenland 2002 PhD Thesis).

Yield: 0.22 g, 0.37 mmol, 51%, (lit 64 %), m.p. 177-180°C.

δ_H from literature (270 MHz; DMSO): 1.28 (2H, m), 1.41 (9H, s), 1.45 (2H, m), 1.58 (1H, m), 1.72 (1H, m), 3.20 (2H, m), 3.73 (1H, m), 4.21-4.31 (m), 6.50 (1H, d, *J* 8.0), 6.69 (1H) 7.31 (2H, t, *J* 7.4), 7.35 (2H, t, *J* 7.0), 7.68 (2H, d, *J* 6.9), 7.87 (2H, d, *J* 7.4), 7.96 (1H, d, *J* 8), 8.31 (1H, s) 8.55 (1H, d, $J < 2$), 8.64 (1H, s), 8.92 (1H, s).

δ_H (600 MHz; DMSO) 1.40 (9H, s, 3($-CH_3$), 12, 16, 17-H), 1.58 (2H, m, CH_2, 21-H), 1.70 (2H, m, CH_2, 20-H), 1.80 (2H, m, CH_2, 22-H), 3.23 (2H, doublet, *J* 6.4, CH_2, 19-H), 3.95 (1H, m, CH, 31-H), 4.22 (1H, t, *J* 6.8, CH, 23-H), 4.30 (2H, d, *J* 7.3, CH_2, 30-H), 6.52 (1H, d, *J* 8.8, CH, 3-H), 7.30 (2H, t, *J* 7.3, 2CH, 37-H and 41-H), 7.42 (2H, t, *J* 7.3, 2CH, 38-H and 42-H), 7.60 (1H, d *J* 8.8, CH, 4-H), 7.77 (2H, d, *J* 7.3, 2CH, 36-H and 40-H), 7.90 (2H, d, *J* 7.3, 2CH, 39-H and 43-H), 8.30 (1H, s, CH, 6-H), 8.60 (1H, s, NH, 7-H), 8.70 (1H, s, NH, 8-H), 8.98 18 or 24-H (1H, s, NH).

δ_C (151 MHz; DMSO) 24.5 (C-21), 29.9 (C-12, 16, 17), 30.5 (C-22), 32.0 (C-20), 40.5 (C-19), 48.5 (C-31), 55.0 (C-23), 67.0 (C-30), 81.0 (C-11), 106.3 (C-3), 121.7 (C-37 and 41), 122.0 (C-5), 126.8 (C-38 and 42), 128.5 (C-36 and 40), 129.0 (C-39 and 43), 138.0 (C4), 142.0 (C-33 and 34), 145.2 (C-32 and 35), 149.0 (C-6), 157.1 (C-25), 158.0 (C-9), 163.0 (C-2), 166.5 (C-13), 175.8 (C-27).

δc (151 MHz; DMSO, DEPT 45 - CH, CH_2, CH_3 all positive) 24.2 (C-21), 29.1 (C-12, 16, 17), 30.3 (C-22), 32.0 (C-20), 40.5 (C-19), 48.0 (C-31), 55.0 (C-23), 67.0 (C-30), 106.0 (C-3), 121.2 (C-39 and 43), 126.5 (C-36 and 40), 128.3 (C-37 and 41), 128.7 (C-38 and 42), 138.0 (C-4), 147.0 (C-6).

δc (151 MHz; DMSO, DEPT 90 – CH only) 48.0 (C-31), 55.0 (C-23), 106.0 (C-3), 121.2 (C-39 and 43), 126.5 (C-36 and 40), 128.3 (C-37 and 41), 128.7 (C38 and 42), 138.0 (C-4), 147.0 (C-6).

δc (151 MHz; DMSO, DEPT 135 – CH and CH_3 positive, CH_2 negative).

CH and CH_3: 29.1 (C-12, 16, 17), 48.0 (C-31), 55.0 (C-23), 106.0 (C-3), 121.2 (C-39 and 43), 126.5 (C-36 and 40), 128.3 (C-37 and 41), 128.7 (C-38 and 42) 138.0 (C-4), 147.0 (C-6).

CH_2: 24.2 (C-21), 30.3 (C-22), 32.0 (C-20), 40.5 (C-19), 67.0 (C-30).

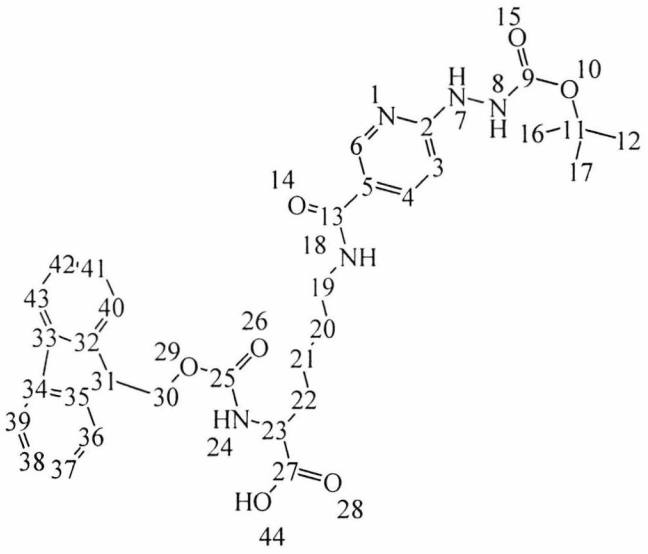

Figure 3.5 Fmoc-Lys-HYNIC-Boc Structure and ^{1}H and ^{13}C NMR assignments

ν_{max} cm^{-1} 3310 (m, N-H *str,* secondary amine), 2978 (m, C-H *str*), 1690 (s C=O *str* ester), 1630 (s, C=O *str* ketone), 1611 (s, C=O *str* amide), 1475, 1450 (N-H *bend*, secondary amine), 1242, 1156 (s, C-O *str* ester).

Analysis by RP HPLC: Eluted at 14.1 minutes. (HPLC / System A / Method 1 / Column 1 / A254, 280, 300 nm). 77% by peak area percent.

$C_{32}H_{37}N_5O_7$ Molecular weight: 603.67, exact mass: 603.27, measured mass of ion: 604.2758.

m/z (ESI) Positive mode, molecular ion $[M + H]^+$:604.2758 100% intensity, $[2M + H]^+$:1207.5443 17% intensity.

Elemental analysis: Formula calculated from $C_{32}H_{37}N_5O_7$

Expected: C 63.7%, H 6.2%, N 11.6%.

Found: C 63.4%, H 6.2%, N 11.0%.

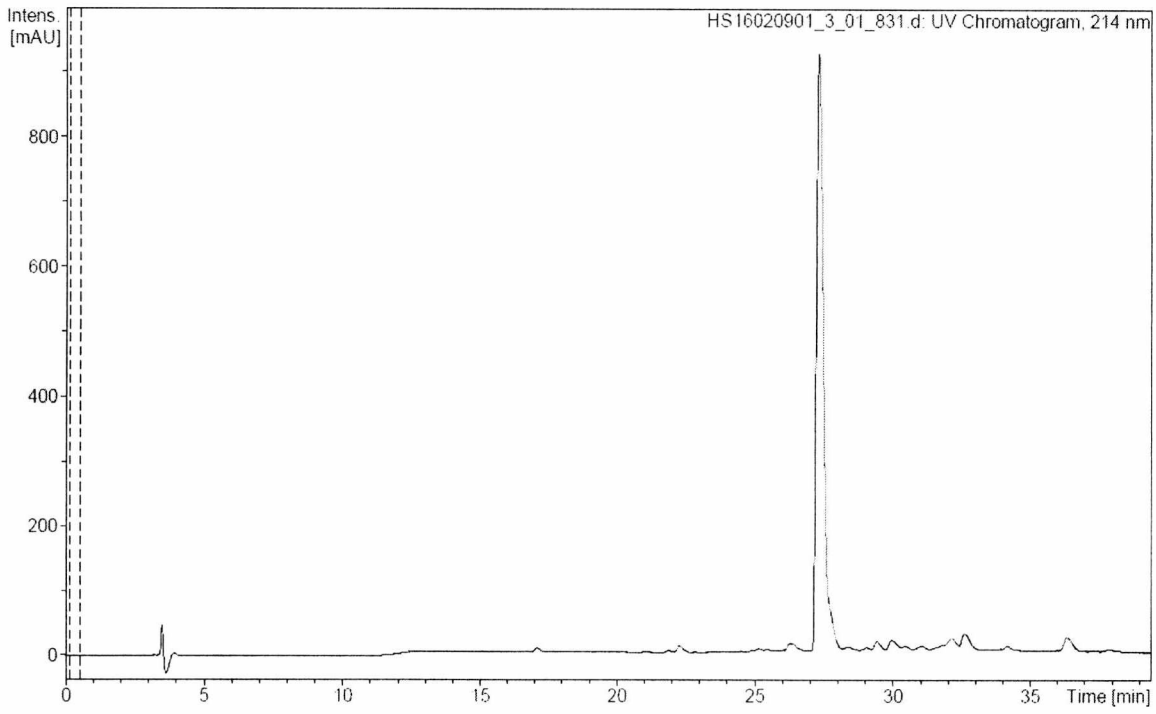

Figure 3.6 HPLC analysis of N-α- Fmoc-Lysine-HYNIC-Boc to show purity. HPLC analysis was carried out with different conditions (see below)

HPLC Conditions for the sample above were:

Mobile phase A: H_2O, 0.05% Trifluoroacetic acid (v/v)

Mobile Phase B: 70% Acetonitrile, 30% H_2O (v/v), 0.045% Trifluoroacetic acid (v/v)

Time	%A	%B
0 min	95	5
5 min	95	5
30 min	0	100
35 min	0	100
40 min	95	5
55 min	95	5

Table 3.0 HPLC gradient; data were collected at 214 nm and for the first 40 minutes only.

3.3.2 Synthesis of N-α- Fmoc-Lysine-HYBA-Boc

3.3.2.1 Synthesis of 4-(*N'*-tert-Butoxycarbonyl-hydrazino)-benzoic acid; 'Boc-HYBA'

To a solution of hydrazinobenzoic acid (HYBA) (7.0 g, 46.0 mmol), anhydrous DMF (10 cm^3) was added with stirring. Di-tert-butyl dicarbonate (10.0 g, 46.0 mmol) was then added. The yellow suspension turned into a clear yellow solution over 1 hour and stirring was continued for 16 hours at room temperature. The reaction mixture was concentrated to remove as much DMF as possible under reduced pressure to give a yellow solid. The resulting yellow paste was dissolved in a minimum amount of ethyl acetate and shaken in a separating funnel with 8 consecutive aliquots of saturated ammonium chloride (100 cm^3 each). The product was dried with sodium sulphate and vacuum filtered to give a clear yellow solution. This was concentrated to dryness and dried in the vacuum oven (60°C 24 h) to yield a pale yellow solid which was used without further purification.

Yield: 10.8 g, 42.9 mmol, 93%, m.p. 167-170°C.

δ_H (270 MHz; DMSO) 1.42 (9H, s, 3(CH_3) 12, 16, 17-H), 6.68 (2H, d, *J* 8.8, 2CH, 3-H and 5-H), 7.78 (2H, d, *J* 8.8, 2CH, 2-H and 6-H), 8.29 (1H, s, NH, 10-H), 8.96 (1H, s, NH, 11-H), 9-H not observed.

δ_C (67.8 MHz; DMSO) 28.0 (C-15, 17, 18), 78.9 (C-14), 110.0 (C-5 and 3), 120.0 (C-1), 132.0 (C-2 and 6), 154.0 (C-4), 157.0 (C-12), 168.0 (C-7).

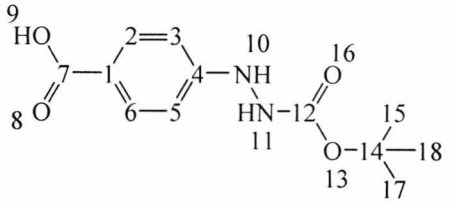

Figure 3.7 HYBA-Boc Structure: ^{1}H and ^{13}C NMR assignments

ν_{max} cm^{-1} 3304 (m, N-H *str,* secondary amine), 2978 (m, C-H sp^3 *str*), 1685 (s, C=O *str* ester), 1681 (s, C=O *str* acid), 1510, 1479 (m, N-H *bend*, secondary amine), 1249, 1154 (s, C-O *str*, ester).

Analysis by RP HPLC: Eluted at 12.5 minutes. (HPLC / System A / Method 1 / Column 1 / A254, 280, 300 nm). 99% by area percent.

$C_{12}H_{16}N_2O_4$ Molecular weight: 252.27, exact mass: 252.11

m/z (ESI) (cone voltage 20V) Positive mode, molecular ion $[M + H]^+$:253.1 20% intensity, 197.0 100% intensity, loss of t-butyl group.

3.3.2.2 Synthesis of Succinimidyl 4-(N'-tert-Butoxycarbonyl-hydrazino)-benzoic acid; 'NHS-HYBA- Boc'

HYBA-Boc (10.6 g, 42.1 mmol), NHS (4.84 g, 42.1 mmol) along with WSC.HCl. (8.06 g, 42.1 mmol) were dissolved in anhydrous DMF (30 cm^3) under an atmosphere of nitrogen gas. The reaction mixture was stirred overnight at RT and resulted in a yellow coloured solution. As much of the DMF as possible was removed under vacuum. The yellow paste remaining was dissolved in a minimum amount of ethyl acetate (30 cm^3) and shaken in a separating funnel with 8 consecutive aliquots of saturated ammonium chloride (100 cm^3 each). The product was dried with sodium sulphate and vacuum filtered to give a clear yellow solution. This was concentrated to dryness and dried in the vacuum oven (60°C 24 h) to yield a pale yellow coloured solid which was used without further purification.

Yield: 3.46 g, 9.90 mmol, 24%, m.p. 190-192°C.

δ_H (270 MHz; DMSO) 1.46 (9H, s, 3(-CH_3) 22, 24, 25-H), 2.90 (4H, s, 2(-CH_2), 15 and 16-H), 6.80 (1H, dd, *J* 8.9 CH, 3-H and 5-H), 7.91 (1H, d, *J* 8.9 CH, 2-H and 6-H), 8.79 (1H, s, NH, 17-H), 9.13 (1H, s, NH, 18-H).

δ_C (67.8 MHz; DMSO) 27.0 (C-15 and 16), 29.0 (C-22, 24, 25), 80.0 (C-21), 112.0 (C-3 and 5), 114.0 (C-1), 133.0 (C-2 and 6), 156.0 (C-4), 157.0 (C-11 and 12), 163.0 (C-19)?, 172.0 (C-7).

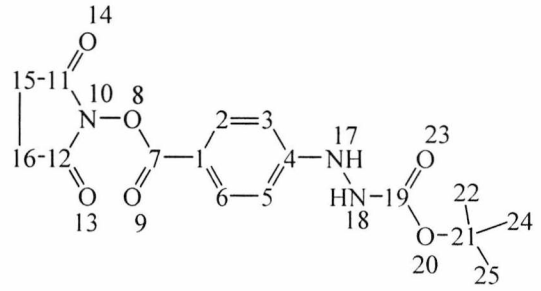

Figure 3.8 NHS-HYBA-Boc Structure: ^{1}H and ^{13}C NMR assignments

ν_{max} cm^{-1} 3312 (m, N-H *str,* secondary amine), 2989 (m, C-H *str*), 1749 (m, C=O *str* ester), 1719 (s, C=O *str* acid), 1606 (m, C=O, *str*, amide), 1261, 1241, 1153, 1052 (s, C-O *str*, ester).

Analysis by RP HPLC: Eluted at 13.9 minutes. (HPLC / System A / Method 1 / Column 1 / A254, 280, 300 nm). 81% by peak area percent.

$C_{16}H_{19}N_3O_6$ Molecular weight: 349.34, exact mass: 349.13, measured mass of ion [M + NH_4]: 367.1611. (Exact mass of $^{+}NH_4$ is 18.03).

m/z (ESI) (cone voltage 20V), Positive mode, molecular ion [M + NH_4] $^{+}$:367.1611 100% intensity.

3.3.2.3 Synthesis of N-α- Fmoc-Lysine-HYBA-Boc

NHS-HYBA-Boc (2.0 g, 5.73 mmol) was added to a round bottom flask along with fmoc-Lys-OH (2.53 g, 6.87 mmol). Anhydrous DMF was then added to the flask (25 cm^3). The reaction mixture was stirred for 2 hours at RT and then water (approx 20 cm^3) was added slowly until the reaction mixture turned from a cloudy suspension to a clear liquid. The solution was stirred overnight at RT. The resulting solution was a yellow colour. The reaction mixture was concentrated to remove water and as much DMF as possible under reduced pressure to give a yellow solid. The resulting yellow paste was dissolved in a minimum amount of ethyl acetate and shaken in a separating funnel with 8 consecutive aliquots of saturated ammonium chloride (100 cm^3 each). The product was dried with sodium sulphate

and vacuum filtered to give a clear pale yellow solution. This was concentrated to dryness. The solid was taken up in ethyl acetate and passed through a 25 cm^3 silica gel 'flash' chromatography column. The column was packed wet and equilibrated with ethyl acetate. Ethyl acetate was passed through the column and the fractions were collected until all product had been eluted. 10% methanol / 90% ethyl acetate was then passed through the column to elute any compounds remaining behind. 10% methanol / 90% ethyl acetate was used for identification by TLC, with the product giving an RF value of 0.28. This was then concentrated to dryness and dried in the vacuum oven (60°C 24h) to yield an intensely yellow solid.

Yield: 0.88 g, 1.45 mmol, 25%, m.p. 150-151°C.

δ_H (600 MHz; DMSO) 1.40 (9H, s, 3(-CH_3), 41, 44, 43-H), 1.55 (2H, m, CH_2, 21-H), 1.70 (2H, m, CH_2, 22-H), 1.78 (2H, m, CH_2, 20-H), 3.30 (2H, m, CH_2, 23-H), 3.97 (1H, m, CH, 1-H), 4.25 (1H, t, *J* 7.3, CH, 19-H), 4.32 (2H, d, *J* 5.9, CH_2, 14-H), 6.70 (2H, d, *J* 8.8 2CH, 31-H and 33-H), 7.35 (2H, t, *J* 7.3, 2CH, 11-H and 7-H), 7.45 (2H, t, *J* 7.3, 2CH, 8-H and 12-H), 7.62 (2H, d, *J* 7.3, 2CH, 6-H and 10-H), 7.63 (2H, dd, *J* 7.3, 2CH, 9-H and 13-H), 7.90 (2H, d, *J* 8.8, 2CH, 30-H and 34-H), 8.02 (1H, s, NH, 36-H), 8.15 (1H, s, NH, 37-H), 8.48 (1H, s, NH, 18 or 24-H), 8.88 (1H, s, NH, 18 or 24-H).

δ_C (151 MHz; DMSO) 24.5 (C-21), 29.8 (C-41, 43, 44), 30.1 (C-20), 32.5 (C-22), 40.5 (C-23), 48.0 (C-1), 55.5 (C-19), 67.0 (C-14), 80.5 (C-40), 112.0 (C-31 and 33), 121.5 (C-9 and 13), 125.5 (C-29), 126.5 (C-6 and 10), 128.5 (C-7 and 11), 129.0 (C-8 and 12), 130.0 (C30 and 34), 142.0 (C-3 and 4), 145.2 (C-2 and 5), 153.5 (C-32), 157.1 (2 peaks) (C-16 and 38), 167.0 (C-25), 175.2 (C-27).

δc (151 MHz; DMSO, DEPT 45 - CH, CH_2, CH_3 all positive) 24.5 (C-21), 29.5 (C-41, 43, 44), 30.3 (C-20), 32.0 (C-22), 40.5 (C-23), 48.0 (C-1), 55.0 (C-19), 67.0 (C-14), 112.0 (C-31 and 33), 121.2 (C-9 and 13), 126.5 (C-6 and 10), 128.5 (C-7 and 11), 129.0 (C-8 and 12), 130.0 (C-30 and 34).

δc (151 MHz; DMSO, DEPT 90 – CH only) 52.0 (C-1), 59.0 (C-23), 115.5 (C-31 and 33), 125.5 (C-9 and 13), 130.5 (C-6 and 10), 132.0 (C-7 and 11), 133.0 (C8 and 12), 133.8 (C-30 and 34).

δc (151 MHz; DMSO, DEPT 135 – CH and CH_3 positive, CH_2 negative).

CH and CH_3: 33.2 (C-12, 16, 17), 52.0 (C-1), 59.5 (C-19), 115.5 (C-31 and 33), 122.5 (C-9 and 13), 130.0 (C-6 and 10), 132.0 (C-7 and 11), 133.0 (C-8 and 12), 134.0 (C-30 and 34).

CH_2: 28.2 (C-21), 34.3 (C-20), 36.0 (C-22), 44.3 (C-23), 71.0 (C-14).

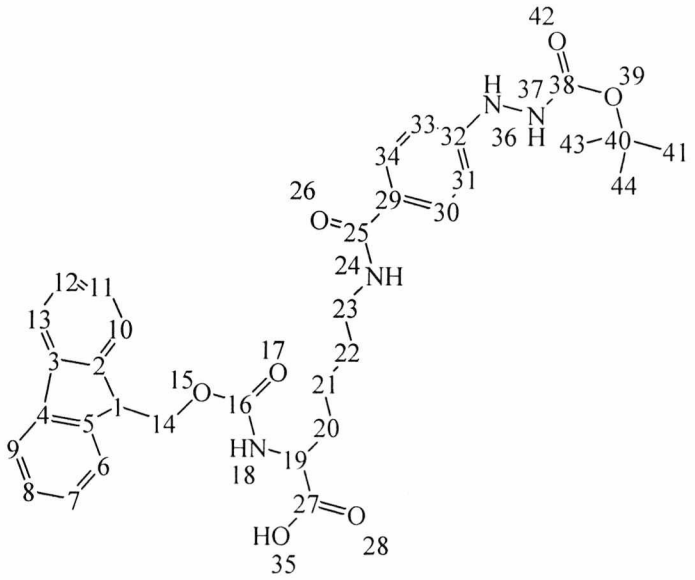

Figure 3.9 Fmoc-Lys-HYBA-Boc Structure: ^{1}H, ^{13}C NMR and DEPT assignments

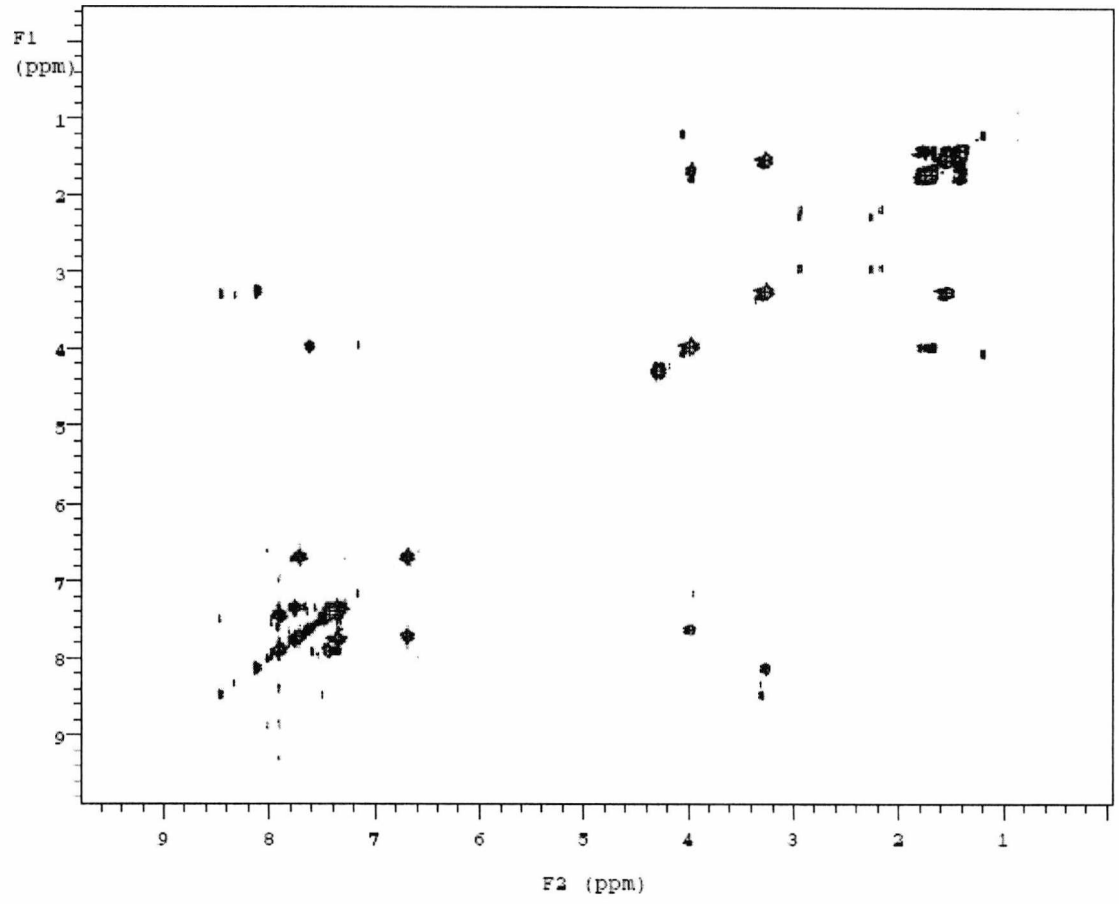

Figure 3.10 2D COSY (Correlation Spectroscopy) NMR spectrum

δ_H (600 MHz; DMSO, 2-D COSY) H-21, H-22, H-20, H-23, H-1, H-19, H-14, H-31 and H-33, H-6 and 10, H-7 and 11, H-8 and 12, H-9 and 13, H-30 and 34, H-18 or 24.

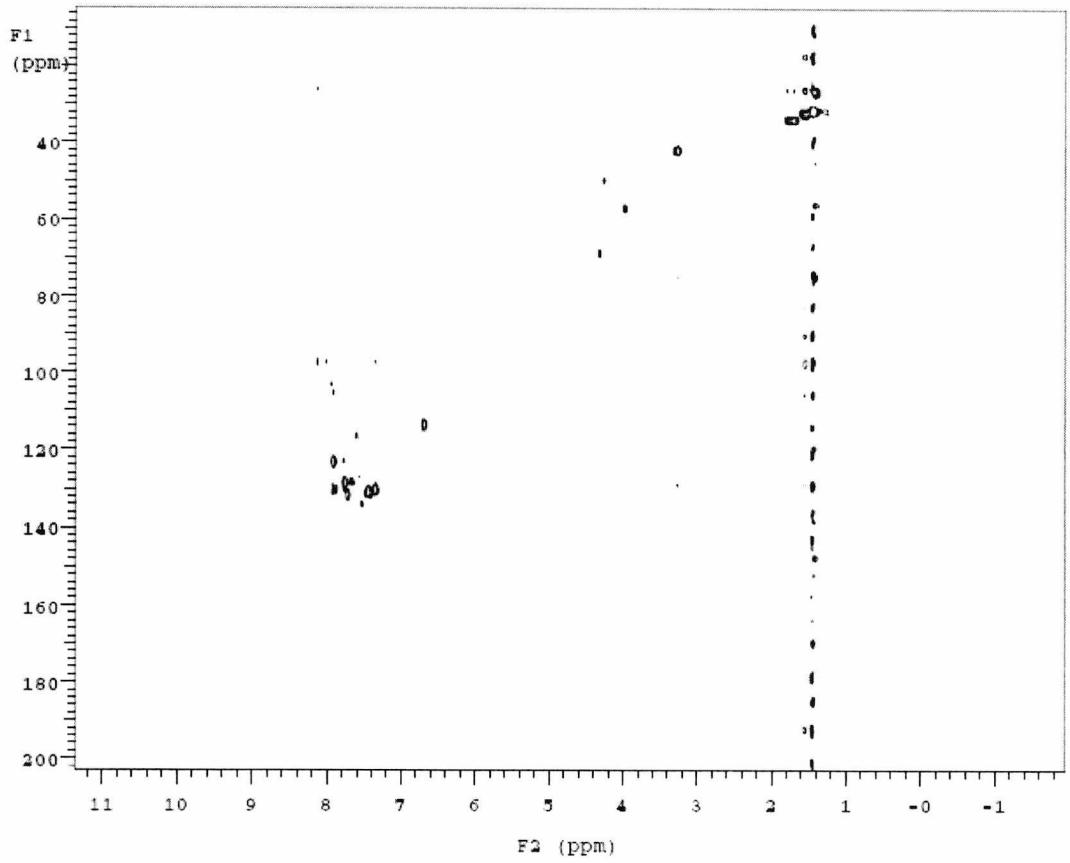

Figure 3.11 Proton-carbon correlation NMR spectrum

δ_H (600 MHz; DMSO, proton-carbon correlation) H-21, H-22, H-20, H-23, H-1, H-19, H-14, H-31 and H-33, H-7 and 11, H-8 and 12, H-6 and 10, H-9 and 13, H-30 and 34.

δ_C (151 MHz; DMSO, proton-carbon correlation) C-21, C-20, C-22, C-23, C-1, C-19, C-14, C-31 and 33, C-9 and 13, C-6 and 10, C-7 and 11, C-8 and 12, C-30 and 34.

ν_{max} cm^{-1} 3291 (m, N-H *str,* secondary amine), 2989 (m, C-H *str*), 1920 (w, -C=C *str*, aromatic ring), 1697 (m C=O *str* ester), 1630 (s, C=O *str* ketone), 1607 (s, C=O *str* amide), 1503 (N-H *bend*, secondary amine), 1241, 1154, 1057 (s, C-O *str* ester).

Analysis by RP HPLC: Eluted at 15.9 minutes. (HPLC / System A / Method 1 / Column 1 / A254, 280, 300 nm). Analysis shown below, 100% purity by peak area.

$C_{33}H_{38}N_4O_7$ Molecular weight: 602.68, exact mass: 602.27, measured mass of ion: 603.2816

m/z (ESI) Positive mode, molecular ion $[M + H]^+$:603.2816 100% intensity.

Elemental analysis: Formula calculated from $C_{33}H_{38}N_4O_7$

Expected: C 65.8%, H 6.4%, N 9.3%.

Found: C 65.7%, H 6.3%, N 8.6%.

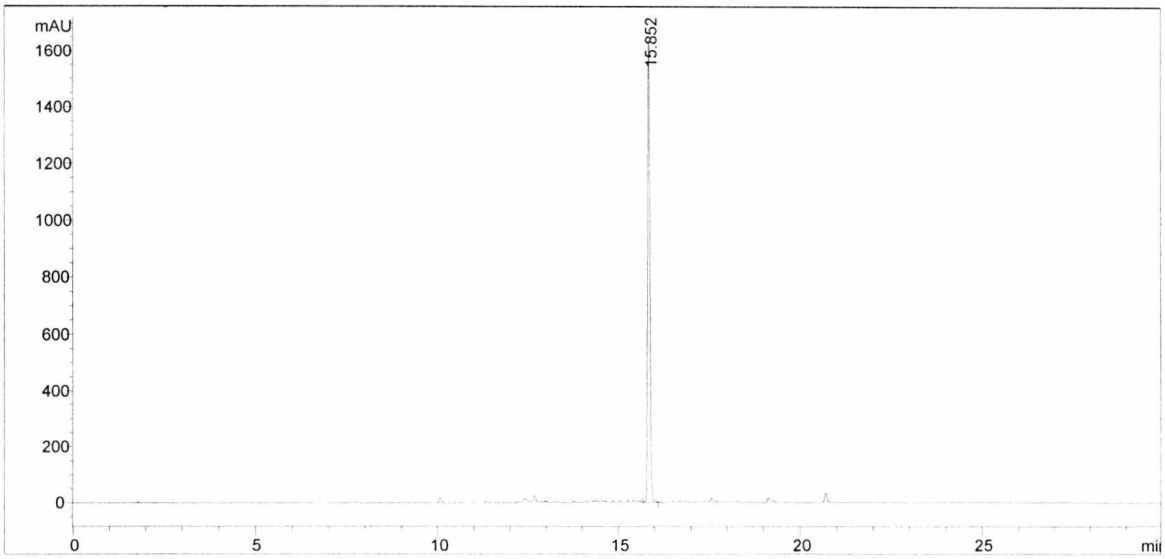

Figure 3.12 HPLC analysis of N-α- Fmoc-Lysine-HYBA-Boc to show purity

3.4 Results and discussion

3.4.1 Synthesis

HYNIC was synthesised with a yield 72% compared to 77% in the literature (Greenland 2002).

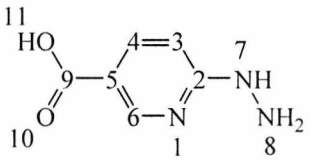

Figure 3.13 HYNIC

The ^1H NMR spectrum did not show the acid proton, which would have been expected at about 12 ppm or the NH_2 protons at position 8. O-H and N-H protons do not always show in an NMR spectrum. Their presence is concentration dependent and their position can alter in the spectrum. In the literature ^1H NMR spectrum, the N-H at position 7 did not show either. N-H protons and O-H protons do not tend to couple with their neighbouring protons as carbon

bonded protons do. N-H and O-H protons can exchange with water protons and so do not always show up in NMR spectra. N-H protons often appear at about 8 ppm, as is the case here for the N-H proton at position 7. The proton in the pyridine ring at position 4 is at a higher chemical shift to the proton at position 3 due to the electron withdrawing effect of the carboxylic acid which is nearer proton 4 than 3. Resonance structures will leave a lack of electron density in the *ortho-* and *para-* positions with respect to the carboxylic acid group (see chapter 2, figure 2.21). Proton 6 is also next to an electron withdrawing nitrogen causing it to appear at a higher frequency in the ^{1}H spectrum compared to proton 4. There is some long range coupling occurring between protons 4 and 6 as well as the expected coupling between protons 3 and 4. As proton 3 is coupling with proton 4 there is a corresponding doublet on the NMR spectrum. Proton 6 is coupling (long range) with proton 4 and so is a doublet. Proton 4 is coupling with both proton 3 and 6 and so is seen as a double doublet. The coupling constants are the same between coupling protons and therefore help to identify protons in the ^{1}H spectrum.

The carbon NMR spectrum showed the carbons labelled 3, 4 and 6 to agree with the assignments in the proton NMR spectrum. The carbon atoms in the 2 and 5 positions, named ipso carbons, with no attached hydrogens, often give smaller signals than those with hydrogen atoms attached to them. This helps with identification. The carbon atom in the 5 position has added electron density from the electron donating (hydrazine) amine group and so is at a lower chemical shift in the NMR spectrum, as the added electron density means it does not feel the full effect of the magnetic field (see chapter 2, figure 2.25). The opposite is true for the carbon in position 2. It has electron density drawn away from it by the carboxylic acid group and so is at a higher chemical shift. The carboxylic acid carbon is subject to the electron withdrawing effect of the oxygens and so is at a high chemical shift of 167 ppm.

For HYNIC, the IR spectrum showed the expected functional groups. As with all the Infra Red spectra discussed in this chapter, not every peak present in the IR spectra has been noted, rather enough peaks to be sure the correct functional groups were present in the spectrum for each compound. An N-H stretch of a secondary amine can be seen at 3315 cm^{-1} with medium intensity, a primary amine N-H stretch at 3226 cm^{-1}, a carboxylic acid O-H stetch at 2726 cm^{-1} and a carboxylic acid carbonyl stretch at 1683 cm^{-1}. These functional groups are all present in the HYNIC molecule and help identify the compound analysed as being HYNIC. The mass spectrum gave the correct mass of 154.1 with 100% intensity. The exact mass of

HYNIC is 153.05 and so once ionised $[M + H]^+$ it can be seen this is the correct ion. The HPLC analysis, according to the peak area, showed the compound was only 72% pure. It is possible that more than one species with differing charges and therefore different retention times is present. The ^1H NMR and ^{13}C NMR spectra showed no impurities and the mass spectrum showed no major impurity peaks.

Boc-HYNIC was synthesised with a yield of 66%.

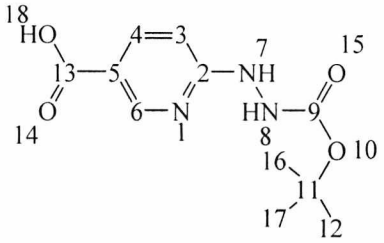

Figure 3.14 Boc-HYNIC

The Boc-HYNIC proton NMR spectrum shows the Boc group at 1.46 ppm in the ^1H spectrum and 29.0 ppm in the ^{13}C spectrum. The methyl groups have a slight electron donating effect which means that because of the three methyl groups, the Boc group has high electron density, as methyl groups are slightly electron donating and so comes at a lower chemical shift than all the other protons (in the ^1H spectrum) and carbons (in the ^{13}C spectrum) in the molecule. Only one peak is seen for the three CH_3 groups; they are all equivalent as the Boc group is symmetrical. Compared to HYNIC, the Boc-HYNIC proton spectrum shows the N-H nitrogen number 8. The N-H proton in position 7 and proton at position 6 have swapped compared to the HYNIC ^1H spectrum. Other than this, the protons in the Boc-HYNIC ^1H spectrum are in the same position as they are in the HYNIC ^1H spectrum with the carboxylic acid proton again not present in the ^1H spectrum. Neither the N-H protons nor the O-H proton are present in the ^1H spectrum from the literature (Greenland 2002), but otherwise the proton ^1H spectra for Boc-HYNIC are in good agreement.

In the ^{13}C NMR spectrum the carbon at position 11 comes at a higher chemical shift than the other carbons in the Boc group as it has no hydrogens directly attached to it and so not as much electron density and is next to an oxygen atom. The other carbon atoms, except numbers 3 and 5 which have swapped over, are in direct agreement with the HYNIC carbon NMR spectrum. There is another carbon atom in the Boc group attached to an oxygen atom at

position 9 which is at 156 ppm. The oxygen atom takes electron density away from the carbon, causing it to appear at a higher chemical shift.

For Boc-HYNIC, the IR spectrum showed the expected functional groups, with an N-H stretch of a secondary amine at 3255 cm^{-1}, a C-H stretch at 2978 cm^{-1}, carbonyl stretches of an acid at 1721, 1712, 1693 cm^{-1} and the C-O stretches of an ester at 1246 and 1150 cm^{-1}. The presence of these functional groups confirms the synthesised compound is the correct compound. The mass spectrum showed the correct mass of 252.0 for $[M - H]^-$, with the exact mass being 253.1. Dimers and trimers were present at 15% intensity of the molecular ion and 5% intensity of the molecular ion respectively. The HPLC analysis showed the Boc-HYNIC eluting at 9.8 minutes and was 94% pure by peak area percent.

The NHS-HYNIC-Boc was synthesised with a yield of 49%. The melting point differed from the literature value by about 5°C. The proton NMR was in agreement with the literature, again the literature did not quote a value for the N-H protons.

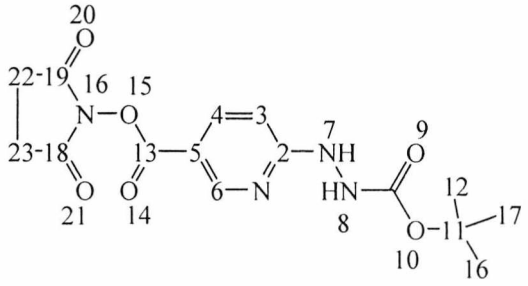

Figure 3.15 NHS-HYNIC-Boc

The succinimidyl CH_2 protons are equivalent and symmetrical and so give rise to one peak at 2.91 ppm. The proton NMR otherwise is the same as the Boc-HYNIC with the exception of the 2 N-H protons which are shifted to a slightly higher chemical shift and reversed so the proton at position 7 is at a lower chemical shift than the proton at position 8. This is easy to see as the NH_2 in position 8 gives rise to a shorter, broader peak than the NH in position 7, perhaps because the proton in position 8 exchanges more readily with water.

The two CH_2 groups in the succinimidyl group are seen before the Boc carbons in the carbon NMR. This is not expected as CH_3 groups usually appear at a lower chemical shift than CH_2 groups in both proton and carbon NMR spectra. The 2 carbonyl carbons are at a higher ppm of 162, just lower than the ester C=O at 167 ppm. The ^{13}C spectrum has differences from the Boc-HYNIC carbon ^{13}C spectrum as carbons 3 and 5 have swapped over as have carbons 2

and 4. This identification has been made because the carbons 5 and 2 have smaller signals than the carbons 3 and 4, as carbons 5 and 2 are ipso carbons.

For NHS-HYNIC-Boc, the IR spectrum showed the expected functional groups, a secondary amine stretch at 3323 cm^{-1}, a C-H stretch at 2978 cm^{-1}, carbonyl stretches for an ester at 1765 and 1730 cm^{-1}, carbonyl stretches for an amide at 1719, 1715 and 1601 cm^{-1} and C-O stretches at 1239, 1201 and 1153 cm^{-1}. The mass spectrum the correct mass of $[M + H]^+$ 351.13, the exact mass is 350.12, showing an additional peak with loss of NHS. There was also a dimer present and a dimer showing loss of NHS. The HPLC analysis showed a purity of 93% from the peak area percent and a retention time of 12.4 minutes.

The Fmoc-Lys-HYNIC-Boc was synthesised with a yield of 51% (Lit. 64% yield). The literature NMR assignments for Fmoc-Lys-HYNIC-Boc differ from the ^1H spectrum assignments taken from the literature. The literature assignments were taken from previous work carried out by the group (Surfraz et al. 2007). The analysis was carried out more thoroughly than before with the DEPT carbon NMR spectra and the proton NMR spectrum on a 600 MHz instrument instead of a 270 MHz instrument.

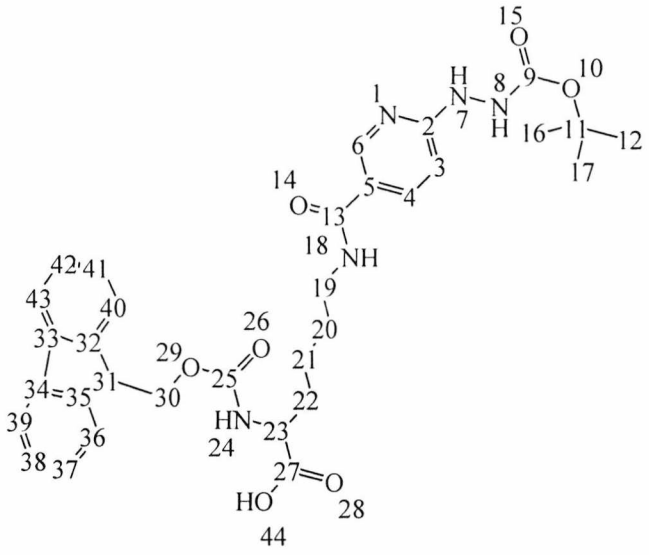

Figure 3.16 Fmoc-Lys-HYNIC-Boc

In the ^1H spectrum, the peak at 1.40 minutes can be identified as the Boc group. The three CH_3 groups have protons in an identical chemical environment and give a single peak just as seen in the ^1H spectrum for Boc-HYNIC and NHS-HYNIC-Boc. The CH_2 protons of the lysine side chain in positions 21, 20, 22, 19 are also at a low chemical shift and the protons at positions 21, 20 and 22 give rise to multiplet peaks as they are all next to two other alkyl

groups. Protons 21 and 20 are next to two other methylene groups and so come at the lowest chemical shifts, 22 is next to a CH_2 and a CH and so is seen next in the ^1H spectrum, proton 19 is next to a CH_2 and an NH and is a doublet as the CH_2 at position 19 does not couple with the NH. The nitrogen of the amine is electron withdrawing as it is not part of a π system and so proton 19 has the highest chemical shift of the CH_2 protons in the lysine alkyl chain. The CH protons 31 and 23 come next in the ^1H spectrum, at a higher chemical shift than the CH_2 protons in the lysine side chain. The CH at position 31 comes first and then 23 as the proton 23 is near carboxylic acid group, which is electron withdrawing and has the effect of moving it to a slightly higher chemical shift and it is also next to an amide group. The CH_2 in position 30 comes at a higher chemical shift than the other CH_2 groups as it is next to an electronegative oxygen atom. Oxygen atoms are more electronegative than nitrogen, so proton 30 appears at a higher chemical shift than proton 19. The aromatic CH in position 3 is next in the ^1H spectrum, in a similar place of 6.52 ppm to where it came in the Boc-HYNIC (6.75 ppm) and NHS-HYNIC-Boc ^1H spectra (6.67 ppm). Protons in positions 37 and 41, then 38 and 42 are next. These four protons are all next to two CH groups. Identifying them correctly was helped by comparison with the proton-carbon correlation NMR spectroscopy carried out on the Fmoc-Lys-HYBA-Boc. The proton at position 4 is next and identification is helped by looking at the coupling constant to check it is the same as for proton 3. The protons 37 and 41 are in an identical chemical environment and so give rise to one peak for both of them. The same is true of the protons; 38 and 42, 36 and 40, 39 and 43. The protons in positions 36 and 40 and 39 and 43 are next. These protons are next to a CH and a quaternary carbon and the effect is that these CH groups compared to the CH groups in positions 37, 41, 38 and 42 feel more of the magnetic field due to having less electron density around them and so are at a higher chemical shift on the ^1H spectrum. The effect is small in this case and all the fluorenyl ring protons come within 0.6 ppm of each other. The proton in position 6 comes at a similar chemical shift (8.3 ppm) to the Boc-HYNIC NMR (8.62 ppm) although no long range coupling is seen this time with proton 4. The NH protons in positions 7 and 8 are identified next with the NH at position 8 being at a slightly higher chemical shift than 7 due to its being closer to the ester than the NH in position 7. There is one more NH in the ^1H spectrum and this is likely to be either the NH at 18 or 24. The OH in position 44 is not seen. From the DEPT spectra, all methyl, methylene, methine and quaternary carbons have been identified. (See discussion of DEPT NMR spectra). Carbon 21 comes before the carbons in the Boc group; this is different to the ^1H spectrum. The carbons in positions 20 and 22 are swapped in

the ^{13}C spectrum when compared to the ^{1}H spectrum. The carbons in positions 19, 31, 23, 30 and 3 are in the same order as in the ^{1}H spectrum. The carbon at position 11 is a quaternary carbon and at 81 ppm it comes where expected with regards to the ^{13}C spectra of Boc-HYNIC and NHS-HYNIC-Boc (80 ppm for both compounds). The fluorenyl carbons 37 and 41, 38 and 42, 36 and 40 and 39 and 43 come in the same order as was seen in the ^{1}H spectrum. C-5 is a quaternary carbon, giving rise to a smaller peak than for those carbons with hydrogens attached. It comes at 122 ppm compared to 117 ppm for the same carbon atom in the NHS-HYNIC-Boc ^{13}C spectrum. The carbon atoms in positions 4, 6 and 2 compare well to those found in the Boc-HYNIC where C-4 was at 139 ppm, here it is 138 ppm, C-6 was at 151 ppm, while in this ^{13}C spectrum it is 149 ppm and C-2 was at 164 ppm and here it is 163 ppm. This is different from the ^{13}C spectrum for NHS-HYNIC-Boc where, as discussed, some of the carbon atoms had swapped positions in comparison to the Boc-HYNIC. It is difficult to distinguish between the carbons in positions 32 and 35 compared to those in 33 and 34. 32 and 35 are in an identical chemical environment and so give rise to one peak as do those in positions 33 and 34 for the same reasons. The difference between them is 3.2 ppm, a very small distance. The C=O carbons come last as they are all next to electronegative oxygen atoms. C-27 is an acid carbon which is found at the highest frequency of 175.8 ppm.

The IR spectrum showed the expected functional groups, at 3310 cm^{-1} there was an N-H secondary amine stretch, at 2978 cm^{-1} a C-H stretch, at 1690 cm^{-1} a carbonyl stretch of an ester, at 1630 cm^{-1} a carbonyl stretch of a ketone and at 1611 cm^{-1} a carbonyl stretch of an amide. At 1475 and 1450 cm^{-1} there was an N-H bend for a secondary amine at 1242 and 1156 cm-1, a C-O ester stretch. The mass spectrum indicated the correct mass of $[M + H]^{+}$ as being 604.28, the exact mass is 603.27. The initial HPLC analysis showed a purity of 77% by peak area percent and the Fmoc-Lys-HYNIC-Boc eluted at 14.1 minutes. However the sample was re-run as it was not known why the extra peaks were present as the sample was shown to be pure from the other analysis carried out. The Fmoc-Lys-HYNIC-Boc was run again under different conditions (see table 3.0) and was shown to be 100% pure by HPLC with the presence of only one peak this time.

The Boc-HYBA was synthesised with a yield of 93%.

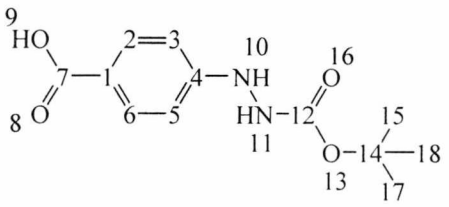

Figure 3.17 Boc-HYBA

The Boc group was found at the lowest chemical shift on the ^{1}H spectrum, as with the Boc-HYNIC, NHS-HYNIC-Boc and Fmoc-Lys-HYNIC-Boc. The aromatic protons in positions 3 and 5, which are in an identical chemical environment, are found at 6.68 ppm. The amine group nearby donates electrons to these protons. The protons in positions 2 and 6 come at a higher chemical shift as these have electron density taken away by the carboxylic acid group. As before, protons 2 and 6 are in an identical chemical environment and so give rise to one peak which is typical of a ^{1}H spectrum of a *para-* substituted benzene ring. Both protons 3 and 5 are next to one proton and so are split by this proton once giving rise to doublet peak. The same can be said for protons 2 and 6. The NH nitrogens come next, with 10-H first and 11-H at a higher chemical shift. The NH_2 proton is a shorter broader peak than the NH proton. The proton in position 9 was not observed.

The Boc group is found at the lowest frequency on the ^{13}C spectrum, followed by the carbon atom in position 14. See discussion of Boc-HYNIC ^{13}C spectrum for explanation of these assignments. As for the ^{1}H spectrum, carbons in positions 3 and 5 are at 110 ppm on the ^{13}C spectrum, and the protons 2 and 6 are at a higher chemical shift of 132 ppm. The ipso carbons in positions 1 and 4 show smaller peaks compared to the other carbons atoms and so can be more easily identified. The carbon in position 1 is has more electron density as it has electron density from the donating amine group. The opposite is true for the C-4, it has electron density taken from it and so comes at a higher chemical shift.

The IR spectrum showed the functional groups, an N-H stretch at 3304 cm^{-1}, a C-H stretch at 2978 cm-1, a carbonyl stretch for an ester at 1685 cm^{-1} and for an acid at 1681 cm^{-1}. Two N-H bends for a secondary amine at 1510 and 1479 cm^{-1} and a C-O stretch at 1249 and 1154 cm^{-1} for an ester. The mass spectrum was done using a higher cone voltage (20V) than for the Boc-HYNIC (10V). The mass spectra for this project were undertaken at Swansea Mass Spectrometry Centre. From the results, it appears that the Boc-HYBA was more difficult to ionise than the Boc-HYNIC and so a higher cone voltage was applied. This had the added effect of causing the t-butyl group to be lost from the HYBA, giving a base peak of 197 instead of the expected 253.1, although that ion was still present at 20% of the intensity of the

base peak. A cone voltage of 10V may have given the molecular ion as the base peak. The HPLC analysis showed the product was 99% pure and the elution time was 12.5 minutes.

The yield of the NHS-HYBA-Boc was 24%. The loss of product was most likely to be during the work up. It was noted that during the liquid liquid extraction procedure, product was lost on the sides of the separating funnel which could not be washed back into solution with solvent.

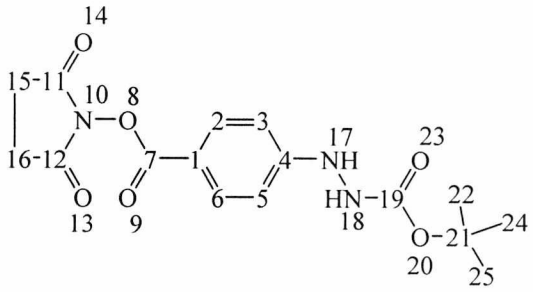

Figure 3.18 NHS-HYBA-Boc

The succinimidyl protons give one peak as they are in identical chemical environments. This peak came after the Boc group on the ^{1}H spectrum at 2.9 ppm. The other peaks in were similarly placed to those in the Boc-HYBA ^{1}H spectrum. The N-H protons in positions 17 and 18 were found at a slightly higher chemical shift compared to those in the Boc-HYBA ^{1}H spectrum. As for NHS-HYNIC-Boc, the carbons in positions 16 and 15 are seen before the Boc group. The quaternary carbon at position 21 comes as expected; at 80 ppm. Carbons 3 and 5 come at 112 ppm. The carbons in positions 1 and 4 come at very similar ppm as for the Boc-HYBA (114 ppm amd 156 ppm compared to 120 ppm amd 154 ppm for the Boc-HYBA) and are again identified by their smaller size. The two other succinimidyl carbons C-11 and 12 give rise to one peak as they are in the same chemical environment. C-7 comes at a higher chemical shift (172 ppm) than C-19 (163 ppm) as the acid carbon is in a more electronegative environment.

The IR showed the functional groups expected, an N-H stretch at 3312 cm^{-1}, a C-H stretch at 2989 cm^{-1}, a carbonyl stretch of an ester at 1749 cm^{-1}, a carbonyl stretch of an acid at 1719 cm^{-1} a carbonyl stretch of an amide 1606 cm^{-1} and at 1261, 1241, 1153, 1052 cm^{-1}, C-O stretches of an ester are found. The mass spectrum showed no loss of NHS that was seen on the NHS-HYNIC-Boc mass spectrum. The molecular ion was identified as the ammonium adduct $[M + NH_4]^{+}$ with a mass of 367.16. The exact mass is 349.13 and the exact mass of $^{+}NH_4$ is 18.03, the total of which is 367.16. The HPLC analysis showed the product eluted at 13.9 minutes and was found to be 81% pure by peak area percent.

The Fmoc-Lys-HYBA-Boc was synthesised with a yield of 25%. The low yield was probably caused by loss of product during the work-up. It was noted that yellow compound was stuck on the sides of the separating funnel which could not be removed with either solvent or water. It is likely that this yellow compound contained product that was inaccessible. It is another possibility that some product remained with the impurities that were removed from the column.

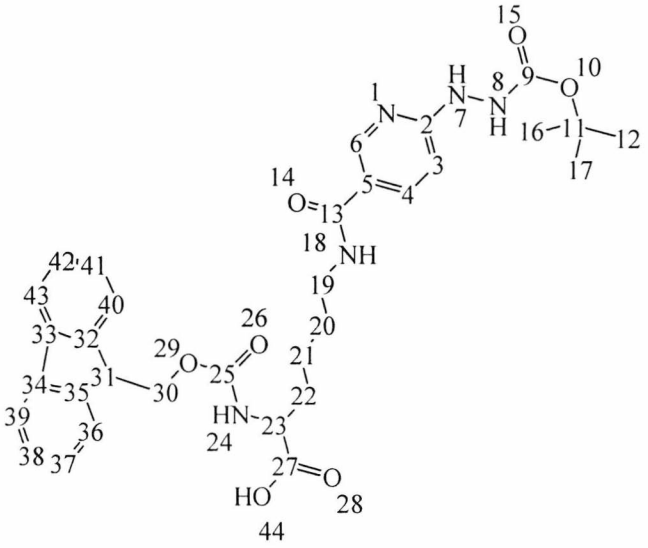

Figure 3.19 Fmoc-Lys-HYBA-Boc

In the ^{1}H spectrum, the peak at 1.40 minutes can be identified as the Boc group. The three CH_3 groups have protons in an identical chemical environment and give a single peak. The CH_2 protons of the lysine side chain in positions 21, 22, 20, 23 are also at a low chemical shift and the protons at positions 21, 22 and 20 give rise to multiplet peaks as they are all next to two other alkyl groups, 21 and 22 are next to two other methylene groups and so come at the lowest chemical shifts, 20 is next to a CH_2 and a CH and so is seen next in the ^{1}H spectrum, proton 23 is next to a CH_2 and an NH and is a doublet as the CH_2 at position 23 does not couple with the NH. The nitrogen of the amine is electron withdrawing as it is not part of a π system and so proton 23 has the highest chemical shift of the CH_2 protons in the lysine alkyl chain. The CH protons 1 and 19 come next in the ^{1}H spectrum, at a higher chemical shift than the CH_2 protons in the lysine side chain. The CH at position 1 comes first and then 19 as the proton 19 is near carboxylic acid group, which is electron withdrawing and has the effect of moving it to a slightly higher chemical shift and it is also next to an amide. The CH_2 in position 14 comes at a higher chemical shift than the other CH_2 groups as it is next to an electronegative oxygen atom. Oxygen atoms are more electronegative than nitrogen, so

proton 14 appears at a higher chemical shift than proton 23. The aromatic protons in position 31 and 33 are next in the ^{1}H spectrum, in a similar place of 6.70 ppm to where they came in the Boc-HYBA (6.68 ppm) and NHS-HYBA-Boc ^{1}H spectra (6.80 ppm). Protons in positions 7 and 11, then 8 and 12 are next. These four protons are all next to two CH groups. Identifying them correctly was helped by comparison with the 2D COSY carried out (see below for discussion of proton-carbon correlation NMR results). The protons 7 and 11 are in an identical chemical environment and so give rise to one triplet peak for both of them. The same is true of the protons; 8 and 12, 6 and 10, 9 and 13. The protons in positions 6 and 10 and 9 and 13 are next. These protons are next to a CH and a quaternary carbon and the effect is that these CH groups compared to the CH groups in positions 7, 11, 8 and 12 feel more of the magnetic field due to having less electron density around them and so are at a higher chemical shift on the ^{1}H spectrum. The effect is small in this case and all the fluorenyl ring protons come within 0.3 ppm of each other. The NH protons in positions 36 and 37 are identified next with the NH at position 37 being at a slightly higher chemical shift than 36 due to its being closer to the ester. There are two more NH groups in the ^{1}H spectrum and they are protons 18 and 24 but the order is not easy to tell and is not helped by the 2D COSY data as that does not distinguish between these NH groups. The OH in position 35 is not seen.

The 2D COSY NMR spectrum only provides information about couplings between protons 3 bonds away from each other. Therefore the protons that do not couple, such as the Boc group protons, do not show up in the 2D COSY NMR spectrum. The spectrum shows the protons in the lysine side chain starting with proton 21 on the top right hand side of the spectrum. The next proton is 22 then 20. Proton 23 comes next then 1, 19 and 14 for the non-aromatic protons. 31 and 33 come first of the aromatic protons, followed by 6 and 10, 7 and 11, 8 and 12, 9 and 13. It is not possible to distinguish the order of these protons from this NMR spectrum. Protons 30 and 34 come at a similar chemical shift to the fluorenyl protons and so it is not possible to distinguish between the fluorenyl protons and 30 and 34 from this spectrum. The NH protons 18 and 24 are present but it is not possible to distinguish between these using this technique. This technique is used in conjunction with 1D NMR and the proton-carbon correlation below to assist with assignments. The data discussed here verifies the data discussed above for the 1D NMR analysis.

Proton-carbon correlation spectroscopy provides information about coupling between protons and heteronuclei. In this case, between carbon nuclei or other heteroatoms and their directly

attached protons. In the spectrum, only cross peaks are observed which correlate a carbon with its attached protons.

In the proton-carbon correlation NMR spectrum, the vertical line on the right hand side should be ignored and only dots on the diagonal taken into account. The ^{13}C NMR spectrum is shown on the vertical axis and the ^{1}H NMR spectrum on the horizontal axis. Both spectra should to a large extent agree i.e. the protons on a molecule in the ^{1}H NMR spectrum should correlate with the attached carbon in the ^{13}C NMR spectrum, although sometimes this is not the case and a proton can be seen on a different place than is expected from the corresponding ^{13}C spectrum. A good example of this is seen in the ^{1}H spectra for NHS-HYBA-Boc and NHS-HYNIC-Boc where the Boc group protons come before the succinimidyl protons, which is in direct contrast with the ^{13}C spectrum where the succinimidyl carbons atoms attached to those protons give a peak before the Boc group.

From the results for the proton-carbon correlation NMR spectroscopy, the Boc group comes first in both the ^{13}C spectrum and the ^{1}H spectrum. It is possible to see that carbon atoms in positions 21 agree, whereas 22 and 20 are swapped around in the ^{13}C spectrum as opposed to the 1H spectrum. Atoms in positions 23, 1, 19, and 14 agree. The aromatic positions 31 and 33 agree and are the first aromatic protons / carbon atoms. The fluorenyl protons and carbon atoms are different as in the ^{1}H NMR spectrum, 11 and 7 come first followed by 8 and 12, 6 and 10 then 9 and 13. In the ^{13}C NMR spectrum, 9 and 13 come first followed by 6 and 10, 7 and 11, then 8 and 12. In both the ^{1}H NMR spectrum and the ^{13}C NMR spectrum, 30 and 34 are the last aromatic protons and carbon atoms. This data supports the data given and discussed above for the 1D ^{1}H NMR and ^{13}C NMR analysis.

From the DEPT spectra, all methyl, methylene, methine and quaternary carbons have been identified. (See discussion of DEPT NMR spectra). Carbon 21 comes before the carbons in the Boc group; this is different to the ^{1}H spectrum. The carbons in positions 20 and 22 are swapped in the ^{13}C spectrum when compared to the ^{1}H spectrum. The carbons in positions 23, 1, 19 and 14 are in the same order as in the ^{1}H spectrum. The carbon at position 40 is a quaternary carbon and at 81 ppm it comes where expected with regards to the ^{13}C spectra of Boc-HYBA and NHS-HYBA-Boc (79 ppm and 80 ppm respectively). The fluorenyl carbons 7 and 11, 8 and 12, 6 and 10 and 9 and 13 come in a completely different order than was seen in the ^{1}H spectrum for example 9 and 13 are seen first in the ^{13}C spectrum and last in the ^{1}H

spectrum. This contrasts with the ^{1}H and ^{13}C spectrum for Fmoc-Lys-HYNIC-Boc where the order of the fluorenyl CH groups were the same in both spectra. C-29 is a quaternary carbon, giving rise to a smaller peak than for those carbons with hydrogens attached. It comes at 125.5 ppm, which is similar to Boc-HYBA where the same carbon comes at 120 ppm. The carbon atoms in positions 30 and 34 (at 130 ppm) compare well to those found in the HYBA-Boc (132 ppm) and NHS-HYBA-Boc ^{13}C spectra (133 ppm). Carbon atom 32 is at 154 ppm and can be compared with the Boc-HYBA ^{13}C spectrum where it was at 154 ppm and the NHS-HYBA-Boc ^{13}C spectrum where it was found at 156 ppm. This is different from the ^{13}C spectrum for NHS-HYNIC-Boc where, as discussed, some of the carbon atoms had swapped positions in comparison to the Boc-HYNIC. It is difficult to distinguish between the carbons in positions 2 and 5 compared to those in 3 and 4. 2 and 5 are in an identical chemical environment and so give rise to one peak as do those in positions 3 and 4 for the same reasons. The difference between them is 3.2 ppm, a very small distance. The C=O carbons come last as they are all next to electronegative oxygen atoms. C-27 is an acid proton which is found at the highest chemical shift of 175.2 ppm. Both the 2D COSY NMR and Proton-Carbon correlation NMR and DEPT NMR data helped in the assignment of the ^{1}H and ^{13}C spectra, for discussion of 2D COSY NMR, Proton-Carbon correlation and DPET NMR data, see below.

The IR spectrum showed the functional groups, an N-H stretch at 3291 cm^{-1}, a C-H stretch at 2989 cm^{-1}, an aromatic –C=C stretch at 1920 cm^{-1}, a carbonyl for an ester stretch 1697 cm^{-1}, for a ketone at 1630 and for an amide at 1607 cm^{-1}. At 1503 cm^{-1} an N-H secondary amine bend was present and C-O stretches of an ester at 1241, 1154 and 1057 cm^{-1}. The mass spectrum showed the molecular ion $[M + H]^{+}$ 603.28 and the exact mass of the compound is 602.27. The HPLC analysis showed a single peak only (100% purity), eluting at 15.9 minutes.

The HPLC results show a trend for the HYNIC compounds eluting earlier than the equivalent HYBA compounds. This is illustrated in the table below:

HYNIC	RT	HYBA	RT
Boc-HYNIC	9.8	Boc-HYBA	12.5
NHS-HYNIC-Boc	12.4	NHS-HYBA-Boc	13.9
Fmoc-Lys-HYNIC-Boc	14.1	Fmoc-Lys-HYBA-Boc	15.9

Table 3.1 Differences in retention times for HYNIC and HYBA compounds

The difference between the HYNIC and HYBA molecules synthesised is the nitrogen in the pyridine ring of the HYNIC compared to the benzene ring of the HYBA. Therefore, it follows that the difference in retention time between equivalent HYNIC and HYBA compounds is due to this nitrogen atom. The nitrogen is possibly becoming protonated, increasing its hydrophilicity and so decreasing the retention time. More hydrophilic compounds elute sooner on a reversed phase HPLC system. This is because the mobile phase is polar and the stationary phase (column) is non-polar. Hydrophilic molecules are retained on the column for a shorter period of time. The effect of this is greatest in Boc-HYNIC compared to Boc-HYBA.

The elemental analysis carried out on the Fmoc-Lys-HYNIC-Boc showed that the percentage of nitrogen found was 0.6% away from that expected which is more than is acceptable for a pure product. However, the carbon and hydrogen found were very close to the expected percentages (carbon 0.3% difference between expected and found and hydrogen no difference between expected and found). For Fmoc-Lys-HYBA-Boc the carbon was exactly as predicted and the hydrogen 0.1% away from what was expected. The nitrogen was 0.7% from what was expected. It should be noted that the difference between the duplicates results for the elemental analysis for Fmoc-Lys-HYBA-Boc was more than 1% and this brings into question the accuracy and therefore relevance, of the analysis. Despite the nitrogen results from these analyses, there is proof of purity for both the compounds from the other analytical analyses carried out.

In the synthesis of succinimidyl 6-Boc-hydrazinopyridine-3-carboxylic acid, water soluble carbodiimide (WSC) was used instead of dicyclohexylcarbodiimide (DCC). DCC produces an

insoluble urea that precipitates from the organic reaction solvent and is equally insoluble in water. Several filtrations are often necessary to remove the DCC. Water soluble carbodiimide is soluble in DMF as DMF is a polar solvent. Using WSC, the urea by-product is formed during the reaction is completely soluble in the aqueous layer of the work-up and so is easy to remove. DMF was used instead of the DMSO used by Greenland (2002) as a solvent in the reactions to produce both Fmoc-Lys-HYNIC-Boc and Fmoc-Lys-HYBA-Boc as DMF is easier to remove due to its lower boiling point than DMSO, but is otherwise a similar solvent as it is also polar and aprotic. DMF is still difficult to remove completely and that is why the organic layers in the liquid extractions were washed so many times; the DMF is washed into the aqueous layer.

(For scheme to show active ester formation using DCC and WSC.HCl, see introduction to chapter 2)

Hydrazinonicotinic acid (HYNIC) is an established bifunctional chelating agent for ^{99m}Tc (King et al. 2007). HYNIC acts as a prosthetic group while bound to a peptide to provide a site specific location for radiolabelling with another molecule, such as an aromatic aldehyde which will react chemoselectively with the hydrazine group on the HYNIC to form a hydrazone bond.

HYBA was chosen to work with as well as HYNIC as they both have the hydrazine group which reacts selectively and rapidly with aldehydes. HYBA has a benzene ring whereas HYNIC has a pyridine ring, otherwise the molecules are identical. Both HYBA and HYNIC were used to give a direct comparison between both molecules. HYBA is much less expensive than HYNIC and so would provide a good alternative for labelling with ^{18}F and other radionuclides with ^{99m}Tc being an exception as in a study carried out by King et al. (2007), HYNIC conjugates formed fewer and more stable labelled species than the corresponding HYBA species. HYNIC has been well studied due to its extensive use as a bifunctional chelating agent with ^{99m}Tc, it has also been used as a bifunctional complexing agent in studies using ^{18}F. However for labelling of peptides with other radionuclides than ^{99m}Tc using HYBA would be an advantage, as already stated, due to cost (for example, 5 g of HYBA costs £9.70 from Acros Organics, whereas 100 mg of HYNIC costs $100 from Solulink) and the possibility of HYBA hydrazones being more stable than HYNIC hydrazones.

Boc-HYNIC and Boc-HYBA were synthesised to be incorporated (separately) into the peptide nanogastrin in place of the lysine residue and also as part of the synthesis of Fmoc-Lys-HYNIC-Boc and Fmoc-Lys-HYBA-Boc, which were also incorporated (separately) into nanogastrin in place of the lysine residue. This gave four peptides based on nanogastrin. The aim was to compare all the peptides synthesised to see which was the best peptide for labelling. The peptides with the lysine residue have an extra $-NH_2$ group compared to the peptides with Boc-HYNIC or Boc-HYBA. This was to further test the selectivity of the aldehyde for the hydrazine group on the HYNIC or HYBA. Fmoc-Lys-HYBA-Boc is a novel compound and so has been fully purified and characterised. King et al. (2007) synthesised a nanogastrin peptide with HYBA attached to the lysine side chain, however nanogastrin was first synthesised and then linked with HYBA, not built into the peptide during solid phase synthesis as it is in this case. Fmoc-Lys-HYNIC-Boc is not a new compound and so was not characterised and purified to the same extent. However the analytical data was checked against the literature to make sure the correct product had been synthesised and the ^{13}C and ^{1}H spectra, including the DEPT NMRs were clean. The HPLC analysis showed one peak. This is a good indication of the product being pure.

The DEPT NMR spectra are presented in the discussion section as it was judged that having the spectra visible would enhance the discussion of the data. From ^{13}C NMR analysis only, it is not possible to easily differentiate between methyl, methylene, methine or quaternary functionality. This is because ^{13}C spectra are broadband decoupled to remove proton couplings with the carbon atoms.

Therefore carrying out DEPT NMR analysis at the same time as ^{13}C NMR analysis helps to distinguish carbons with no hydrogen atoms, carbons with one hydrogen, carbons with two hydrogens and carbons with three hydrogens directly bonded.

In a DEPT 45 experiment, CH, CH_2 and CH_3 are all positive therefore from a comparison of the ^{13}C NMR spectrum and the DEPT 45, the carbons with no hydrogen atoms attached can be definitely identified.

From a comparison between the ^{13}C and the DEPT 45 spectra for Fmoc-Lys-HYBA-Boc, C-40 at 80.5 can be identified as a carbon with no hydrogen atoms attached. This helps to identify this carbon as the quaternary carbon of the BOC group. C-29 and C-32 are also quaternary carbons (ipso carbons). The DEPT NMR analysis cannot help to identify which is

which, however. The same can be said of C-2 and C-5 as well as C-3 and C-4, all of which are quaternary carbons that are therefore absent from the DEPT NMR spectra. C-16, C-38, C-25 and C-27 are all C=O carbons in either ester (C-16 and C-38), acid (C-27) or amide (C-25) functional groups.

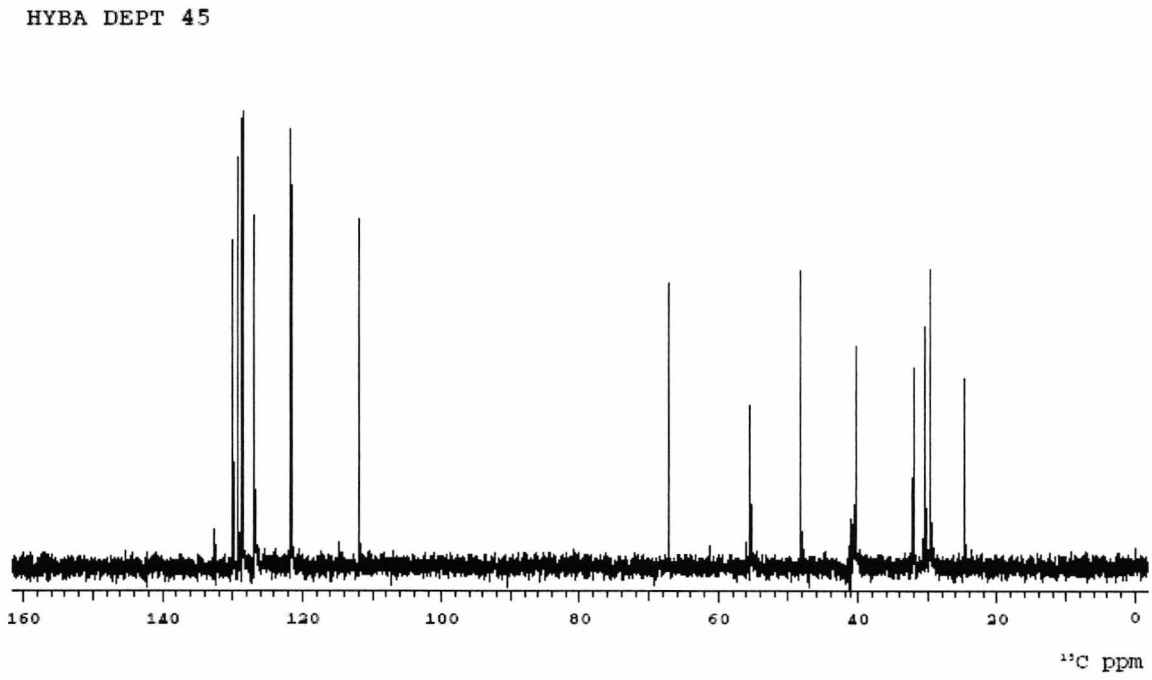

Figure 3.20

When the DEPT 135 (CH and CH_3 positive, CH_2 negative) is compared to the DEPT 45, this helps to distinguish the CH_2 carbons from the CH and CH_3 carbons. For Fmoc-Lys-HYBA-Boc, C-21, C-20, C-22, C-23 and C-14 are all CH_2 carbons according to the DEPT 135 NMR analysis.

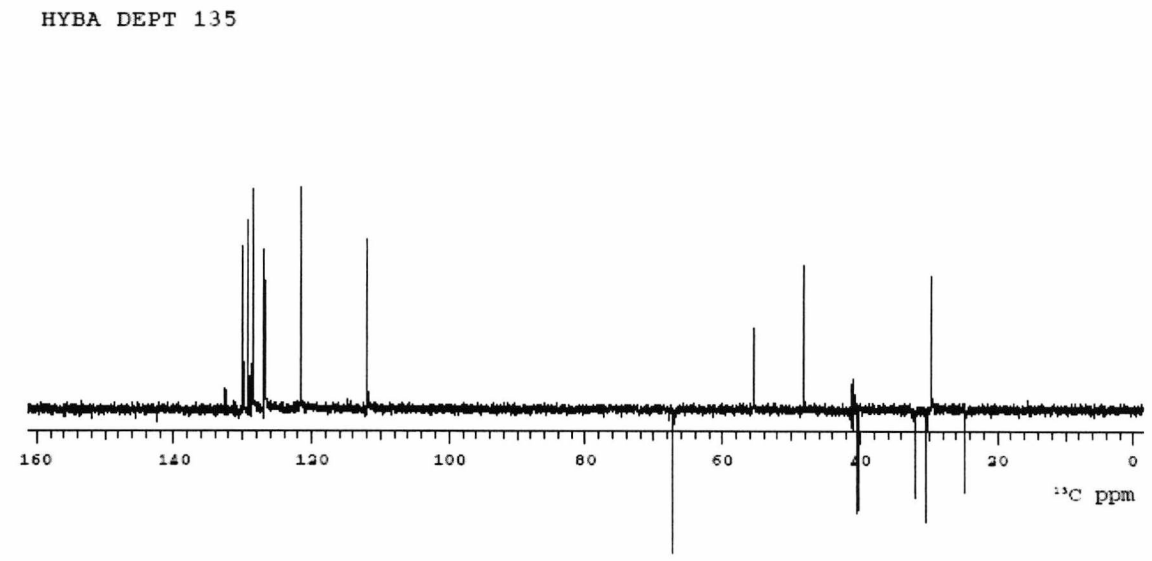

Figure 3.21

The DEPT 90 spectrum shows only CH carbons and therefore helps distinguish between CH and CH_3 carbons. When the DEPT 90 spectrum for Fmoc-Lys-HYBA-Boc is compared to the positive part of the DEPT 135 spectrum (CH and CH_3 only), only one peak is in the DEPT 135 spectrum is missing from the DEPT 90 spectrum and that is the CH_3 carbons at 24.5 (C-41, C-43 and C-44) that correspond to the Boc group.

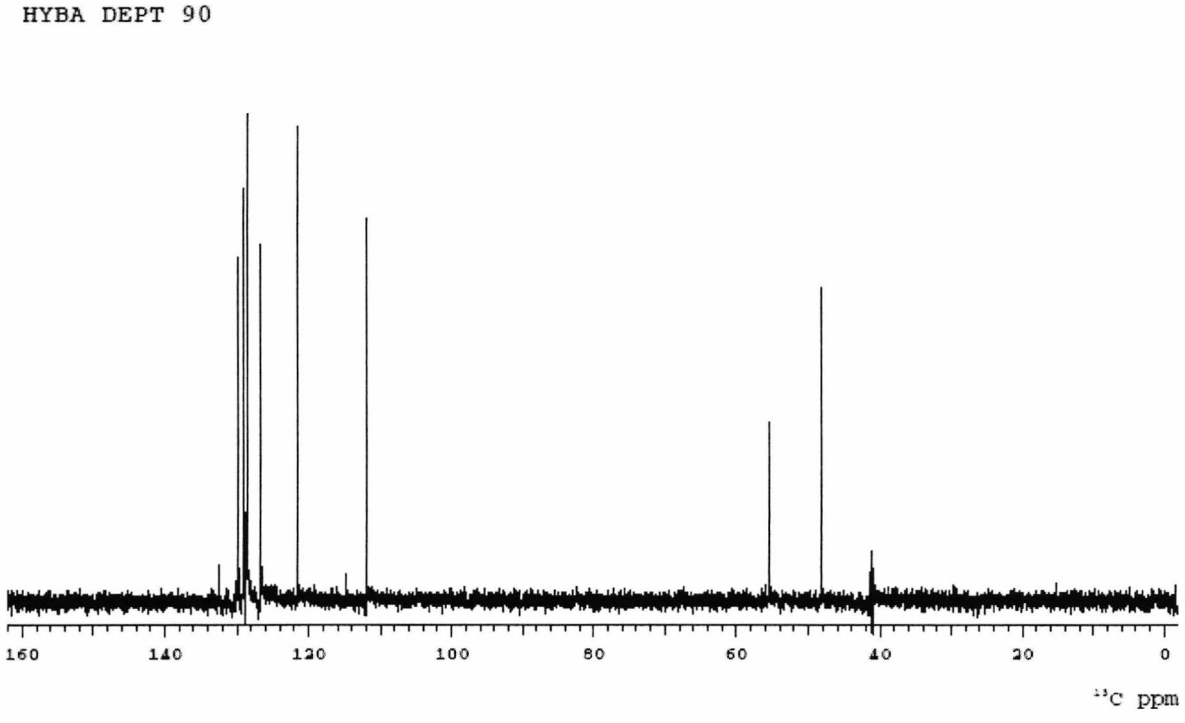

Figure 3.22

The DEPT NMR spectra for Fmoc-Lys-HYNIC-Boc can be analysed in the same way.

C-11 can be identified as a quaternary carbon, belonging to the boc group. C-2 and C-5 are also quaternary carbons (ipso carbons). C-33 and C-34 as well as C-32 and C-35 are quaternary carbons belonging to the fmoc group. C-13 and C-27 are an amide C=O carbon and an acid C=O carbon respectively. C-9 and C-25 are ester carbons.

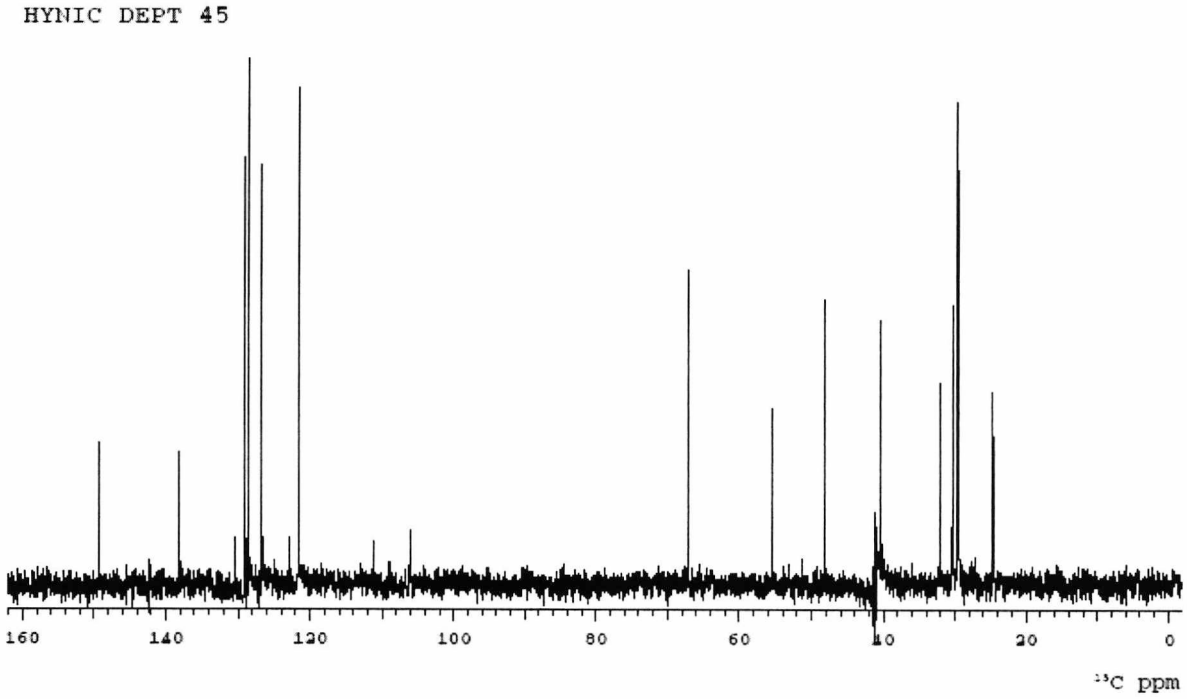

Figure 3.23

From the DEPT 135 NMR spectrum, C-21, C-22, C-20, C-19 and C-30 are all CH_2 carbons.

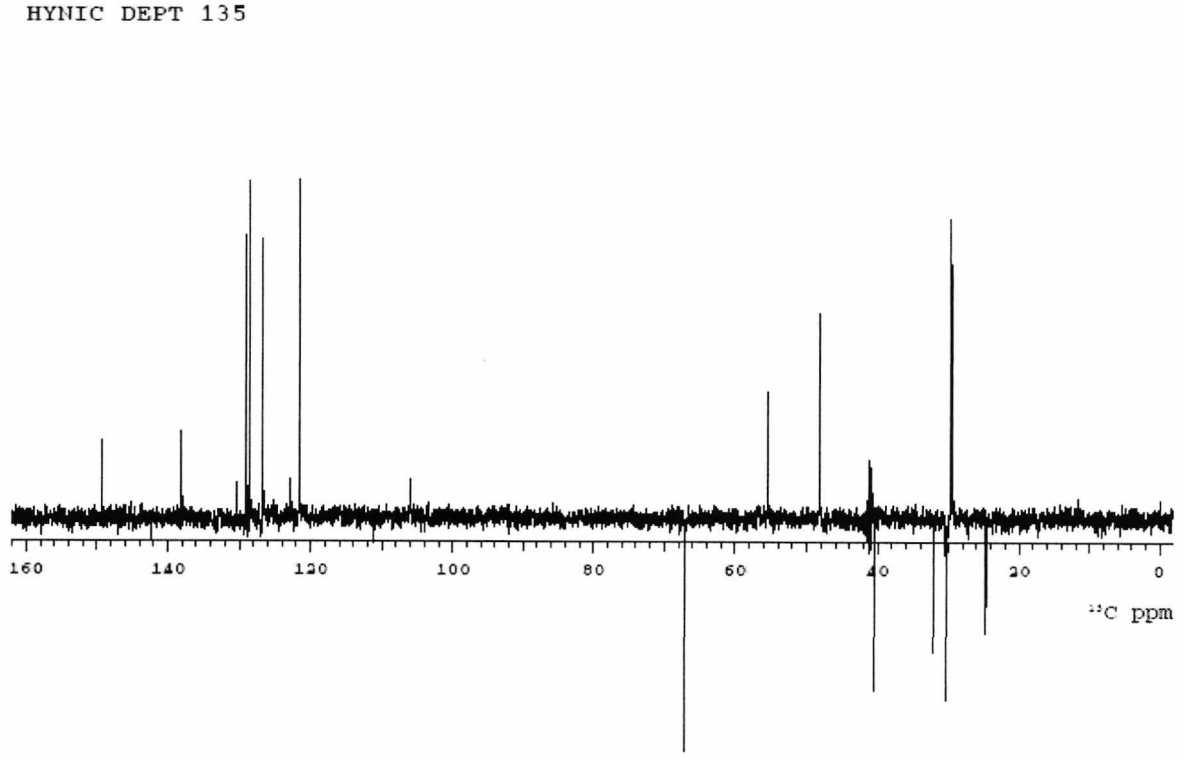

Figure 3.24

When a comparison is made of the positive aspect of the DEPT 135 spectrum (CH and CH_3) with the DEPT 90 spectrum (CH only), the only peak that is carbons in CH_3 groups is the Boc group at 24.5. Again, this can then be definitely identified as the Boc group.

188

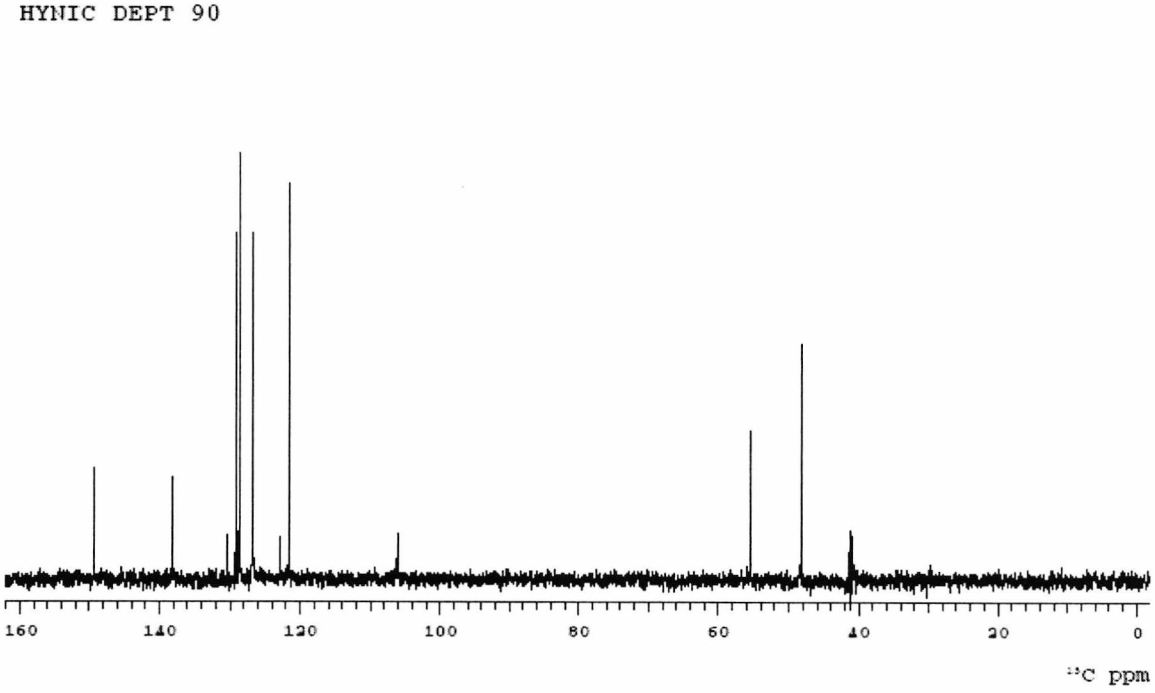

Figure 3.25

3.5 Conclusion

Fmoc-Lys-HYBA-Boc and Fmoc-Lys-HYNIC-Boc were successfully synthesised and the Fmoc-Lys-HYBA-Boc, which is a new molecule, was fully characterised. Fmoc-Lys-HYNIC-Boc was characterised in a more comprehensive way than has been done previously. HYBA-Boc and HYNIC-Boc were also successfully synthesised. These four amino acid synthons were incorporated into peptides for radiolabelling (see chapter 4).

NHS-HYBA-Boc could be incorporated into proteins for chemoselective labelling.

References

Abrams MJ, Juweid M, tenKate CI, Swartz DA, Hauser MM, Gaul FE, Fucello AJ, Rubin RH, Strauss HW and Fischman AJ, (1990). Technetium-99-m-human polyclonal IgG radiolabeled via the hydrazine nicotinamide derivative for imaging focal sites of infection in rats. *Journal of Nuclear Medicine*, **31**, 2022-2028.

Babich JW, Soloman H, Pike MC, Kroon D, Graham W, Abrams MJ, Tompkins RG, Rubin RH, Fischman AJ (1993). Tc-99m-labelled hydrazine-nicotinamide derivatised chemotactic peptide analogues for imaging focal sites of bacterial infection. *Journal of Nuclear Medicine* **34**, 1964-1974.

Banerjee S, Pillai MRA, Ramamoorthy N (2001). Evolution of Tc-99m in diagnostic radiopharmaceuticals. *Seminars in Nuclear Medicine* **31**, 260-277.

Bangard M, Behe M, Bender H, Guhlke S, Risse J, Grunwald F, Maeke HR, Biersack H-J (1998) *European Journal of Nuclear Medicine* **23**, 837

Bruus-Jensen K, Poethko T, Schottelius M, Hauser A, Schwaiger M, Wester H-J (2006). Chemoselective hydrazone formation between HYNIC-functionalised peptides and 18F-fluorinated aldehydes. *Nuclear Medicine and Biology* **33**, 173-183.

Chang YS, Jeong JM, Lee YS, Kim HW, Rai GB, Lee SJ, Lee DS, Chung JK, Lee MC (2005). Pre*para*tion of ^{18}F-human serum albumin: a simple and efficient protein labelling method with ^{18}F using a hydrazone-formation method. *Bioconjugate Chemistry* **16**, 1329-1333.

Fichna J and Janecka A (2003). Synthesis of target-specific radiolabelled peptides for diagnostic imaging. *Bioconjugate Chemistry* **14**, 3-17.

Greenland WEP, Howland K, Hardy J, Fogelman I, Blower PJ (2003). Solid-phase synthesis of peptide radiopharmaceuticals using Fmoc-N-ε-(HYNIC-Boc)-lysine, a technetium-binding amino acid: Application to Tc-99m labelled salmon calcitonin. *Journal of Medicinal.Chemistry* **46**, 1751-1757.

Greenland WEP (2002). Radionuclide conjugates of calcitonin for imaging of bone disease and cancer. PhD thesis, University of Kent.

King RC, Surfraz MB-U, Biagini SCG, Blower PJ, Mather SJ (2007). How do HYNIC-conjugated peptides bind technetium? Insights from LC-MS and stability studies. *Dalton Transactions* 4998-5007.

Lee Y-S, Jeong JM, Kim HW, Chang YS, Kim YJ, Hong MK, Rai GB, Chi DY, Kang WJ, Kang HK, Lee DS, Chung J-K, Lee MC, Suh Y-G (2006). An improved method of 18F peptide labelling: hydrazone formation with HYNIC-conjugated c(RGDyK). *Nuclear Medicine and Biology* **33**, 677-683.

Rennen HJJ, Laverman P, van Eerd EM, Oyen WJG, Corstens FHM, Boerman OC (2007). PET imaging of infection with a HYNIC-conjugated LTB4 anatagonist labelled with F-18 via hydrazone formation. *Nuclear Medicine and Biology* **34**, 691-695.

Shao J, Tam JP (1995). Unprotected peptides as building blocks for the synthesis of peptide dendrimers with oxime, hydrazone and thiazolidine linkages. *Journal of the American Chemical Society* **117**, 3893-3898.

Surfraz M B-U, King R, Mather SJ, Biagini SCG, Blower PJ (2007). Trifluoroacetyl-HYNIC peptides: Synthesis and ^{99m}Tc radiolabelling. *Journal of Medicinal Chemistry* **50**, 1418-1422.

Chapter 4

Synthesis of peptides for radiolabelling

4.0 Introduction

4.1 Solid phase peptide synthesis; background

Solid phase synthesis is a process by which chemical transformations can be carried out on a solid support in order to prepare a wide range of synthetic compounds. The idea was developed by Robert Bruce Merrifield (Merrifield 1963) to synthesise polypeptides and earned him the Nobel Prize in 1984. Solid phase peptide synthesis is now the widely accepted methodology for peptide synthesis. Solid phase chemistry offers many advantages over conventional synthesis in terms of efficiency as well as convenient work-up and purification procedures. Solid phase peptide synthesis (SPPS) allows the incorporation of unnatural amino acids and the synthesis of D-amino acids which can be incorporated into peptides and proteins. SPPS also enables post translational modifications to be carried out. SPPS allows the synthesis of up to 120 amino acid residues which in turn, allows most polypeptide hormones to be synthesised via this route. Other methods of peptide or protein synthesis such as genetic engineering only allow for the twenty amino acids defined by the genetic code to be incorporated. Genetic engineering is the preferred method for the synthesis of larger polypeptides (Barrett and Elmore 1998).

During SPPS, α-amino and side-chain protected amino acid residues are added sequentially to an insoluble polymeric support thereby allowing the peptide to be synthesised by coupling the carboxyl group (*C*-terminus) of one of the amino acids to the amino group (*N*-terminus) of another. Chemical peptide synthesis usually starts at the *C*-terminus of a peptide which contrasts with protein biosynthesis *in vivo*, which starts at the *N*-terminus. Protecting groups are required for SPPS; temporary protection for the *N*-α amino group and permanent protection for the *N*-ε amino and carboxyl groups. Protecting groups are necessary to stop unintended side reactions occurring. Therefore, the general principle of SPPS is one of

coupling and deprotection; the free *N*-terminal amine of a solid phase attached peptide is coupled to the carboxylic acid group of an incoming *N*-protected amino acid. The amino acid is deprotected and a new *N*-terminal amine is revealed.

Since its conception in 1963, SPPS methodology has been improved with the introduction of Fmoc chemistry (Atherton et al. 1978, Chang and Meinhofer 1978). The Fmoc (9-fluorenylmethoxycarbonyl) group is stable to acids and is removed using a secondary base e.g. piperidine (30% piperidine in DMF). Piperidine removes the proton as shown below to produce the highly reactive dibenzofulvene which reacts with piperidine to form a stable adduct. The Fmoc group has UV absorbing properties (300-320 nm) allowing deprotection to be followed spectrophotometrically (Barrett and Elmore 1998).

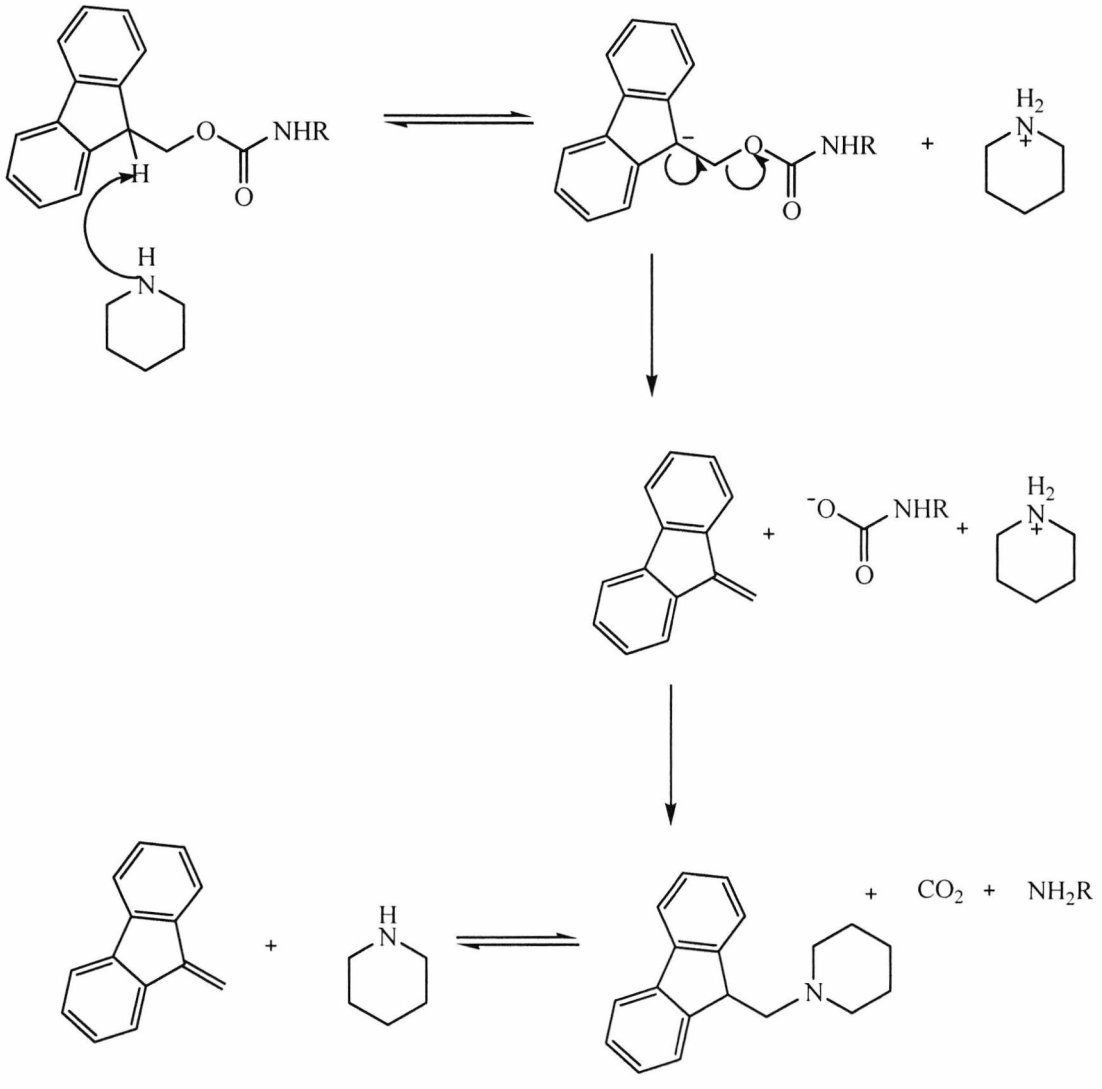

Scheme 4.0 Removal of the Fmoc group using piperidine

Due to amino acid excesses used to ensure complete coupling during each synthesis step, incoming amino acids require protection of their amino group in order to obtain coupling to a free amino acid attached to the resin, this is achieved using the Fmoc group. The Fmoc strategy's main advantage is that it eliminates the need for strong acids such as trifluoroacetic acid (TFA) for deprotection and hydrofluoric acid (HF) for removal from the resin, providing a much milder approach to deprotection (removal of the Fmoc group under mild basic conditions) that it is easily automated. The repeated exposure of resin-bound peptides to TFA may result in premature cleavage of the permanent protecting groups and detachment from the resin leading to peptide impurities and reduced yields (Atherton et al. 1978). The stronger acids are also hazardous to use, especially HF. The milder conditions allow the use of acid labile protecting groups that are stable under basic conditions, such as benzyl and Boc (butoxycarbonyl) groups. The amino acid side chain benzyl protection groups and the t-Boc protection are removed by TFA, deionised water and triisopropylsilane (TIS; a carbocation scavenger). Therefore the deprotection steps rely on two different mechanisms.

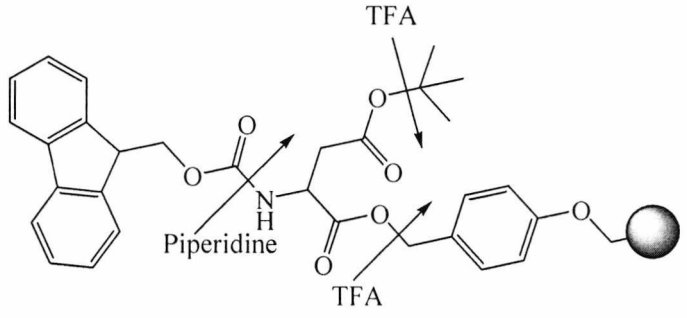

Figure 4.0 Protection strategy in Fmoc SPPS. The arrows represent cleavage sites.

4.2 Solid phase peptide synthesis; the process

SPPS is generally performed in the C→N direction. First, a resin is selected and a linker is attached. The resin must be insoluble, yet porous and has functional units attached called 'linkers'. It is onto the linker that the peptide chain is built. This linker acts as protection for the *C*-terminal α-carboxyl group of the peptide during the elongation process. The peptide remains covalently bound to the linker until cleaved at the end of the process. This allows

reagents and by-products of synthesis to be washed away. Once the linker is attached, the first amino acid, protected at the *N*-terminal and activated at the *C*-terminal, is coupled to the linker. The temporary amino protecting group is removed and a second protected and activated amino acid attached. Activation speeds up the rate of reaction; to enhance the electrophilicity of the carboxyl group, the negatively charged oxygen must first be activated into a better leaving group. The carboxyl group of an amino acid e.g. Fmoc-Phe-OH, is activated using (e.g. Fmoc-Phe-OH:) HBTU:HOBt:DIEA, 1:1:1:2 where DIEA (diisopropyl ethylamine) is a proton scavenger. The active ester is introduced as a uronium (in this instance) salt of a non-nucleophilic anion e.g. HBTU. Addition of HOBt can prevent racemisation and dehydration of asparagine and glutamine side chains.

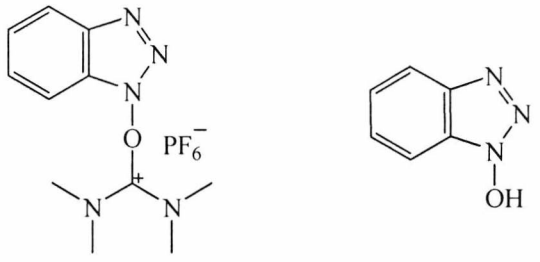

Figure 4.1 Structures of HBTU (left) and HOBt (right)

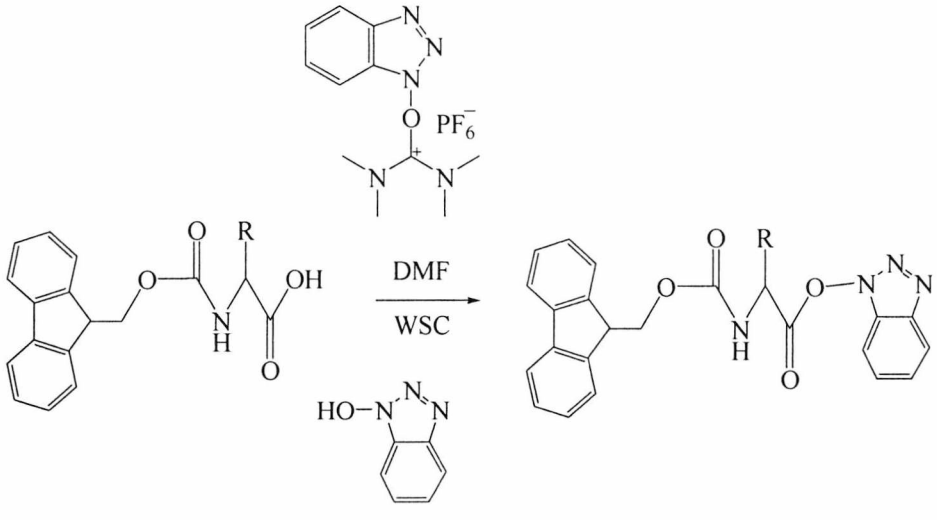

Scheme 4.1 Formation of the HBTU / HOBt active ester

These steps are repeated until the desired peptide chain is obtained. Once the peptide is complete, it is removed from the solid support with simultaneous removal of the side chain protecting groups using a cocktail of reagents, usually in the presence of carbocation scavengers, such as TIS and H_2O. Carbocation scavengers are electron donating nucleophilic reagents which stabilise the carbocations, preventing them re-attaching to the peptide to form impurities. The solid support (resin) must be completely insoluble in any of the solvents and must be physically and chemically stable. The linker on the resin is permanently attached and must be easily cleavable from the peptide at the end of the synthesis. Depending on the linker used, a variety of *C*-termini can be obtained e.g. acids, amides, hydrazides and alcohols. For this work, NovaSyn® TGR (Novabiochem) resin was used. This has a primary amine which leaves a peptide amide on final TFA cleavage. A peptide amide, when compared to a peptide acid, is less prone to action *in vivo* by carboxypeptidases thereby giving the peptide amide a longer half-life than a peptide acid. Purification of the peptide is achieved by washing away excess reagents with DMF while it is still attached to the resin. This simple purification is the major advantage of SPPS. Once the peptide is fully assembled, it must cleaved from the resin. The side chain protection must also be removed which is accomplished at the same time as cleaving the peptide from the solid support using TFA. This step results in the formation of reactive carbocations which must be scavenged. The peptide is isolated by either precipitation from TFA or precipitation after evaporation of TFA and volatile scavengers. The peptide is extracted into water, lyophilised and stored at -20°C. It is then analysed by LC-MS. (Sutcliffe-Goulden 2000, Greenland 2002)

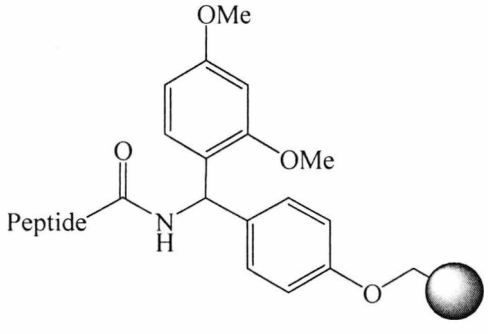

Figure 4.2 NovaSyn® TGR resin

4.3 Gastrin and CCK-2 receptor

The success achieved in targeting somatostatin receptor expressing tumours has led to interest in targeting other receptors that are over-expressed in various tumour types. (King et al. 2007). There has been much recent interest in imaging tumours that express cholecystokinin type 2 (CCK-2) receptors. (Nock et al. 2005, Reubi 2003, Behe and Behr 2002, Smith et al. 2004, Biagini et al. 1997, McWilliams et al. 1998, Mather et al. 2007). The gastrointestinal peptides gastrin and CCK exist in different molecular forms. Gastrin is present in the bloodstream in three different forms; 'big gastrin' is a thirty four residue native peptide and 'little gastrin' is a 17 residue native peptide while 'minigastrin' is a fourteen residue native peptide. CCK is also a thirty four amino acid peptide which exists in several bioactive forms (Mather et al. 2007). CCK-1 is cholecystokinin A receptor, a human protein that binds non-sulfated members of the cholecystokinin family of peptide hormones. The receptor is a major physiological mediator of pancreatic enzyme secretion and smooth muscle contraction in the gall bladder and stomach. In the central nervous system (CNS) and peripheral nervous system (PNS), this receptor regulates satiety and the release of β-endorphin and dopamine (Entrez Gene a). CCK-2 is cholecystokinin B receptor, a human protein receptor for CCK and gastrin which are regulatory peptides of the brain and gastrointestinal (GI) tract. The receptor has a high affinity for both sulfated and non-sulfated CCK analogues and is found mainly in the CNS and GI tract (Entrez Gene b). Gastrin and CCK, as biologically active peptides have the same five amino acids at their carboxyl terminus. They act as neurotransmitters in the brain, as regulators of various functions of the gastrointestinal tract, mainly concerning the stomach, pancreas and gallbladder (Walsh 1994). They act as growth factors in most parts of the gastrointestinal tract (Hakanson and Sundler 1991, Johnson 1989) and also as growth factors in several neoplasms, such as those discussed below. CCK-2 receptors are present in the greatest concentration in the gut mucosa, pancreas and the brain (Mantyh et al. 1994, Saillan-Barreau et al. 1999, Reubi et al. 1997b).

The gastrin/CCK-2 receptor has increased levels of expression in several tumour types, including medullary thyroid cancer (MTC) (Reubi and Waser 1996), neuroendocrine tumours (Reubi and Waser 2003) astrocytomas, stromal ovarian tumours, gastroenteropancreatic neuroendocrine tumours and in extrememly high densities in gastrointestinal stromal tissues and small cell lung cancer (Reubi et al. 1997, Reubi and Waser 2003). However, the role of gastrin, CCK and their receptors (CCK-2/gastrin-R or CCK-1-R) in gastric and colon cancer

is still disputed (Reubi et al. 1997, Upp et al. 1989, Imdahl et al. 1995). There has been interest, in light of the above, in development of radiolabelled gastrin/CCK analogues for targeted diagnostic imaging and therapy of CCK-2/gastrin expressing tumours (Nock et al. 2005). Radiolabelled analogues of the CCK-2 receptor ligands, gastrin and CCK, have shown promise in the detection of CCK-2 receptor-positive tissue in humans (Behe and Behr 2002) for example, [DTPA-D-Glu]-minigastrin radiolabelled with ^{111}In for detection and ^{90}Y for the therapeutic purposes have been evaluated clinically in MTC (Behe et al. 2003).

'Nanogastrin' is a synthetic truncated form of gastrin comprising the *C*-terminal domain with the sequence NH_2-Lys-Glu-Ala-Tyr-Gly-Trp-Met-Asp-Phe$CONH_2$.

A ^{99m}Tc-labelled nanogastrin analogue incorporating a HYNIC moiety at the *N*-terminus has been shown to have good receptor binding affinity and serum stability and is a good candidate for *in vivo* evaluation as an imaging agent (von Guggenberg et al 2004). For this reason, nanogastrin was chosen for this project.

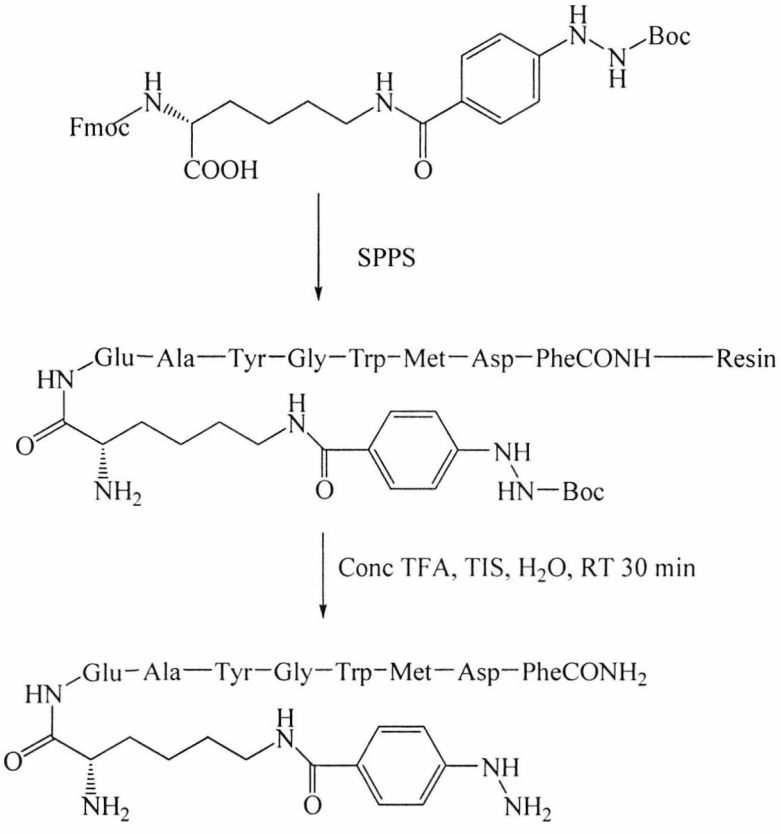

Scheme 4.2 HYBA nanogastrin synthesis using conventional solid phase Fmoc chemistry (Surfraz et al. 2007).

4.4 Aims and objectives

The aim of the work carried out in this chapter was to synthesise the peptides to be radiolabelled with ^{18}F. Nanogastrin was chosen as the peptide and so all the peptides synthesised were based on 'nanogastrin'; these peptides were HYBA-nanogastrin (minus Lys) where HYBA replaced the lysine residue in the peptide, HYNIC-nanogastrin (minus Lys), where HYNIC replaced the lysine residue in nanogastrin and HYBA-nanogastrin and HYNIC-nanogastrin, where HYBA and HYNIC respectively were added to nanogastrin, in effect, after the last residue (lysine). The HYBA-nanogastrin (minus Lys) and the HYNIC-nanogastrin (minus Lys) have the hydrazine group that is selective for the aldehyde and so should form a hydrazone bond for chemoselective labelling. The HYBA-nanogastrin and HYNIC-nanogastrin have both the hydrazine group and a lysine side chain with an amine. It is expected that these two peptides should label as selectively as the HYBA- and HYNIC-nanogastrin (minus Lys) peptides should i.e. with formation of a hydrazone bond, but the selectivity was to be further tested by having the lysine side chain amine group present on the same peptide.

4.5 Materials and methods

All amino acids were purchased from Novabiochem, all solvents were purchased from Fisher. DIEA (*N,N*-diisopropyl ethylamine) and TIS (triisopropylsilane) were bought from Aldrich. HBTU (*O*-benzotriazole-*N,N,N',N'*-tetramethyl-uronium-hexafluoro-phosphate) and HOBt (*N*-hydroxybenzotriazole) were bought from AGCT bioproducts. Dimethylformamide (DMF) and trifluoroacetic acid (TFA) were purchased from Rathburn.

4.5.1 Peptide Synthesis

Solid-phase peptide synthesis (SPPS) of the nanogastrin peptides was performed using conventional Fmoc chemistry as detailed below:

The peptide synthesis was carried out by K. Howland using the procedure detailed below: The peptides (10 μmole) were synthesised on a Shimadzu PSSM-8 Multiple Peptide Synthesiser using the Fmoc strategy. Standard side chain protecting groups were utilised and the peptide assembled on TGR amide resin (NovaSyn® TGR resin) using HBTU (*O*-(benzotriazol-1-yl)-1,1,3,3-tetramethyluronium hexafluorophosphate) mediated coupling. The resin was suspended in DMF and mixed by bubbling N_2 through it. Briefly, the Fmoc group

was removed by two 5 minute treatments with 30% piperidine in DMF (*N,N*-dimethylformamide) followed by 5 washes with DMF. The amino acid (8 equiv) was dissolved in DMF, mixed with 0.5M HOBt(N-hydroxybenzotriazole)/0.5M HBTU in DMF (8 equiv) and 1.0M DIEA (diisopropyl ethylamine) in DMF (16 equiv) and added to the resin. The reaction was mixed by nitrogen bubbling for 60 minutes after which the resin was washed 5 times with DMF. This process was repeated until the required sequence was assembled. The final Fmoc group was removed, the resin washed with DMF followed by methanol and then vacuum dried for 1 hour.
The peptides were released from the resin and side chain deprotected by a 30 minute treatment with 95% TFA (trifluoroacetic acid), 2.5% H_2O, 2.5% TIS (triisopropylsilane). The peptide was isolated by precipitation in ice-cold diethyl ether. The peptides were pelleted by centrifugation and washed a further two times with ice-cold ether. Each was dissolved in water and recovered by freeze-drying.

4.5.2 Instrumentation

A micrOTOF-QII mass spectrometer was used for the analysis of the synthesised peptides. Samples were separated on-line by reverse-phase HPLC on a Vydac 218TP52 column (C18, 5 μm, 300Å, 2.1 mm x 250 mm) running on an Agilent 1100 HPLC system at a flow rate of 0.2 ml/min using a water, acetonitrile, 0.05% TFA gradient: mobile phase A, 0.05% TFA in water; mobile phase B, 70% acetonitrile, 0.045% TFA in water; 5% mobile phase B then a linear gradient 5 – 100% mobile phase B in 25 minutes. The eluant was monitored at 214 nm and then directed into the electrospray source at 4.5 kV and mass spectra recorded from 50-3000 m/z. Data were analysed with Bruker's Compass Data Analysis software.

Buffer A: H_2O, 0.05% Trifluoroacetic acid (v/v)
Buffer B: 70% Acetonitrile, 30% H_2O (v/v), 0.045% Trifluoroacetic acid (v/v)

Time	%A	%B
0 min	95	5
5 min	95	5
30 min	0	100
35 min	0	100
40 min	95	5
55 min	95	5

Table 4.0 HPLC gradient conditions for the peptide analysis

Data were collected at 214 nm and for the first 40 minutes only. The mass spectrometer was a Bruker micrOTOF-Q II high resolution instrument with a mass range of m/z 50-3000. Source type: ESI, ion polarity: positive.

4.5.3 Synthesis of Nanogastrin

NH_2-Lys-Glu-Ala-Tyr-Gly-Trp-Met-Asp-Phe$CONH_2$

m/z (ESI) Positive mode, molecular ion $[M + H]^+$:1145.49 approx 90% intensity, $[M + 2H]^{2+}$:573.25 approx 100% intensity

$C_{54}H_{72}N_{12}O_{14}S$, molecular weight: 1145.29, exact mass: 1144.50.

Measured mass of ion: 1145.49. ($[M + H]^+$)

Purity: 95% by HPLC by peak area percent.

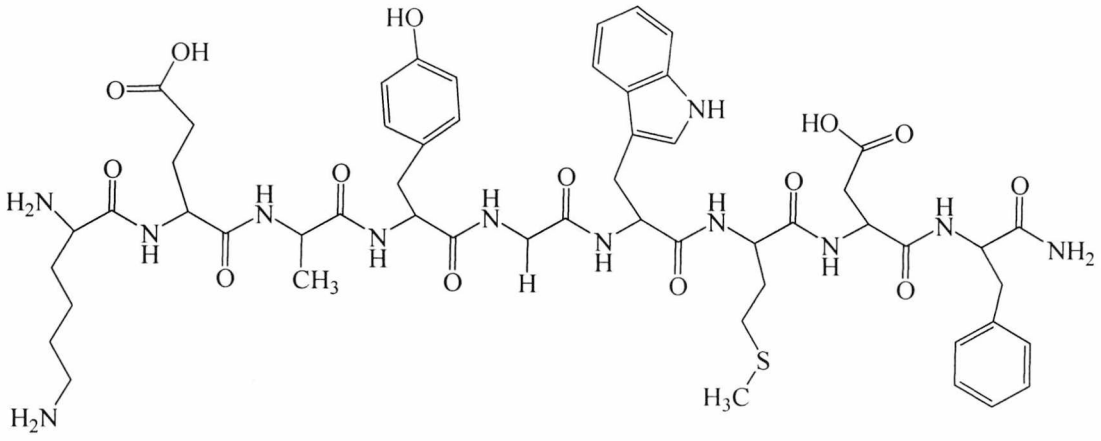

Figure 4.3 Structure of nanogastrin

4.5.4 Synthesis of HYBA-nanogastrin (minus Lys)

The following peptide was synthesised; HYBA-Glu-Ala-Tyr-Gly-Trp-Met-Asp-PheCONH$_2$. The lysine residue of nanogastrin was replaced by HYBA in this peptide. HYBA was introduced into the peptide in the same way the other amino acids were in the form of Boc-HYBA. The Boc group is removed at the same time as removal from the resin i.e. with the addition of TFA.

m/z (ESI) Positive mode, molecular ion $[M + H]^+$:1151.50 approx 90% intensity, $[M - HYBA + OH]^+$:1017.44 100% intensity, loss of 134.06 equivalent to HYBA molecule minus OH group (cleaves between R and NH on the HYBA nanogastrin structure below).

$C_{55}H_{66}N_{12}O_{14}S$, molecular weight: 1151.25, exact mass: 1150.45.

Measured mass of ion: 1151.50.

Purity: 80% by HPLC by peak area percent.

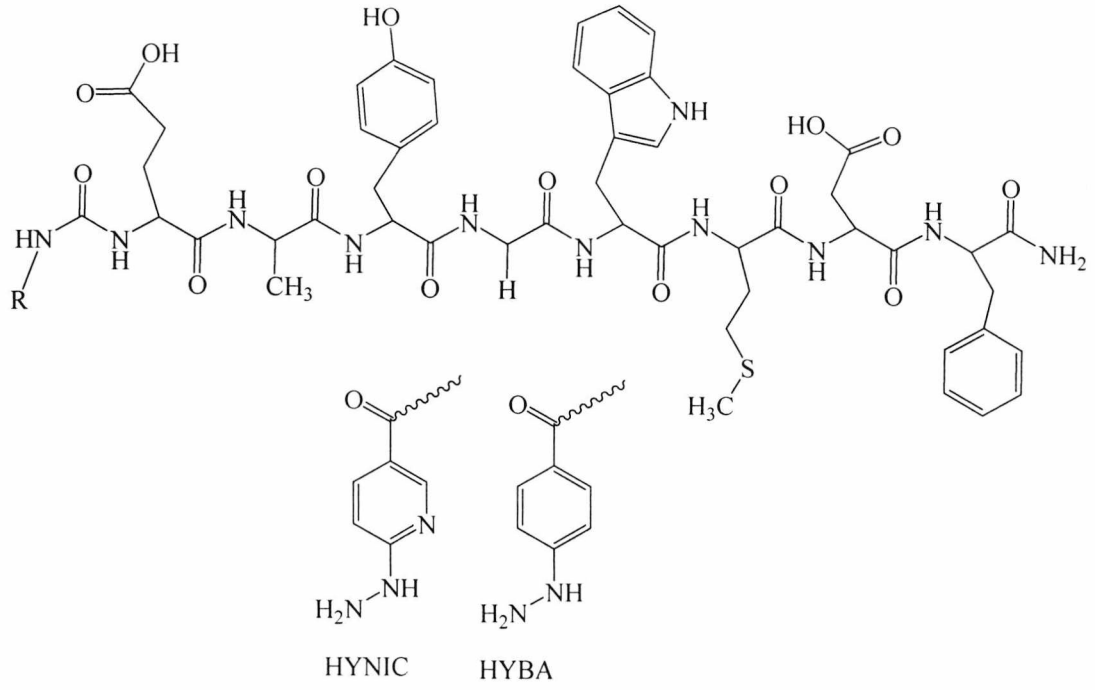

Figure 4.4 Structure of HYNIC-nanogastrin (minus Lys) and HYBA-nanogastrin (minus Lys).

4.5.5 Synthesis of HYNIC-nanogastrin (minus Lys)

The following peptide was synthesised. The peptide was based on the nanogastrin peptide, but with the lysine residue replaced by HYNIC; HYNIC-Glu-Ala-Tyr-Gly-Trp-Met-Asp-PheCONH$_2$. HYNIC was introduced into the peptide in the same way the other amino acids were, in the form of Boc-HYNIC. The Boc group is removed at the same time as removal from the resin i.e. with the addition of TFA.

m/z (ESI) Positive mode, molecular ion $[M + H]^+$:1152.47 100% intensity.

$C_{54}H_{65}N_{13}O_{14}S$, molecular weight: 1152.24, exact mass: 1151.45

Measured mass of ion: 1152.47.

Purity: 95% by HPLC by peak area percent.

4.5.6 Synthesis of HYBA-nanogastrin

The following peptide was synthesised; nanogastrin peptide with HYBA as an extra residue; HYBA-Lys-Glu-Ala-Tyr-Gly-Trp-Met-Asp-PheCONH$_2$.

m/z (ESI) Positive mode, molecular ion $[M + H]^+$:1279.53 approx 40% intensity, $[M + 2H]^{2+}$: 640.27 100% intensity.

$C_{61}H_{78}N_{14}O_{15}S$, molecular weight: 1279.42, exact mass: 1278.55.

Measured mass of ion: 1279.53.

Purity: 33% by HPLC by peak area percent.

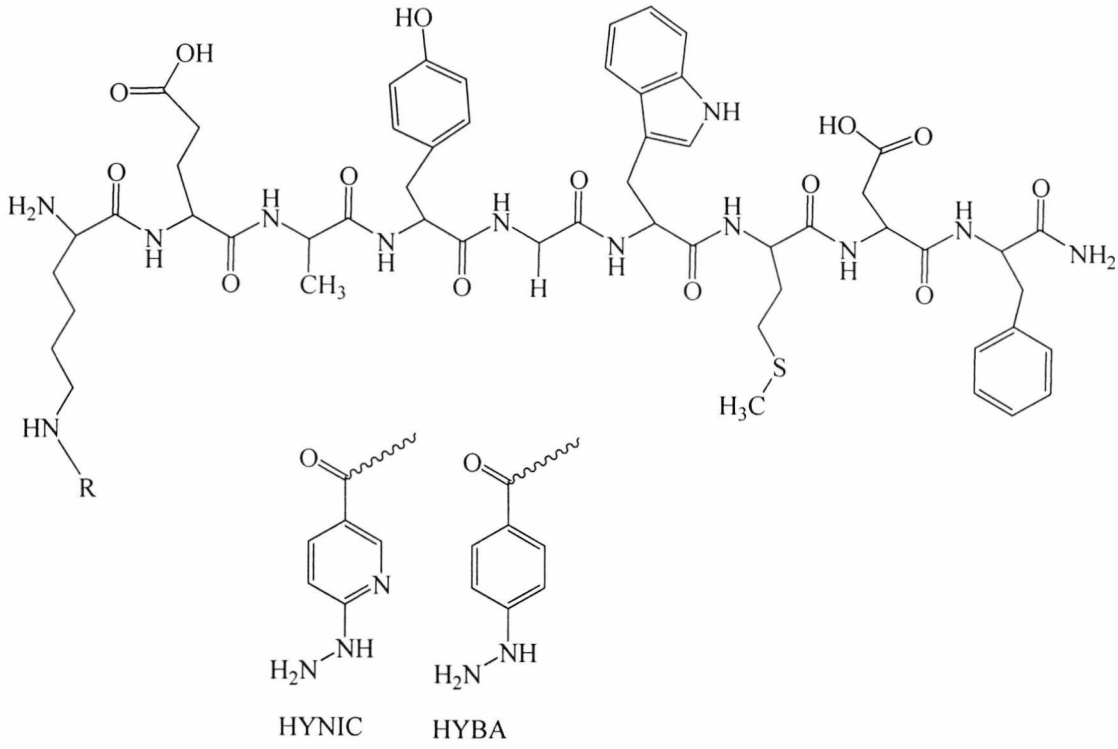

Figure 4.5 Structure of HYNIC-nanogastrin and HYBA-nanogastrin.

4.5.7 Synthesis of HYNIC-nanogastrin

The following peptide was synthesised; nanogastrin peptide with HYNIC as an extra residue; HYNIC-Lys-Glu-Ala-Tyr-Gly-Trp-Met-Asp-PheCONH$_2$.

m/z (ESI) Positive mode, molecular ion $[M + H]^+$:1280.53 approx 30% intensity, $[M + 2H]^{2+}$: 640.77 100% intensity.

$C_{60}H_{77}N_{15}O_{15}S$, molecular weight: 1280.41, exact mass: 1279.54.

Measured mass of ion: 1280.53.

Purity: 87% by HPLC by peak area percent.

4.6 Results and discussion

Peptide synthesis needs to be 99+ % efficient for addition of each individual amino acid to the growing peptide chain to give good yields and purity at the end of the process. The yield for each peptide synthesised is not calculated as when the peptides are freeze-dried, some TFA is still present as a salt. Water is also trapped in the peptides. Therefore unless the peptides are sent for amino acid analysis (which these were not), calculating the yield from the freeze-dried product is inaccurate. Due to this, yield is not very commonly given for peptides.

All peptides were successfully synthesised. The purity of the peptides was derived from the area percent of the chromatograms from the LC-MS analysis. The purity of the peptides varied between 80% for the HYBA-nanogastin (minus Lys) peptide to 95% for the nanogastrin peptide, with the exception of the HYBA-nanogastrin peptide which was 33% pure. The impurities present are likely to be closely related to the synthesised peptide, for example, a peptide missing an amino acid. From the purity results, it appears that adding HYBA to the peptides is not as efficient a process as adding HYNIC (especially for HYBA-nanogastrin compared to HYNIC-nanogastrin), the mechanism for this is not clear. It can be seen that the HYBA molecule can detach from the peptide as is seen with HYBA-nanogastrin (minus Lys), although this did not occur with the HYBA-nanogastrin peptide.

It has been found that when labelling with ^{99m}Tc, the labelling efficiency of HYBA is much lower than that of HYNIC with tricine and trisodium triphenylphosphine-3,3',3"-trisulfonate (TPPTS) as coligands (Kim et al. 2006), and in another study by King et al. (2007) that for each co-ligand system, HYNIC conjugates formed fewer and more stable labelled species than the corresponding HYBA conjugates. In this study LC-MS analysis found that all HYNIC and HYBA conjugates contained one hydrazine moiety bound to ^{99m}Tc but that the HYNIC conjugate contained fewer co-ordinating co-ligand molecules than the HYBA conjugate indicating HYNIC is more able to satisfy the oxidation requirement of ^{99m}Tc.

In comparison with work carried out by King et al. (2007), the HYBA-nanogastrin peptide did not show an ion at 2 mass units below the mass expected; there was no oxidation of the hydrazine group to give a postulated diazene during ionisation in the mass spectrometer.

It has been shown that removal of HYNIC-Boc derivatised peptides from the SPPS resin, conventionally accomplished with TFA, can give rise to trifluoroacetyl-HYNIC as well as the

free HYNIC compound (Greenland et al. 2003). Formation of trifluoroacetyl-HYNIC can be kept to a minimum by keeping the incubation time in TFA as short as possible (Surfraz et al. 2007). This effect was not seen here as no ions corresponding to HYNIC trifluoroacetylation were seen in the mass spectra of the peptides synthesised for this project.

Nanogastrin, HYBA-nanogastrin and HYNIC-nanogastrin all gave ions with a +2 charge. Ions with a +2 charge require a smaller magnetic field to deflect them towards the detector as they are deflected twice as much as singly charged ions of the same mass and therefore show up on the mass spectrum at half the m/z value. The LC-MS instrument used for analysis of the peptides is very efficient at ionisation and therefore often gives the 2+ ion as well as the singly charged ion, as can be seen with the peptides synthesised for this project.

The purity of the peptides will not affect the next step i.e. radiolabelling, as at this stage it is more important to see if radiolabelling of the peptide is possible. This can be investigated using a peptide that is not 100% pure.

4.7 Conclusion

All peptides were successfully synthesised and characterised by LC-MS analysis. The HYNIC peptides both were synthesised with greater purity relative to the HYBA peptides, with the HYBA-nanogastrin being only 32.8% pure. However despite this, all peptides are suitable for radiolabelling with ^{18}F as the aim of this project was to assess chemoselectivity of the [^{18}F]4-fluorobenzaldehyde for the hydrazine group on the peptide for site specific radiolabelling of peptides and this can be achieved using peptides that are not 100% pure.

4.8 Summary of chapters 2 to 4

When HYBA was reacted with an active ester instead of an aldehyde, there was very little reactivity between HYBA and the active ester, whereas, it can be clearly seen in all the competition reactions involving the aldehydes that they reacted very specifically with HYBA in preference to the competing amines. Active esters are less reactive with HYBA and less selective than aldehydes. Therefore it can be concluded that labelled aldehydes will be better prosthetic groups than labelled active esters for reaction with HYNIC or HYBA-containing molecules.

When the rate of hydrazone formation between 2-iodobenzaldehyde or 4-fluorobenzaldehyde with HYBA was investigated, HYBA reacted with either 2-iodobenzaldehyde or 4-fluorobenzaldehyde and only one product was formed, rapidly, with little or no heating. This was the case even in the presence of the competing amine, benzylamine. Therefore it can be concluded that aldehydes react with HYBA with complete specificity over amines. This reaction occurs rapidly even at room temperature.

Four molecules were synthesised to be incorporated into peptides for chemoselective labelling via hydrazone formation. Fmoc-Lys-HYBA-Boc and Fmoc-Lys-HYNIC-Boc were successfully synthesised and the Fmoc-Lys-HYBA-Boc, a new molecule, was fully characterised. Fmoc-Lys-HYNIC-Boc was characterised in a more comprehensive way than has been done previously. HYBA-Boc and HYNIC-Boc were also successfully synthesised. The peptides containing HYBA, HYNIC and HYBA and HYNIC amino acid synthons were were successfully synthesised and characterised ready for radiolabelling with [^{18}F]fluorobenzaldehyde.

NHS-HYBA-Boc could be incorporated into proteins for chemoselective labelling.

Unforunately, the radiolabelling of the peptides synthesised in this chapter was not completed in time for the results to be included in this thesis. However, early indications are that the strategy presented here of hydrazone bond formation between a peptide containing HYBA and a ^{18}F labelled aldehyde does work as theorised.

4.9 Future Work

An investigation into the relative stabilities of HYNIC hydrazone bond versus HYBA hydrazone bond would be a good starting point for future work because there is a possibility that HYBA hydrazones may be more stable. This is due to the possibility that the pyridyl N of HYNIC hydrazone compound could act as a nucleophilic catalyst and accelerate hydrolysis or the protonated pyridine could act as an acid catalyst. If HYBA hydrazones were found to be more stable, it would be a good reason to use HYBA rather than HYNIC when labelling peptides or other biomolecules with ^{18}F via [^{18}F]fluorobenzaldehyde.

It would also be prudent to investigate which is the best way of labelling peptides using either the hydrazone or oxime methodology, as the two are very similar. Namely, to investigate the serum stabilities of the hydrazone versus the oxime bond, also to assess the labelling kinetics

including which of the two methodologies could be used at the lowest concentration and rate of formation of the oxime bond versus the hydrazone bond at a temperature compatible with labelling peptides. Then next step would be to demonstrate labelling with ^{18}F and to optimise labelling conditions. From the current literature on these two methods for labelling, it is difficult to say which would be the better option and so a thorough investigation would appear to be a logical step forwards.

Only benzaldehyde and glucose have been used as aldehydes for labelling to date and other aldehydes should be tested to find the one that is easiest to label with ^{18}F, easiest to couple to the peptide and also which has the best hydrazone stability and changes the lipophilicity of the peptide the least.

The results obtained in the competition reactions for 4-formylphenyl boronic acid deserve special mention as the addition of this aldehyde to a peptide via a hydrazone bond could provide a 1-step labelling strategy due to the affinity fluorine has for boron. The results obtained here show that in the presence of Fmoc-Lys-OH as the competing amine, 4-FPB reacts selectively with HYBA. However in the presence of ABAME as a competing amine, the reaction mixtures from both competition reactions (one with equimolar amounts and one with 3-fold excess of the competing amine) showed significant amounts of starting material. 4-FPB did not react with ABAME when the two were reacted together separately. When benzylamine was used as the competing amine, the reaction between HYBA and 4-FPB yielded 60% 4-[N'-(4-boronobenzylidene)hydrazino]-benzoic acid in the presence of 1 equivalent of benzylamine and when 10 equivalents of benzylamine was present the reaction mixture contained only 4-[N'-(4-boronobenzylidene)hydrazino]-benzoic acid wth no starting material present. Due to the fact that using boron as a binding site for fluorine would produce a 1 step labelling strategy and that the results presented here are not easy to interpret, it may be worth investigating these reactions further.

References

Atherton E, Fox H, Harkiss D, Logan CJ, Sheppard RC, Williams BJ (1978). A mild procedure for solid phase peptide synthesis:- Use of fluorenylmethoxycarbonyl amino acids. *Journal of the Chemical Society Chemical Communication*, 537-539.

Barrett GC, Elmore DT (1998) Amino acids and Peptides. Methods for the synthesis of peptides (chapter 7). Cambridge University Press pp130-173.

Behe M, Becker W, Gotthardt M, Angerstein C, Behr TM (2003). Improved kinetic stability of DTPA-DGlu as compared with conventional monofunctional DTPA in chelating indium and yttrium: preclinical and initial clinical evaluation of radiometal labelled minigastrin derivatives. *European Journal of Nuclear Medicine and Molecular Imaging* **30**, 1140.

Behe M, Behr TM (2002). Cholecystokinin-B (CCK-B)/gastrin receptor targeting peptides for staging and therapy of medullary thyroid cancer and other CCK-B receptor expressing malignancies. *Biopolymers* **66**, 399-418.

Biagini P, Monges G, Vuaroqueaux V, Parriaux D, Cantaloube JF, De Micco P (1997). The human gastrin/cholecystokinin receptors: type B and type C expression in colonic tumours and cell lines. *Life Science* **61**, 1009-1018.

Chang D and Meinhofer J (1978). Solid phase peptide synthesis using mild base cleavage of fluorenylmethoxycarbonyl amino acids. Exemplified by the synthesis of dihydrosomatostatin. *International Journal of Protein Research* **11**, 5401-5402.

Entrez Gene a; CCKAR cholecystokinin A receptor

Entrez Gene b; CCKBR cholecyctokinin B receptor

Greenland WEP (2002). Radionuclide conjugates of calcitonin for imaging bone disease ans cancer. *PhD Thesis*.

Greenland WEP, Howland K, Hardy J, Fogelman I, Blower PJ (2003). Solid-phase synthesis of peptide radiopharmaceuticals using Fmoc-N-ε-(Hynic-Boc)-lysine, a technetium-binding amino acid: Application to Tc-99m labelled salmon calcitonin. *Journal of Medicinal Chemistry* **46**, 1751-1757.

Hakanson R, Sundler F (1991). Trophic effects of gastrin. *Scandinavian Journal of Gastroenterology Supplement* **180**, 130-136.

Johnson LR (1989). Trophic effects of gut peptides. In: Makhlouf GM, ed. Handbook of physiology, section 6. Bethesda, MD: American Physiological Society; 291-310.

Kim YS, He ZJ, Hsieh WY, Liu S (2006). A novel ternary ligand system useful for preparation of cationic Tc-99m-diazenido complexes and Tc-99m-labeling of small biomolecules. *Bioconjugate Chemistry* **17**, 473-484

King RC, Surfraz MB-U, Biagini SCG, Blower PJ, Mather SJ (2007). How do HYNIC-conjugated peptides bind technetium? Insights from LC-MS and stability studies. *Dalton Transactions*, 4998-5007.

Mantyh CR, Pappas TN, Vigna SR (1994). Localisation of cholecystokinin A and cholecystokinin B / gastrin receptors in the canine upper gastrointestinal tract. *Gastroenterology* **107**, 1019-1030.

Mather SJ, McKenzie AJ, Sosabowski JK, Morris TM, Ellison D, Watson SA (2007). Selection of radiolabelled gastrin analogues for peptide receptor-targeted radionuclide therapy. *The Journal of Nuclear Medicine* **48**,615-622.

Merrifield RB (1963). Solid phase peptide synthesis. I. The synthesis of a tetrapeptide. *Journal of the American Chemical Society* **85**, 2149-2154.

McWilliams DF, Watson SA, Crosbee DM, Michaeli D, Seth R (1998). Co-expression of gastrin and gastrin receptors (CCK-B and delta CCK-B) in gastrointestinal cell lines. *Gut* **42**, 795-798.

Nock BA, Maina T, Behe M, Nikolopoulou A, Gotthardt M, Schmitt JS, Behr TM, Macke HR (2005). CCK-2/gastrin receptor-targeted tumour imaging with (99m)Tc-labelled minigastrin analogs. *Journal of Nuclear Medicine* **46**, 1727-1736.

Reubi JC (2003). Peptide receptors as molecular targets for cancer diagnosis and therapy. *Endocrine Reviews* **24**, 389-427.

Reubi JC, Schaer JC, Waser B (1997). Cholecystokinin CCK-A and CCK-B/gastrin receptors in human tumours. *Cancer Research* **57**, 1377-1386.

Reubi JC, Waser B (1996). Unexpected high incidence of cholecystokinin-B/gastrin receptors in human medullary thyroid carcinomas. *International Journal of Cancer* **67**, 644-647.

Reubi JC, Waser B (2003). Concomitant expression of several peptide receptors in neuroendocrine tumours:molecular basis for in vivo multireceptor tumour targeting. *European Journal of Nuclear Medicine and Molecular Imaging* **30**, 781-793.

Reubi JC, Waser B, Laderach U, Stettler C, Freiss H, Halter F, Schmassmann A (1997b). Localisation of cholecystokinin A and cholecystokinin B / gastrin receptors in the human stomach and gallbladder. *Gastroenterology* **112**, 1197-1205.

Saillan-Barreau C, Dufresne M, Clerc P, Sanchez D, Corominola H, Moriscot C, Guy-Crotte O, Escrieut C, Vaysse N, Gomis R, Tarasnova N, Fourmy D (1999). Evidence for a functional role of the cholecystokinin-B / gastrin receptor in the human fetal and adult pancreas. *Diabetes* **48**, 2015-2021.

Smith JP, Stanley WB, Verderame MF, Zagon IS (2004). The functional significance of the cholecystokinin-C (CCK-C) receptor in human pancreatic cancer. *Pancreas* **29**, 271-277.

Surfraz MB-U, King R, Mather SJ, Biagini SCG, Blower PJ (2007). Trifluoroacetyl-HYNIC peptides: Synthesis and 99mTc Radiolabelling. *Journal of Medicinal Chemistry* **50**, 1418-1422.

Sutcliffe-Goulden J (2000). *PhD Thesis.*

Von Guggenberg E, Behe M, Behr TM, Saurer M, Seppi T, Decristoforo C (2004). ^{99m}Tc labelling and in vitro and in vivo evaluation of HYNIC-and (Nα-His)acetic acid-modified [D-glu1]-minigastrin. *Bioconjugate Chemistry* **15**, 864-871.

Walsh JH (1994). Gastrin. In: Walsh, JH, Dockray GJ, eds. Gut peptides: biochemistry and physiology. New York: Raven Press, 75-121.

Chapter 5

Ruthenium(III) EDTA complex synthesis, ion exchange and stability studies

5.0 Introduction

5.1 Fluoride and metals

Due to its high electronegativity, the fluoride ion is classified as a hard base. It has a strong affinity towards multivalent metal ions (hard metal ions), including Al(III), Ca(II), Fe(III), Zr(IV) and a series of lanthanide metal ions (Doherty and Hoffman 1991).

The H bonds formed between water and fluoride is one of the stronger H bonding interactions known (Dunitz and Taylor 1997). Even small amounts of a protic solvent can lead transition metals fluorides to become kinetically labile, which leads to easy ionisation (Branan et al. 1987). In aprotic solvents, for a number of metal complexes, the fluoro derivative may be the most stable in the halogen series. Traditionally metal fluoride complexes have been perceived to be unstable in comparison to analogues of the heavier halogens (Pagenkopf and Carreira 1999).

One of the central objectives in organometallic chemistry is the preparation of transition metal complexes with open co-ordination sites or easily displaced ligands (Beck and Sunkel 1988). These molecules facilitate the first step of any catalytic cycle which involves substrate co-ordination at the metal (Murphy et al.1997). Easy displacement of weakly coordinating ligands by fluoride has proven to be a very promising route to organometallic fluoride compounds. In several systems, net metathesis of fluoride for chloride has been accomplished cleanly and in good yield via abstraction of chloride using AgOTf or $AgBF_4$, followed by addition of fluoride from organic solvent-soluble sources (Doherty and Hoffman 1991). The reactivity and stereochemistry of substrate binding in organometallic systems may be manipulated by the switching of halide substituents, in particular fluoride and chloride, with bromide to a lesser extent (Murphy et al. 1997).

Yuchi et al. (1996) studied complexes of hard metal ions with polyaminocarboxylates as fluoride receptors. Metal complexes Zr^{4+}, Hf^{4+} and Th^{4+} reacted so quickly with fluoride that the process could not be followed by monitoring with a fluorine ion selective electrode. The reaction of Al^{3+} with fluoride proceeded more slowly. These metal ions have a high affinity for fluoride, although extensive hydrolysis especially of Zr(IV) and Hf(IV) interfered with quantitative evaluation. The stability constants for coordination of the first fluoride were estimated to be $10^{6.4}$ for Al^{3+}, $10^{9.0}$ for Zr^{4+}, $10^{8.6}$ for Hf^{4+} and $10^{7.7}$ for Th^{4+}. Stability constants for fluoride decreased with an increasing number of donor atoms of a ligand for any metal ions. For Zr^{4+} and Hf^{4+} the ligand DTPA (diethylenetriamine-*N,N,N',N'',N''*-pentaacetic acid) had just the necessary and sufficient number of donor atoms to encircle each metal ion. All the sites on the metal ion were occupied by the donor atoms of the ligand and one of the acetate groups had to be detached to create a space for accommodating fluoride (Yuchi et al. 1996). The zirconium(IV) complex of *N*-methyliminodiacetic acid was an excellent fluoride acceptor; fluoride was quantitively fixed on the complex at pH < 4.5 and reversibly expelled at pH 9 within a short time period.

Tanaka et al. (2002), studied the reaction between fluoride and Zr(IV) complexes by ^{19}F NMR and potentiometry using $K_2[Zr(CO_3)EDTA]$ and $[Zr(H_2O)_2EDTA]$ as the model compounds. As the Zr(IV) complex is very stable, they attempted to make a Zr(IV) complex of a polymer resin having an EDTA functional group for selective removal of fluoride ions. According to x-ray structural analysis of $[Zr(H_2O)_2EDTA]$, Zr(IV) was surrounded by hexadentate EDTA and two water molecules corresponding to a zirconium coordination number of eight (Pozhidaev et al. 1974). The coordinated water could be replaced by more strongly binding molecules such as organic bidentate ligands (Intorre and Martell 1964). The significant shift of ^{19}F peaks from the location of free fluoride ion was attributed to the direct coordination of fluoride to Zr(IV). The peak intensity of the complexed fluoride relative to free fluoride decreased with the increase in pH implying that complexation of fluoride with Zr(IV) was unfavourable in the higher pH region. The optimum pH for maximum peak ratio of complexed fluoride ranged from pH 3 to 6. The NMR data suggested that direct complexation of fluoride on the metal was the most plausible mechanism of retention and that the Zr(IV) loaded chelating resins retained fluoride by ternary complex formation. The high selectivity of the zirconium loaded chelating resins for fluorine could not be interpreted simply by an ion exchange mechanism which is based on electrostatic force. The data also implied that the

Zr(IV) EDTA complex could capture up to two fluoride ions by direct coordination to the Zr(IV) centre. The presence of anions including chloride, nitrate, sulfate and acetate up to one hundred times the concentration of fluoride did not interfere with the adsorption of fluoride but the presence of phosphate significantly affected adsorption.

Takahashi et al. (2002) investigated a ligand exchange reaction for detection of fluoride in aqueous solution. They used a detection system based on a decrease in fluorescence when a solution of flavonol (3-hydroxyflavone) and $[Zr(H_2O)_2EDTA].2H_2O$ had fluoride added to it. The change was associated with ligand exchange between flavonol coordinated to Zr(IV) with fluoride. The scheme is shown below.

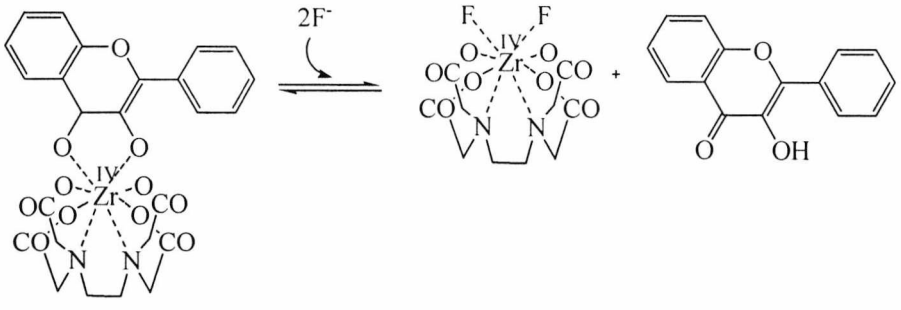

Scheme 5.0 Showing the Zr(IV) EDTA-flavonol complex which changes to the Zr(IV) EDTA-F_2 complex on addition of 2 F^-

The fluorescence signal intensity changed most sensitively between pH 4.5 and 6 where ligand exchange between flavonol and fluorine took place most favourably. Time course experiments showed that the change of fluorescence signal intensity was rapid and terminated within one minute upon addition of fluoride (pH 5) at 50°C. It was found ternary complex formation with flavonol seemed favourable at a pH ranging from 5 to 9. The presence of common anions including chloride, sulphate, nitrate, acetate and interestingly, in this paper as compared with Tanaka et al. (2002), phosphate did not interfere significantly with the signal intensity even in concentrations up to one hundred times that of fluoride ions (0.2 ppm). Metal cations including Al(III), Fe(III), Cu(II) interfered due to competing complexation of flavonol with these metal ions.

A study by Yuchi and Matsuo (2005) assessed the affinities of Zr(IV) and Ti(IV) to 25 different anions and found the affinities of Zr(IV) to anions in general were much stronger than those of Ti(IV) due to the greater tendency of Ti(IV) towards hydrolysis.

It has been suggested by Yuchi et al. (1999) that adsorption of fluoride ion on Zr(IV) complexes takes place by dual mechanisms; an ion-exchange mechanism in strongly acidic media and by an addition reaction in weakly acidic media.

Ligand (-L) exchange: $[(\text{-L})Zr(OH)_2] + H^+ + F^- \rightleftharpoons [(\text{-L})Zr(OH)F]$

Addition: $[(\text{-L})Zr(OH)_2] + K^+ + F^- \rightleftharpoons [(\text{-L})Zr(OH)_2F^-, K^+]$

The contribution of the addition mechanism increases with an increase in pH and thereby enhanced co-adsorption of K^+.

Among the 25 anions tested, fluoride had the highest affinity to Zr(IV), which was exemplified by the largest adsorption constant, by the formation of a 1:2 species and also by the presence of an addition mechanism even in a relatively low pH range of 3-4 (Yuchi and Matsuo 2005).

Yuchi et al. (1993) found that when a complex of Zr(IV) with the ligand SXO (semi-xylenol orange) was reacted with fluoride that at a pH of about 2, the partially hydrolysed complex was predominant and its reaction with fluoride ion could be expressed by (where L is the SXO ligand):

$Zr_2(OH)_4(HL)_2^{2-} + 2F\text{-} \rightleftharpoons 2ZrLF^- + 2OH^-$

At a high pH, the equilibrium above shifts to the left and the reactivity with fluoride is reduced. The reaction with F^- was therefore highly pH dependent.

The reactivity of some trivalent metal ions (Al^{3+}, Ga^{3+}, In^{3+}, Fe^{3+}, Sc^{3+}, Y^{3+}, La^{3+}) with fluoride were studied by Yuchi et al (1987). It was found that the reactivity of the metal ion with fluoride generally decreased upon coordination to a polyaminocarboxylate. Two of the polyaminocarboxylates studied (NTA and HEDTA) formed complexes that held more than one coordinated water molecule and because of this, formation of ligand complexes with trivalent metal ions corresponded to substitution of water molecules for fluoride ions as formation of simple fluoro complexes. It was suggested that for the polyaminocarboxylate EDTA, the complexes formed with Ga(III), Fe(III) and Sc(III) involved one arm of the carboxylate group becoming free on formation of the complex and also that the parent

complexes involved the complete hexadentate chelation of EDTA irrespective of the coordination number of the metal ions.

In another paper by Yuchi et al. (1990) eight coordination for the Zr(IV) EDTA complex in solution was proposed due to the strong tendency to form complexes with bidentate ligands. MLF (mixed ligand complex of a metal and EDTA with fluoride) was identified only for tetravalent metal ions of a moderate size, these being Zr(IV) and Hf(IV) as opposed to the other tetravalent metals studied; Ge(IV), Ti(IV), Sn(IV), and Th(IV) (Yuchi et al. 1990).

Yuchi et al. (1995a) found that when complexes of tetravalent metal ions with chromogenic chelating reagents were examined for fluorometric determination of fluoride, Zr(IV) and Hf(IV) were superior to Th(IV) as a central metal ion.

Yuchi et al. (1994) found that using Zr(IV) fixed on a hydrophilic chelating polymer having iminodiacetate groups, fluoride was rapidly adsorbed on the polymer complex in acidic media and quantitively desorbed in basic media. More than 95% of fluoride was adsorbed if the F:Zr molar ratio was kept lower than 0.2. With an increase in the ratio, the recovery of fluoride decreased and finally Zr(IV) started to leak when fluoro complexes with ratios higher than 2 were present. At higher pH, the hydroxide ion can expel the adsorbed fluoride through the formation of mixed ligand complexes only with the hydroxide ions which are reversibly converted to the starting complex by any acids. Both the forward and reverse reactions were completed within a few minutes.

In a study of determination of fluoride in the presence of tetravalent metal ions with an ion selective electrode, Yuchi et al. (1995b) found that as long as L (ligand or chelating group e.g. EDTA, DTPA, CDTA, TTHA) is in excess over M (metal ion), the equilibrium given by equation below is completely shifted to the right. Due to the fact that only one fluoride is left in the mixed ligand complex and the experimental conditions are chosen so that at least 80% of the fluoride is recovered by this reaction any further rise in recovery from 80% depends on the equilibrium process of the equation below:

$$MF_n + L \rightleftharpoons MLF + (n\text{-}1)F^-$$

The position is determined only by the stability constant of the mixed ligand complex, irrespective of an excess concentration of L. The low recovery found at pH values less than 5

is due to the protonation of the liberated fluoride. Formation of HF in strongly acidic media interferes with the reaction of fluoride with metal complexes. At higher pH levels, mixed-ligand complexes can react with hydroxide ions to expel fluoride by the reaction below:

$$MLF + OH \rightleftharpoons ML(OH) + F^-$$

The use of the fluoride ion selective electrode is limited to pH values lower than 6 because of interference from hydroxide ions. It was found that Hf(IV) complexes have a relatively high affinity for hydroxide ions as well as for fluoride ions whereas Th(IV) complexes have a relatively low affinity for hydroxide ions (Yuchi et al. 1995b).

A paper by Filippou et al. (2002) states that the one-electron oxidation of the chromium(III) triamidoamine complex $[Cr(N_3N)]$ $\{(N_3N)^{3-} = [(Me_3SiNCH_2CH_2)_3N]^{3-}\}$ with silver(I) salts is a valuable method for the synthesis of rare and thermally stable chromium(IV) halides and pseudohalides of the general formula $[Cr(N_3N)X]$ (X=F, Cl, I, CN). The strong π-donating ability of the N_3N ligand is expected to reduce the oxidising power of these compounds making them good starting materials for the organometallic chemistry of chromium(IV). Chromium is another metal with a strong affinity for fluoride.

5.2 Ruthenium and fluoride

Several Ru-pac (ruthenium-polyaminocarboxylate) complexes have been reported to have anti-tumour properties, these include $Ru(EDTA\text{-}H_3)Cl_2.4H_2O$, $H[Ru(PDTA\text{-}H_2)Cl_2].4H_2O$ and $[Ru(CDTA\text{-}H_2)Cl_2].2H_2O$ (Jolley et al. 1999). The anti-tumour mechanism is still largely unknown (Chatterjee and Mitra 2006). Ruthenium(III) EDTA was investigated as a potential NO scavenger to be used as antitumour / antiangiogenic agents (Morbidelli et al. 2003). Ru EDTA was able to bind tightly and inactivate NO in solution. The complex formed exhibits spectral behaviour that is diagnostic of a stable ruthenium-nitrosyl species i.e. the appearance of an intense IR transition at 1900-1800cm^{-1} and the disappearance of hyperfine signals in the ^1H NMR spectra owing to loss of paramagnetism. The study was able to demonstrate that Ru(III) EDTA complexes do inhibit angiogenesis *in vivo*.

A study by Chatterjee and Mitra 2006 found ruthenium(III) complexes containing polyaminocarboxylate ligands (Ru-pac) to have features which indicate they may be suitable for biological applications. Ru-pac complexes can bind to biomolecules through a rapid aquo-

substitution reaction. The donor character of the pac ligand is comparable with that of many biological enzymes which make use of the carboxylate and amine donors from amino acids to bind to a metal centre. The pac ligand, such as EDTA, can form very stable 1:1 (metal:ligand) complexes with Ru. The chemistry of [Ru(III)(pac)(H_2O)] complexes is dominated by their lability towards aquo-substitution reactions which gives an easy and straightforward means of synthesising mixed-ligand complexes (Chatterjee 1998). Ruthenium complexes with pac ligands demonstrate potential as metallodrugs because they have a number of stable oxidation states, have rapid ligand exchange and an ability to bind to certain biological molecules. *In vitro* studies have shown the ability of Ru EDTA complexes to scavenge NO in biological systems (Chatterjee and Mitra 2006).

$[Ru(III)(EDTA)(H_2O)]^- + NO \rightarrow [Ru(II)(NO^+)(EDTA)]^- + H_2O.$

Ru EDTA complexes have been studied due to their ready conversion from one oxidation state to another and also because of the tendency of its compounds to undergo hydrolysis and polymerisation. Comparison of the EDTA compounds of Ru(III) with those of iron(III) and rhodium(III) with regards to bond strength with nitrogen and oxygen atoms of the ligand and also with chlorine atoms, demonstated the marked similarity between Ru(III) and Fe(III) compounds (Ezerskaya and Solovykh 1966).

Conversely, Ru(III) EDTA was found to be significantly less reactive than Fe(III) EDTA according to Bajaj and van Eldik (1988). The substitution reactions of Ru(III) EDTA were accompanied by significant spectral changes. When Ru(III) was bound to EDTA its lability was increased by at least 7 orders of magnitude and it underwent substitution more rapidly than Ru(II) (Matsubara and Creutz 1978). Labile means constantly undergoing or likely to undergo change or breakdown. EDTA in a complex with Ru(III) has been shown to be pentadentate in aqueous solution and the sixth coordination site of the metal centre is occupied by a water molecule at low pH and a hydroxide ion at high pH (Matsubara and Creutz 1979). Kinetic studies on the substitution behaviour of these complexes indicate a maximum reactivity at pH 4-6 where the observed rate constant is practically independent of pH. This has been ascribed to the extreme lability of Ru(III) EDTA H_2O (Matsubara and Creutz 1979). The study by Bajaj and van Eldik (1988) found that in aqueous solution rapid hydrolysis of $K[Ru(HEDTA)Cl].2H_2O$ from $Ru(HEDTA)Cl^-$ in solution to $Ru(HEDTA)H_2O$ occurred. The lability of the Ru EDTA complex decreased above a pH of 6.5 because of the

deprotonation of the coordinated water molecule to produce a less labile hydroxo species. The complex Ru HEDRA (where HEDRA is *N*-(hydroxyethyl)-ethylenediaminetriacetic acid), was substantially less labile than (Ru EDTA) H_2O^- complex, demonstrating the important effect of the pendant carboxylate group in the latter case playing a role in the rapid substitution reactions of Ru EDTA complexes (Bajaj and van Eldik 1989).

When Ru(III) (EDTA) H_2O^- was mixed with 1 M thiocyanate ion in a study by Matsubara and Creutz (1979), visible spectral changes associated with the binding of one or two thiocyanate ions were resolvable and over a period of hours, changes occurred that corresponded to the binding of a third and maybe forth thiocyanate ion were observed. Changes were also observed for coordination of iodide to the Ru(III) complexes. It is suggested that both H_2O and a free carboxylate group are required for maximal activity in a Ru(III) EDTA complex and that the labilisation of Ru(III) is accompanied by a sharp pH dependence.

The aim of this chapter was to assess the feasibility of using a transition metal attached to a peptide to chelate fluoride in one easy reaction step. There is a great deal of literature available that relates to transition metals in mixed ligand complexes. From the literature reviewed, zirconium(IV) complexes with aminopolycarboxylates appear to have the greatest affinity for and generate the most stable complexes with fluoride. Ruthenium(III) EDTA complexes appear to be labile in aqueous solution but are able to form stable complexes with NO *in vivo* and ruthenium(III) forms complexes with EDTA leaving a chloride available for easy ion exchange. While none of this literature is directly about PET applications, having been written with other applications in mind, a great deal can be learnt about the nature of complexes involving fluorine and transition metals bound to organic molecules from reading these papers. The literature discussed in this introduction shows that many compounds have been made that are very similar in nature to compounds of interest for this project, despite having been developed for different applications. While some of the information is conflicting, such as the stability of the oxidation states of ruthenium, many of the conclusions in these papers imply that it may well be possible to develop a compound for PET applications using a transition metal as a binding site for fluorine, for example with regards to compounds being water soluble and being stable at neutral pH. The metal complex would have to be kinetically stable and resist hydrolysis. As discussed earlier, ruthenium was identified as the metal to start with for this strategy.

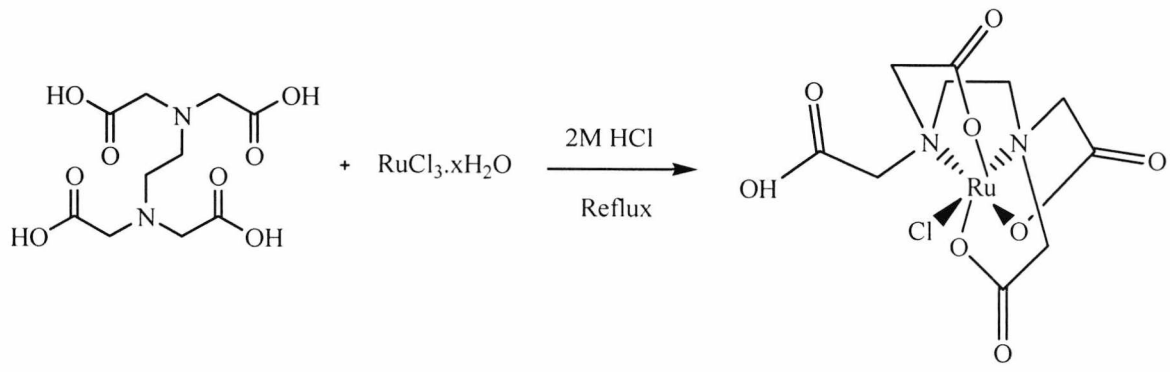

Scheme 5.1 Synthesis of Ruthenium(III) EDTA $[Ru(III)(EDTA)Cl]^-$ complex. (Jolley *et al.* 1998)

Proof of principle in the long term would be to develop an ^{18}F labelled peptide that could be synthesised very quickly in the minimum of reaction steps as well as to determine its labelling efficiency and stability. This could then be used as a tracer for PET imaging.

5.3 Aims and objectives

Initially the aim of this project was to develop a new binding site for fluoride to give a one step labelling technology that could be applied to the development of a wide range of peptide and protein based radiopharmaceuticals. An additional longer term aim was to apply this labelling technology to produce a novel ^{18}F radiolabelled peptide that could be used for PET imaging. The new compound would use a metal ion bound to a peptide to bind fluoride in one reaction step.

The aim therefore focuses on finding new binding sites for fluoride. Present technology relies on creation of a carbon-fluorine (C-F) bond which is a lengthy procedure, involving multiple reaction steps (see chapter 1 for discussion of present ^{18}F labelling techniques). This causes an unwanted decrease in the specific activity of the ^{18}F labelled radiopharmaceutical during preparation. It also increases the chances of contamination of the radiopharmaceutical which should be sterile for injection into patients as well as increasing radiation exposure to the operator.

It was proposed to use a metal to bind fluoride as this strategy would be a one step process. The metal would already be conjugated to a peptide or protein before addition of fluoride. This strategy would be the basis of the new labelling technology which could then be adapted for use with different peptides, proteins or other biomolecules to provide radiopharmaceuticals that could be labelled easily and rapidly.

The polyaminocarboxylate compound EDTA (ethylenediaminetetraacetic acid) was chosen as a chelating agent for the metal. EDTA has one uncoordinated carboxylate group which provides a means of linking to a peptide. Ruthenium(III) was chosen as the metal initially because ruthenium(III) binds to EDTA leaving one bound chlorine atom that could be involved in a one step anion exchange reaction with a fluoride ion in an aqueous solution.

The objective was to synthesise a Ru(III) EDTA ($[Ru(III)(EDTA)Cl]^{2-}$) complex that was stable under aqueous conditions and therefore not susceptible to hydrolysis or further ion exchange after incorporation of fluoride. This would enable labelling with ^{18}F by anion exchange in one easy step.

Eventually the aim was to extend the strategy to other hard metals to identify ones with optimal fluoride binding characteristics.

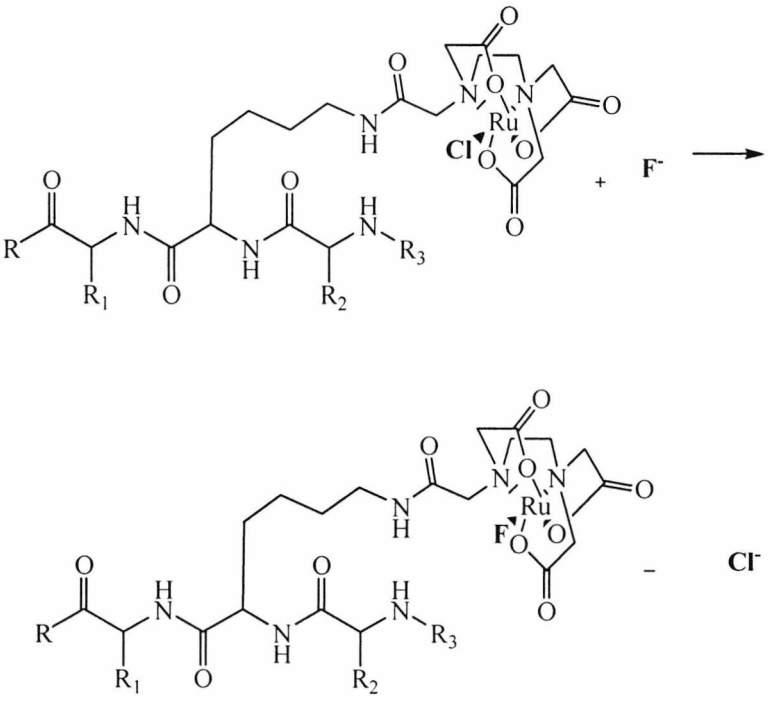

Scheme 5.2 Ruthenium(III) EDTA complex attached to a peptide showing chloride for fluoride anion exchange (shown in bold for clarity)

5.4 Materials and methods

Ruthenium(III) chloride hydrate and ethylenediaminetetraacetic acid (99%) were purchased from Acros Organics. Hydrochloric acid (37% solution in water) was purchased from BDH Laboratory Supplies. Ethanol (analytical reagent grade) was purchased from Fisher Scientific. All reagents were used as received.

5.4.1 Synthesis of Ruthenium {[2-(Bis-carboxymethyl-amino)-ethyl]-carboxymethyl-amino}-acetic acid (Ruthenium(III) EDTA or [Ru(III)(EDTA)Cl]$^-$)

A solution of $RuCl_3.xH_2O$ (0.33 g, 1.24 mmol) and EDTA (0.60 g, 1.44 mmol) in 2M HCl (25 cm^3) was heated under reflux overnight. The colour changed from dark brown to yellow. The 2M HCl was partially removed under vacuum and crystals formed over a period of 1 to 2 weeks. The yellow crystals were collected by filtration and recrystallised from ethanol. The crystals were dried with ethyl acetate. (Jolley *et al.* 1998)

Yield: 0.27 g, 0.63 mmol, 51%, decomposition temperature 260-265°C.

Ruthenium(III) is paramagnetic therefore no NMR spectroscopy was carried out on the product.

ν_{max} cm^{-1} 2750 (br, m, OH *str*), 2984 (m, sp^3, C-H *str*), 1743 (s, C=O, *str*, ester), 1719 (s, C=O, *str*, acid).

m/z (ESI) (cone voltage **10**V) Negative mode, ion $[M + Cl - H]^-$:462.1 100% intensity, $[M - H]^-$:426.2 12% intensity, (where M is the molecular ion), (cone voltage **50**V) $[M - Cl - H]^-$: 390.1 100% intensity, $[M - H]^-$:426.2 20% intensity, $[M + Cl - H]^-$:462.1 18% intensity.

Molecular formula: $C_{10}H_{13}ClN_2O_8Ru$

Exact mass: 425.94 taking ruthenium to be 102, which is the most abundant isotope of ruthenium.

Molecular weight: 425.74

Elemental analysis: Formula calculated from $C_{10}H_{13}ClN_2O_8Ru$

Expected: C 28.2%, H 3.1%, N 6.6%.

Found: C 32.2%, H 5.0%, N 5.5%.

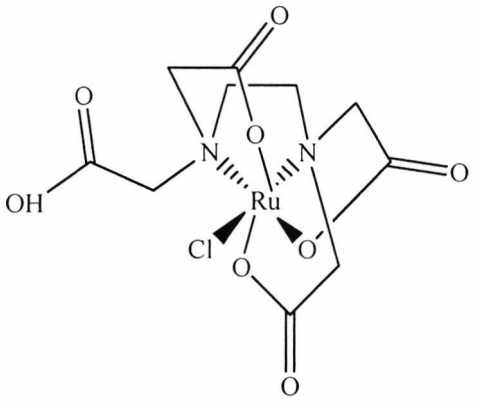

Figure 5.0 Structure of [Ru(III)(EDTA)Cl]$^-$

5.4.2 Anion exchange reactions

Anion exchange reactions were carried out and analysed by UV/visible spectroscopy and mass spectrometry to determine whether the chlorine on the complex could be replaced by another halogen ion. Three different halogenated inorganic salts were used; potassium fluoride (UV/visible spectroscopy experiment only), sodium iodide, sodium bromide.

5.4.2.1 Mass Spectrometry experiment

Three 2 mmol solutions of the $[Ru(III)(EDTA)Cl]^{2-}$ complex in water were made and each had either water or equimolar amounts of the halogen salts NaBr or NaI added giving:

2 mmol $[Ru(III)(EDTA)Cl]^{2-}$ in water

2 mmol $[Ru(III)(EDTA)Cl]^{2-}$ in 2 mmol aqueous NaBr

2 mmol $[Ru(III)(EDTA)Cl]^{2-}$ in 2 mmol aqueous NaI.

The $[Ru(III)(EDTA)Cl]^{2-}$ sample in water with no added anion acted as a control sample. Data were obtained using a cone voltage of 10V, 20V, 50V and 90V to compare 'soft' ionisation with less gentle ionisation. Mass spectrometry was carried out at t=0, t=24 and t=48 for each of the three solutions.

5.4.2.2 UV/visible spectroscopy experiment

1 mmol $[Ru(III)(EDTA)Cl]^{2-}$ in water

1 mmol $[Ru(III)(EDTA)Cl]^{2-}$ with 1 mmol aqueous NaBr

1 mmol $[Ru(III)(EDTA)Cl]^{2-}$ with 1 mmol aqueous NaI

1 mmol $[Ru(III)(EDTA)Cl]^{2-}$ with 1 mmol aqueous KF

The solutions were monitored over a period of 168 hours with measurements taken at t=0, t=24, t=48, t=72 and t=168 h to see if there was any change in absorbance over the time period.

5.5 Results and discussion

5.5.1 Synthesis

In NMR spectroscopy, there can be paramagnetic shifts produced by unpaired electrons. These unpaired electrons give rise to large dipolar magnetic fields which can result in substantial nuclear shielding or deshielding which can result in the protons in a compound having a chemical shift that is not within the normal chemical shift for a proton NMR and therefore will not show up in the ^{1}H NMR spectrum. Certain oxidation states of metals produce paramagnetism (Hore 1995), such as the ruthenium(III) used for this work. It is also possible the signal is broadened so much that it is not detected.

The IR spectroscopy results showed evidence for the presence of the correct functional groups for $[Ru(III)(EDTA)Cl]^{2-}$. There was a broad OH stretch at 2750 cm^{-1}, a C-H stretch at 2984 cm^{-1}, a carbonyl ester stretch at 1743 cm^{-1} and a carbonyl acid stretch at 1719 cm^{-1}. The presence of these functional groups helps to confirm the presence of the $[Ru(III)(EDTA)Cl]^{2-}$ complex. The IR spectrum of $[Ru(III)(EDTA)Cl]^{2-}$ was compared to that of EDTA and found to be different. The IR spectrum of EDTA showed and CH stretch at 3017 cm^{-1} and one broad C=O stretch at 1681 cm^{-1}.

The elemental analysis results were not as expected. The results for carbon, hydrogen and nitrogen had a difference of more than 5% from the predicted elemental analysis. It is possible that some solvent or water was present in the sample. The $[Ru(III)(EDTA)Cl]^{2-}$ synthesised

was crystalline and the crystals uniform in colour and size which is an indication of a pure product.

5.5.1.1 Powder x-ray diffraction results

X-ray diffraction was also carried out and the results compared against Ru(III) EDTA diffraction data available from the CSD (Cambridge Structural Database). The X-ray diffraction data obtained showed differences from the CSD database comparison.

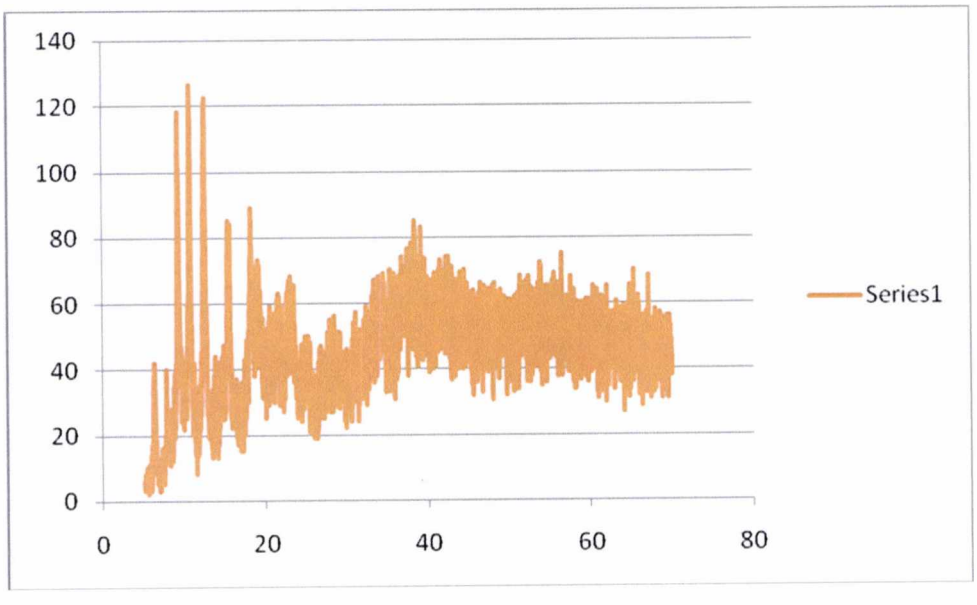

Figure 5.1 Sample 'HS50' $[Ru(III)(EDTA)Cl]^{2-}$

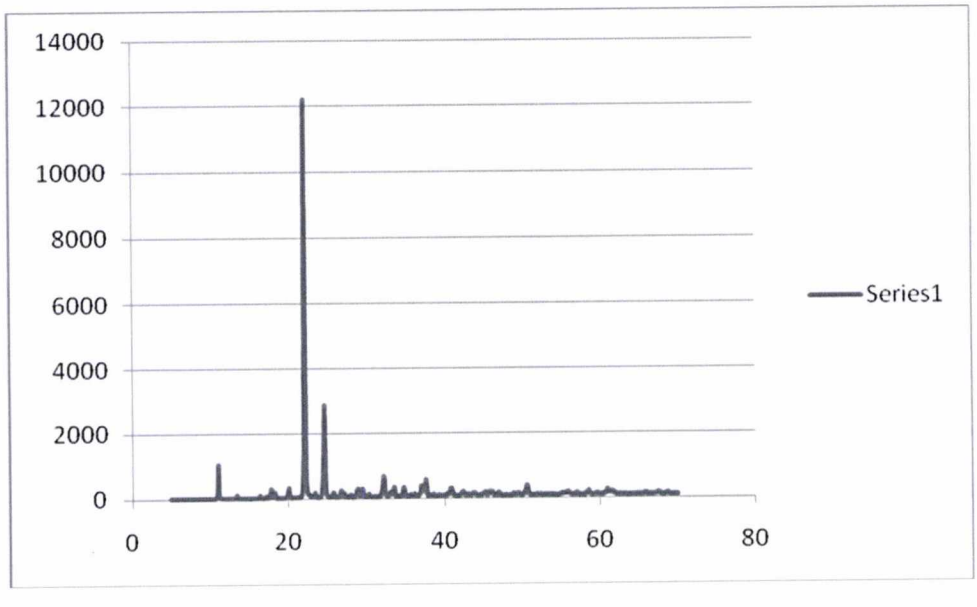

Figure 5.2 Ru(III) EDTA from CSD database

Although the scales are very different on the Y axis (the Y axis scale is set automatically depending on the height of the peaks in the sample), it can be seen that there is an absence of the two large peaks in sample HS50 when compared to the sample from the CSD database. This implies that the complex synthesised was not the one expected or it is possible the sample was too weak to give a good spectrum. However the IR data showed the presence of EDTA in a form different to the starting material and mass spectral data showed the presence of EDTA and ruthenium therefore it was thought to be worthwhile continuing with this work and carrying out anion substitution reactions.

For the mass spectrometry, the isotope pattern for $[Ru(III)(EDTA)Cl]^{2-}$ was calculated using Sheffield ChemPuter (available from the Sheffield University Chemistry Department website).

Mass	**%**	
420	14.4	_____
421	1.7	_
422	9.8	_____
423	34.4	_____
424	38.5	_____
425	59.9	_____
426	100.0	_____
427	26.6	_____
428	78.6	_____
429	9.5	_____
430	17.2	_____
431	2.0	_
432	0.4	

Figure 5.3 $[Ru(III)(EDTA)Cl]^{2-}$ isotope pattern

The isotope pattern above shows the percentages of the various isotopes of ruthenium present in a sample of $[Ru(III)(EDTA)Cl]^{2-}$ (formula: $C_{10}H_{13}ClN_2O_8Ru$). The most abundant isotope gives a mass of 426. The other isotopes of ruthenium give the other masses present in the above diagram.

The mass spectrometry was carried out in Swansea at the National Mass Spectrometry Centre. The mass spectral data proved difficult to obtain, with only weak spectra being obtained. When more sample was added, the results became 'spikey' (i.e. no meaningful ions present), possibly due to poor spraying. This could have been because there was too much water present (water was used as a solvent for the samples). Another contributing factor was that the negatively charged halogen ions appeared to affect the spray and ionisation was poor. The results from the mass spectra analysis indicate that at a low cone voltage of 10V, the principal ion found (100% intensity) was the $[Ru(III)(EDTA)Cl]^{2-}$ molecular ion plus a chlorine atom (formula: $C_{10}H_{13}Cl_2N_2O_8Ru$). This means at the low cone voltage of 10V, the $[Ru(III)(EDTA)Cl]^{2-}$ complex is bonding with two chlorine atoms more commonly than the one chlorine atom, according to the mass spectra results. It is possible that more non-ionised species are present that are not detected by the mass spectrometer. When the cone voltage is increased to 50V, the complex has a strong tendency to lose a chlorine atom, ($[M - Cl - H]^-$: 390.1, 100% intensity) as well as bonding with one extra chlorine atom ($[M + Cl - H]^-$:462.1, 18% intensity), according to the mass spectra results. The molecular ion ($[M - H]^-$) was present at 20% intensity.

5.5.1.2 Mass Spectrometry results for the anion exchange reactions

The anion exchange reactions and analysis were carried out in Swansea. For the analysis, it was found that negative ionisation was again complicated by the negative halogen ions present, which appeared to affect the spray and cause poor ionisation of the complex. The mass spectra obtained showed no binding of the other anions (I or Br) to the ruthenium complex and no changes over time in any of the samples. Many ions were found with the isotope pattern characteristic of ruthenium containing compounds. The molecular formulas of the ions that were expected for each compound, had the experiment been successful, and for the $[Ru(III)(EDTA)Cl]^{2-}$ control have been put in a table to show what ions were sought in the the mass spectra.

Molecular formula	Exact mass
$[Ru(III)(EDTA)Cl]^{2-}$: $C_{10}H_{13}ClN_2O_8Ru$	425.94
$C_{10}H_{13}IN_2O_8Ru$	517.88
$C_{10}H_{13}BrN_2O_8Ru$	469.98

Table 5.0

Below are the results for the control compound; $[Ru(III)(EDTA)Cl]^{2-}$ ($C_{10}H_{13}ClN_2O_8Ru$) and H_2O at t=0. This demonstrates that there were many peaks present in this mass spectrum. From the ions present is possible to see ions that correspond to loss of Cl (390.1), gain of Cl (462.0). There are also ions present that are more difficult to identify structurally, for example the difference of 28 between 462.0 and 490.0 and between 490.0 and 518.0 and the difference of 64 between the molecular ion ($[M - H]^-$) and 490.0. It is possible that a loss of 28 may correspond to the loss of a carbon atom and an oxygen atom. A loss of 64 does not correspond to two chlorines, and is more likely to correspond to the loss of a functional group, although it is not a carboxylic acid. The higher the cone voltage, the more peaks are present, which is to be expected as the molecule is being broken into more fragments in the instrument.

The results for the $[Ru(III)(EDTA)Cl]^{2-}$ solution left for 48 hours with the NaI and the NaBr are very similar in that there are many ions in the mass spectra and it is very difficult to say exactly what complex each ion corresponds to. One thing that can be said is that ruthenium is present in each as the characteristic splitting pattern of ruthenium is present in all ions in the spectra. The ions in the table above were not present in any of the mass spectra showing that the ion exchange of Cl with I or Br is not occurring or at least, the products are not being detected here. No coordination with water was detected. Below is shown data obtained for $[Ru(III)(EDTA)Cl]^{2-}$ in H_2O at t=0. The data obtained are shown as an example of the complexity of the data and the difficulty in interpretation.

$[Ru(III)(EDTA)Cl]^{2-}$ in water at t=0

m/z (ESI) (cone voltage **10V**) Negative mode: $[M - H]^-$:426.2 5% intensity, $[M + Cl - H]^-$:462.0 35% intensity, $[M + 64 - H]^-$:490.0 100% intensity, $[M + 92 - H]^-$:518.0 60% intensity.

(Cone voltage **20V**): $[M - H]^-$:426.2 5% intensity, $[M + Cl - H]^-$:462.0 35% intensity, $[M + 64 - H]^-$:490.0 100% intensity, $[M + 92 - H]^-$:518.0 60% intensity.

(cone voltage **50V**): $[M - Cl - H]^-$: 390.1 50% intensity, $[M - 16 - H]^-$:410.1 30% intensity, $[M - H]^-$:426.2 10% intensity, $[M + 28 - H]^-$:454.0 100% intensity, $[M + 64 - H]^-$:490.0 50% intensity, $[M + 92 - H]^-$:518.0 80% intensity.

(Cone voltage **90V**): $[M - Cl - H]^-$: 390.1 45% intensity, $[M - 16 - H]^-$:410.1 17% intensity, $[M - H]^-$:426.2 20% intensity, $[M + 28 - H]^-$:454.0 60% intensity, $[M + 64 - H]^-$:490.0 100% intensity, $[M + 92 - H]^-$:518.0 80% intensity.

5.5.1.3 UV/Visible spectroscopy results for the anion exchange reactions

Metal complex chromophores arise from the splitting of d-orbitals by binding of a transition metal to ligands. A molecule absorbs certain wavelengths of visible light and transmits or reflects others which gives the molecule colour. A chromophore is a region in a molecule where the energy difference between two different molecular orbitals falls within the range of the visible spectrum. Visible light that hits the chromophore is absorbed and excites an electron from its ground state into an excited state. To further investigate the binding characteristics of halogens to the $[Ru(III)(EDTA)Cl]^{2-}$ complex UV/visible data were obtained from the same halogenated inorganic salts (plus KF) that were sent for mass spectral analysis. A change in absorbance of the solution over time would indicate changes occurring within the complex that relate to exchange of chloride ion with another anion or with water.

The $[Ru(III)(EDTA)Cl]^{2-}$ sample in water with no added anion acted as a control sample in case there were changes such as the loss of the chloride ion with subsequent binding to a hydroxyl ion which would also cause changes in UV absorption.

The results are shown in figures 5.4 and 5.5.

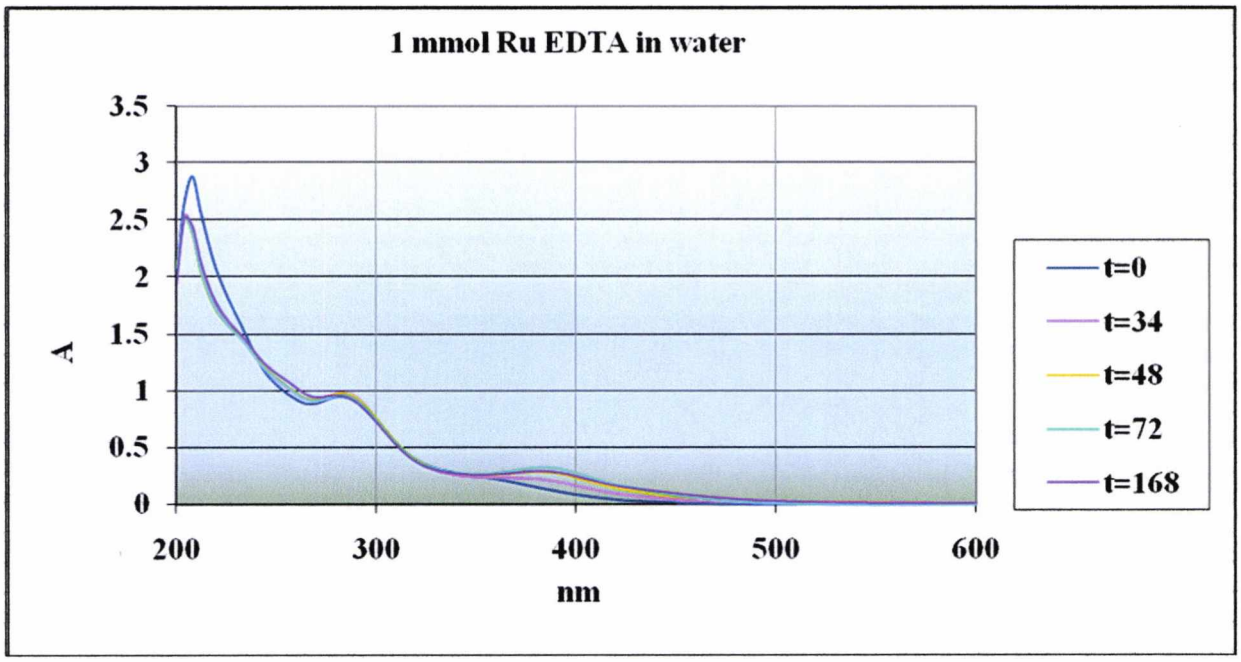

Figure 5.4 1 mmol $[Ru(III)(EDTA)Cl]^{2-}$ in water: UV absorption over 168 hours

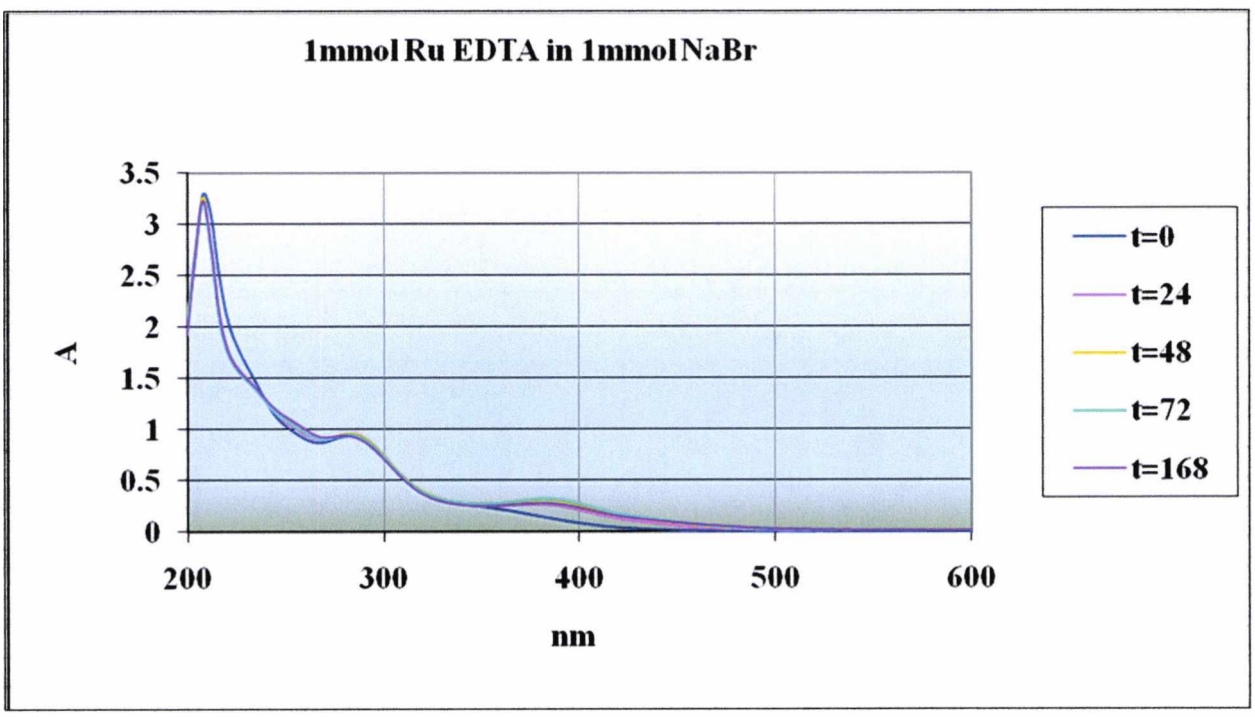

Figure 5.5 1 mmol $[Ru(III)(EDTA)Cl]^{2-}$ in 1 mmol NaBr: UV absorption over 168 hours

Both UV/visible spectra show a change in absorbance over time at 350 to 500 nm i.e. mainly in the visible region. This is consistent with observed colour changes. This data shows a change is occurring over time which could be due to bromide ions complexing with the

$[Ru(III)(EDTA)Cl]^{2-}$. However, the same change is occurring in the control solution (without bromide ion present) meaning it is more likely the change occurring is not due to exchange of Cl with Br. It is possible that hydrolysis is occurring, although there was no evidence of this from the mass spectral data. The other anions NaI and KF gave essentially the same results with the same changes noticed between 350 and 500 nm. It is also possible that ruthenium(III) is being reduced to ruthenium(II). It is mentioned in the introduction that Ru undergoes ready conversion from one oxidation state to another (Ezerskaya and Solovykh 1966). This would also give rise to spectral changes.

When radiolabelling a peptide for PET imaging, the solvent used would preferably be aqueous. The information from the literature that even small amounts of a protic solvent can lead transition metal fluorides becoming kinetically labile leading to easy ionisation (Branan et al. 1987) was always a potential problem for the rationale employed here. Stable complexes are needed for radiolabelling with ^{18}F for PET applications; the complex must be kinetically stable, in other words, once formed, the complex must not quickly undergo further reactions including the reverse reaction back to the starting material. From the literature, as mentioned in the introduction, it appears that Ru(III) EDTA complexes undergo ready conversion from one oxidation state to another and there is a tendency for its compounds to undergo hydrolysis and polymerisation. The results obtained in this chapter reflect this. Zirconium may represent a better choice of metal than ruthenium as Zr(IV) EDTA complexes appear to be much more stable. This represents an area of research that could be continued in the future.

5.6 Conclusion

It was decided after assessing the lack of positive results obtained from the UV/visible spectral data, the mass spectral data and X-ray diffraction data, not to proceed with this strategy any further. This was because ultimately, in a clinical setting, the strategy would have involved using the ion exchange mechanism discussed above to swap a chlorine ion for a fluorine-18 ion in one step. The results obtained from these studies combined with the information from the literature concerning the lability in aqueous solution of the $[Ru(III)(EDTA)Cl]^{2-}$ complex indicate that this is not a feasible way of labelling $[Ru(III)(EDTA)Cl]^{2-}$ with ^{18}F.

References

Bajaj HC, van Eldik R (1988). Kinetics and mechanism of ligand substitution reactions of ethylenediaminetetraacetate complexes of ruthenium(III) in aqueous solution. *Inorganic Chemistry* **27**, 4052-4055.

Bajaj HC, van Eldik R (1989). Kinetics and mechanism of the ligand substitution reactions of *N*-(hydroxyethyl)ethylenediaminetriacetate complexes of ruthenium(III) in aqueous solution. *Inorganic Chemistry* **28**, 1980-1983.

Beck W, Stunkel K (1988). Metal-complexes of weakly coordinating anions – precursors of strong organometallic lewis-acids. *Chemical Review* **88**, 1405-1421

Branan DM, Hoffman NW, McElroy EA, Miller NC, Ramage DL, Schott AF, Young SH (1987**).** Anion affinity of carbonylbis(triphenylphosphine)rhodium(I) in CH_2Cl_2-fluoride vs its halide analogs. *Inorganic Chemistry* **26**, 2915-2917.

Chatterjee D (1998). Properties and reactivities of polyaminopolycarboxylate (pac) complexes of ruthenium. *Coordination Chemistry Reviews* **168**, 273-293.

Chatterjee D, Mitra A (2006). Ruthenium polyaminocarboxylate complexes: Prospects for their use as metallopharmaceuticals. *Platinum Metals Review* **50**, 2-12.

N. Doherty, N. W. Hoffman (1991).Transition-metal fluoro compounds containing carbonyl, phosphine, arsine and stibine ligands. *Chemical Review* **91**, 553-573.

Dolle F (2005). Fluorine-18-labelled fluoropyridines: advances in radiopharmaceutical design. *Current Pharmaceutical Design* **11**, 3221-3235.

Dunitz JD, Taylor R (1997). Organic fluorine hardly ever accepts hydrogen bonds. *Chemistry-A European Journal* **3**, 89-98.

Ezerskaya NA, Solovykh TP (1966). Compounds of ruthenium with ethylenediaminetetra-acetic acid. *Russian Journal of Inorganic Chemistry* **11**, 991-995.

Filippou AC, Schneider S, Ziemer B (2002). Syntheses and molecular structures of chromium(IV) halides and psuedohalides bearing a triamidoamine ligand. *European Journal of Inorganic Chemistry* 2928-2935.

Gansow OA (1991). Newer approaches to the radiolabeling of monoclonal antibodies by the use of metal chelates. *Nuclear Medicine and Biology* **18**, 369-381.

Hicks RJ (2005). The role of PET in monitoring therapy. *Cancer Imaging* **5**, 51-57.

Hore PJ (2005). Nuclear Magnetic Resonance. Oxford Chemistry Primers. Oxford University Press, UK.

Intorre BJ, Martell AE (1964). Aqueous zirconium complexes. II. Mixed ligand chelates. *Journal of the American Chemical Society* **83**, 3618-3623.

Jolley J, Campbell CJ, Castineiras A, Yanovsky AI, Nolan KB (1999). Reactions of *N,N* '-dicarboxamido-*N,N* '-dicarboxymethyl-1,2-diaminoethane (EDTA-diamide) with hydrated ruthenium(III) chloride and potassium tetrachloroplatinate(II). Crystal and molecular structures of the pentadentate EDTA-H complex $NH_4[Ru(EDTA\text{-}H)Cl]\cdot 2H_2O$ and the EDTA-imide complex $PtCl_2[_2(HOOCCH_2)NCH_2CH_2NCH_2CONHCOCH_2]\cdot 2H_2O$. *Polyhedron* **18**, 49-55.

Kilbourn MS, Dence CS, Welch MJ, Mathias CJ (1987). Fluorine-18 labeling of proteins. *Journal of Nuclear Medicine* **28**, 462-470.

Matsubara T, Creutz C (1978). Inverted redox catalysis - catalysis on ruthenium(II) by an extraordinarily labile ruthenium(III) metal center. *Journal of the American Chemical Society* **100**, 6255-6257.

Matsubara T, Creutz C (1979). Properties and reactivities of pentadentate ethylenediaminetetraacetate complexes of ruthenium(III) and -(II). *Inorganic Chemistry* **18**, 1956-1965.

Murphy EF, Murugavel R, Roesky HW (1997). Organometallic fluorides: Compounds containing carbon-metal-fluorine fragments of d-block elements. *Chemical Review* **97**, 3425-3468.

Okarvi SM (1999). Recent developments in ^{99m}Tc-labelled peptide-based radiopharmaceuticals: an overview. *Nuclear Medicine Communications*, **20**, 1093-1112.

Okarvi S (2001). Recent progress in fluorine-18 labelled peptide radiopharmaceuticals. *European Journal of Nuclear Medicine* **28**, 929-938.

Pagenkopf BL and Carreira EM (1999). Transition metal fluoride complexes in asymmetric catalysis. *Chemistry-A European Journal* **5**, 3437-3442.

Pozhidaev I, Porai-Koshits MA, Polynova TN (1974). Crystal structure of zirconium ethylenediaminetetraaceticacetate tetrahydrate. *Zhurnal Strukturnoi Khimii* **15**, 644-650.

Schormann M, Roesky HW, Noltemeyer M, Schmidt H-G (2002). Diphenyllead difluoride and triphenylbismuth difluoride – new fluorinating reagents for the chlorine-fluorine metathesis reactions of group 4 and 5 compounds. *Journal of Fluorine Chemistry* **101**, 75-80.

Shreve PD, Anzai Y, Wahl RL (1999). Pitfalls in oncologic diagnosis with FDG PET imaging: Physiologic and benign variants. *Radiographics* **19**, 61-77.

Sluka JP, Griffin JH, Mack DP, Dervan PB (1990). Reagents and Methods for the Solid-Phase Synthesis of Protein-EDTA for Use in Affinity Cleaving. *Journal of the American Chemical Society* **112**, 6369-6374.

Suzuki TM, Tanaka DAP, Tanco MAL, Kanesato M, Yokoyama T (2000). Adsorption and removal of oxo-anions of arsenic and selenium on the zirconium(IV) loaded polymer resin functionalised with diethylenetriamine-*N,N,N',N'*-polyacetic acid. *Journal of Environmental Monitoring* **2**, 550.

Takahashi Y, Tanaka DAP, Matsunaga H, Suzuki TM (2002). Fluorimetric detection of fluoride ion by ligand exchange reaction with 3-hydroxyflavone coordinated to a zirconium (IV) – EDTA complex. *Journal of the Chemical Society-Perkin Transactions* **2**, 759-762.

Tanaka DAP, Kerketta S, Llosa Tanco MA, Yokoyama T, Suzuki TM (2002). Adsorption of fluoride ion on the zirconium (IV) complexes of the chelating resins functionalised with amine-*N*-acetate ligands. *Separation Science and Technology* **37**, 877-894.

Wilbur DS (1992). Radiohalogenation of proteins: An overview of radionuclides, labeling methods and reagents for conjugate labeling. *Biconjugate Chemistry* **3**, 433-470.

Yuchi A, Hotta H, Wada H, Nakagawa G (1987). Mixed ligand complexes of trivalent metal ions with an amine-*N*-polycarboylate and fluoride. *Bulletin of the Chemical Society* **60**, 1379-1382.

Yuchi A, Ban T, Wada H, Nakagawa G (1990). Mixed-ligand complexes of tetravalent metal ions with amine-*N*-polycarboxylates and fluoride. *Inorganic Chemistry* **29**, 136-138.

Yuchi A, Hokari N, Wada H, Nakagawa G (1993). Semi-xylenol orange complex of zirconium (IV) as a photometric reagent system for fluoride based on mixed ligand complex formation. *Analyst* **118**, 219-222.

Yuchi A, Terao H, Niwa T, Wada H (1994). Rapid adsorption and desorption of fluoride on zirconium (IV) complex with hydrophilic chelating polymer. *Chemistry Letters*, 1191-1194.

Yuchi A, Murase H, Wada H (1995). Structural features of organic reagents suitable for spectrophotometric or fluorimetric determination of fluorine based on mixed-ligand complex formation. *Analytical Sciences* **11**, 221-226

Yuchi A, Niwa T, Wada H (1995b). Determination of fluoride in the presence of tetravalent metal ions with an ion-selective electrode: Application to raw materials of fluoride glasses. *Analyst* **120**, 167-170.

Yuchi A, Hokari N, Terao H, Wada H (1996). Complexes of hard metal ions with amine-*N*-polycarboxylates as fluoride receptors. *Bulletin of the Chemical Society of Japan* **69**, 3173-3177.

Yuchi A, Matsunaga K, Niwa T, Terao H, Wada H (1999). Preparation and preconcentration of fluoride at the ng ml^{-1} level with a polymer complex of zirconium(IV) followed by potentiometric determination in a flow system. *Analytica Chimica Acta* **388**, 210-208.

Yuchi A, K.Matsuo K (2005). Adsorption of anions to zirconium (IV) and titanium (IV) chemically immobilised on gel-phase. *Journal of Chromatography A* **1082**, 208-213.